Proceedings

of the

Symposium

on the

Physics of Superconducting Devices

held

April 28-29, 1967

at

University of Virginia, Charlottesville

Sponsored by the Office of Naval Research, Physics Branch

PROCEEDINGS

OF THE

SYMPOSIUM

ON THE

PHYSICS OF SUPERCONDUCTING DEVICES

SPONSORED BY

OFFICE OF NAVAL RESEARCH, PHYSICS BRANCH

GRANT # NONR(G)00015-67

HELD AT THE

UNIVERSITY OF VIRGINIA, APRIL 28-29, 1967

PHYSICS DEPARTMENT

UNIVERSITY OF VIRGINIA

CHARLOTTESVILLE 22903

CONTENTS

LIST OF PARTICIPANTS

ADKINS, C. J., University of Cambridge, England; now Department of Physics, Rutgers University, New Brunswick, New Jersey 08903

ALGER, R. S., USN Radiological Defense Laboratory, San Francisco, California 94135

BARATOFF, A., Department of Physics, Brown University, Providence, Rhode Island

BARBEE, Troy W., Stanford Research Institute, 333 Ravenswood Avenue, Menlo Park, California

BARDEEN, John, Department of Physics, University of Illinois, Urbana, Illinois

BEAMS, Jesse W., Department of Physics, University of Virginia, Charlottesville, Virginia 22903

BEASLEY, Malcolm R., Department of Physics, Cornell University, Ithaca, New York 14850

BEHRINGER, Robert E., Office of Naval Research, 1030 East Green Street, Pasadena, California 91101

BERWIN, Robert W., Jet Propulsion Laboratory, 4800 Oak Grove Drive, Pasadena, California 91103

BHATNAGER, Anil, Department of Physics, University of Maryland, College Park, Maryland

BIRMINGHAM, B. W., Atomic Energy Commission, Washington, D. C. 20545

BLOCH, Felix, Department of Physics, Stanford University, Stanford, California 94305

BROWN, Robert E., Magnetism and Metallurgy Division, U. S. Naval Ordnance Laboratory, Silver Spring, Maryland 20910

BURGESS, Ronald E., Department of Physics, University of British Columbia, Vancouver 8, British Columbia, Canada

CABRERA, Nicolas, Department of Physics, University of Virginia, Charlottesville, Virginia 22903

CARSON, John W., NASA Electronics Research Center, 575 Technology Square, Cambridge, Massachusetts 02139

CARTER, John T., Department of Physics, Rice University, Houston, Texas 77001

CAUSEY, C. W., Office of Naval Research, Code 422, Washington, D. C. 20360

CELLI, Vittorio, Department of Physics, University of Virginia, Charlottesville, Virginia 22903

CHASZEYKA, Michael A., Office of Naval Research, 219 South Dearborn Street, Chicago, Illinois 60604

CHERRY, William H., RCA Laboratories, Princeton, New Jersey 08540

CHEVRIER, Jean Claude, Dupont, Wilmington, Delaware

CHILTON, Frank, Physics Division, Stanford Research Institute, Menlo Park, California 94025

CLARKE, John, Darwin College, Cambridge, England

CAFFEY, Howard T., Westinghouse Research Laboratories, Beulah Road, Pittsburgh, Pennsylvania 15235

COHN, George I., Quantum Engineering, Inc., 660 South Arroyo Parkway, Pasadena, California

COLEMAN, Robert V., Department of Physics, University of Virginia, Charlottesville, Virginia 22903

CRAIG, Paul, Brookhaven National Laboratory, Upton, New York 11973

D'AIELLO, Robert V., RCA Laboratories, Princeton, New Jersey

DAHM, Arnold, Department of Physics, University of Pennsylvania, Philadelphia, Pennsylvania 19104

DAUNT, John G., Department of Physics, Stevens Institute of Technology, Hoboken, New Jersey 67030

DAVIS, H. A., Plastics Department, DuPont Experimental Station, Wilmington, Delaware 19898

DAYEM, A. H., Bell Telephone Laboratories, Murray Hill, New Jersey

DEATON, B. C., General Dynamics Corporation, Fort Worth Division, P. O. Box 748, Fort Worth, Texas 76101

DEAVER, Bascom, Department of Physics, University of Virginia, Charlottesville, Virginia 22903

DEBS, Robert J., National Aeronautics and Space Administration, N-213-8 Ames Research Center, Moffett Field, California 94035

DeREGGI, Aime S., Department of Physics, University of Virginia, Charlottesville, Virginia 22903

DRAUTMAN, J. J., Gardner Cryogenics Corporation, 2136 City Line Road, Bethlehem, Pennsylvania 18017

DUNNINGTON, Leroy T., U. S. Navy Marine Engineering Laboratory, Code 632, Annapolis, Maryland 21401

EATON, III, Russell, Power Technology Laboratory, USAERDL, Ft. Belvoir, Virginia 22060

EDELSACK, E. A., Office of Naval Research, 1076 Mission Street, San Francisco, California 94103

EDELSTEIN, Alan S., International Business Machines, T J Watson Research Center, Yorktown Heights, New York 10598

EISENBERG, Judah M., Department of Physics, University of Virginia, Charlottesville, Virginia 22903

ERDMAN, Robert J., Keithley Instruments, 28775 Aurora Road, Cleveland, Ohio 44139

EVERITT, C. W. F., Department of Physics, Stanford University, Stanford, California 94022

FAIRBANK, Henry A., Department of Physics, Duke University, Durham, North Carolina 27706

FAIRBANK, William M., Department of Physics, Stanford University, Stanford, California

FERRELL, Richard A., Visiting Professor, Department of Physics, University of Virginia, Charlottesville, Virginia; now University of Maryland, College Park, Maryland

FREEMAN, Jr., Donald C., Speedway Reserve Laboratories, Linde Division, Union Carbide, 1500 Poloco Street, P. O. Box 24184, Indianapolis, Indiana 46224

FULTON, T. A., Bell Telephone Laboratories, Room 10302, Murray Hill, New Jersey 07971

GARDNER, Carl G., Laboratory for Physical Science, National Security Agency, 7338 Baltimore Boulevard, College Park, Maryland

GARDNER, Frank S., Office of Naval Research, 495 Summer Street, Boston, Massachusetts 02210

GARDNER, Murray, N-213-8, Ames Research Center, Moffett Field, California 94035

GARSTENS, Martin A., Office of Naval Research, Washington, D. C. 20360

GAULE, Gerhart K., OSAECOM-XL-E, Institute for Explor. Research, Fort Monmouth, New Jersey

GIAEVER, Ivar, General Electric Research and Development Center, P. O. Box 8, Schenectady, New York 12301

GLOVER, Rolfe E., Department of Physics, University of Maryland, College Park, Maryland

GOLDMAN, A. M., Department of Physics, University of Minnesota, Minneapolis, Minnesota 55455

GOLDMAN, Robert, Philco-Ford Corporation, Philadelphia, Pennsylvania

GOODKIND, John M., Department of Physics, University of California (San Diego), La Jolla, California 92037

GOREE, William S., Stanford Research Institute, 333 Ravenswood Avenue, Menlo Park, California

GRIMES, Charles C., Bell Telephone Laboratories, Murray Hill, New Jersey 07971

GRUENBURG, L., Department of Electrical Engineering, Massachusetts Institute of Technology, Cambridge, Massachusetts

HADEN, C. R., School of Electrical Engineering, University of Oklahoma, Norman, Oklahoma 73069

HAFSTROM, John W., Metallurgy Department, Room 8-411, Massachusetts Institute of Technology, Cambridge, Massachusetts 02139

HAGENA, O. F., RLES, University of Virginia, Charlottesville, Virginia

HAHN, Harold, IE Fourth, Accelerator Department Building 923, Brookhaven National Laboratory, Upton, New York 11973

HAKE, R. R., North American Aviation Science Center, 1049 Camino Dos Rios, Thousand Oaks, California 91360

HALAMA, Henry, Building 911, Brookhaven National Laboratory, Upton, New York 11973

HAMILTON, William O., Department of Physics, Stanford University, Stanford, California 94305

HAMMONS, Warren, Mail Stop R312, National Security Agency, Ft. George C. Mead, Maryland 20755

HAMMOND, Donald L., Hewlett Packard Company, 1501 Page Mill Road, Palo Alto, California 94304

HANRAHAN, Donald J., Code 5230, Naval Research Laboratory, Washington, D. C.

HENDRICKS, John B., Magnet Laboratory, Oak Ridge National Laboratory, P. O. Box 4, Building 9201-2, Oak Ridge, Tennessee 37831

HILDEBRANDT, Alvin F., Department of Physics, University of Houston, Allen Boulevard, Houston, Texas 77004

HODDER, Robert E., United Aircraft Research Laboratories, Silver Lane, East Hartford, Connecticut 06108

ISAKSON, Frank B., Physics Branch, Office of Naval Research, Washington, D. C. 20360

JAMES, Richard, Keithley Instruments, 28775 Aurora Road, Cleveland, Ohio 44139

JOHNSON, Robert C., Central Research Department, E. I. du Pont de Nemours and Co. Experimental Station, Wilmington, Delaware 19898

JONES, Clifford K., Cryophysics Department, Westinghouse Research Laboratories, Pittsburgh, Pennsylvania 15235

KAO, Y. H., State University of New York, Stonybrook, New York 11790

KAMPER, Robert A., Cryogenics Division, National Bureau of Standards, Boulder, Colorado 80302

KUNZLER, J. E., Bell Telephone Laboratories, Murray Hill, New Jersey 07971

KINDERMAN, E. M., Stanford Research Institute, Menlo Park, California

KING, Jr., Creston A., Department of Physics, Loyola University, 6363 St. Charles Avenue, New Orleans, Louisiana 70118

KIWI, Miguel G., Department of Physics, University of Virginia, Charlottesville, Virginia 22903

KWIRAM, A. L., Chemistry Department, Harvard University, Cambridge, Massachusetts

LABUSCH, Reiner, Department of Engineering Physics, College of Engineering, Cornell University, Ithaca, New York 14850

LARSON, Donald, Department of Physics, University of Virginia, Charlottesville, Virginia 22903

LEE, David M., Department of Physics, Brookhaven National Laboratory, Upton, Long Island, New York 11973

LESKOVAR, Branko, Lawrence Radiation Laboratory, University of California, Berkeley, California

LEVINE, James L., I.B.M. Watson Laboratory, 612 West 115th Street, New York, New York 10025

LIPSCHULTZ, Fred, Brookhaven National Laboratory, 20 Pennsylvania, Upton, New York 11973

LITTLE, William A., Department of Physics, Stanford University, Stanford, California 94305

LONG, H. M., Union Carbide Corporation, P. O. Box 44, Tonawanda, New York

LOVE, Roy, Solid State Physics Department, Corning Glassworks, Sullivan Park, Corning, New York

LUCAS, Edward J., Avco-Everett Research Laboratory, 2385 Revere Beach Parkway, Everett, Massachusetts 02149

MACVICAR, M. L. A., Metallurgy Department, Room 8-413, Massachusetts Institute of Technology, Cambridge, Massachusetts 02139

MARCUS, Paul M., International Business Machines Research Center, Yorktown Heights, New York 10598

MATISOO, Juri, IBM Thomas J. Watson Research Center, P. O. Box 218, Yorktown Heights, New York 10598

MCASHAN, Michael S., High Energy Physics Laboratory, Stanford University, Stanford, California 94305

McCANDLESS, E. L., Union Carbide, 270 Park Avenue, New York, New York

McCONE, Gordon, Aeronutronic Division, Philco-Ford Corporation, Ford Road, Newport Beach, California 92663

McCUMBER, D. E., Bell Telephone Laboratories, Mountain Avenue, Murray Hill, New Jersey 07971

McVEY, Eugene S., Electrical Engineering, University of Virginia, Charlottesville, Virginia 22903

MEINCKE, Peter, Room 1D-322, Bell Telephone Laboratories, Murray Hill New Jersey

MELICH, Michael E., Department of Physics, Rice University, Houston, Texas 77001

MERCEREAU, James E., P. O. Box A, Ford Motor Company, Newport Beach, California 92663

MESERVEY, Robert, Massachusetts Institute of Technology, National Magnet Laboratory, 170 Albany Street, Cambridge, Massachusetts 02139

MASON, Peter V., Jet Propulsion Laboratory 198-220, California Institute of Technology, Pasadena, California 91103

MILLER, Barry I., Room IE 416B, Bell Telephone Laboratories, Murray Hill, New Jersey

MITCHELL, John W., Department of Physics, University of Virginia, Charlottesville, Virginia 22903

NITZ, Allen, Allis Chalmers, P. O. Box 512, West Allis, Wisconsin

NORDMAN, James E., Department of Electrical Engineering, University of Wisconsin, Madison, Wisconsin 53706

OPFER, James E., Department of Physics, Stanford University, Stanford, California 94305

PARKER, Herman M., Aerospace Engineering and Engineering Physics, University of Virginia, Charlottesville, Virginia 22903

PARKER, William H., Department of Physics, University of Pennsylvania, Philadelphia, Pennsylvania 19104

PIERCE, John M., Department of Physics, Stanford University, Stanford, California 94305

QUELLE, Jr., Fred W., Boston Branch, Office of Naval Research, 495 Summer Street, Boston, Massachusetts 02210

REYNOLDS, Joseph M., Louisiana State University, P. O. Box 16070, Baton Rouge, Louisiana 70803

RENTON, C. A., National Aeronautics and Space Administration, Electronics Research Center, 575 Technology Square, Cambridge, Massachusetts 02139

RIES, Roger P., 1707 West Clark Street, Champaign, Illinois 61820

ROSE, R. M., Room 4-132, Massachusetts Institute of Technology, Cambridge, Massachusetts 02139

ROSENBLUM, Bruce, University of California, Santa Cruz, California 95060

ROWE, Irving, Office of Naval Research, 207 West 24 Street, New York, New York 10011

ROSS, Raymond, ASAECOM-XL-E, Institute F. Explor. Research, Fort Monmouth, New Jersey

ROWELL, John M., Bell Telephone Laboratories, ID-342 Murray Hill, Murray Hill, New Jersey 07971

SANDIFORD, David J., Department of Physics, Manchester University, Manchester 13, England

SASS, Andrew R., R.C.A. Laboratories, Princeton, New Jersey

SATTERTHWAITE, C. B., Department of Physics, University of Illinois, Urbana, Illinois 61803

SCALAPINO, D. J., University of Pennsylvania, Philadelphia, Pennsylvania

SCHMIDT, Hartwig, Department of Physics, University of Virginia, Charlottesville, Virginia 22903

SCHOOLEY, James F., National Bureau of Standards, Washington, D. C. 20234

SCHWABL, Franz, Department of Physics, University of Virginia, Charlottesville, Virginia 22903

SCHWARTZ, Brian B., National Magnet Laboratory, Massachusetts Institute of Technology, Cambridge, Massachusetts 02139

SCHWETTMAN, Alan, Department of Physics, Stanford University, Stanford, California

SCOTT, Warner C., Texas Instruments, Incorporated, P. O. Box 5936 MS134, Dallas, Texas 75222

SCHWIDTAL, Klaus, Attn: AMSEL-XL-E, United States Army Electronics Command, Fort Monmouth, New Jersey 07703

SEIDEL, George, Department of Physics, Brown University, Providence, Rhode Island

SEKULA, S. T., Solid State Division, Oak Ridge National Laboratory, P. O. Box X, Oak Ridge, Tennessee 37830

SERIN, Bernard, Department of Physics, Rutgers - The State University, New Brunswick, New Jersey 08903

SHAPIRO, Sidney, Room IB-405, Belle Telephone Laboratories, Murray Hill, New Jersey 07922; now Department of Electrical Engineering, University of Rochester, Rochester, New York 14627

SHEN, L. Y. L., Room 10302, Bell Telephone Laboratories, Murray Hill, New Jersey 07971

SHOSTAK, Arnold, ONR, Washington, D. C.

SIEGEL, Kenneth, Division of Cutler Hammer, Airborne Instrument Laboratory, Walt Whitman Road, Melville, Long Island, New York 11746

SILVER, Arnold H., Ford Scientific Laboratory, P. O. Box 2053, Dearborn, Michigan 48121

SMITH, Todd I., Department of Physics, Stanford University, Stanford, California 94305

SOULEN, Robert J., National Bureau of Standards, Washington, D. C. 20234

SPOHR, D. A., Cryogenics Branch, Naval Research Laboratory, Washington, D. C. 20390

STANFORD, A. L., School of Physics, Georgia Institute of Technology, Atlanta, Georgia

STEVENS, Donald K., Metallurgy and Materials Programs, U. S. Atomic Energy Commission, Washington, D. C. 20545

STEVENS, Howard O., Code 632, U. S. Navy Marine Engineering Laboratory, Annapolis, Maryland 21401

STEWART, J. W., Department of Physics, University of Virginia, Charlottesville, Virginia 22903

STEWART, W. C., R.C.A. Laboratories, Princeton, New Jersey 08540

SZEPFALUSY, Nora, Department of Physics, University of Virginia, Charlottesville, Virginia 22903; now Institute of Theoretical Physics, Roland Eötvös University, Puskin, U.T.C.A. 5-7, Budapest VIII, Hungary

SZEPFALUSY, Peter, Department of Physics, University of Virginia,Charlottesville, Virginia 22903; now Institute of Theoretical Physics, Roland Eötvös University, Puskin, U.T.C.A. 5-7, Budapest VIII, Hungary

TAYLOR, Barry N., R.C.A. Laboratories, Princeton, New Jersey 08540

TAYLOR, Henry, Department of Physics, Rice University, Houston, Texas 77027

TINKHAM, Michael, Department of Physics, Harvard University, Cambridge, Massachusetts 02138

TROUTMAN, Ronald, ONR, Department of the Navy, Washington, D. C.

VAN VEE, James, Chemistry Department, Harvard University, Cambridge, Massachusetts

VERNON, Jr., F. L., Aerospace Corporation, P. O. Box 95085, Los Angeles, California 90045

VICTOR, Joe M., Southwest Research Institute, 8500 Culebra, San Antionio, Texas 78206

WEAVER, Harry, Varian Associates, 611 Hansen Way, Palo Alto, California 94303

WEBB, Watt W., Rockefeller Hall, Cornell University, Ithaca, New York 14850

WHEATLEY, John C., Department of Physics, University of California (San Diego), P. O. Box 109, La Jolla, California 92037

WHITEHEAD, W. D., Center for Advanced Studies, University of Virginia, Charlottesville, Virginia 22903

WILSON, B. J., Code 5230, Naval Research Laboratory, Washington, D. C.

YNTEMA, George B., United Aircraft Research Laboratories, East Hartford, Connecticut 06108

YOUNG, William, Department of Physics, Rice University, Houston, Texas 77001

ZAR, Jacob L., Avco-Everett Research Laboratory, 2385 Revere Beach Parkway, Everett, Massachusetts 02149

ZIMMERMAN, J. E., Ford Scientific Laboratory, P. O. Box 2053, Dearborn, Michigan

ZUCKERMANN, Martin, Department of Physics, University of Virginia, Charlottesville, Virginia 22903; now Department of Physics, Imperial College of Science and Technology, Prince Consort Road, London, S. W. 7, England

INTRODUCTION

The Symposium on the Physics of Superconducting Devices was held at the University of Virginia in Charlottesville on April 28 and 29, 1967. The meeting was sponsored by the Office of Naval Research, Physics Branch, with additional support from the Physics Department of the University.

The purpose of the Symposium was to exchange ideas on new applications of superconductivity. Techniques and devices made possible by the unique properties of superconductors were discussed with emphasis on the basic physics and inherent limitations of the devices. Computers and high field magnets were specifically not included in order to limit the size of the meeting.

In spite of the rather severe topical limitation, the meeting grew considerably beyond expectation to 180 participants in four sessions which included 23 papers. The session chairmen, Felix Bloch, John Bardeen, John Daunt and Richard Ferrell, are due particular thanks for keeping the packed agenda within the schedule of the brief and busy meeting.

The Organizing Committee for the Symposium consisted of Bascom S. Deaver, Jr. (University of Virginia), Chairman, Edgar A. Edelsack (Office of Naval Research, San Francisco), William M. Fairbank (Stanford University), Richard A. Ferrell (University of Virginia, Visiting Professor), William S. Goree (Stanford Research Institute), and John W. Stewart (University of Virginia).

The enthusiastic cooperation and support of Nicolas Cabrera, Chairman, and other members of the Physics Department as hosts and the assistance provided through the Center for Advanced Studies by W. D. Whitehead, Director, were indispensable to the success of the meeting.

Local arrangements were handled by Vittorio Celli, Aime DeReggi, Acar Isin, Donald Larson and Martin Zuckermann, with the assistance of most other members of the Physics Department in one capacity or another. Special thanks are due to John Stewart for the well planned transportation, including

chartered buses to and from Washington and to Donald Larson for the outstanding luncheon and banquet on Friday.

We are particularly indebted to E. A. Edelsack for his guidance and experience in conducting scientific meetings and to Frank B. Isakson, Head, Physics Branch, Office of Naval Research, for making the meeting possible.

It was originally expected that the meeting would be somewhat smaller than was in fact the case, and only an informal summary was to be published (a summary did appear in Physics Today, September 1967). However, during the course of the meeting it was decided that a proceedings would be issued. In order to assist the speakers in preparing written versions of their talks, since they had not been asked to prepare formal papers, the sessions were tape recorded. A reporter was engaged to make a stenotypic record in addition, however, he became overwhelmed by the unfamiliar language of the physicist (although, in fact, the company has successfully reported other technical meetings). Each speaker was provided with the resulting, somewhat garbled, transcription of his talk, with several options suggested to him:

To edit the transcription so that it could be published simply as an edited talk,

To provide a more formal paper if he had prepared one,

To provide an abstract of his talk and a literature reference if the work had been subsequently published or accepted for publication.

This choice accounts for the variety of forms in which the talks are reported in this proceedings. The intent was to make easily accessible in printed form all the ideas discussed at the symposium with no attempt at literary consistency. The editors would like to thank the speakers for their cooperation in this unexpected effort.

Especial thanks are due to Michael Tinkham for his excellent summary of the proceedings, which he gave in the last talk of the Symposium.

The meeting served to emphasize the strikingly wide range of applications of superconductors. Devices and techniques using superconductors

are making possible new kinds of experiments and are vastly extending the range of sensitivity for measuring a variety of physical quantities. This phenomena, which has for so long been mostly a tantalizing curiosity to the technologist, now promises to add a whole family of new instruments to the already important list of applications in computers and magnets.

The incidence of discussion about fluctuations and noise in superconductors during the meeting indicated a growing concern with these topics, both from a fundamental point of view and as limitations on devices.

Additional copies of these proceedings are available through Office of Naval Research, Physics Branch, Code 421, Main Navy Building, Washington, D. C., Attention: E. A. Edelsack.

Bascom S. Deaver, Jr.
University of Virginia

William S. Goree
Stanford Research Institute

August 1967

A SUPERCONDUCTING LINEAR ACCELERATOR AND THE USE OF SUPERCONDUCTIVITY IN SOME FUNDAMENTAL EXPERIMENTS IN PHYSICS

W. M. Fairbank
Stanford University

Ever since the discovery of superconductivity[1], in 1911, and the discovery of superfluidity[2], in 1937, it has been realized that in the electrical conductivity of superconductors and the superfluid heat conductivity of liquid helium, there exist absolutely unique properties in nature. Yet as late as the General Electric Low Temperature Research Conference in 1952 - some people say, "That is not so late" - the main speaker suggested that there were no practical applications possible in low temperature physics. This was the one ivory tower field which was perfectly safe; that nuclear physics used to be this way, but nobody would conceivably cool something down to four degrees above the absolute zero just to make use of these peculiar properties.

With the discovery of the cryotron in 1956 by Dudley Buck[3] and the discovery of high field superconducting magnets by Kuntzler[4] in 1959, a great deal of excitement and anticipation of real practical applications of superconductivity became prevalent. Yet, today, in 1967, we still do not have superconducting computers. In fact, the effort in this field has decreased. The effort in the magnetic field is increasing, but most of the effort so far is with modest scale research magnets, although this is certainly changing.

I would like to suggest that in the superconducting accelerator an application exists for both the near-zero resistance of superconductors and the superfluid properties of liquid helium which will revolutionize the construction of accelerators[5] and cannot be duplicated at room temperature. I think that this development has the possibility of taking low temperatures out of the research stage into the practical area of development. It requires hundreds of feet of superfluid helium, refrigerators operating below the lambda point and removing hundreds of watts. It requires 24 hour operations without any breakdown. I think that the fact that high energy physics is willing to pay for this may be the crucial point that makes this a practical application.

In a conference last year in Boulder, Colorado, Weil was asked to give a talk about the applications of superconductivity to electromagnetism. He told me ahead of time that he was going to say there were not any practical applications. I said, "What about the superconducting accelerator?" He answered, "Nobody would pay a million dollars to a low temperature laboratory to develop one of these devices." I said, "Nobody would pay for that out of low temperature budgets. However, if SLAC, the Stanford Linear Accelerator, were to be modernized to increase the voltage by 20 BEV, the estimated budget is $53 million, to increase by a factor of 4 the klystrons and modulators. For $53 million you can buy a lot of refrigeration." He agreed and changed his talk.

First of all what is a linear accelerator and why do superconductivity and superfluidity offer such a tremendous possibility for improvement?

The first figure shows a diagram of a linear accelerator. It is a linear chain of microwave cavities. The individual cavities are coupled to their neighbors through a hole on the accelerator axis so that the entire assembly resonates as a single microwave structure. For the $\pi/2$ mode shown in the figure, the electric field in one-half of the cavities is zero. The electric field in the remaining cavities lies along the accelerator axis and alternates in direction from one excited cavity to the next. Since the fields vary sinusoidally with time, one-half cycle later these fields have reversed in direction. The distance from the center of one excited cavity to the center of the next is exactly one-half of a free-space wave length. Thus electrons traveling at the speed of light through the accelerator stay in phase with the accelerating fields and absorb energy from each of the excited cavities. Since the electrons cannot absorb energy in those cavities where the field is zero, these unexcited cavities are made as short as is convenient. To accelerate protons for the first few BEV, the cavities would be placed closer together since the protons would have a velocity less than the velocity of light.

The purpose of all accelerators is to accelerate particles to very high energy. It is desirable to have the maximum energy. Since the length of the accelerator is limited by the National Budget, one needs to have the maximum voltage per foot. The maximum voltage per-unit-length that can be obtained in an

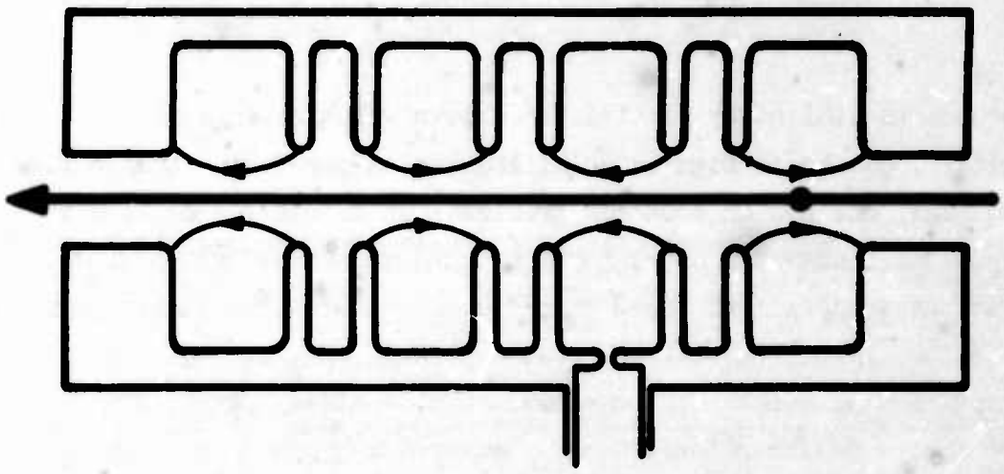

Fig. A-1 Standing wave bi-periodic $\pi/2$ mode accelerator structure.

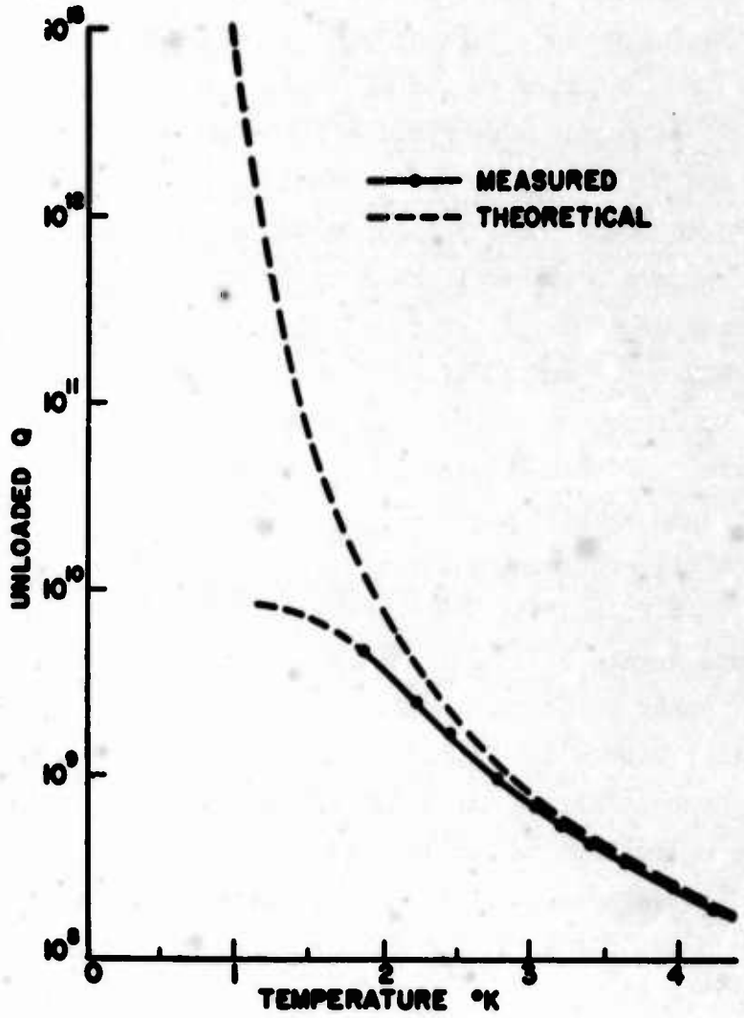

Fig. A-2 Measured Q of superconducting lead cavity as a function of temperature.

accelerator is limited by electric breakdown which, according to the experiments of Kapitza[6], can be as high as 30-million volts-per-foot. Long before one reaches this voltage, one has an economic problem. To maintain 4 million volts per foot requires 1 million watts of rf power at the optimum frequency of 3,000 megacycles, which is the frequency of the Stanford accelerator, just to overcome the losses in the copper. This is with the best available copper. Even if one were to cool the copper down, because of the anomalous skin effect, one can not gain a factor of more than a few over these losses. Therefore, one has to have very high power klystrons. The development of 20-megawatt klystrons by Hansen at Stanford was a key to the present accelerators. A 20-megawatt klystron cannot be operated continuously. Therefore, the accelerator is turned off most of the time, being on for 1 or 2 microseconds and off for a thousand times as long.

As an example, the world's biggest linear accelerator, SLAC, is 10,000 feet long. It accelerates electrons by two million volts per foot up to 20 BEV. To maintain that rf field requires over two billion watts. It is kept on for one or two microseconds and turned off for a thousand times as long. The average power consumed in the walls of the cavity is over two million watts. If SLAC were to operate at the breakdown power that has been developed by Kapitza in Russia, it would require over a hundred billion watts of peak rf power. Even a generous administration in Washington cannot afford this.

There are other problems. First, to keep the beam very homogeneous is difficult due to transient effects caused by the short pulsed operation of the accelerator and the frequency shift due to changes in the temperature of the cavity when large amounts of power are dissipated in the cavity walls. Second, a low duty cycle makes it difficult to observe rare events. For these rare event coincidence experiments a gain of approximately 1 thousand in sensitivity is obtained by an accelerator which is on continuously over an accelerator where the power is bunched in pulses with a duty cycle of only 1 in a thousand.

In summary, because of the large losses in the copper walls of existing linear accelerators, a limit is put on the total voltage output of the accelerator, the duty cycle of the accelerator, the homogeneity of the beam, and the ability to observe rare events in coincidence experiments.

A great effort is being made to make high duty cycle accelerators. The Los Alamos accelerator and the MIT accelerator are solving this problem by having a very long accelerator with a low voltage per unit foot. But this is very expensive and represents a brute force solution to the problem.

We have demonstrated, that in a superconducting accelerator the losses in the walls of the cavities can be reduced by a factor of about 500,000. This is a magic number. If we make a duty cycle unity, we have to dissipate a thousand times more power, and then remove that power at $2^{o}K$. This costs about a thousand times as much in refrigeration power. A thousand times a thousand is a million. Since klystrons are not as efficient as compressors, we end up with about a factor of 500,000 giving exactly the same power to keep a superconducting accelerator continuously on as is required to maintain a 1/10% duty cycle at room temperature. This was recognized very early. I even wasted some time when, as a graduate student, I was working on the Q's of superconducting cavities and thinking about superconducting accelerators. But it was absurd to build a superconducting accelerator in 1946 for two reasons. One, you could only make a litre of helium per day or so, and secondly the observed Q's of cavities[7] were a hundred times lower than in present experiments[8]. Also, there was a residual resistance.

About 1960, because of the development in SLAC and the desire to modernize the High Energy Physics Laboratory at Stanford, we decided to see if we couldn't obtain higher Q superconducting cavities. The next speaker, John Pierce, as an entering new graduate student worked with Perry Wilson and myself. That means that John did all the work. He succeeded in just a fraction of a year in improvthese Q's by almost one hundred[9]. Since that time, H. S. Schwettman[10], T. Smith, M. McAshan, J. Turneaure[14], J. M. Pierce[13], P. B. Wilson and E. E. Chambers and myself have all worked on the superconducting accelerator problems. As this goes to press cavity Q's in excess of 10^{10} at 10,000 megacycles have been obtained with both lead and niobium[11].

In room temperature accelerators the losses for a given accelerating voltage per foot decreases inversely as the square root of the frequency. Therefore the accelerators are made at as high a frequency as possible. For a superconductor one gains linearly as one reduces the frequency. The Stanford superconducting

accelerator is being built at 956 megacycles. The cavities are about 10 inches in diameter.

Figure 2 shows the Q's obtained by John Turneaure[14] on a lead cavity at 10,000 MHz. Also shown is the theoretical Q from the theory of Mattis and Bardeen[12]. You will hear more about this in the talk later on this morning.

There are interesting problems with what causes residual losses. Trapped flux, and other things are involved. We will hear more about this in M. McAshan's talk later this morning.

Now, how high a field can be maintained in these cavities? The field will be limited by electric breakdown. Supposedly that is very similar to room temperature breakdown. But what about the critical magnetic field?

The next figure shows some experiments at Stanford[10]. It is seen that the dc critical magnetic field and the ac critical magnetic field, where the Q begins to drop, are the same for tin.

Here is the second magical thing about superconducting cavities. How big is the critical magnetic field compared with the breakdown for electric fields? The best electric breakdown that has been obtained is in Russia, by Kapitza, 30 million volts per foot. This corresponds to a magnetic field in an accelerator cavity of about 1500 Gauss. That is just above the critical magnetic field for niobium. Thus the very best magnetic field that can be obtained in a Type I superconductor turns out to be almost identical with the best electric breakdown, a pure accident. Just the factor of 500,000 reduction in losses is what is needed to produce a CW accelerator with the same loss as a room temperature accelerator with a duty cycle of 1/1000.

We have built a five foot accelerator in a ten foot dewar. The cavities are about 10 inches in diameter, operating at 956 megacycles The accelerating cavity is twice as long as the zero field coupling cavity. The cavities are connected by indium "O" rings in the unexcited cavities. Each excited cavity is plated through the hole in the cavity, which is about 2 3/4 inches. One has a series of cavities that can be bolted together. The ten foot dewar holds 700 litres of helium.

We have operated the five foot accelerator with an rf accelerating field of about 10 Mev. We actually got about 6 Mev particles out of it because the

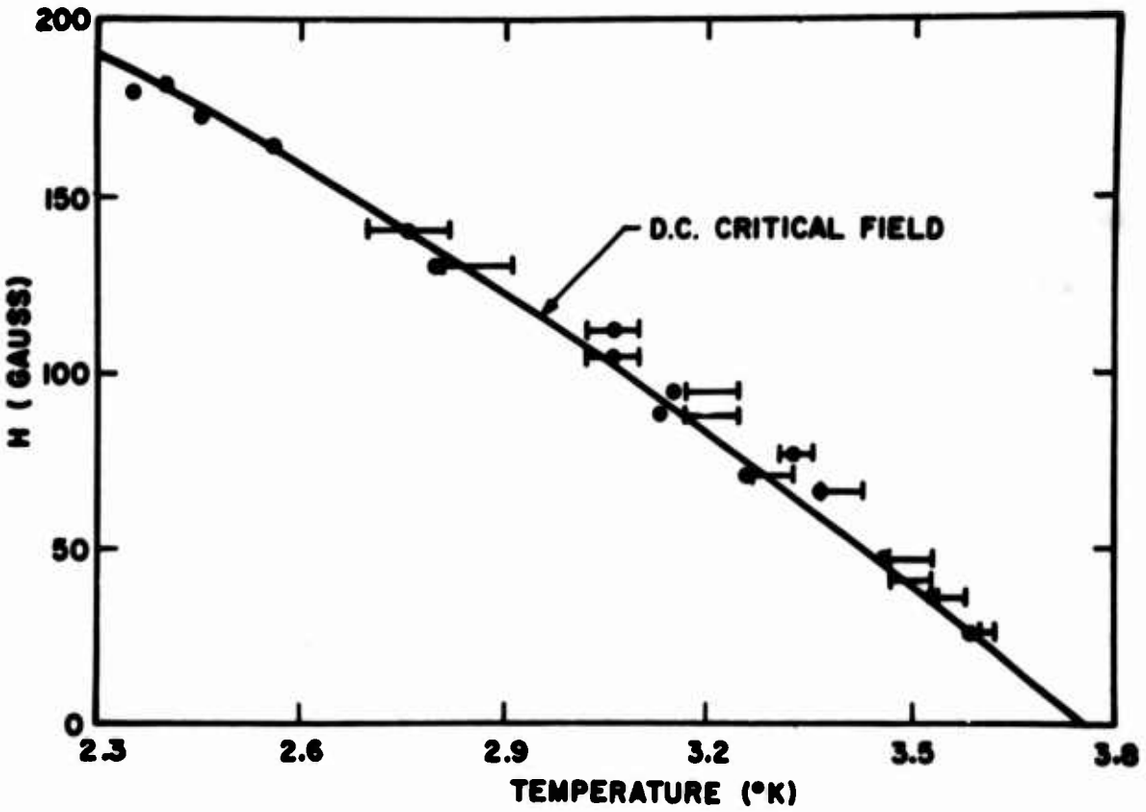

Fig. A-3 The ac critical magnetic field of tin as a function of temperature. The dots and the bars represent two methods of analyzing the data.

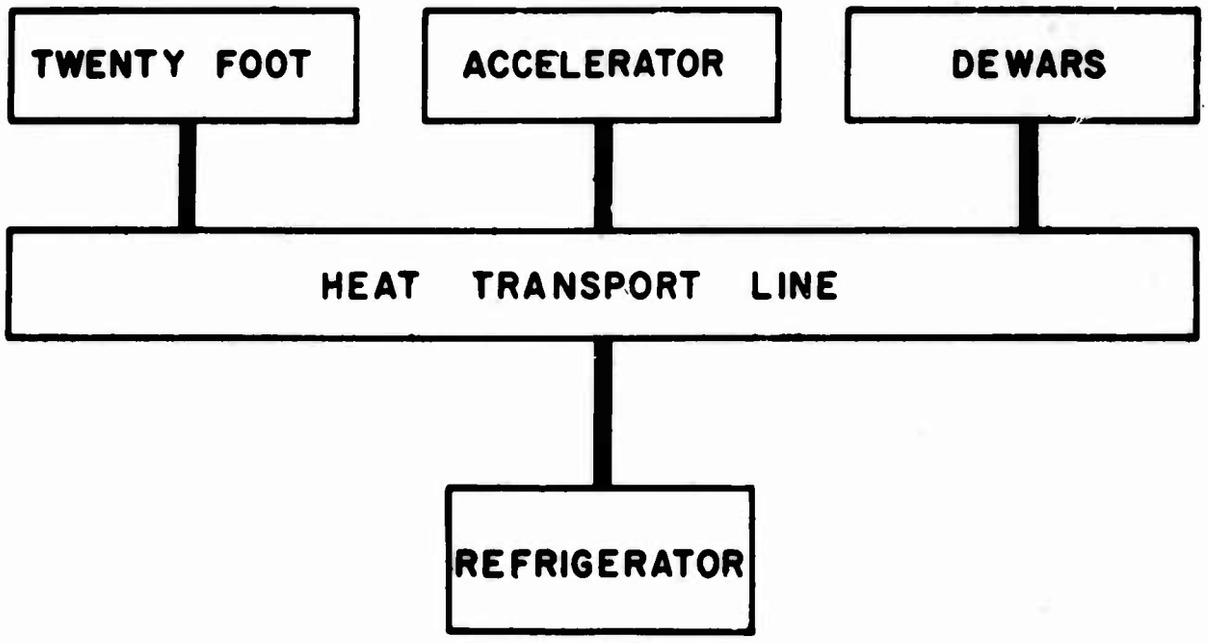

Fig. A-4 Schematic of a cryogenic system for superconducting accelerator.

injection was sufficiently below the velocity of light that we did not have quite the right phase. We calculated what we would have gotten with velocity of light electrons and obtained a figure of about 10 Mev. This meant that the peak voltage in the cavities was about 20 Mev in five feet. This is about where we have been getting rf breakdown in other lead cavity experiments. The present breakdown is probably caused by whiskers, dirt or oxygen on the surface and supposedly can be improved. This will be discussed by M. McAshan. Higher voltages are expected from niobium.

How is such a cavity kept cold, and how does it really operate?

Although the unloaded cavity Q's are over 10^9 the beam loaded Q's will be about 10^7. Because the temperature coefficient of expansion becomes almost zero at helium and because one is introducing 500,000 times less heat, it is possible to keep the accelerator beam very much more homogeneous. The biggest factor affecting the resonant frequency of the superconducting accelerator is the changing pressure of the helium as the temperature is changed. For a homogeneity of one part in 10^4 the temperature has to be kept constant to $0.03^{\circ}K$.

We have ordered a refrigerator, which Arthur D. Little is making, at a cost of $405,000. It is a remarkable achievement, because this refrigerator is no more expensive than equivalent refrigerators at $4^{\circ}K$ and will remove continuously 300 watts at $1.85^{\circ}K$. We estimate its operating costs for 24 hours a day to be $50,000 a year; if we pay four cents a litre for the liquid nitrogen and one cent per kilowatt hour for the electricity. This is considerably less than we pay at present to run the accelerator at the Stanford High Energy Laboratory.

Superfluid helium turns out to be all important in this process. In order to remove several hundred watts over several hundred feet and keep the temperature within $.03^{\circ}K$, it would require a bus bar of copper 100 feet in diameter. This is not very practical. It turns out that nine inches of superfluid helium will do the same thing. Now the superfluid properties of helium become all important. We imagine a test laboratory where we can try all kinds of devices for superfluid helium, running over a distance of 500 feet or more, and maintaining a temperature equilibrium within a few hundredths of a degree. I think it is possible that this is the way in the future one might have a really large scale low temperature

laboratory, on board a ship or in some kind of an installation where one central refrigerator would cool several hundred feet.

The specific heat of helium, although we normally think it is not very big, is 1/10 the specific heat of water. The Stanford accelerator will have about a foot cross section of liquid helium, about 30 liters per foot of length, so the specific heat to raise the temperature one degree is about 6,000,000 joules. If we should increase the heat the refrigerator can remove continuously by a factor of 100, we could still keep this increased power on for several seconds before the temperature would rise by .03°K. So if we have to go to pulsed operation, we do not need modulators. Because of the specific heat of helium, we can leave the accelerator on several seconds, long enough to turn it on and off with a switch.

Figure 4 shows schematically an accelerator and heat transport dewar operating from one refrigerator, which keeps the temperature constant over the whole length of the laboratory.

Figure 5 shows another possible modification of a superconducting accelerator made possible because of low temperatures. Higher voltages can be obtained by using a superconducting bending magnet to reverse the beam and send it back through the accelerator on the other half of the cycle and then again in the forward direction. For such an operation the length must be kept very constant because the beam is passing through the standing wave machine in two directions. But the length doesn't change at helium temperatures. Calculations indicate 700 feet can be kept constant to within a few thousandths of an inch very easily.

Now, I would like to mention a few other applications which we are developing using low temperature techniques. This is to illustrate at this conference that low temperatures are providing means of doing some very exotic experiments.

Figure 6 shows an experiment suggested by Leonard Schiff[15] to test Einstein's general theory of relativity by means of a gyroscope which is forced to go around the earth in a satellite. Schiff has calculated from Einstein's general theory of relativity that a perfect gyroscope subject to no external torques will experience an anomalous precession with respect to the fixed stars as it travels around the earth. A second anomalous precession arises due to the rotation of the earth. The figure shows the two effects on two seperate gyros in a polar

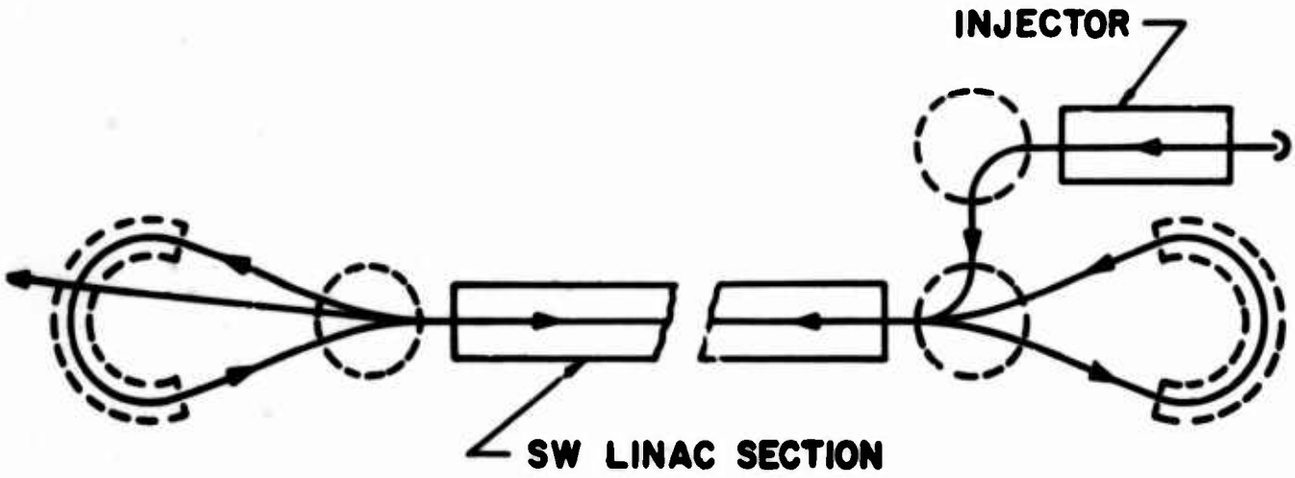

Fig. A-5 Schematic of recirculating linac using superconducting bending magnets.

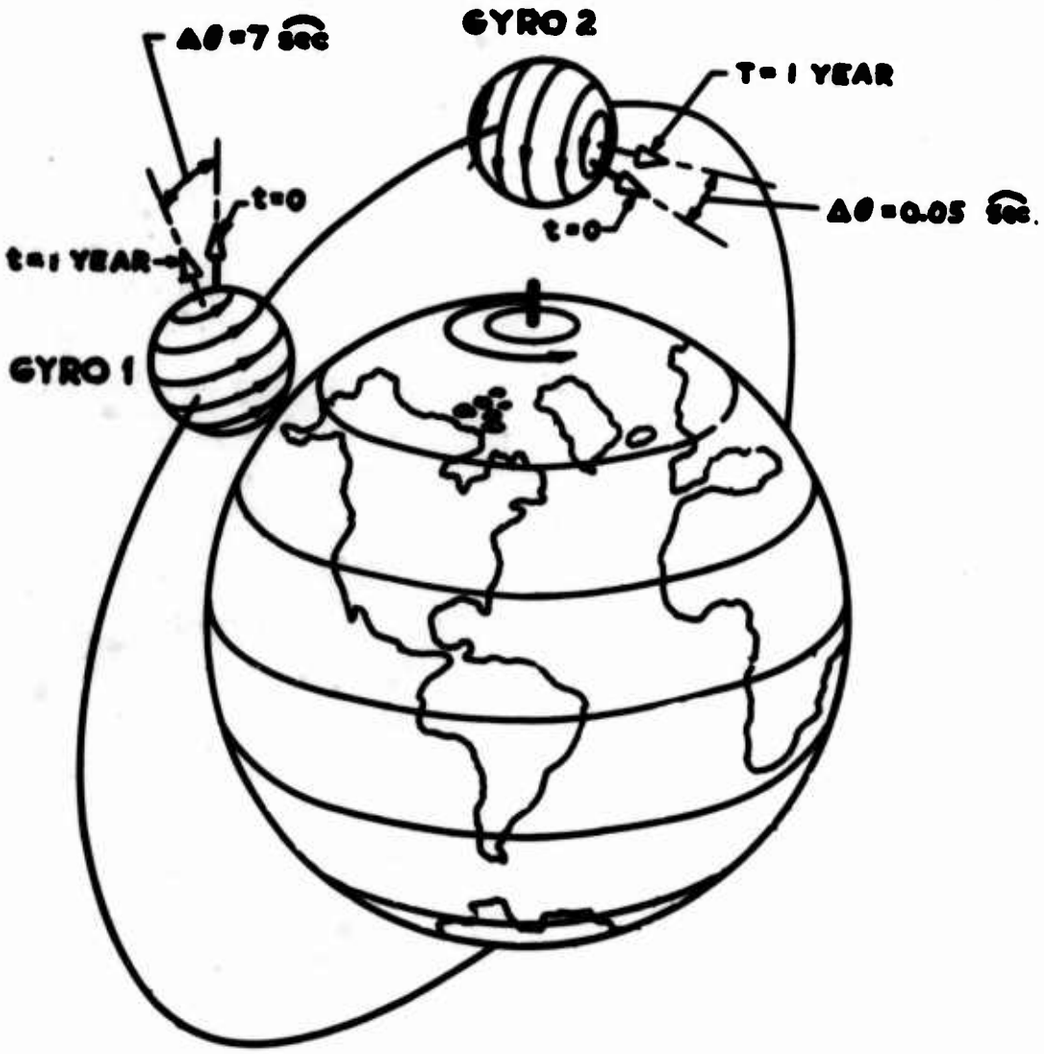

Fig. A-6 Relativistic precessions of gyroscopes in 500 mile polal orbit according to the Schiff calculations from Einsteins general theory of relativity.

orbit. The spin axis of gyro 1 is parallel to the axis of the earth and at right angles to the axis of the orbit. The predicted precession of such a gyroscope is 7 seconds of arc per year in the direction shown. This is the effect due to rotation 15 times a day about the earth. The axis of gyro 2 is oriented parallel to the satellite orbit and at right angles to the axis of the earth. The predicted precession of the axis of this gyro due to the rotation of the earth is 0.05 seconds of arc per year in the direction shown in the diagram. Under the conditions shown the two effects do not interfere.

There has been only one experiment which tests the equations of motion in Einstein's theory, that is the precession of the perihelion of Mercury. Recently Dickey has caused a lot of excitement by suggesting that this 1% check of Einstein's theory may really be in error by 8% because the sun is not quite spherical. Everyone does not believe this, especially the physicists who believe very strongly in Einstein. But Dickey is one of our best experimentalists, and he certainly has raised an exciting experimental question. The Schiff experiment would check such an effect.

In order to check the Dickey effect, one would like to measure both effects predicted by Schiff to a few percent accuracy. This requires an experiment accurate to a few thousandths of a second of arc per year. Such an experiment would give a completely new check to the general theory of relativity. We have addressed ourselves to the problem of how such a gyroscope can be made. It should be capable of being readout to a few thousandths of a second of arc and should have a drift rate due to all external torques of less than a few thousandths of a second of arc per year.

Because of the necessity of supporting the gyroscope against the gravitational pull of the earth it is impossible to make a mechanical gyroscope on earth which approaches within several orders of magnitude these requirements on drift rate. However in a satellite it is possible to reduce the effective gravitational field sufficiently to reduce the support torques to the required level. The gravity-gradient torques which exist on any gyroscope which is not perfectly spherical remain as large in the satellite as they are on earth. To reduce the drift from these torques to less than a few thousandths of a second of arc per

year it is necessary to have the ball as nearly as possible perfectly spherical. This poses a readout problem. Conventional readouts require knowing the position of the axis of rotation with respect to the ball. If the moments of inertia of all the axes of the ball are the same it is impossible to anticipate about which axis the gyroscope will spin. Furthermore if the experiment is done at helium temperatures any cooling of the ball must be done by black body radiation since the gyro ball will be spinning in a vacuum. Therefore the readout must introduce extremely small quantities of heat into the ball.

Superconductivity provides through the London moment[16,17,18,19] a unique way of solving this readout problem. A spinning superconductor produces along its axis of spin a magnetic field of $10^{-7}\ \omega$ gauss. It is expected that the gyro ball in the experiment will be made of quartz, coated with a thin layer of niobium. The ball will be an inch and one half in diameter, and the gyro spin speed will be 2×10^{3} radians/sec. This will produce a magnetic field of 2×10^{-4} gauss along the axis of spin. The question then arises how can one detect to a few thousandths of a second of arc the orientation of such a gyroscope by use of this very small magnetic field. Figure 7 shows the readout which makes use of a superconducting loop. Shown in the figure is a spinning superconductor with a magnetic field as indicated along the axis of the spin. Around the spinning sphere is placed, as a method of readout, a superconducting loop. As the orientation of the gyro ball changes, the magnetic flux through the loop changes. An accurate reading of this flux gives the direction of the axis of the ball. This will in practice be done with a double loop shown in Figure 8. This double loop, with a variable inductance produced by a moving ground plane mounted to a quartz crystal, is a parametric amplifier. This magnetometer will be discussed by John Pierce. Theoretical calculations indicate that the sensitivity of this magnetometer is sufficient to measure a few thousandths of a second of arc. We are working toward making experimental results equal to the theory.

Figure 9 shows the experiment[20]. It consists of a quartz telescope, which is always kept pointed at a fixed star, and the gyroscope. The gyroscope is surrounded by a four inch superconducting shield from which the last quantum of flux will hopefully have been eliminated. The gyroscope and telescope readouts in the helium temperature and zero-g environment will not change with respect to each other by more than a few thousandths of a second of arc per year.

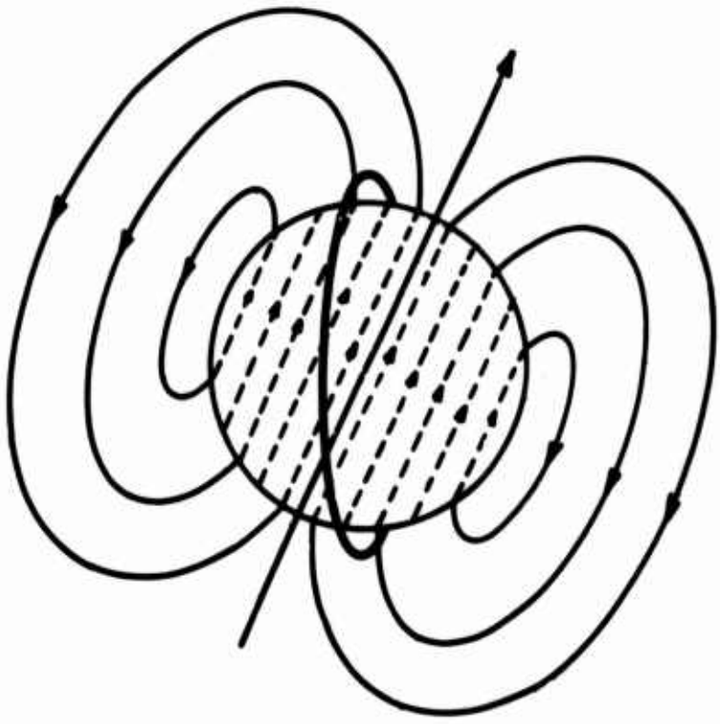

Fig. A-7 Principle of the London moment readout.

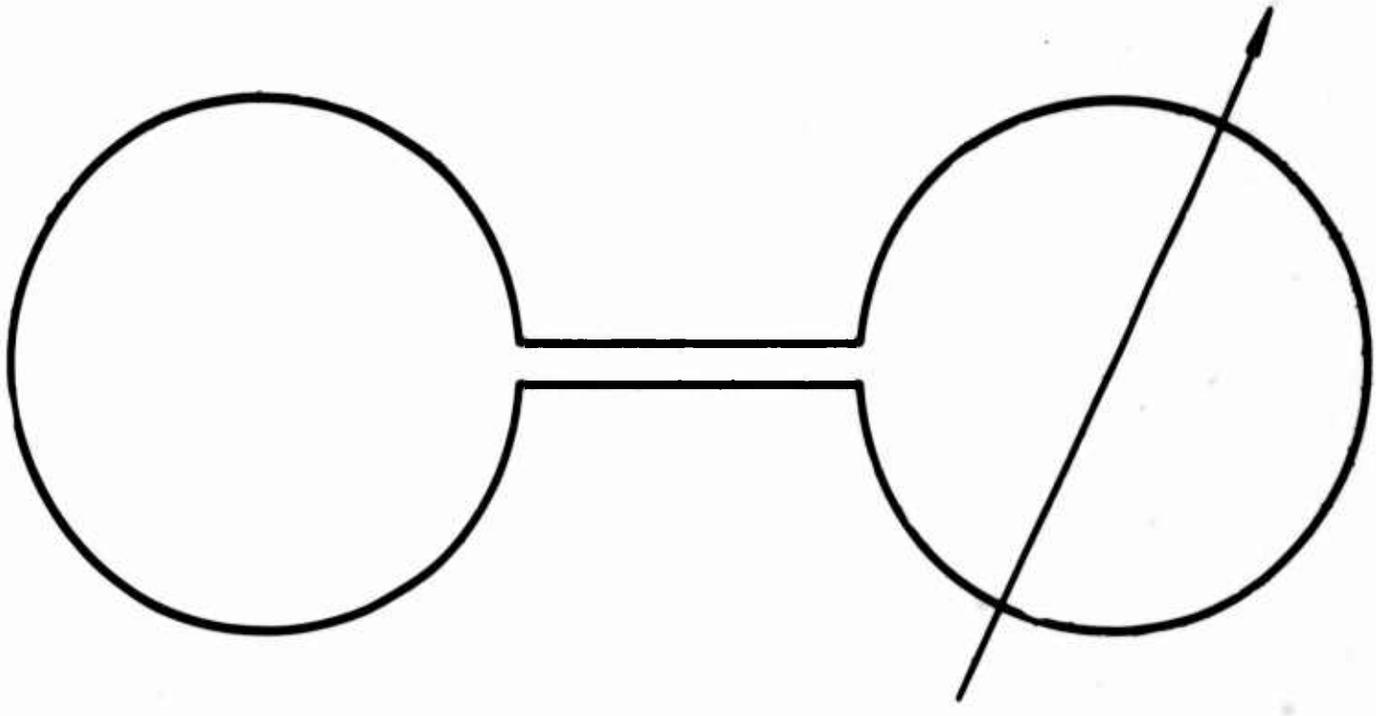

Fig. A-8 Schematic illustration of the superconducting detection circuit. The arrow indicates that the inductance of that loop can be varied periodically.

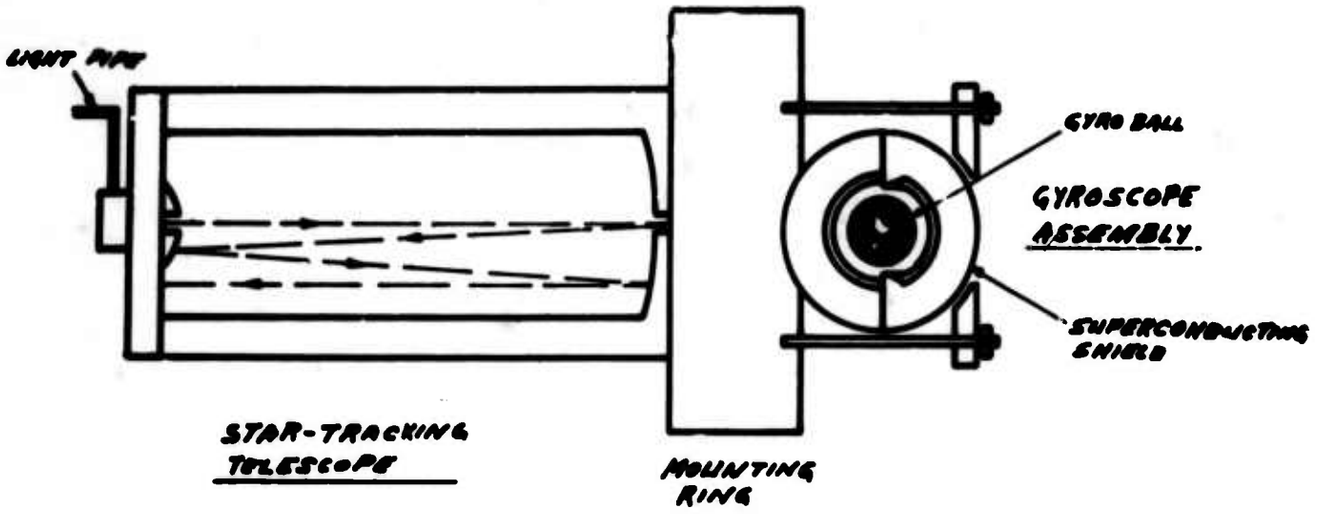

Fig. A-9 Gyroscope and telescope mounted together for laboratory test of relativity experiment.

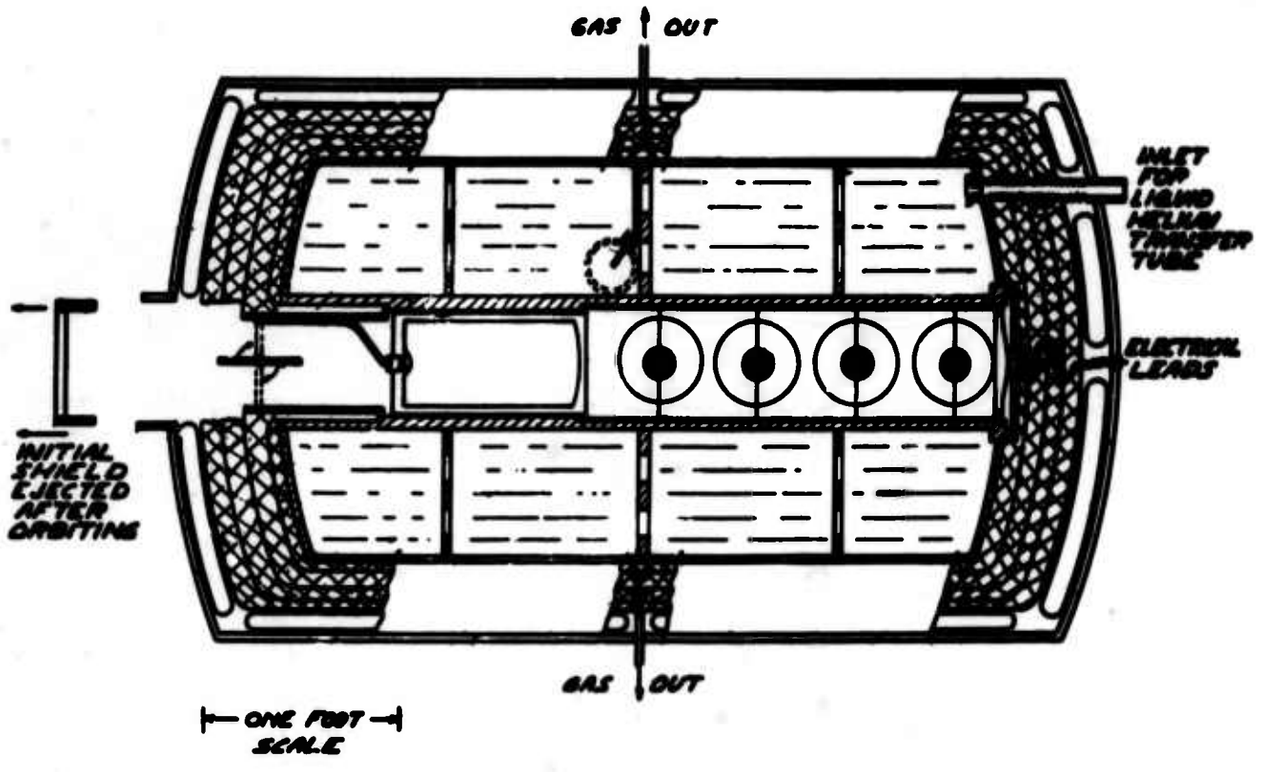

Fig. A-10 Flyable low temperature apparatus for relativity experiment.

Figure 10 shows the dewar surrounding the complete experiment. It will contain 250 litres of liquid helium surrounding four gyroscopes and a telescope. Two gyroscopes will measure each of the relativity effects. Two hundred layers of super-insulation will be compressed by inflatable pillows during take off. In space, the pillows will be deflated and the superinsulation allowed to expand to provide sufficiently good insulation to keep the helium for a year in space.

The liquid helium will be maintained below the lambda point and removed through a superfluid filter to gas jets at room temperature which will control with the helium gas the attitude of the satellite so as to be always pointed at the star. The use of a superfluid filter eliminates the difficulty of containing and pumping on a liquid in a zero-g environment.

Now, could one perform the relativity experiment on earth? It turns out nature has made what physicists believe is a perfect gyroscope, a spinning nucleus. The ideal nucleus is the nucleus of He^3 since it is contained in a non-magnetic atom. Such a gyroscope is in principle like the superconducting gyroscope mentioned above. It produces along its axis of spin a magnetic field. However, it has such a small moment of inertia compared to its magnetic moment, that a very small magnetic field will cause it to precess. To perform the relativity experiment on the He^3 nucleus on earth would require an external field less than 10^{-18} gauss. Up until now a field of less than 10^{-7} gauss has been impossible to obtain. However, superconductors give us the hope of obtaining very much smaller fields.

Figure 11 shows a diagram of the cylinder used in the quantized flux experiment comprising Bascom Deaver's Ph.D. Thesis at Stanford[21]. When the tiny tin cylinder was cooled below the transition temperature in less than half a flux unit, there was no flux trapped in the central hole. This gives the possibility of obtaining larger regions of zero magnetic field If one could cool a spherical superconducting shell through its transition temperature in less than half a quantum of flux, in such a way that no thermal fluctuations introduce trapped flux, then one should obtain in the region inside the sphere, zero magnetic field. If polarized He^3 nuclei are placed inside such a zero magnetic field region in a completely symmetrical way, then the He^3 nuclei will remain polarized and pointing

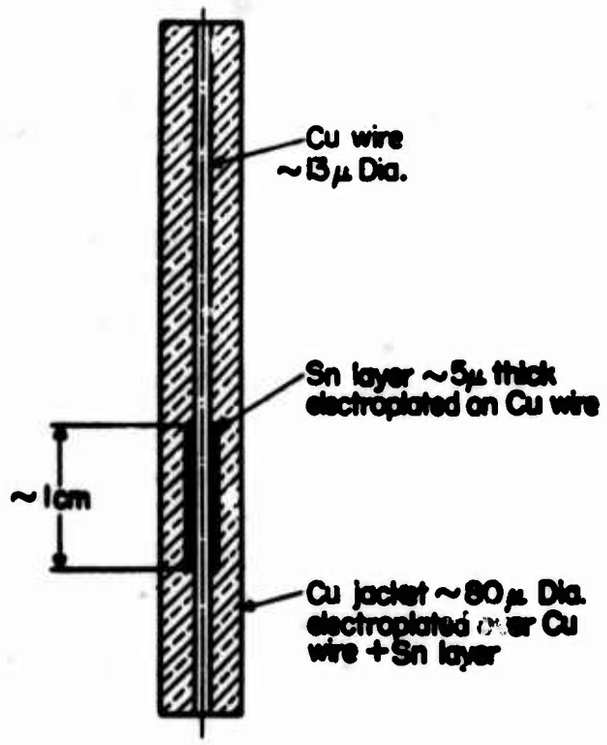

Fig. A-11 Details of sample construction for quantized flux experiment.

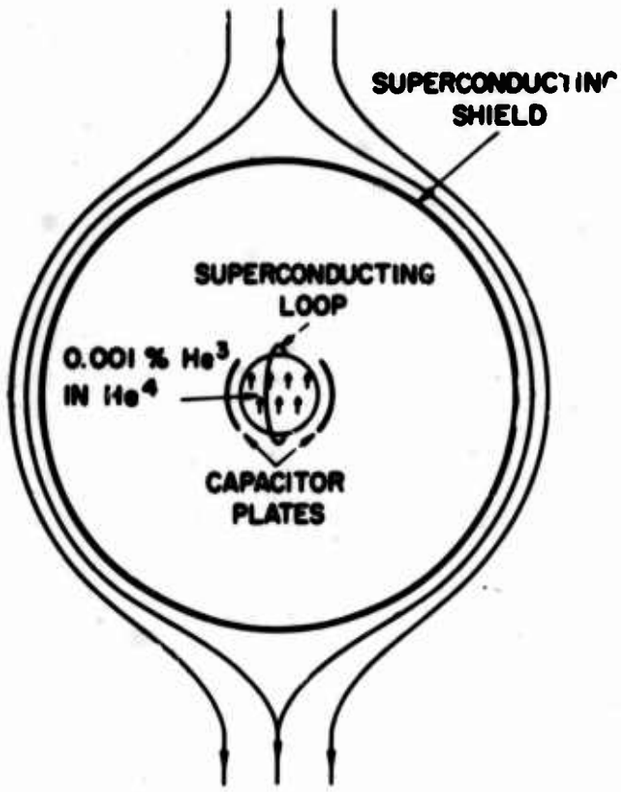

Fig. A-12 Schematic of the free precession nuclear gyroscope. The condenser plates are for use in the experiment to seek nuclear electric dipole moment of He^3.

in the same direction for T_1 or T_2, which ever is the shortest. Such a nuclear gyroscope could be readout with a superconducting loop magnetometer exactly in the same way as described for the relativity experiment in space.

Figure 12 shows such a nuclear gyroscope being made by W. O. Hamilton[20] at Stanford. The outside sphere is made of quartz, spherical to a few millionths of an inch. It will be coated with niobium. The polarized He^3 will be diluted with He^4 to increase the relaxation time. It can be made theoretically longer than a year by diluting to 1 part in 10^5 He^3 in He^4. The He^3 will be polarized by optical pumping at room temperature.

The actual experiment to be done with this He^3 gyro will not be the relativity experiment but an easier experiment to determine whether or not the He^3 nucleus is a perfect gyroscope. In other words, to determine whether or not the positive and negative charges have the same center of charge, i.e. whether there exists a permanent electric dipole moment along the spin axis of the He^3 nucleus. In order to check this, the He^3 nuclei will be immersed in an external electric field at right angles to the axis of spin. Just as the gravity gradient will cause an elliptical gyroscope to precess in space, so a permanent electric dipole moment will cause the He^3 nuclei to precess in the electric field gradient which exists in the He^3 atom in the presence of an external electric field. The existence of a permanent electric dipole moment would violate time reversal invariance. The recent experiments at Brookhaven by the Princeton group have suggested that there may be such a time reversal invariance violation[22]. The zero magnetic field region will be obtained, if existing attempted experiments are successful, by the expansion of a series of concentric lead socks in an initially small external magnetic field[20]. Each sock, when cooled through its transition temperature and then expanded, will cause a reduction in the field by more than an order of magnitude according to preliminary experiments performed thus far. W. O. Hamilton is spending his full research time on the electric dipole moment experiment and C. W. F. Everitt on the relativity experiment.

In summary, superconductivity coupled with low temperature environment offers the possibility of improving linear accelerators, of checking Einstein's general theory of relativity, of performing a time reversal invariance experiment

more accurately than the best existing high energy experiments and also other experiments which I have not had time to mention, such as a gravity meter to search for quarks. I am sure that other ideas for the use of superconductors in the solution of basic research problems are already being exploited by many of you.

Acknowledgments

The superconducting linear accelerator development is a cooperative program between the Physics Department and the High Energy Physics Laboratory at Stanford. I wish to particularly acknowledge the important contribution of Professor Schwettman and Drs. E. E. Chambers, M. S. McAshan, J. M. Pierce, T. I. Smith, J. P. Turneaure and P. B. Wilson. The project has been supported by the Office of Naval Research.

The relativity experiment, supported by NASA, has received full time support and direction from Dr. Francis Everett. The He^3 gyro experiment has been supported by the Air Force Office of Scientific Research, the Air Force Avionics Laboratory and the Air Force Aeronautical Research Laboratory and been under the full time direction of Professor Hamilton.

References

1. H. K. Onnes, Commun. Phys. Lab. Univ. Leiden, No. 120b (1911); Commun. Phys. Lab. Univ. Leiden, No. 122b (1911).
2. P. L. Kapitza, Nature, London, 141, 74 (1938); J. F. Allen and A. D. Misener, Nature, London 141, 75 (1938).
3. D. A. Buck, Proc. I.R.E. 44, 482 (1956).
4. J. E. Kunzler, E. Buehler, F. S. L. Hsu, and J. E Wernick, Phys. Rev. Letters 6, 89 (1961).
5. H. A. Schwettman, J. P. Turneaure, W. M. Fairbank, T. I. Smith, M. S McAshan, P. B. Wilson and E. E. Chambers, The 1967 U.S National Particle Accelerator Conference (to be published).
6. S. P. Kapitza, V. P. Bykov, and V. N. Melekhin, Sovient Phys. JETP 14, 266 (1962).
7. H. London, Proc. Roy. Soc. A176, 522 (1940).
8. For a review of such experiments see: E. Maxwell, Progress in Cryogenics, vol. IV, (Heywood, London, 1964).
9. W. M. Fairbank, J. M. Pierce, and P. B Wilson, Proceedings of the VIII International Conference on Low Temperature Physics (Butterworths, Washington, 1963).
10. H. A. Schwettman, P. B Wilson, J. M. Pierce, and W. M. Fairbank, Advances in Cryogenic Engineering, vol. 10 (Plenum Press, New York, 1965).
11. Niobium cavities have been prepared for us by Varian Associates and the Linde Division of Union Carbide.
12. D. C. Mattis and J. Bardeen, Phys. Rev. 111, 412 (1958).
13. J. M. Pierce, Ph.D. Thesis, Stanford University, 1967 (unpublished).
14. J. P. Turneaure, Ph.D. Thesis, Stanford University, 1967 (unpublished).
15. L. I. Schiff, Proc. Natl. Academy 46, 871 (1960).
16. F. London, Superfluids, Vol. I (John Wiley and Sons, New York, 1950 and Dover Publications, Inc., New York 1961).
17. M. Bol and W. M. Fairbank, Proc. of IX Int. Conf. on Low Temp. Phys., Columbus, Ohio, August 31 - September 4, 1964 (Plenum Press, p. 451 1965).
18. A. F Hildebrandt, Phys. Rev. Let. 12, 190 (1964).

19. A. King, Jr., J. B. Hendricks, and H. E. Rorschach, Jr , Proc. IX Int. Conf. on Low Temp. Phys. (Plenum Press, p. 466 (1965).
20. William M. Fairbank, William O. Hamilton and C. W. F. Everitt, Proceedings of the Research Applications Conference Office of Aerospace Research U. S. Air Force, Washington, D. C. Processed for the Defense Documentation Center Defense Supply Agency.
21. B. S Deaver, Jr. and W. M Fairbank, Phys. Rev. Let. 7, 43 (1961).
22. J. H. Christenson, J. W. Cronin, V. L. Fitch and R. Turlay, Phys. Rev. Let. 13, 138 (1964).

A PERSISTENT CURRENT MAGNETOMETER WITH NOVEL APPLICATIONS*

John M. Pierce
Physics Department
Stanford University

The magnetometer circuit described in this paper is central to several experiments which are being done in our group at Stanford. In addition to the relativity experiment and the He^3 gyroscope mentioned by Dr. Fairbank in the preceeding paper, it is being used to measure the magnetic susceptibility of large biomolecules in dilute solutions and to measure the EPR spectrum of biomolecules in water solution. The latter experiment is discussed in some detail below, because in it are used most of the unique features of this magnetometer.

With such varied applications of the circuit being made, it is not surprising that several people have made important contributions to its development. This paper is a review of the entire development program, and no attempt will be made to sort out the contributions of various individuals.

Fig. 1 shows the basic magnetometer circuit. The loop L_1- L_2 is a closed superconducting circuit, a portion of which can be driven normal by the switch heater, S. As long as the switch is closed, the total flux linking the loop is constant. The quantity to be measured is a change, Φ, in the flux from external sources which links the coil L_1. Its introduction causes persistent current, $i_o = n_1\Phi/(L_1 + L_2)$, to flow in the loop. If L_2 is now varied, i_o must also vary, and finite voltages are produced. Thus current flows in the central branch of the circuit and power is delivered to the load R. If L_2 is varied sinusoidally by a small fraction α, and if the system is properly matched, then the steady-state output power indicated in Fig. 1 is obtained.

One can compare this circuit to the Foner magnetometer[1] by noting that the output power is approximately the same as that obtained in a normal LR circuit

*Work supported in part by the U.S. Office of Naval Research.

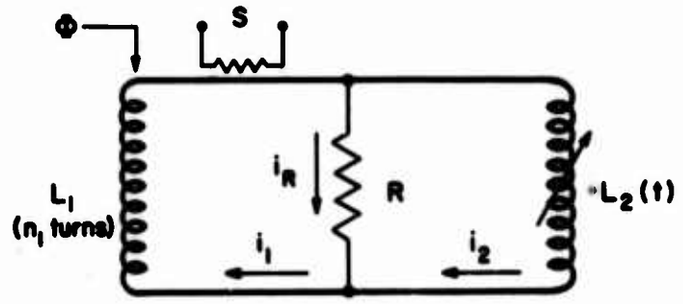

$$L_1 i_1 + L_2 i_2 = n_1 \Phi$$

$$i_R R = \frac{d}{dt}(L_2 i_2)$$

$$i_1 - i_2 = i_R$$

$$L_2^0\left[1 + a \sin(\omega t)\right] = L_2(t)$$

$$P \cong \frac{n_1^2 \Phi^2}{2L_1} \frac{2}{27} a^2 \omega$$

Where:

$$R = \omega L_1^0 \qquad L_1 = 2L_2^0$$

$$L_1^0 = \frac{L_1 L_2^0}{L_1 + L_2^0}$$

$$a << 1$$

Fig. B-1 Basic Magnetometer Circuit.

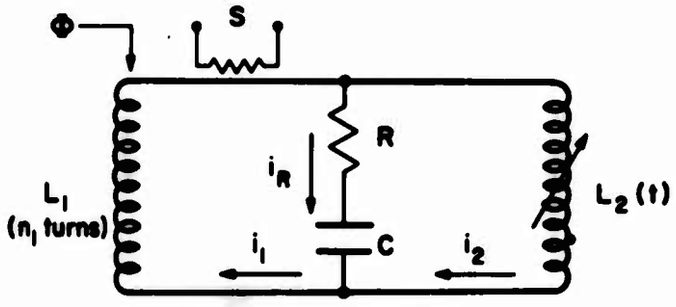

$$L_1 i_1 + L_2 i_2 = n_1 \Phi$$

$$R \frac{d}{dt}(i_R) + \frac{1}{C} i_R = \frac{d^2}{dt^2}(L_2 i_2)$$

$$i_1 - i_2 = i_R$$

$$L_2^0\left[1 + a \sin(\omega t)\right] = L_2(t)$$

$$P \cong \frac{n_1^2 \Phi^2}{2L_1} \frac{2}{27} a^2 \omega Q$$

Where:

$$\omega = \left[L_1^0 C\right]^{-\frac{1}{2}} \qquad L_1 = 2L_2^0$$

$$L_1^0 = \frac{L_1 L_2^0}{L_1 + L_2^0} \qquad Q = \left[\omega C R\right]^{-1}$$

$$a << 1$$

Fig. B-2 Resonant Magnetometer Circuit.

if a magnetized sample producing a flux Φ is vibrated at frequency ω so that the flux linking the coil varies a fraction α. The great sensitivity of our circuit is due to the fact that it is possible to make $\alpha \approx 1/10$ at $\omega \approx 2\pi \times 10^6$. Thus the output power is orders of magnitude greater than one could ever obtain by actually moving a sample.

The performance of the basic circuit can be improved by resonating it with a capacitor, as shown in Fig. 2. The output power is just that obtained from the nonresonant circuit multiplied by the Q of the resonant circuit. The Foner magnetometer can also be improved by resonating the circuit. However, since our circuit is superconducting, a Q of 10^4 or more is not difficult to achieve.

Let us now calculate the expected sensitivity of this circuit. Since the circuit is entirely superconducting, the ultimate limit will be the input noise of the room-temperature receiver. The minimum detectable change in the magnetic field linking a single loop of wire of radius 1 cm (L_1) should be

$$B_{min} \approx 1 \times 10^{-10} \text{ gauss.}$$

Here we assume a receiver with 3 db noise figure in a bandwidth of one cycle, and we assume values for the other parameters as indicated above.

A further physical insight into the behavior of the circuit can be obtained by noting that the quantity $(n_1\Phi)^2/2L_1$ can be written as $\frac{1}{2} L_1 i_o^2$. Here i_o is the original dc persistent current. Alternatively it can be written as $(B^2/2\mu_o)V_{eff}$. Here V_{eff} is the effective volume of the coil L_1. Thus this energy is just the field energy contained in the sample taken by L_1. This energy is delivered to the load roughly $\alpha^2\omega Q$ times per second, and this rate can be made $\sim 2\pi \times 10^8$ sec^{-1}. The output energy of course comes from the modulator, not the field.

Now obviously the heart of this system is the modulator, the means by which the inductance of L_2 is varied 10% at frequencies $\sim 10^6$ Hz. Fig. 3 shows the modulator we have developed most completely. It is essentially a hollow cylinder of superconductor (the indium film) which can be thermally switched between the normal and superconducting states by means of an electric current in the coaxial heater formed by the aluminum and aluminum-copper films. The length of the

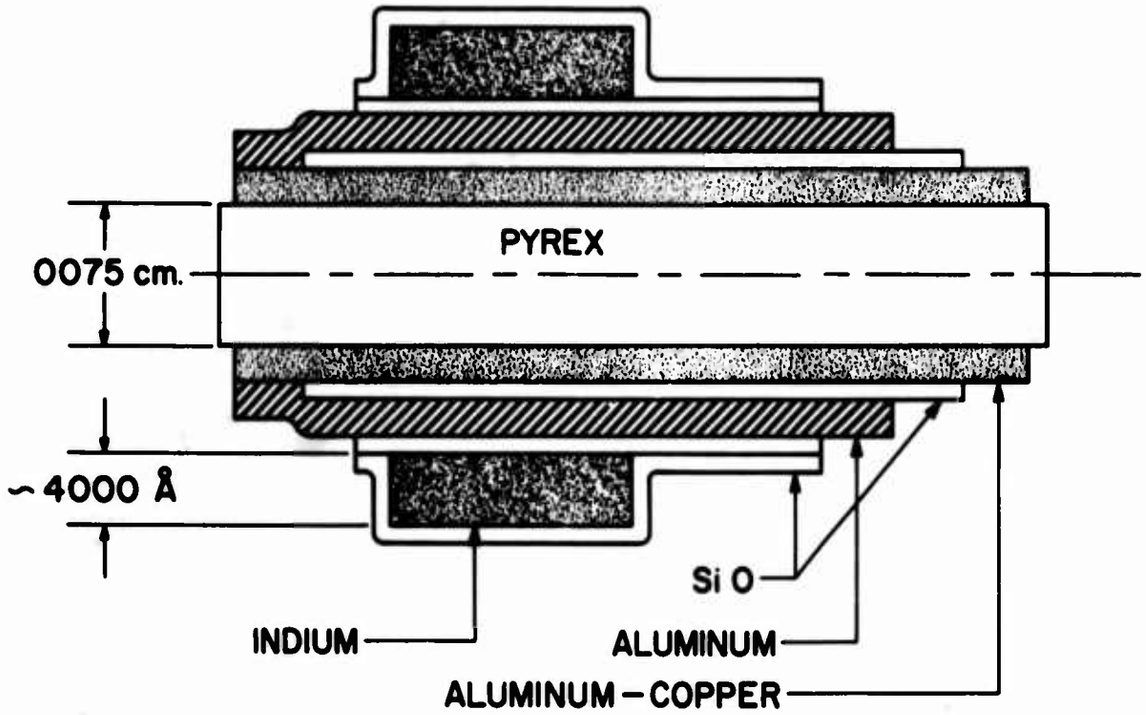

Fig. B-3 Thermally Switched Modulator.

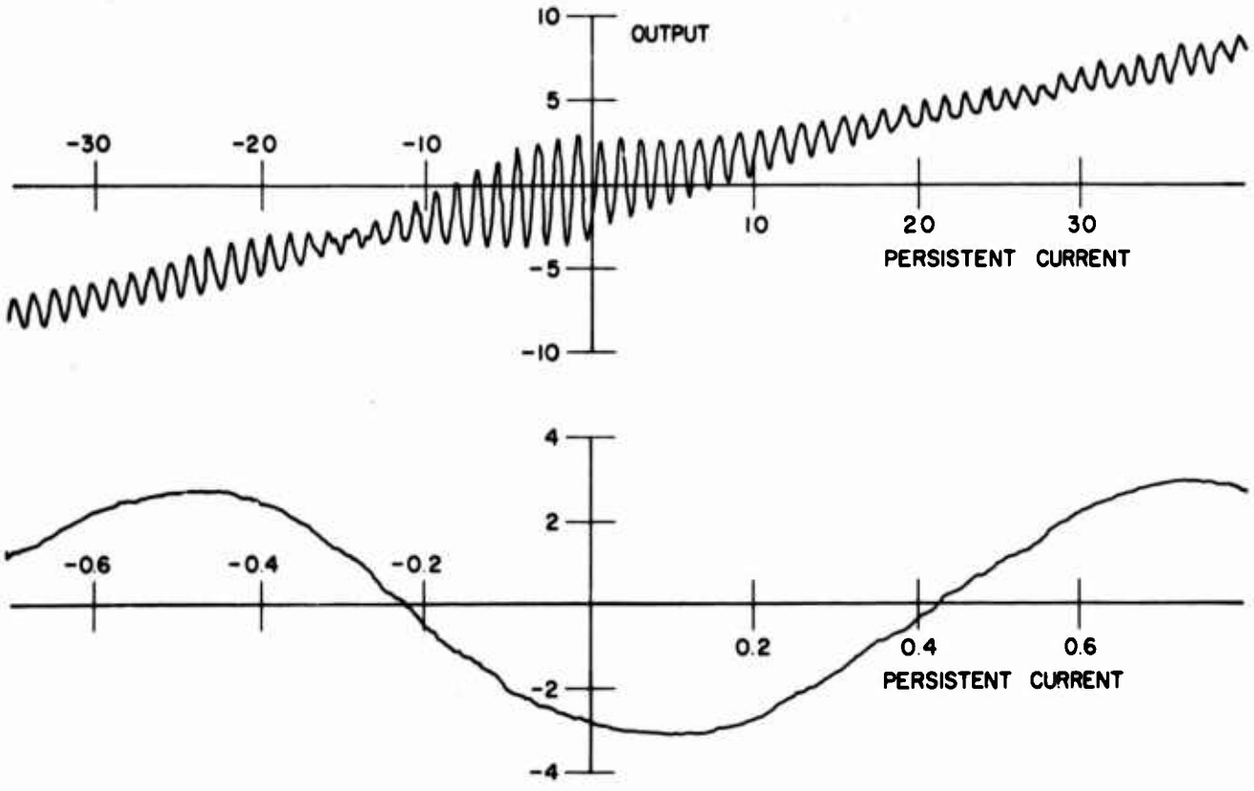

Fig. B-4 Circuit Output Versus Persistent Current.

indium cylinder is approximately 1 cm. This device is prepared by vacuum evaporation, and it is inserted in a coil of .002" diameter Nb wire space-wound with a .006" inside diameter. The assembly is immersed horizontally in liquid helium maintained about 100 millidegrees below the transition temperature of indium. The liquid is free to circulate vertically between the turns of the coil to cool the modulator. About 5 milliwatts of heater power is sufficient to operate the modulator.

With this device we have modulated the inductance of the little coil as measured at several MHz by 10% at frequencies up to 100 kHz. But such a device does not simply modulate the inductance of a coil. When a hollow cylinder of superconductor is cooled through the transition in a field such that less than one half quantum of flux links it, then it excludes all the flux from its area. This is the effect desired; work is done in excluding the flux which eventually can be delivered to the load. When, however, the flux is greater than one half quantum, the cylinder adjusts it to the nearest quantum. Thus the output of the circuit is a semi-periodic function of the persistent current, as shown in Fig. 4. Plotted here is the output of a phase-sensitive receiver, using the heater power for a phase reference. The zero offset between the two curves is not significant. The large waves correspond to flux quanta[2] in the modulator, and the washing out at high quantum numbers is due to gradients in the field produced by the small coil L_2. The overall slope is due to the Meissner effect in the indium film.

The noise which is apparent on the lower curve is not receiver noise. It is in fact about three orders of magnitude larger than receiver noise. This noise is due to fluctuations of the field inside the high-permeability ferromagnetic shielding around the apparatus.

A modulator of this type is as sensitive to field applied directly to it as it is to field produced by the persistent current in the coil L_2. Hence, to use this device as we have described, it is necessary to operate the modulator in a region where the field is constant in time roughly to the sensitivity desired for the magnetometer. It is further necessary that the field gradient along the modulator be less than the field associated with a quantum of flux ($\sim$1 milligauss).

Otherwise the sensitivity is drastically reduced as in Fig. 4 for high quantum numbers.

A region of quite constant magnetic field can be produced with a superconducting shield,[3] but attempts to date to use such a shield with this modulator have been unsuccessful. The reason is that when a container plated with superconductor is cooled even in a very low magnetic field ($< 10^{-4}$ gauss) highly inhomogeneous fields $\sim 10^{-2}$ - 10^{-1} gauss are nearly always produced in it. The large field gradients ruin the sensitivity of the circuit. We have, however, recently traced this phenomenon to thermoelectric currents flowing between the superconductor and the substrate on which it is plated, and we expect to overcome this difficulty in the near future.[4]

Fig. 5 shows the circuit refined for measuring magnetic field. Except for the configuration of L_1 it is similar to the circuits used for the other purposes mentioned above. L_1 can be rotated to measure absolute field. The triaxial mount for the modulator is shown schematically. It is designed to reduce pickup from the modulator heater voltage to the circuit. The round dots represent silver-paint contacts to the heater films on the modulator. Note that both heavy loops are persistent; they are coupled inductively so that the coil of optimum geometry for the modulator, L_2, can be matched to L_1. We have added the coil L_3 so that a known flux can be inserted in the circuit and the modulator used as null-detector only. The resistor R_s shorts out L_1 at the modulation frequency to prevent radiation and other undesirable effects.

A completely different type of modulator is also under development. Fig. 6 shows the basic idea. The inductor L_2 is now a long line photoetched in a sputtered niobium film on an optically flat substrate. Right above the line, about 2000 Å away, we place a ground plane. This is another niobium film sputtered onto an x-cut quartz crystal resonant in the longitudinal mode at the modulation frequency. Now the inductance of such a line near enough to a ground plane is proportional to the distance between the plane and the line. Thus when the crystal vibrates $\sim$ 1000 A at 1 MHz, the inductance is modulated by a large fraction at this frequency. We have modulated a capacitor $\sim$ 10% at

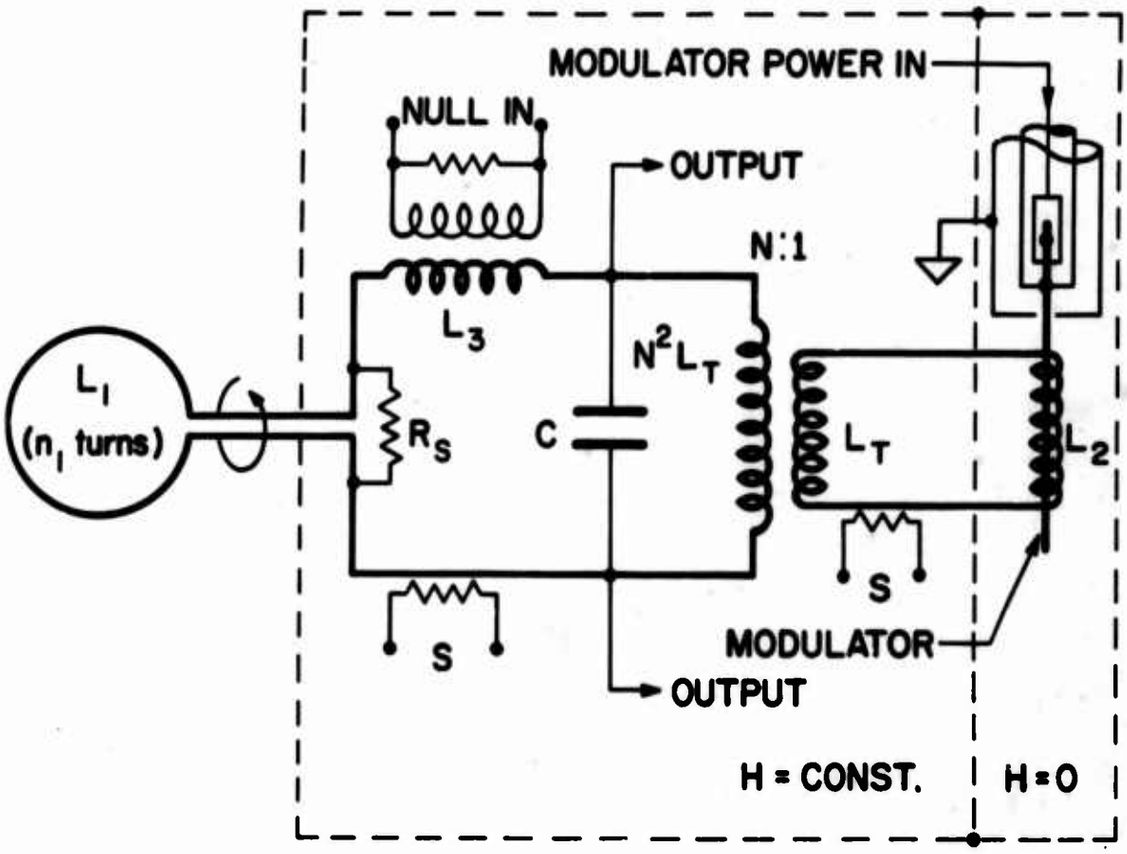

Fig. B-5 Magnetometer Circuit for Magnetic Field Measurement.

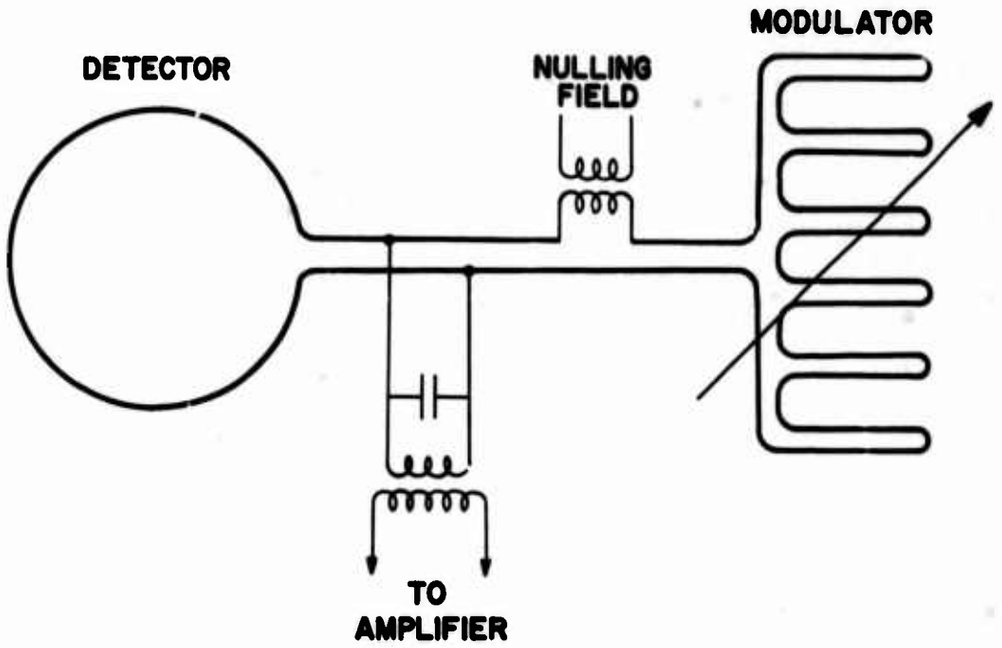

Fig. B-6 Schematic of Circuit Using Vibrating Modulator.

1 MHz, and we expect to have the techniques of fabricating the line perfected in the near future.

One of the novel experiments to which we are applying this circuit is the experiment to measure EPR in water solutions. The problem with conventional paramegnetic resonance, in which the microwave power absorbed by the spins is measured, is that water is a stronger absorber of microwaves. With this magnetometer circuit we plan to measure the magnetization of the spins produced by the resonance, not the absorbed power.

This experiment uses two features of the circuit that were not emphasized previously. First, the coil L_1 can be in quite a high magnetic field as long as it is constant in time; only the modulator must be in a low field. Second, the circuit has a memory. If the flux Φ is present when the switch is closed and is subsequently removed, the persistent current provides a record of its presence.

The experiment we visualize is as follows: The room-temperature sample of solution is contained in a small dewar inserted into L_1. The switch is opened and a persistent superconducting magnet is set to the desired magnetic field. With the switch still open, the sample is irradiated with a pulse of microwave power sufficient to magnetize the spins. The switch is then closed and the power turned off. After the spins have relaxed the persistent current can be measured at leisure with no dissipation in the water.

Calculations indicate that the sensitivity should be about 5×10^{13} spins per cc with a measuring time $\sim 10^{-2}$ sec. The experiment is still in its early stages, and many problems remain to be solved, not the least of which is the perfection of a superconducting switch which can be operated in a fraction of a microsecond without introducing spurious persistent currents. Still it is quite a novel experiment and it illustrates the potential of the circuit.

A region of extremely low magnetic field is vital to several experiments in progress, especially the He^3 gyroscope. An experiment is well under way which should produce fields very near zero by cooling a superconducting shield in such a way that not even one flux quantum is trapped through the walls. Fig. 7 shows

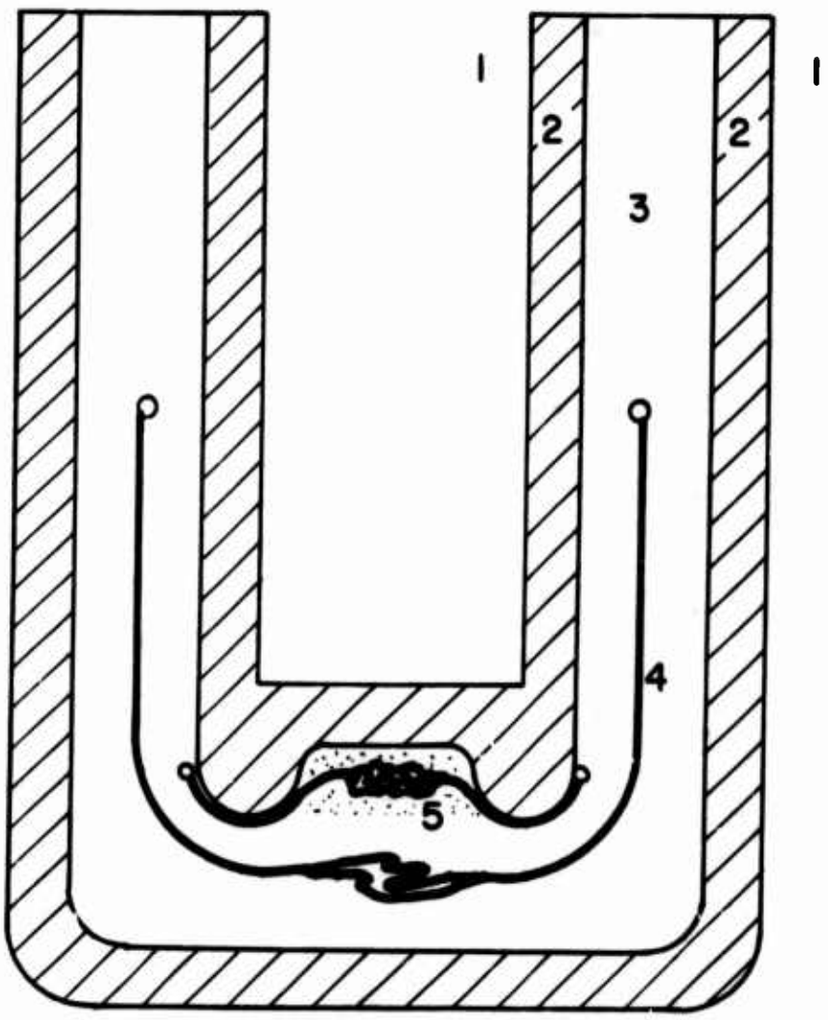

Fig. B-7 Schematic of Zero-Field Apparatus.

the basic idea. A series of flexible plastic bags laminated with thin lead foil are crumpled up, cooled and expanded, each inside the previous ones. As each bag expands, it forces flux out and produces a region of lower field inside. Finally, the last one can be cooled in a low enough field so that no quanta are trapped. Care must be taken in cooling to avoid the thermoelectric effects mentioned above and also trapping due to the fundamental thermal noise present in the shield just before it cools through the transition.

References

1. Foner, S., Rev. Sci. Instr. 30, 548 (1959).

2. A device similar to our modulator was used by A. L. Kwiram and B. S. Deaver, Jr., Phys. Rev. Letters 13, 189 (1964), to measure quantized flux. This device is a further development of theirs designed to operate efficiently as a modulator at higher frequency.

3. J. E. Mercereau, paper delivered at this Symposium. Note that Mercereau's magnetometer is not particularly sensitive to a field gradient.

4. Similar effects have been observed by others. See for example the paper delivered at this Symposium by A. F. Hildebrandt. We think that the effects observed by him can also be explained by thermoelectricity.

THE APPLICATION OF SUPERCONDUCTORS IN THE CONSTRUCTION OF HIGH-Q MICROWAVE CAVITIES*

M. S. McAshan
High Energy Physics Laboratory
Stanford University
Stanford, California

In the course of the developmental work for the superconducting accelerator at Stanford, we have been pursuing a study of the microwave properties of superconducting surfaces. This paper deals with the progress and present status of this work and describes some possibly useful applications of single superconducting microwave cavities.

The significant quantity describing the behavior of radiation incident upon a conducting surface is the surface impedance

$$Z_s = R_s + iX_s \ .$$

Here R_s is the surface resistance and X_s is the surface reactance.

This quantity is defined as the ratio of the tangential E and H fields at the surface, so that the Poynting vector normal to the surface is

$$\underset{\sim}{S} = \frac{c}{4\pi}(EXH^*) = \left(\frac{c}{4\pi}\right)^2 Z\,|H_{tan}|^2\hat{n} \ .$$

Thus the real part of Z, R_s, describes the power absorbed by the surface, and the imaginary part X_s describes the power density in the metal itself. This last is usually expressed as an effective skin depth

$$\delta = \frac{X_s c^2}{4\pi\omega} \ .$$

For superconductors at low frequencies $\hbar\omega \ll \epsilon$ the skin depth is approximately equal to the penetration depth λ.

*Work supported in part by the U. S. Office of Naval Research, Contract [Nonr 225(67)].

Our work has been with microwave cavities in which case the measured quantities are the unloaded Q of the cavity and its resonant frequency. These are related to the surface properties by

$$Q = G/R_s$$

$$\omega = \omega_o(1 - X_s/2G) \ .$$

Here G is a geometrical factor depending on the cavity shape, and ω_o is the resonant frequency calculated from Maxwell's equations assuming perfectly conducting walls.

In this way we have studied the surface resistance of tin and lead at 2.8 and 11.2 GHz, and the surface reactance of tin at 11.2 GHz. Measurements of this kind have, of course, been made before; however, the very high Q's of our cavities have permitted measurement of good accuracy over a sufficient range of values to permit careful comparisons with theory.

Considering first the results for surface resistance: We have assumed the form

$$R_s = R_{res} + AR_{theo.}$$

as the relation between the measured quantity R_s and the resistance calculated for an ideal superconductor. The parameters R_{res} and A have been included to account for non-ideal behavior. R_{res} one wishes to make as small as possible and can be taken as a figure of merit for a superconducting surface. A should be close to unity.

To illustrate the behavior of these terms, the first figure shows a set of data points, measurements of Q as a function of temperature. The residual Q of this cavity is about two billion. The rapid rise of Q with decreasing temperature is due in the BCS theory to the fact that for frequencies for which $\hbar\omega \ll \epsilon$, the surface resistance is roughly proportional to the number of electrons in the quasi-continuous excitation spectrum. Thus it is approximately exponential with temperature

$$R_s \approx e^{-\epsilon/2KT}$$

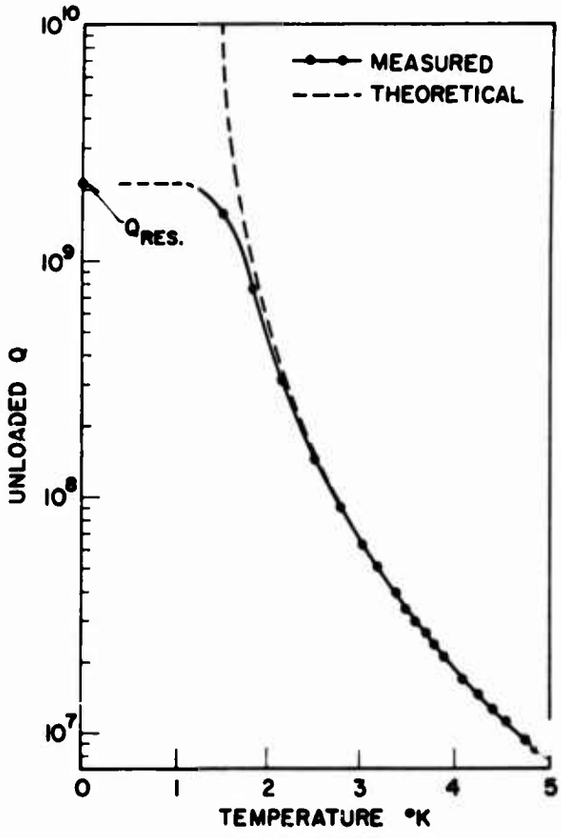

Fig. C-1

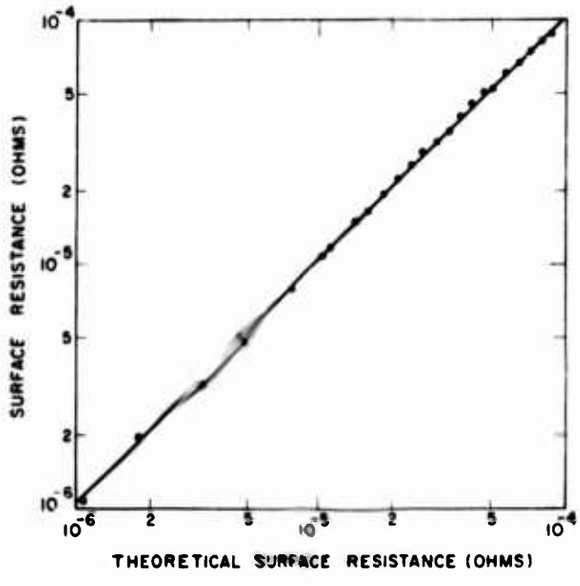

Fig. C-2 A Graph Showing the Experimental Surface Resistance Data and the Best Fit of the Experimental Data to the Mattis and Bardeen Theoretical Results for Lead at 11.2 GHz. The data are represented by the dots and the best fit is represented by the straight line.

For R_{theo} in the above expression we have tried three functions: the semi-empirical Pippard function, which is based on the two-fluid model and has a t^4-type dependence, the Mattis and Bardeen[1] calculation, and the Mattis and Bardeen calculation in the Pippard limit. This is the limit in which the coherence length and the electron mean free path are allowed to approach infinity. The Pippard function did not fit at all well, and indeed gave a negative value for R_{res}. The Mattis and Bardeen calculation fit very well at both frequencies and for both tin and lead. The Pippard limit fit reasonably well at low reduced temperatures except that the resulting values of A were high, about 5. When data at higher reduced temperatures were included, this expression did not fit well.

Figure 2 shows an example of the fit of the Mattis and Bardeen theory to the data for lead at 11.2 GHz. The fitting was done with R_s, A, and ϵ_o, the reduced energy gap at zero temperature, left as free parameters. The other parameters in R_{theo} were less critical, and no reasonable values were taken from the literature leaving A to take up the slack. The typical values of A derived were, however, quite close to 1, always being between 0.7 and 1.05.

Actually ϵ_o is known from other types of measurement, so ϵ_o is not really a free parameter as the quality of the fit can be judged by the resulting value of ϵ_o. The values of ϵ_o derived from the fitting at the two different frequencies agreed to within their estimated errors. For tin and lead these are

$$\epsilon_o = 3.58 \pm 0.02 \text{ for tin}$$

$$\epsilon_o = 4.08 \pm 0.03 \text{ for lead} \quad .$$

These are to be compared with

tin	lead	from
3.47 ± 0.07	4.26 ± 0.08	tunneling
3.6 ± 0.2	4.14 ± 0.1	infrared absorption

The value for tin seems to be in agreement. The value for lead may be a little low. Here one may be seeing a result of the stronger coupling in lead.

The Mattis and Bardeen calculations also agree very well with our surface reactance measurements. Because it is impossible to measure the cavity

dimensions accurately enough to determine ω_o sufficiently well, the absolute surface reactance could not be measured. Thus the expression

$$X_s = X_{so} + \Delta X$$

was used to fit the data. Here X_{so} is a parameter related to ω_o and ΔX is the measured relative surface reactance.

Figure 3 shows the results of such a fit. Here the surface reactance at zero temperature, which is determined from the calculation, has been subtracted out. From this fit it is possible to extrapolate the surface reactance to zero frequency and zero temperature and so to determine λ_o, the penetration depth at zero temperature. This value is for tin

$$\lambda_o = 5.55 \pm 0.02 \times 10^{-6} \text{ cm} .$$

This agrees with previously measured values, and so one can have confidence in the absolute surface reactances calculated from the Mattis and Bardeen theory.[2]

It seems to us that the temperature dependent part of the surface resistance and the surface reactance are well described by the Mattis and Bardeen theory and that we have a good understanding of these terms. The same cannot be said of the residual surface resistance however. There is a great deal of black magic in producing good superconducting surfaces, and our approach has been to make a series of cavities and test them and follow what patterns seem to emerge. Our efforts at the present time are concentrated in two areas.

The first is the study of niobium surfaces: We have tried both solid and plated TE_{011} cavities at X band with various surface preparation. The best residual Q values have been about 600 million for polished, solid cavities although some plated cavities have been nearly as good. Niobium is different from lead in that surface preparation has more effect on the residual Q. We are not far enough along in this work to have made good sense out of the results as yet. Measurements of the temperature dependence of the surface resistance, however, agree very well with values calculated from the Mattis and Bardeen theory using the published values of ϵ_o.

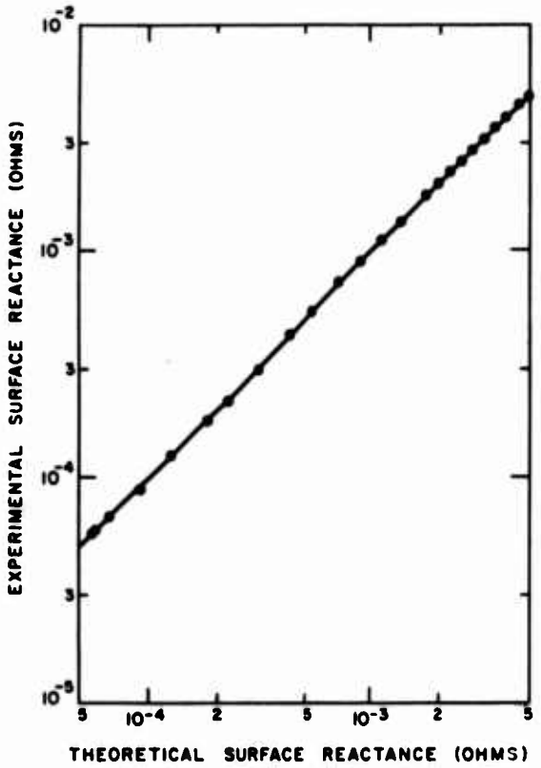

Fig. C-3 A Graph Showing the Experimental Surface Reactance Data and the Best Fit of the Experimental Data to the Mattis and Bardeen Theoretical Results for Tin at 11.2 GHz. The data are represented by the dots and the best fit is represented by the straight line. The surface reactance at $0^{o}K$ has been subtracted from the data shown in this figure.

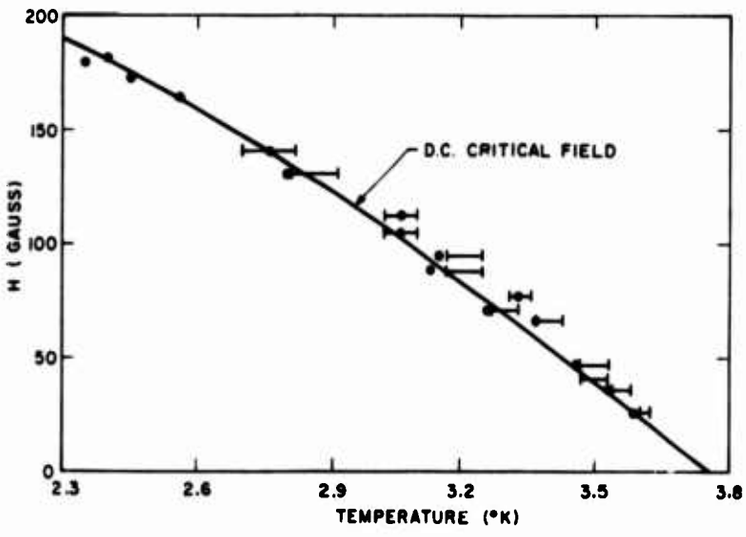

Fig. C-4 The AC Critical Field of Tin as a Function of Temperature. represents data for which the temperature is corrected from a measurement of the loaded Q and ⊢——⊣ represents data for which the temperature is corrected from a knowledge of the thermal properties and the power dissipation.

The second area of work is the continuing effort to improve lead surfaces. The residual Q of our lead cavities in the TE_{011} mode is subject to considerable seemingly random fluctuations between about 1 and 6 billion. We suspect that either differential thermal contraction between the lead and the substrate, or frozen-in flux lines from thermoelectric or Thomson currents induced during the cooling-down. These hypotheses are supported by the fact of very good residual Q values recently increased in a few cavities of lead plated or aluminum. Aluminum matches lead in thermal contraction better than copper, and in plating aluminum, a layer of bronze, presumably with a large electrical resistance, is first applied. This layer might lend to diminish the currents causing frozen-in flux.

To test these hypotheses we are planning measurements in solid lead cavities and building an apparatus to permit control over the cool down rate. Also Mr. John Pierce has been making measurements in an X-band cavity in which the first three TE_{01n} modes can be excited. This will give data on the frequency dependence of the residual resistance which should be valuable in assessing its origins.

Another property of superconductors at microwave frequencies that we have studied is the critical field. The most complete set of these measurements is for tin. These were made by placing a tin-plated endplate on a lead cavity (S-band) and observing the Q as a function of applied power. It remains essentially unchanged until at some power level breakdown of the superconducting state is observed. The magnetic field at the breakdown power is calculated from the measured Q value, and the temperature of the superconducting surface is estimated in two ways. Either the measured Q is used to give the temperature or the temperature is calculated from a knowledge of the heat input and the sample geometry.

Figure 4 shows breakdown fields plotted against temperature for tin. The solid line is the bulk dc critical field, and one can see that within the accuracy of the measurements there is agreement.

Actually it seems to us that rather than the bulk critical field, the superheating critical field should be observed for microwave frequencies. The

appearance of this higher critical field, however, is probably suppressed by the surface roughness of the plated sample.

[Note added in August 1967: In the last few months we have succeeded in attaining residual Q's as high as $\sim$ 18 billion in lead and $\sim$ 15 billion in niobium TE_{011} mode cavities at X-band. However, there is still no convincing experimental evidence that the residual losses can be attributed to trapped flux, or any other specific mechanism, for that matter.]

References

1. D. C. Mattis and J. Bardeen, Phys. Rev. 111, 412 (1958).

2. These measurements and their analyses were made principally by Mr. John Turneaure. He is at present preparing a paper which describes this work in greater detail.

THE MEASUREMENT OF SMALL VOLTAGES USING A QUANTUM INTERFERENCE DEVICE

J. Clarke
Cavendish Laboratory
Cambridge, England

The properties of Josephson tunnelling junctions[1] or more generally of weak-link devices are by now very well known. These weak-links are able to sustain a supercurrent up to a well-defined maximum known as the critical current. For values of current greater than this, a voltage appears and the voltage-current relationship becomes essentially a resistive one.

For our present purpose, we are concerned with the properties of two such junctions connected in parallel in an otherwise superconducting ring. This system was first studied experimentally by Jaklevic et al.[2] They showed that the critical current of the double junction was an oscillatory function of a magnetic field applied at right angles to the ring. The period was one flux quantum (ϕ_o) that is, about 2×10^{-7} gauss cm^2.

This property enables us to make a very simple digital voltmeter. Consider the configuration of Figure 1. We have two weak-links or tunnelling barriers connected in parallel in a superconducting ring. A current, i, passed through the junctions, develops a voltage, v, across them which is used to determine the critical current in some way. An external primary coil, of inductance L_o, is tightly coupled to the double junction and has in series with it a resistance R_o and a stray inductance L_s. The current in the primary required to create one flux quantum in the double junction and thus one oscillation in critical current is $I_o = \phi_o/L_o$ and the voltage sensitivity thus

$$V_o = I_o R_o = \phi_o R_o/L_o. \qquad (1)$$

The effective inductance of the circuit is $L_s + \alpha L_o$, where α is a coefficient of the order of unity which allows for the possible modification

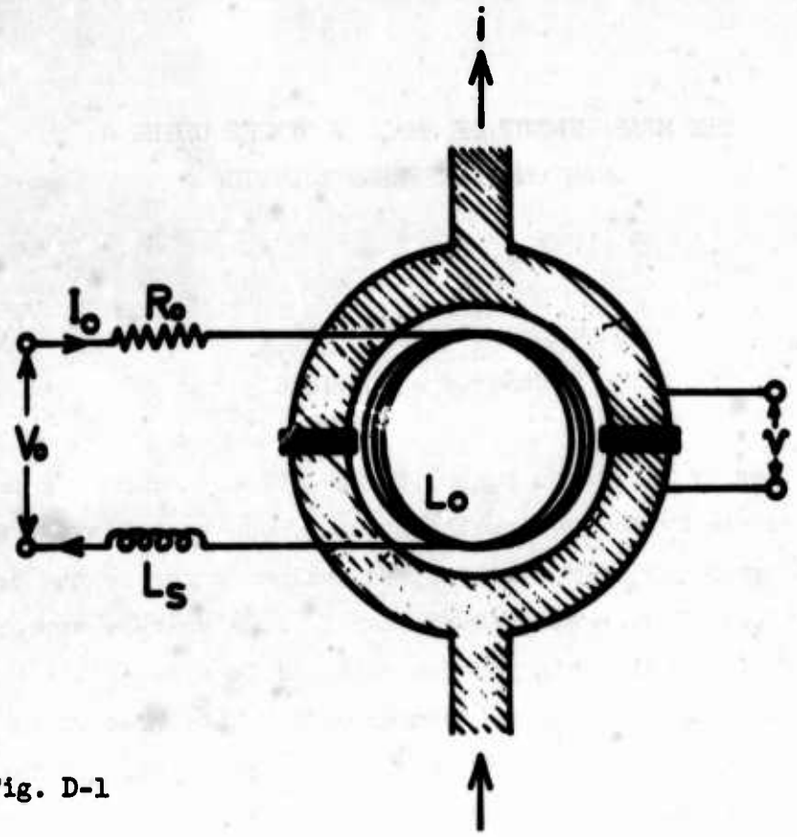

Fig. D-1

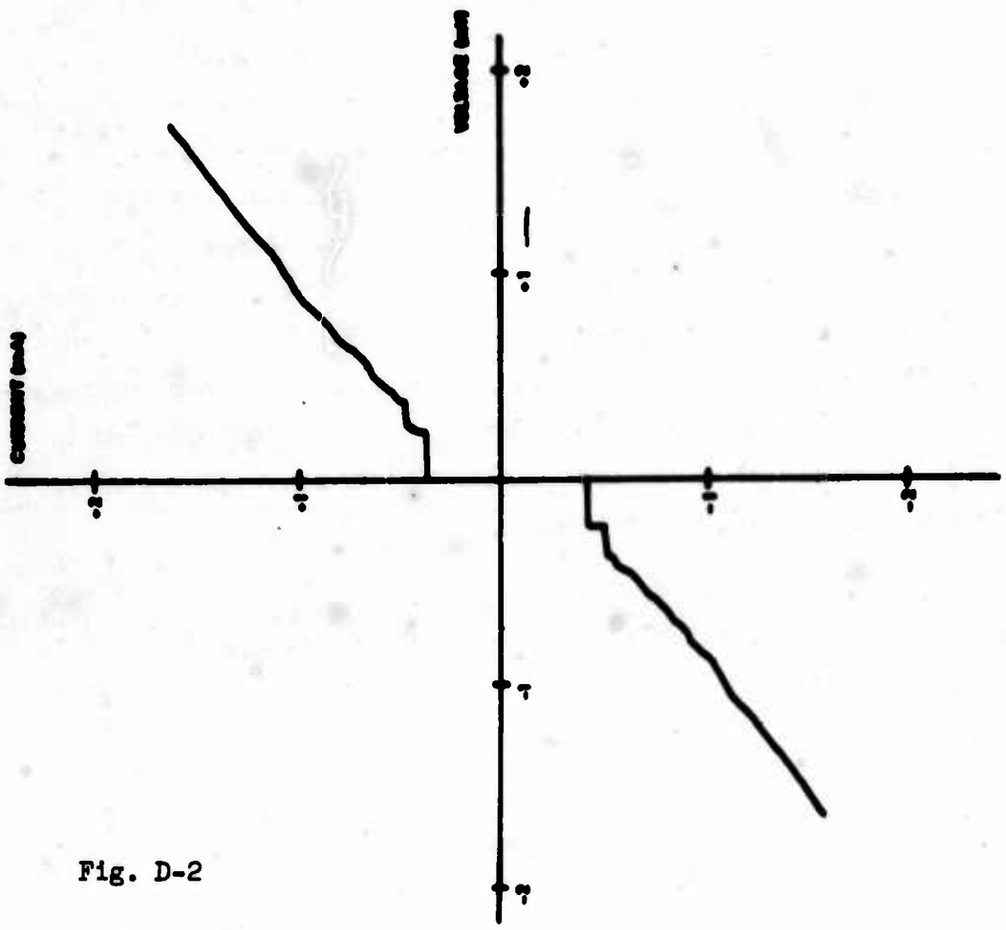

Fig. D-2

of the effective inductance by the presence of the double junction.[3] If for the time being we ignore the stray inductance and take $\alpha = 1$, we see that

$$V_o = \phi_o/\tau, \qquad (2)$$

where $\tau = L_o/R_o$ is the time-constant of the system. If we take $\tau = 1$ second, then the digital voltage sensitivity of the system is 2×10^{-15} volts. However, if we could detect a small fraction of an oscillation in critical current, we should be able to measure an even smaller voltage. For example, if we could detect 1/2% of one oscillation, the voltage sensitivity would be 10^{-17} volts, although of course the measurement would no longer be digitized.

I should now like to discuss the practical application of this principle. It has proved possible to make very reliable weak-link or tunnelling devices by simply enclosing a length of bare niobium wire in a blob of tin-lead solder. Tunnelling is supposed to occur between the wire and the solder through the oxide barrier; the solder does <u>not</u> alloy with the niobium but makes a tight mechanical contact around the wire. Two additional leads connected to the solder enable the resistance between wire and solder to be determined in a four-terminal arrangement. It was found that specimens with a room temperature resistance of the order of one ohm invariably displayed tunnelling characteristics at liquid helium temperatures, the critical current being typically 1 mA. A typical i-v characteristic obtained using a current source is shown in Figure 2; the steps on the resistive part are due to the Josephson A.C. effect which gives rise to resonances within the junctions. The fact that the slope at higher voltages extrapolates to a finite current at zero voltage suggests that the specimen is not simply a superconductor-oxide-superconductor tunnelling junction; however, the exact nature of the junction is of no great importance for the present purpose. These specimens also have the considerable advantage of not deteriorating under repeated thermal cycling, so that they can be used indefinitely.

The device is familiarly known at a "SLUG" or "Superconducting Low-inductance Undulating Galvanometer".

It is not yet clear what the Slug has to do with the principle which I discussed earlier. One would expect, of course, that a junction made in this way would have a more or less continuous oxide barrier, that is, it would be a single junction. In fact, this is very far from being the case, as the following experiment demonstrated. The junction characteristics were monitored continuously on an oscilloscope using a 50 c/s sweep current. It was found that the critical current was an oscillatory function of an additional direct current passed along the niobium wire. The period was typically a few hundreds of microamps but varied considerably from specimen to specimen. It appears that the Slug behaves in some way as a double junction and although the exact mechanism is not clear, it is possible to see roughly how the oscillations occur.

Figure 3 shows schematically a longitudinal section through the device. Let us suppose for the moment that there is a junction between wire and solder at each of two points (A, B) near the ends of the solder blob but not elsewhere. A current I flowing along the niobium wire generates a magnetic field 2I/r (r being the radius of the wire) in the penetration layers of both superconductors, that is, within the dotted lines of the sketch. The configuration of the section is thus similar to that of the double junction we considered earlier, except in that the magnetic field is generated by a current flowing along one of the superconductors rather than being applied externally. The area threaded by the field is $\ell(\lambda_{Nb} + \lambda_s)$, ℓ being the length of the blob and λ_{Nb} and λ_s the penetration depths of the niobium and solder respectively. Thus the change in current flowing along the wire required to produce one oscillation in critical current is

$$\Delta I \approx \frac{\phi_o r}{2\ell(\lambda_s + \lambda_{Nb})} \qquad (3)$$

Taking $r = 5 \times 10^{-3}$ cm, $\ell = 0.5$ cm and $(\lambda_s + \lambda_{Nb}) = 2000$ Å gives $\Delta I \approx$ 500μA.

There is of course no obvious reason why the junctions should occur only at the ends of the blob. I feel the most likely explanation is that

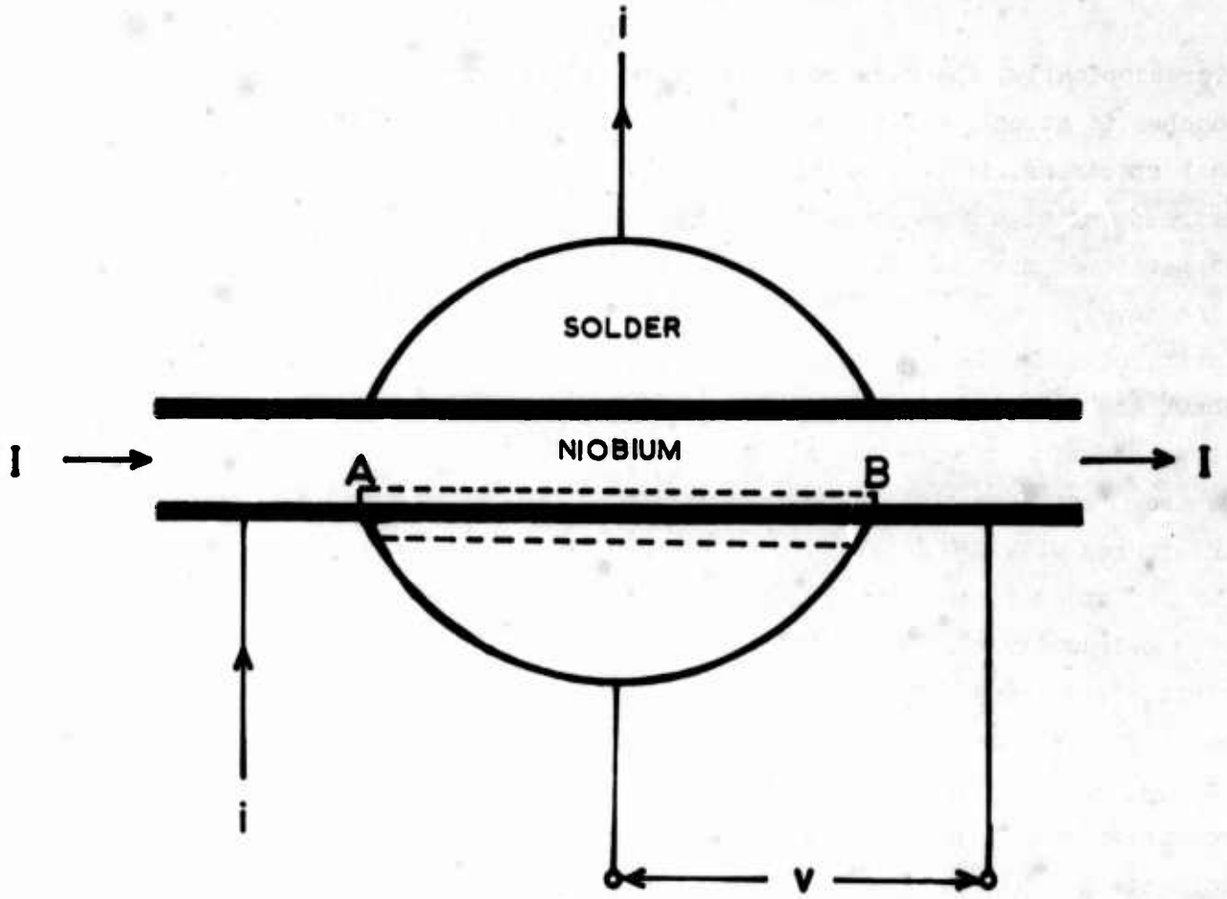

Fig. D-3

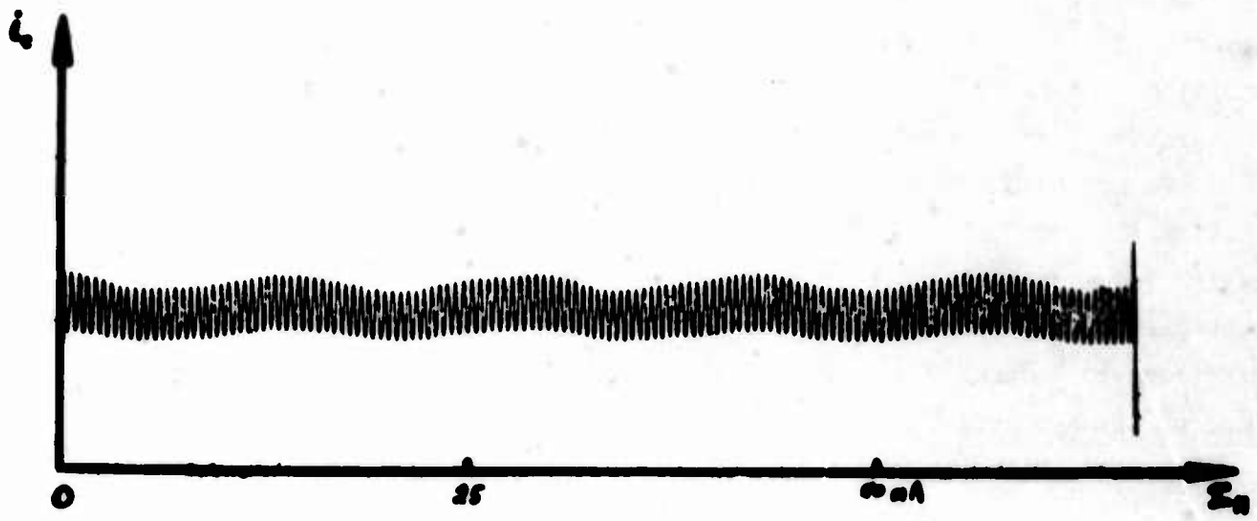

Fig. D-4

microscopically, the surface of the wire is very rough, so that the solder touches it at only a few discrete points at which tunnelling occurs. In most specimens, it is possible to observe several thousand oscillations without any sign of a diminution in their amplitude. This means that the contact area must be very small, otherwise we should expect to see a Fraunhoper-like envelope due to the effect of the magnetic field on the individual junctions. However, quite often there are more than two contacts. Figure 4 shows the variation in critical current (i_c) with the current (I) flowing along the niobium wire for a typical Slug. Two of the contacts give rise to the "fast" oscillations with a period of about 500μA and a third junction interferes with one of the others to produce the "slow" period.

In order to use the Slug as a practical instrument, one needs a method of continuously monitoring the critical current. A sinusoidal current sweep confined to the positive half of the characteristic is applied to the junction. Below the critical current no voltage is developed; at the critical value, a voltage suddenly appears and for higher currents there is an essentially resistive behaviour. As the current is reduced, the voltage jumps back to zero again. By squaring up these pulses electronically we obtain a square-wave output whose mark-space ratio is a function of the critical current, so that by measuring the mean voltage of the square-wave we can determine the critical current. In practice, it is very easy to detect a change of 1μA in the current flowing along the niobium wire, provided that the junction is biased (by another current along the niobium wire) at the point where the critical current has its mean value, that is, di_c/dI is a maximum. An alternative way of measuring i_c has recently been described by McWane et al.[4]

We now have a device with the following properties: a current sensitivity of about 1μA; a resistance which is zero; and a circuit inductance which is essentially that of the piece of niobium wire, say 10nH. To make the galvanometer into a voltmeter, we connect in series a resistance (R_o) of (say) 10^{-8} ohms. The sensitivity of the voltmeter, is then 10^{-14} volts and the time-constant (L_s/R_o) about 1 second. Notice that this is down by a factor of about 10^3 on the figure mentioned earlier. This is because the

inductance L_o is just the very small inductance between the wire and solder; the stray inductance, L_s, is very much greater and dominates the effective inductance of the circuit.

The voltmeter has invariably been used as a null-reading instrument: a current is fed into the standard resistor (R_o) so as to maintain the current flowing through the Slug at its zero value. A servomechanism has been developed to atuomatically balance the circuit by feeding an appropriate current into R_o; this not only facilitates the taking of readings but also substantially reduces the effective time-constant of the circuit.

There is one point about the use of the Slug as a voltmeter that I should like to emphasize and that is the fact that it behaves essentially as an impedance converter. A change of 1μA in the primary circuit, whose resistance is 10^{-8} ohms, gives rise to a comparable change in the critical current in an impedance of about 1 ohm. We have thus achieved a power gain of about 10^8.

I should now like to discuss the possible sources of noise which limit the sensitivity of the voltmeter:

(1) Short and long-term drifts in the various biases and detecting signals applied to the Slug. These can be made negligible by careful electronic design.

(2) Noise referred to the input of the amplifier into which is fed the voltage produced by the Slug. This can be eliminated with the aid of standard low-noise techniques.

(3) Temperature fluctuations in the helium bath above the λ-point which give rise to noise in two ways:

   (i) fluctuations in the critical current which is temperature-dependent in this region;

   (ii) voltages generated in the circuit resistances by the Thomson effect.

   Both of these effects are important above the λ-point but seem to disappear below it, where presumably the fluctuations in the bath temperature are much smaller.

(4) E.M.F.'s introduced into the low-temperature circuit from sources external to the cryostat. These effects have been minimized by enclosing the circuit itself in a superconducting lead can and by screening the cryostat leads; nevertheless, it appears that extraneous noise governs the detection limit of the present system.

(5) Johnson noise generated in the standard resistor, which is given by:

$$\overline{V_N^2} = \frac{kTR_o}{\tau} . \qquad (4)$$

Taking $T = 2^{o}K$, $R_o = 10^{-8}$ ohms and $\tau = 1$ second, the r.m.s. noise is about 5×10^{-16} volts. This figure is an order of magnitude below the detection limit and therefore unlikely to be a limiting factor.

(6) Fluctuations in the critical current of the junctions: this subject is discussed in detail by Professor Scalapino in a later paper but the voltages involved seem likely to be much smaller than the other noise levels.

I have recently made attempts to reduce the noise level of the system with the aid of a superconducting transformer, which produces current gain within the superconducting can. The principle of this is quite simple. The niobium wire on which the Slug has been made is bent into a circle and the ends welded together so as to form a superconducting ring. An applied magnetic field generates a circulating current which may be measured by the Slug: in fact the field sensitivity is quite good, about 10^{-7} gauss. Figure 5 shows the principle of the transformer: a superconducting primary coil of N turns in series with a resistance R and an inductance L_s is coupled to the superconducting ring and the voltage to be measured applied to the terminals. Now if the primary coil is ideally coupled, it will not contribute to the inductance of the circuit: the flux in the superconducting secondary cannot change and consequently neither can that in the primary. In this case we have achieved a voltage sensitivity N times better than with the Slug alone, with more or less the same time-constant, L_s/R.

TRANSFORMER

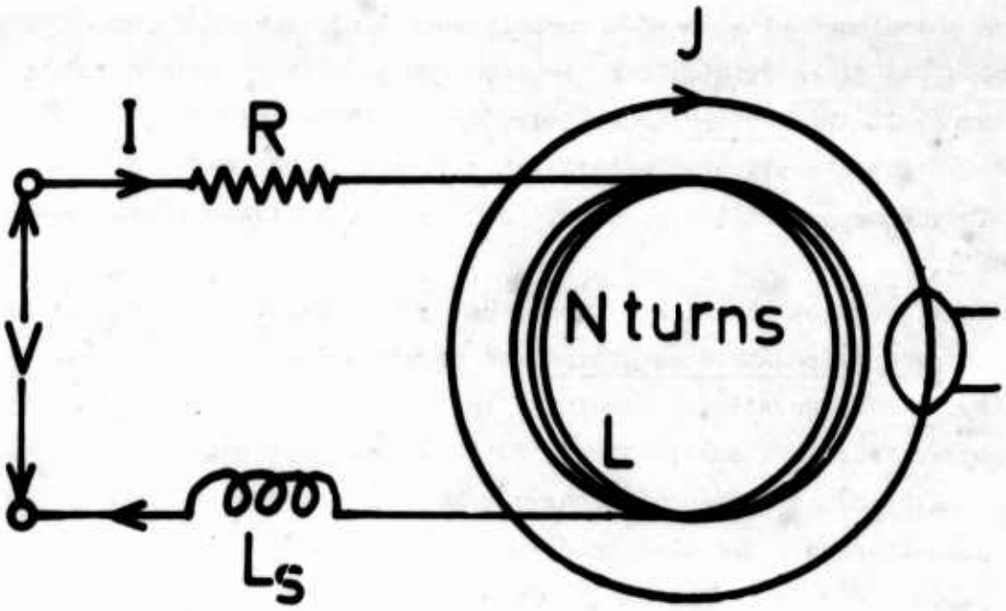

Fig. D-5

AMPLIFIER

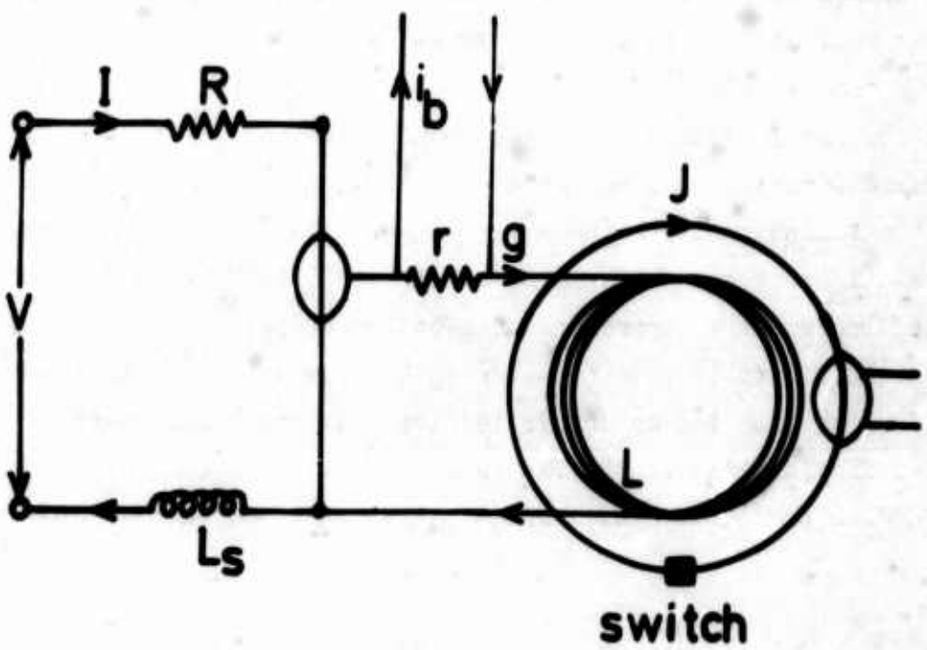

Fig. D-6

Unfortunately, it is not possible in practice to couple the coil ideally, even with the aid of an iron core. Thus there is always a stray inductance associated with the N-turn coil which increases the time-constant appreciably, and it is difficult to achieve any worthwhile gain from the system. However, the current sensitivity may be increased almost indefinitely with the aid of the coil; this is extremely useful when the ultimate in voltage sensitivity is not required but a higher input impedance is desirable.

The configuration just described opens up the possibility of using a second Slug as an impedance transformer to obtain a far higher voltage sensitivity. To discuss this principle, let us turn back for a moment to the i-v characteristic shown in Figure 2. The important point to realize is that when the critical current is changed, the current flowing at small voltages also changes. The Slug is driven from a steady voltage source (i.e. of impedance $r \ll 1$ ohm) which biases the Slug on to a portion of the characteristic where di/dv is low. If we change the current flowing in the niobium wire, the critical current and hence the current flowing through the voltage source will change by a comparable amount, but in a circuit whose resistance is of the order of 1 ohm. We can thus use a second Slug to match a low-impedance circuit (say 10^{-8} ohms) to a high-gain superconducting transformer without introducing a long time-constant.

A practical circuit is shown in Figure 6. The first circuit is just the usual voltmeter circuit, with $R = 10^{-8}$ ohms, say, and $\tau \approx 1$ second. The N turn-coil of inductance L is superconducting and the resistance r is small compared with the Slug resistance (r_s), say 10^{-1} ohms. The system is set up in the following way: the superconducting switch in the final loop is opened and i_b increased from zero; for $i_b < i_c$, the current flows through the Slug and the superconducting coil. At $i_b = i_c$, the system is unstable but stability is obtained when i_b becomes sufficiently large to drive the Slug on to a region of finite slope, a substantial part of the current then flowing through r. The superconducting switch may now be closed: it was opened to prevent the build up of large currents in the superconducting loop.

A voltage V applied to the input terminals produces a current $I = V/R$ in the niobium wire of the Slug. The current g produced in the N-turn coil is of comparable value and gives rise to a current $j \approx N_g \approx NI$ in the superconducting loop, which is measured in the usual way. The time-constant of the transformer is rather less than $L/(r + r_s)$, so that L may be of the order of a few Henries before the time-constant becomes inconveniently large. A servomechanism may also be added to this system.

The system has been tried experimentally with $R = 10^{-8}$ ohms, $r = 10^{-1}$ ohms and $N = 10^3$, so that the theoretical ultimate sensitivity was about 10^{-17} volts. This of course is much less than the thermal noise developed in R; in fact the noise level at $2^{\circ}K$ was less than 10^{-15} volts, that is, the sensitivity was apparently limited by thermal fluctuations.

It would appear that this represents the ultimate voltage sensitivity which may be achieved with a Slug at He^4 temperatures, although it may be possible to utilize the available sensitivity more fully by going to temperatures attainable in a dilution refrigerator or adiabatic demagnetization cryostat. However, it would certainly be necessary to take the most stringent precautions against external noise: probably one would need to work in a completely shielded room.

I should like to conclude on a highly speculative note. We could replace the input circuit of the amplifier with a superconducting loop so as to make a magnetometer with a sensitivity of about 10^{-10} gauss. In principle, it should be possible to add another amplifying stage to this loop to achieve an overall sensitivity of about 10^{-13} gauss.

DISCUSSION

Chilton (S.R.I) asked why the double junction characteristics could not follow from the Meissner effect in the junction which would screen out the current from the interior of the Slug.

Clarke replied that the dependence of the critical current upon applied magnetic field in a self-field limited tunnelling junction was not

an interference-type pattern. At low fields, the relationship was essentially a linear one; above the H_{c_1} of the junction (of the order of 1 gauss, corresponding to a few tens of milliamps in the niobium wire) the flux would completely penetrate the junctions and a Fraunhofer-type pattern would result. In any case, the penetration layers at each end of the junction would be typically of the order of 1 mm, far larger than the size necessary to give the double junction characteristic with no diffraction pattern.

REFERENCES

1 Josephson, B. D., 1962, Phys. Letters, 1, 251;
1964, Rev. Mod. Phys., 36, 216;
1965, Adv. Phys., 14, 419.

2 Jaklevic, R. C., Lambe, J., Silver, A. H. and Mercereau, J. E.,
1964, Phys. Rev. Letters, 12, 159.

3 Clarke, J., 1966, Phil. Mag., 13, 115.

4 McWane, J. W., Neighbor, J. E. and Newbower, R. S.,
1966, Rev. Sci. Instru., 37, 1602.

A SUPERCONDUCTING GRAVIMETER*

W. M. Prothero, Jr. and J. M. Goodkind
University of California
San Diego, at La Jolla, California

Among the many possible uses of superconductors and liquid helium, their application to research on gravity has been most fascinating to us. The gravity meter which we herein describe will have immediate applications in geophysics and we hope to apply the techniques which we have developed to investigations of properties of the gravitational field. The geophysical applications follow from the high stability of persistent currents in superconductors. The drift rate in existing gravimeters (of order 10^{-8} g's per day) makes observations of slow variations in the earth's gravitational force impossible. Our device supports a test mass with a magnetic field generated by persistent current magnets which are, in principle, perfectly stable. In practice we anticipate a stability of about 10^{-12} g's and our first objective is to record the two week component of the earth tides which should be about 10^{-9} g's.

The principle of the device is to levitate a superconducting ball over a persistent current magnet. The field geometry is arranged so that the force gradient on the ball in the vertical direction is small. Then, its position in that direction is monitored very accurately. The ball is a hollow aluminum shell, one-inch diameter, with .04 inch wall thickness and has a .001 inch thick layer of lead on its outside. It weighs 4.5 grams.

The small force gradient is produced by using a pair of coils, as shown in Fig. 1, with the ball floating just above the plane of the upper coil.

---

*Work supported by the National Science Foundation.

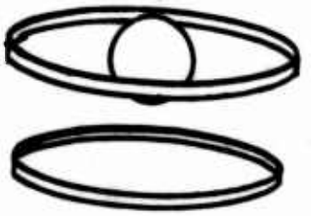

Fig. E-1

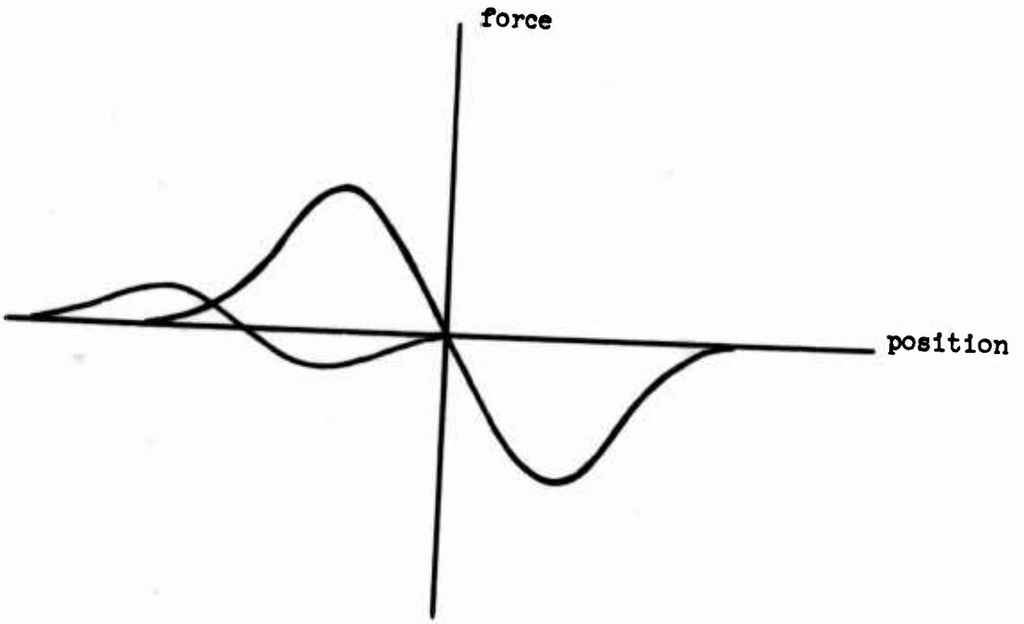

Fig. E-2

Qualitatively, the effectiveness of this scheme for producing a small force gradient can be seen from the plot in Fig. 2. The larger curve is the force from the field of the lower coil and the smaller one is the force from a much smaller field in the upper coil. The net force from the two coils is then roughly the sum of the two. Thus, by adjusting the ratio of the currents in the two coils a region of essentially zero slope can be produced. With appropriate feedback arrangements we have arranged the controls so that one knob adjusts the ratio of the currents in the two coils. Figure 3 is a plot of the force as a function of position measured for various current ratios. In practice, the smallest force gradient which we have used is of the order of 60 dyne/cm. This corresponds to a resonant frequency of 6/10 cycles/sec.

In a practical device it is not desirable to simply produce the smallest possible force gradient. Rather, there is an optimum which is dictated by the thermal driving forces which result from the damping. The force gradient should be chosen in such a way that the thermal forces will produce a "noise" signal approximately equal to the noise generated in the rest of the system (e.g., in the electronic amplifier). If the gradient is chosen larger than this the device will be less sensitive. If it is chosen smaller than this, no improvement in signal to noise will be obtained but the device will be more easily overdriven by large disturbances. In fact, if the gradient were small enough, the thermal forces themselves could overdrive the device and make it totally useless. At present, in our instrument these forces amount to 10^{-11} g's for a 1/40 cycle band width and correspond to a .05 Angstrom displacement of the ball in a gradient of 100 dynes/cm.

Two different detection schemes are currently in use, one magnetic, the other electrostatic. The first uses a superconducting transformer and flux detector, Fig. 4, to measure the changes in the flux pattern caused by the motion of the ball. If the ball moves, it will alter the flux pattern in the left hand side of the transformer and therefore force a current to flow. The resulting field in the right hand side of the transformer is then measured with a flux detector. Until recently we have been using a detector invented by Bascom Deaver. It is a solid tin wire inside of a pick up coil. The wire is thermally switched between normal and superconducting state so that any

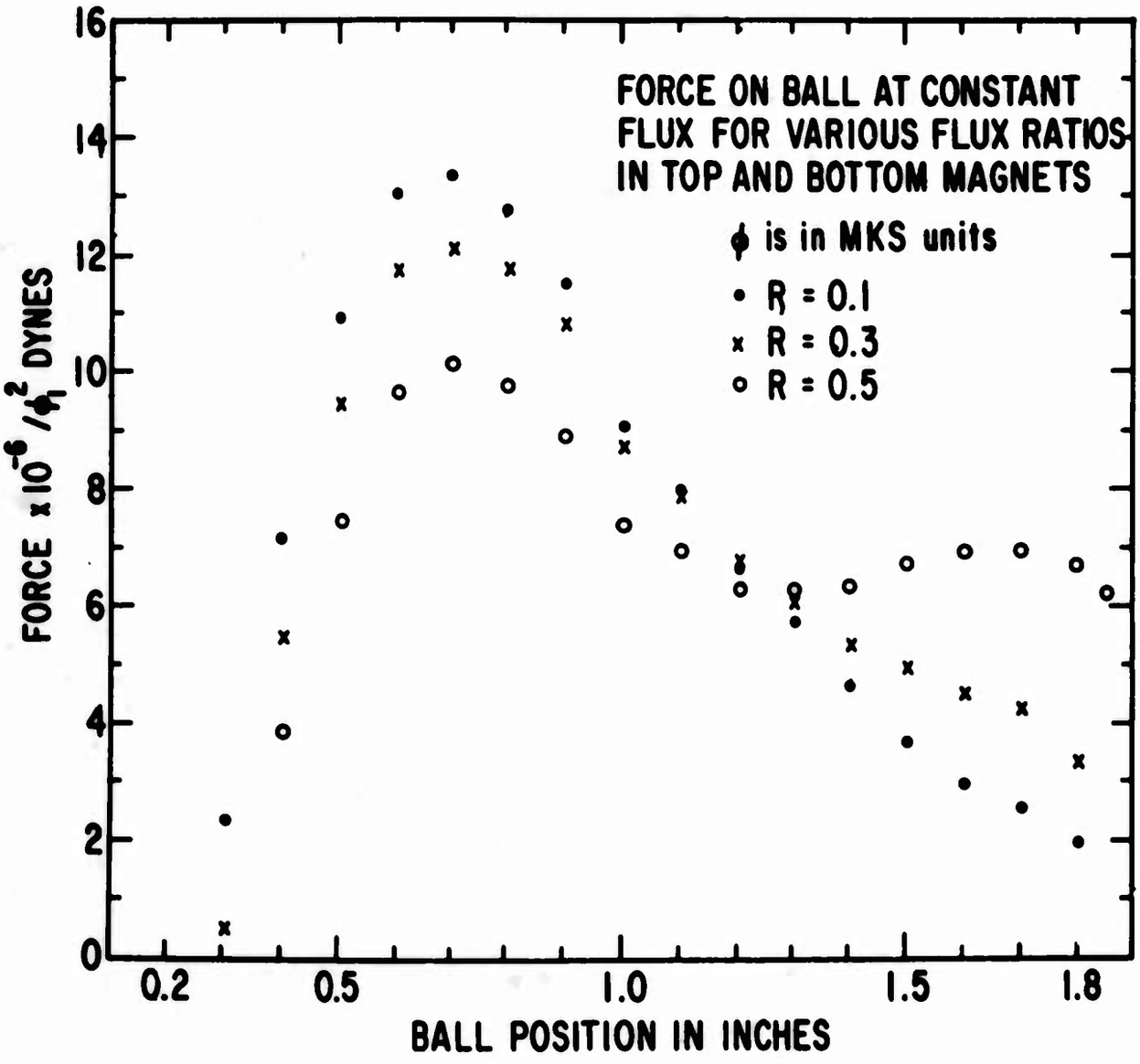
FORCE ON BALL AT CONSTANT
FLUX FOR VARIOUS FLUX RATIOS
IN TOP AND BOTTOM MAGNETS
ϕ is in MKS units
• R = 0.1
× R = 0.3
○ R = 0.5
FORCE x 10⁻⁶ /ϕ₁² DYNES
BALL POSITION IN INCHES
0
2
4
6
8
10
12
14
16
0.2
0.5
1.0
1.5
1.8

Fig. E-3

flux which is present is pushed in and out of the coil. This produces a voltage which is proportional to the flux threading the wire in its normal state. With this detector we are able to see a displacement of the ball corresponding to about 10^{-9} g's. Presently we are using an exciting new device developed by the people at the Ford Laboratories. The basic sensitivity of the device as we are using it is 2×10^{-4} flux quanta when used with a filter of .1 second time constant on the output of the phase sensitive amplifier. This is between 10^3 and 10^4 times more sensitive than the solid wire detector.

The electrostatic detection scheme uses a capacitance bridge arranged as shown in Fig. 5. When the ball is centered, the capacitance between the ring and each end plate is the same so that no voltage is observed. If the ball moves off of center a voltage is observed with a phase which depends on the direction of displacement. The geometry of our present apparatus leads to a sensitivity of 0.5 Å displacement for a one-fortieth cycle bandwidth. Although this sensitivity can be improved by a number of means, it is adequate at present. If the force gradient is reduced an order of magnitude to 10 dynes/cm, the thermal displacements will then be 0.5 A^{o}, i.e., equal to the noise in the capacitance bridge. Thus the sensitivity and stability of the device will not be affected by either detection scheme.

The final instrumental feature which I wish to discuss is the feedback and readout systems. Any system which can be operated as a null device with negative feedback will, as a consequence, offer improved linearity, range of operation, and stability. In this case we apply negative feedback directly to the ball through electrostatic forces from the same capacity plates described above. Direct current voltages are used as shown in Fig. 6. With equal and opposite voltages on each of the end plates and the ball in the center, no force is exerted on it. A voltage of appropriate sign applied to the center ring will exert a force in the direction desired. Furthermore, the force will be directly proportional to the voltage so that the feedback voltage is the readout for the instrument. Currently, the best digital voltmeters can approach an accuracy of a part in 10^6 so that ultimately

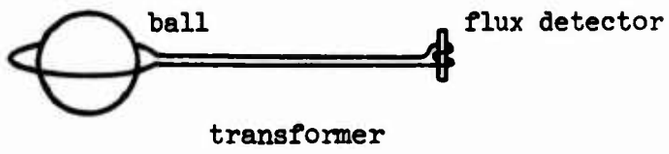

Fig. E-4

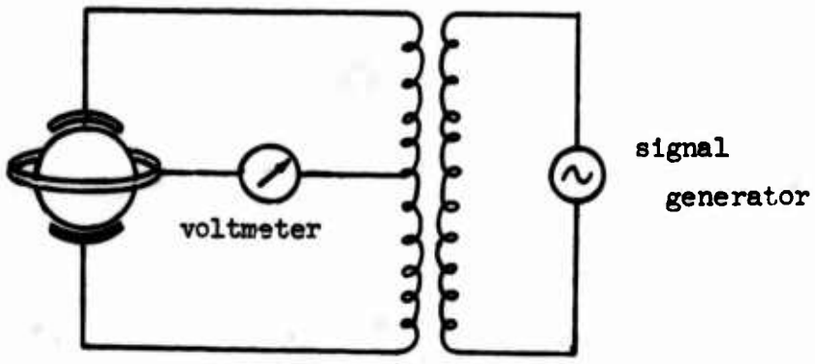

Fig. E-5

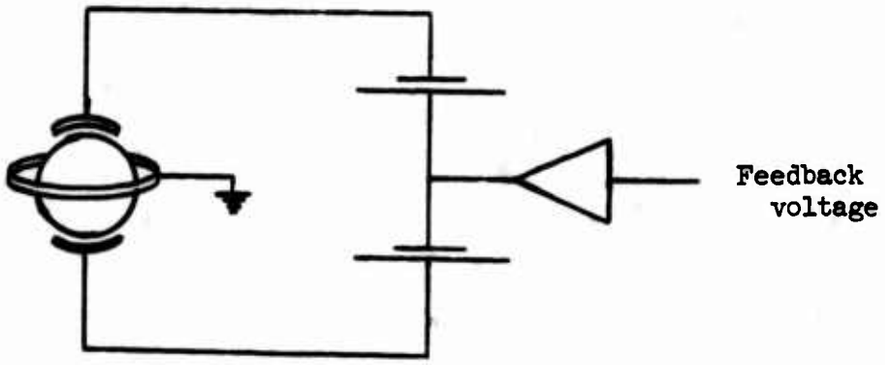

Fig. E-6

we expect this to be the dynamic range of the gravimeter. Thus, without filtering the dominant microseisms which are of the order of 10^{-6} g's we should be able to measure a disturbance of 10^{-12} g's. In order for this to be true the device must have sufficient dynamic range that the large disturbances do not drive it into a non-linear region when the gain is sufficient to observe the smallest disturbances. The data which we present will indicate that the device does indeed have this capability.

I would like now to tell you about some of the problems that we have dealt with thus far. The question of the stability of the field from persistent current magnets was, of course, a major concern from the start. Thus, we have used the flux detector with a sensitivity corresponding to 10^{-9} g's to measure the field stability. In particular, we expected difficulties from the flux creep phenomenon. Our expectations seemed to be borne out by the results shown in Fig. 7. This was the field measured as a function of time in a pair of Niobium Zirconium coils. It shows the dependence on the logarithm of the time which is expected for flux creep. Regardless of whether it was truly flux creep or not, the effect reproduced itself when the coils were rewound but disappeared when we used pure Niobium wire for the coils. The field generated by the coils is below H_{c2} for Niobium.

Another source of field instability was temperature dependent susceptibilities of the materials used to construct the device. The apparatus is currently made entirely of aluminum and quartz and some o.f.h.c. copper. With these conditions we are now unable to measure any variation of the magnetic field with temperature.

The variations in the earth's magnetic field must be shielded in order to achieve the stability we seek. In order to do so a μ metal shield is placed around the dewar. Then a lead plated shield in the liquid helium bath surrounds the entire apparatus. We have had recurring problems with such shielding with a temperature dependence and with an apparent increase in the static field inside of the shield at low temperatures. At one point it appeared as if the field increase remained when the lead was heated above its transition temperature. Whatever the cause of the effect, it could also be responsible for

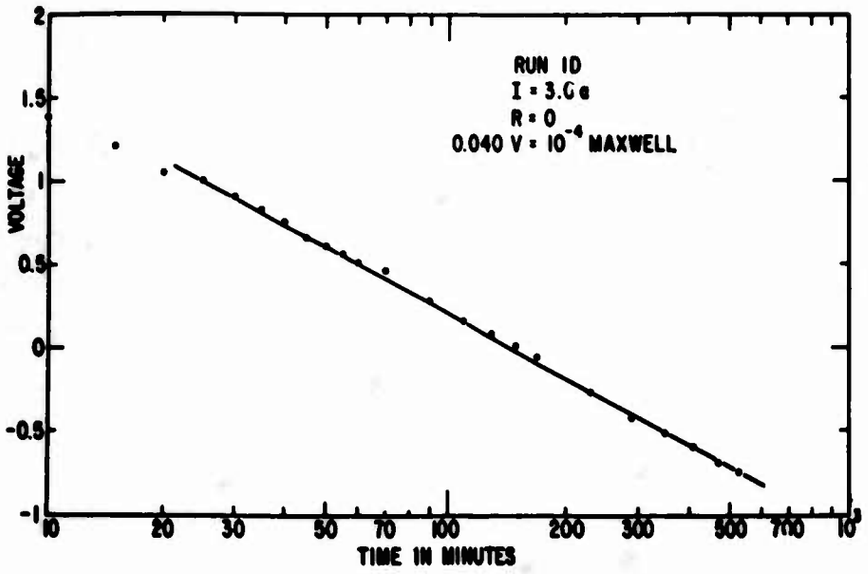

Fig. E-7

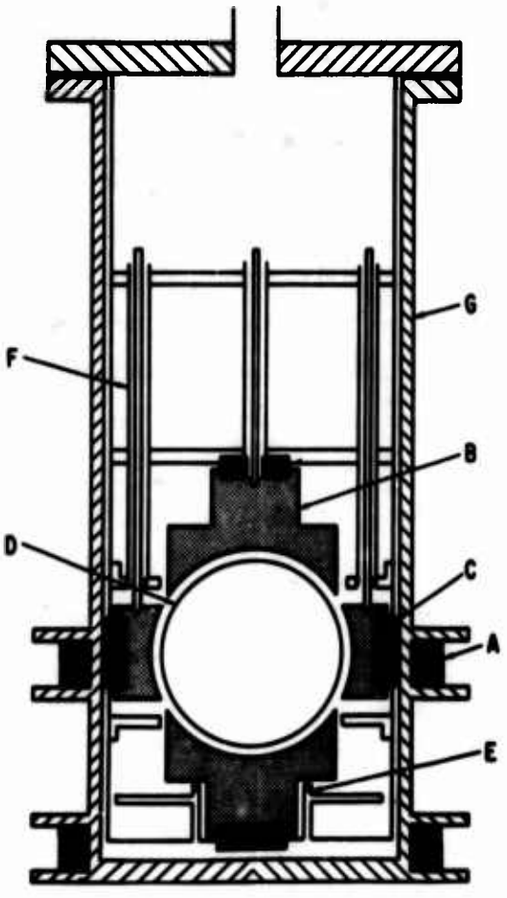

Fig. E-8 A-support coil; B-capacitor plate; C-quartz insulator; D-ball; E-notch for flux detector transformer; F-coaxial cable for capacitor; G-vacuum can.

the flux trapping that the Stanford group considers to be the limitation on the Q of their cavities. In any case, I think a warning against simply assuming that lead plated on copper is a good shield, is in order. In the cases where we have achieved good shielding the overall field stability was better than the sensitivity of the flux detector (about 1 part in 10^8 in this case).

There are many possible sources of spurious signals in addition to field variations. I will simply list those which we have considered and state that all of them have been shown to be insignificant at our present level of sensitivity and will not appreciably affect measurements at the 10^{-12} g level.

A change of the penetration depth of lead with temperature will change the apparent size of the ball and therefore change the supporting force.

A small amount of He gas must be left in the vacuum chamber to keep the ball from heating up (we use 100μ). The bouyant force of this small amount of gas will change with temperature as its density changes.

If the ball collects a net charge it will experience a force from the feedback voltage on the capacitor plates.

Thermal emf's in the feedback circuit can generate a net force on the ball.

Gas desorbtion from the ball can change its mass.

Finally, I would like to show you a diagram of the apparatus and some data showing the earth tides, which was obtained with this device.

Figure 8 is a schematic diagram of the apparatus.

Figures 9, 10 and 11 are data taken with the flux detector as the position sensing device and with no feedback on the ball. The solid lines are earth tides as calculated from the position of the sun and moon. In every case you will see that the phase is correct, but there is some question about the amplitude (i.e., calibration). There are several lessons to be learned from this data. First of all, it does demonstrate a high degree of linearity in the device even without feedback. The earth tides of order 10^{-8} g's are observable in the presence of higher frequency variations of order 10^{-6} g's and greater.

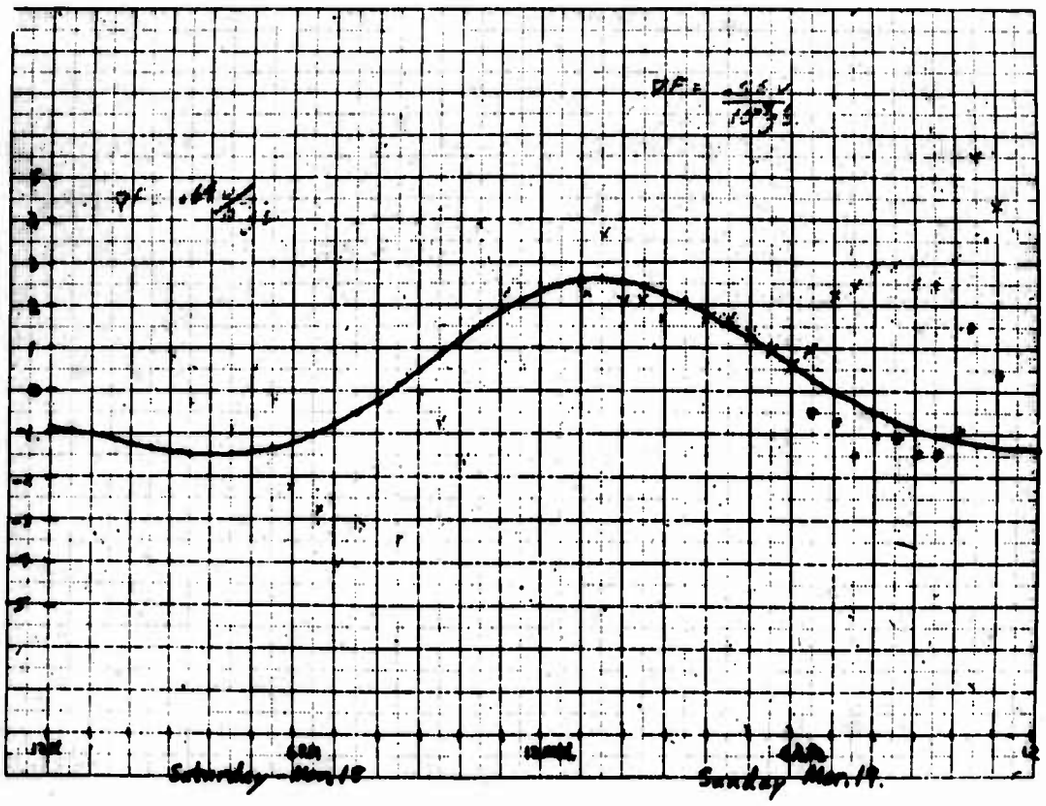

Fig. E-9

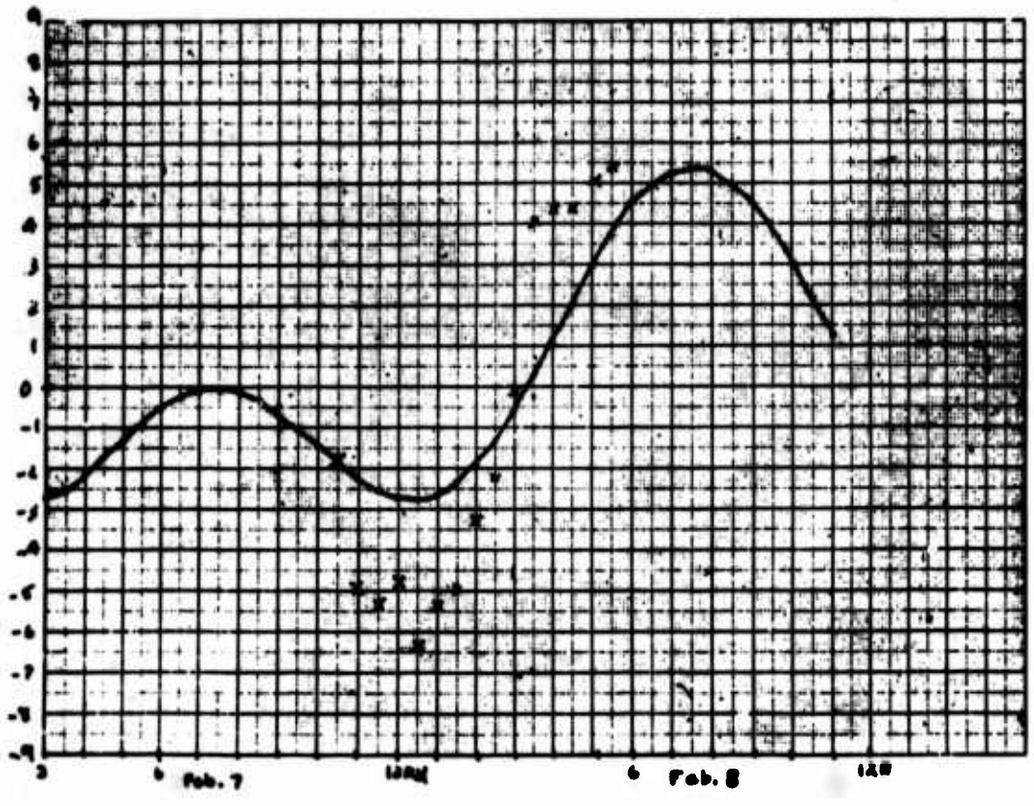

Fig. E-10

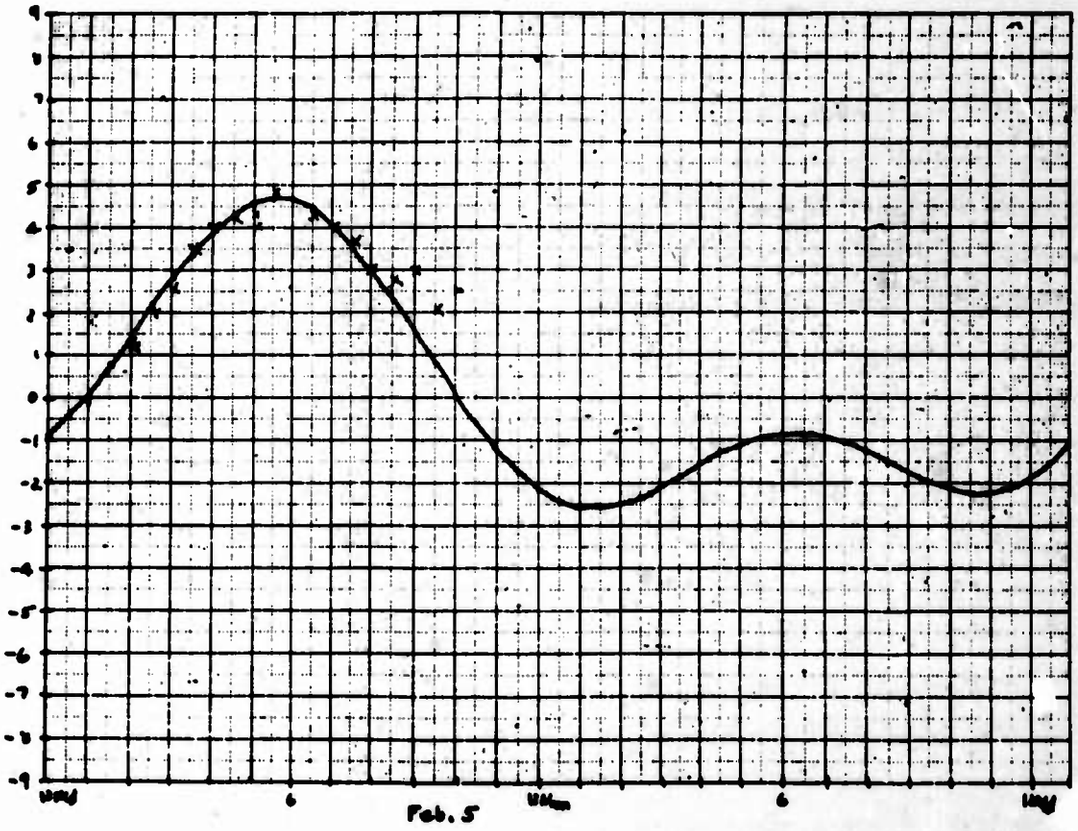

Fig. E-11

In addition, the deviations of our data from the calculated earth tide can be interpreted as an upper limit on the drift rate of the device. For this data the largest deviations correspond to a drift rate of 10^{-8} g's per hour. More meaningful information on the drift rate will be forthcoming when we receive a new dewar which is designed to allow us uninterrupted runs of thirty days. We have also built a vibration-isolator block to reduce the noise from the building.

Finally, I would just like to point out the possibilities for future experiments on the gravitational field itself. With this device we have produced a force which is stable to at least one part in 10^{8}. Such stabilities are rare in the laboratory. One fascinating possibility that we are considering is to use this force to balance the gravitational attraction between two masses in the laboratory. In this way we could look for a possible variation in the gravitational constant.

A SUPERCONDUCTING OSCILLATOR-DETECTOR

A. H. Silver
Scientific Laboratory, Ford Motor Company, Dearborn, Michigan

The title of this talk may give the impression that I am going to describe some new instruments which you may go to your local store and buy, but in fact that is not the case. I want to talk about some experiments we have completed in our laboratory in the last few years, and discuss some ideas about what we think are the important mechanisms. The end result of this looks like a nice oscillating detector which can be used in at least cryogenic experiments if not in some other more general way.

The basic ideas which we will be involved with really stem from the ac Josephson effect and the macroscopic quantization of superconductors. We have accomplished a marriage of these two ideas and come up with what can best be described as a mode of operation of superconductors, in which they become very sensitive and interesting detectors.

We have been engaged in this particular aspect for about a year, but this draws rather heavily upon the work that has been done in the last three or four years, both in our laboratory and in other places around the country, particularly other places with work on the ac Josephson effect. And I would like to just say that the collaborators on this work have been myself and J. E. Zimmerman from our Laboratory in Dearborn.

The area of interest, as you may have guessed already, is going to be some multiply-connected configuration which incorporates a weak link, or weak contact, between two different pieces of super conductor. Initially I want to review some of the properties of such configurations which are entirely superconducting, and then get over to systems in which they are not entirely superconducting, but in fact a finite resistance is incorporated within this ring.

First I shall say a few words about these weak connections. I guess historically the understanding and ideas came from Josephson's prediction of superconducting tunneling, but in the last few years there have been several types of weak

contacts or weak couplings developed. As you heard this morning there is the solder blob, there is also a thin film connection, there is the tunneling junction, and there is a configuration that we have developed and worked with, point contact. This is made by adjusting a pointed superconducting screw, and therefore is an adjustable point contact. While all these experiments could in principle be performed with any one of these devices, we have concentrated on the adjustable point contacts. We found them very convenient to use, particularly for experiments where one wishes to change the properties of the contacts since we can do a lot of experiments in a short period of time without the need of going in and out of the dewar.

I will quickly review the pertinent properties of these multiply-connected superconducting rings, which contain one weak link. There is a difference in a ring with one link compared to a ring containing two weak links such as was discussed by Clarke this morning, since there are no dc effects that you are going to observe by running a current through it or connecting a dc meter to it. However, we have been using an ac technique for several years which is very simple to use and has a number of distinct advantages. I don't think this has been used too widely, and I will say more about the details of it in a few minutes.

One of the things we have done is to determine experimentally the magnetic behavior of such rings. Figure 1 shows the experimentally measured behavior of superconducting rings containing one weak link. We have plotted the field vertically as a function of an applied field which is plotted at an angle for experimental reasons. For several adjustments of this contact for a given inductance we observed the quantized behavior. In fact the quantity that is quantized is not the flux but the phase integral, as we already knew. If the contact is sufficiently weak that there will be transitions between adjacent states, and these transitions can have essentially two different forms. They can be discrete discontinuous transitions as in cases A and B at the top, or they can be continuous transitions from one quantum state to the next, as in the lowest two curves. The criterion which we have derived to determine whether the behavior will be reversible or irreversible depends upon both the inductance

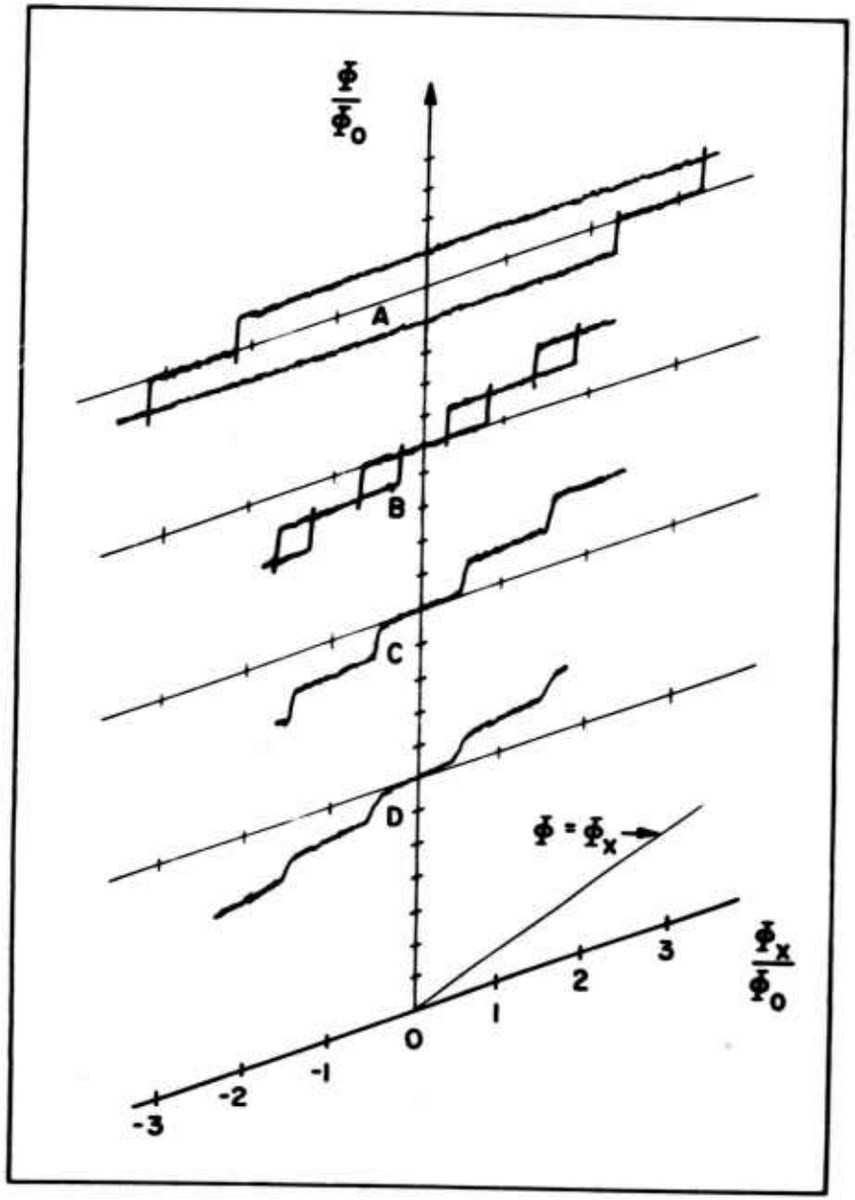

Fig. F-1

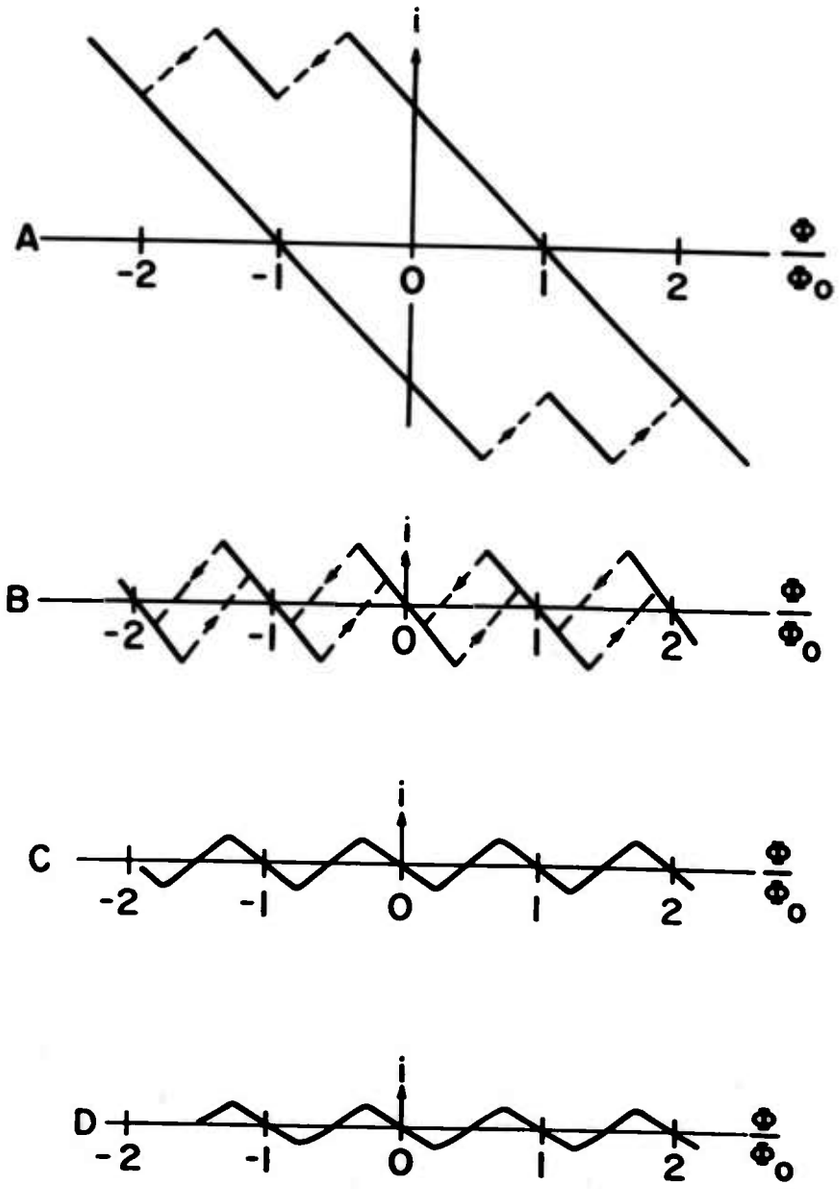

Fig. F-2

of the ring and the critical current of contact. In fact the transition is reversible or irreversible if the product of the inductance of the ring and the critical current of the contact is less than or greater than $\Phi_o/2$, respectively, where Φ_o is the flux quantum. We might just as well have taken this set of curves by varying the inductance of the ring with a fixed contact. In fact, we have performed such experiments to verify that the behavior can be changed merely by changing this product. This is stated to point out that it is not a change in the details of the contact that is responsible for the nature of the transitions.

I should say a few words about the nature of the contact before I proceed. We visualize these contacts, and we have to visualize them because we can't see them, as being of a dimension small enough that they cannot contain or trap a vortex within the contact itself. Now, there may be other types of contacts which will give similar behavior, but we feel certainly if you satisfy this condition that quantum behavior will be observable. This can be accomplished with Josephson tunneling junctions which are smaller than the Josephson length, and one should get similar behavior.

One further interesting point here is that in the reversible behavior the current backs off and goes to zero at the half quantum point, and this is no doubt related to a current induced depairing or gapless behavior in the region of the contact.

Figure 2 shows data derived from Figure 1 in which we have computed the circulating current i as a function of the flux in the ring. One sees that for the first two cases there is not too much of interest. There are just straight lines because one does not have reversible behavior. But in the lower two curves if we consider the region $-\frac{1}{2} < \Phi/\Phi_o < \frac{1}{2}$ we have essentially a plot of the current as a function of the quantum phase across the contact. The thing which distinguishes these point contacts from the tunneling junction is that about the zero phase region the slope is linear, as best we can determine, right up to the critical current. Upon reaching the critical current the current begins to decrease and, depending upon how large $L\, i_c$ is compared to $\Phi_o/2$, the decrease can be essentially linear or we may begin to get curvature. This curvature resembles a portion of a sinefunction. It is in this region that we believe

gaplessness occurs in the contact. The phase across the contact goes beyond 90 degrees, and is limited at 180 degrees when the current in the contact has reduced to zero and the flux in the ring is $\Phi_o/2$.

I have given this as a review, but since the experiments which we wish to discuss are in reality an extension of this work, I think this will aid the continuity. From the first figure, we can readily recognize that, if you were to apply a linearly increasing magnetic field to one of these rings, the flux inside the ring will not change in a simple linear fashion but will have a spectrum. The fundamental frequency for that spectrum will be given by the ratio of the rate of change of the external flux with time to the flux quantum,

$$\nu_o = \frac{1}{\Phi_o} \frac{d\Phi_x}{dt} .$$

There will be an emf induced in the ring which is going to be given by the actual rate of change of flux, and this emf will have the same fundamental frequency, which is really nothing more than the Josephson ac frequency. That is, there is an applied emf given by $d\Phi_x/dt$, and a resultant oscillation of the ring at the Josephson frequency.

The first experiment in this area which we performed was to put a resonant circuit at 30 Mcps around the ring and adjust a magnetic field ramp to the Josephson frequency and observe the output of a 30 Mcps receiver. In fact we did get a signal out when the ramp was adjusted to the proper value. However, it is difficult to control such a ramp precisely. Furthermore, you have to stop and turn it around, and so it is not a very satisfactory way to generate radiation and we then thought that we had a better idea. The basic problem is to produce a small controllable emf in this ring. One needs a low emf, low impedance source element which can be inserted in series with the point contact and there are no batteries in the range of interest, the microvolt and submicrovolt region.

We attempted to calculate what should happen if we put a small resistor and a small emf in our original weakly-connected superconducting ring. Consider the

following equivalent circuit

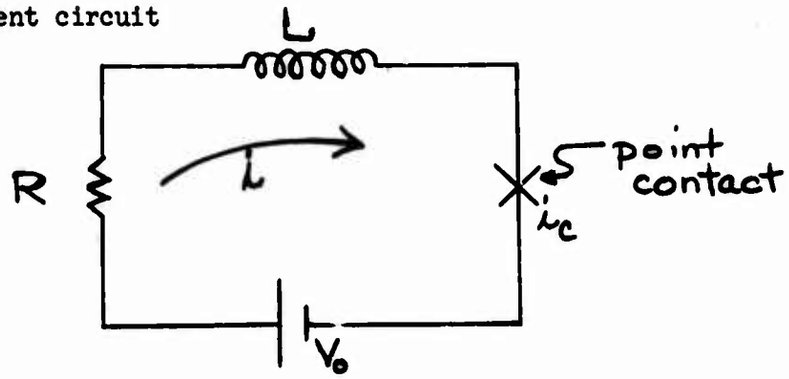

where R and V_o are the resistance and emf equivalents of a voltage source, L is the inductance of the ring, and i_c the critical supercurrent of the contact. In order to compute the dynamical behavior of the circulating current i we require some tractable mathematical form for the currentvoltage behavior of the contact. In this instance the Josephson relations are convenient approximations,

$$i = i_c \sin \varphi,$$

and

$$V_J = \frac{\Phi_o}{2\pi} \frac{d\varphi}{dt} \quad ,$$

where V_J is the voltage across the contact, and φ is called the gauge-invariant quantum phase difference across the contact. Thus one can write the standard Kirchoff equations for this circuit, and integrate the differential equation yielding the solution

$$\frac{i-\alpha i_c}{|i_c-\alpha i|} = \sin\left[\omega_o\sqrt{1-\alpha^2}\left(t + \frac{L}{R} \ell n\left[1-\frac{\alpha i}{i_c}\right]\right)\right],$$

$$\alpha = \frac{i_c R}{V_o} < 1 \quad ,$$

$$\omega_o = 2\pi V_o/\Phi_o \ .$$

The general oscillatory nature of i is now apparent and we have plotted i(t) in Fig. 3 for three values of α. The upper curve, $\alpha = 0$ is for a superconducting ring, $R \doteq 0$, and R increases in the lower curves. Since the current is plotted in units of $(\Phi_o/2\pi L)$ these are universal curves for various values of i_c. The central curve for each α corresponds to $i_c = \Phi_o/2\pi L$ and is the crossover between

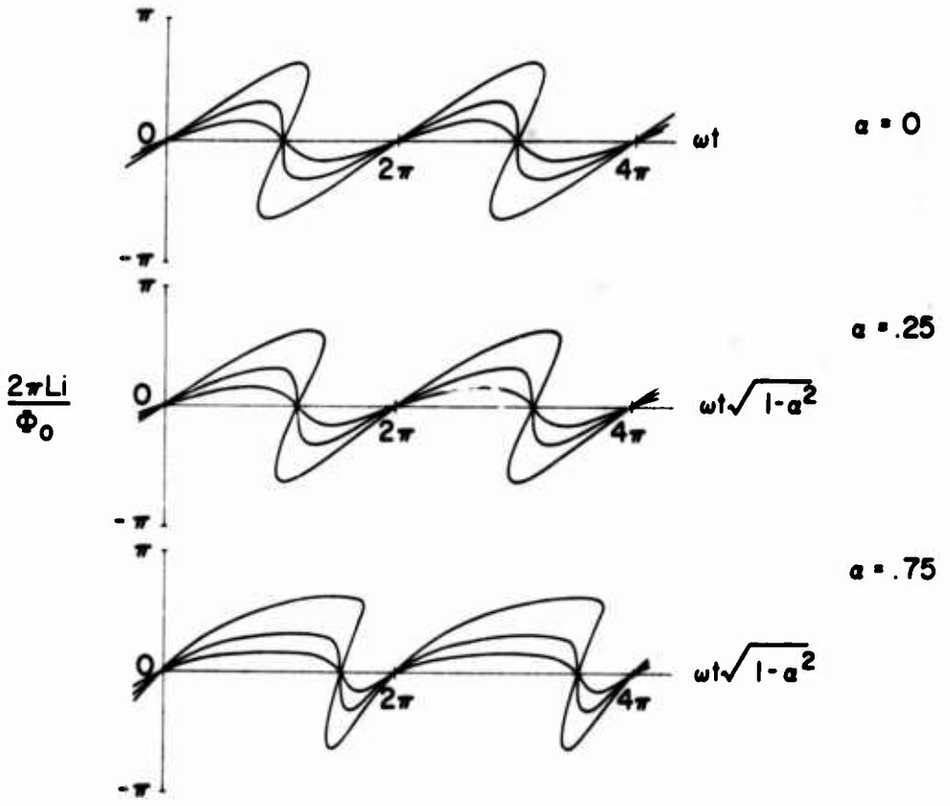
π
0
-π
2π
4π
ωt
α = 0
α = .25
α = .75
2πLi/Φ0
ωt√(1-α²)

Fig. F-3

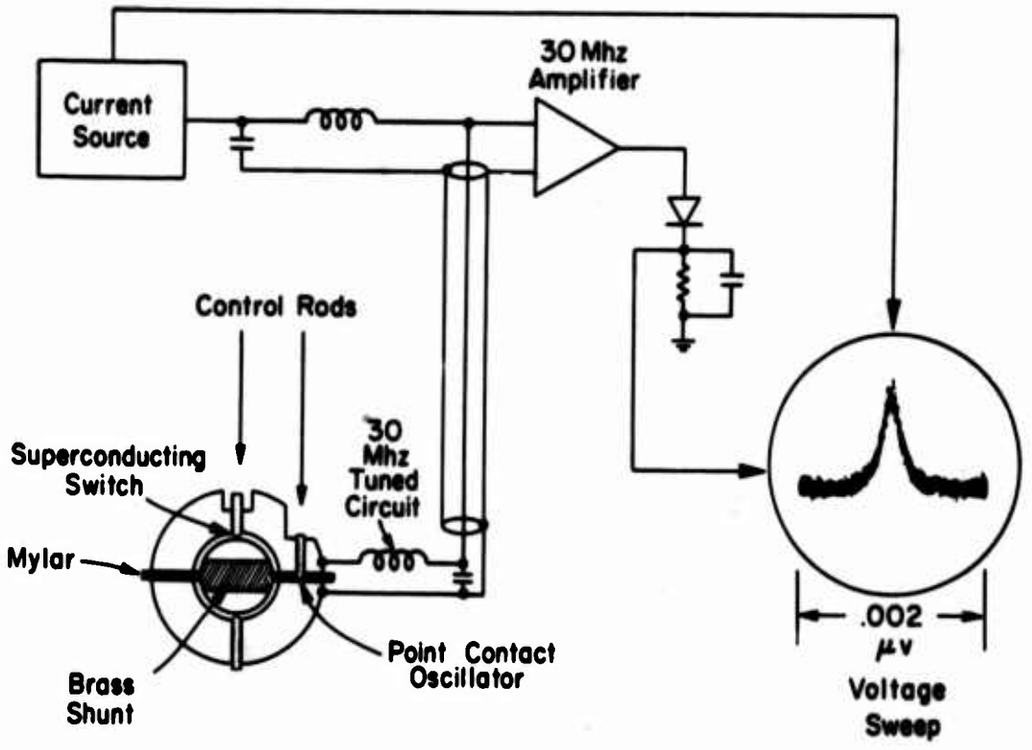
Current Source
30 Mhz Amplifier
Control Rods
Superconducting Switch
30 Mhz Tuned Circuit
Mylar
Brass Shunt
Point Contact Oscillator
.002 μv
Voltage Sweep

Fig. F-4

reversible and irreversible behavior in the case of Josephson tunneling junctions (assumed in the calculation). This time dependence then becomes equivalent to the field dependence of i for a superconducting ring. Thus for $i_c > \Phi_o/2\pi L$ we expect i to make irreversible transitions to its lower value. This corresponds to an instantaneous change of Φ_o in the fluxoid and of approximately Φ_o in the flux in the ring. For $\alpha > 0$ the frequency is slightly modified by $\sqrt{1-\alpha^2}$ and becomes slightly skewed because of the dc losses in R.

Since we know what qualitative modifications are required in describing point contacts compared to Josephson tunneling junctions, we had every reason to believe on the basis of this calculation that you could generate an oscillating current flowing in the ring. This is essentially the Josephson ac effect, but what I would call the uniform mode. I think the majority of experiments on Josephson tunneling junctions are such that the Josephson frequency is determined by the dimensions of the junction, and the currents that flow are principally internal in the junction. And of course this is one reason why there is trouble getting power out of them. In the present case the alternating current flows through the contact, the inductor and the resistor. Thus the current actually flows in the circuit external to the contact itself.

We set out to try this experiment principally near 30 Mcps and at X-band. Just to refresh you on the voltages involved, at 30 Mcps the voltage required is 6×10^{-8} volts, at X-band it is a little more handy, 20 microvolts. But one still doesn't have such a battery, and the way we get around this problem is shown in Figure 4. Here you can see the history of our experiment, because this is one of our rings which originally contained a double contact. We have removed one point contact and placed a brass resistance across the center of this ring. The ring is superconducting niobium and the brass shunt has a resistance of 3.5 micro-ohms. We use a current source at the top left, which generates a current through the brass resistor, and it is this IR which produces the voltage V_o for us. When you adjust IR of the system to be equal to $\Phi_o\nu$, we get an output signal in our diode detector which is shown at the right-hand side.

In this case the band-width and the response function is exactly that of the receiver because we can control the current very well and we have a fairly

wide band resonant circuit, about a couple hundred kilocycles. So it is not at all a test of band-width of the radiation.

Figure 5 shows the experiment at X-band where we used a similar configuration. The actual device is at the top of the X-band cavity and is placed off center as shown in order to couple to the magnetic field of the cavity. The circulating current in the device couples to the magnetic field in the cavity and the observed output is shown at the right-hand side of the figure. Because this was an almost degenerate cavity with several modes close together we were able to observe the three responses shown.

We use a biasing current through this small resistance to produce the voltage V_o. The voltage V_o is not precisely IR because the current through the resistor is essentially the external current minus the critical current of the contact. So there is some correction one has to make if one wishes to know a priori what V_o is. However, as I will describe shortly, we have a technique for measuring the critical current of these rings when it is either completely superconducting or almost superconducting as in the present case.

The power generated is very small. In fact the magnitude of this power is very similar to that given in the very first talks today. The power generated at a frequency ν is

$$P = \frac{\Phi_o^2}{2L} \nu \quad .$$

The inductances that we have used are typically 10^{-9} to 10^{-10} henrys. These are reasonably easy to achieve and give powers of the order of 10^{-10} watts at X-band.

However, from the point of view of coupling out, the impedance of this system is roughly ωL which for these inductances is about 6 ohms at X-band. Consequently it is not a difficult problem at all to couple to this point contact oscillator.

I wish to emphasize that this voltage biased configuration is a uniform mode of the point contact with the current flowing in the external circuit. The oscillation with frequency determined by IR occurs regardless of whether there is any resonant electromagnetic circuit there or not. I think some of the things I

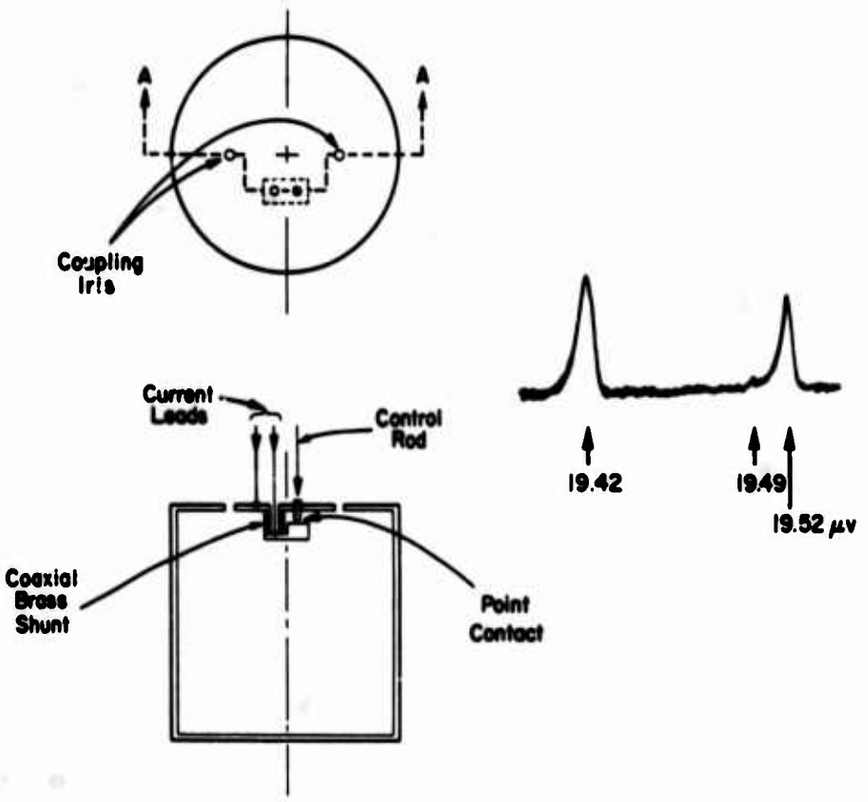
A
A
Coupling Iris
Current Leads
Control Rod
Coaxial Brass Shunt
Point Contact
19.42
19.49
19.52 μv

Fig. F-5

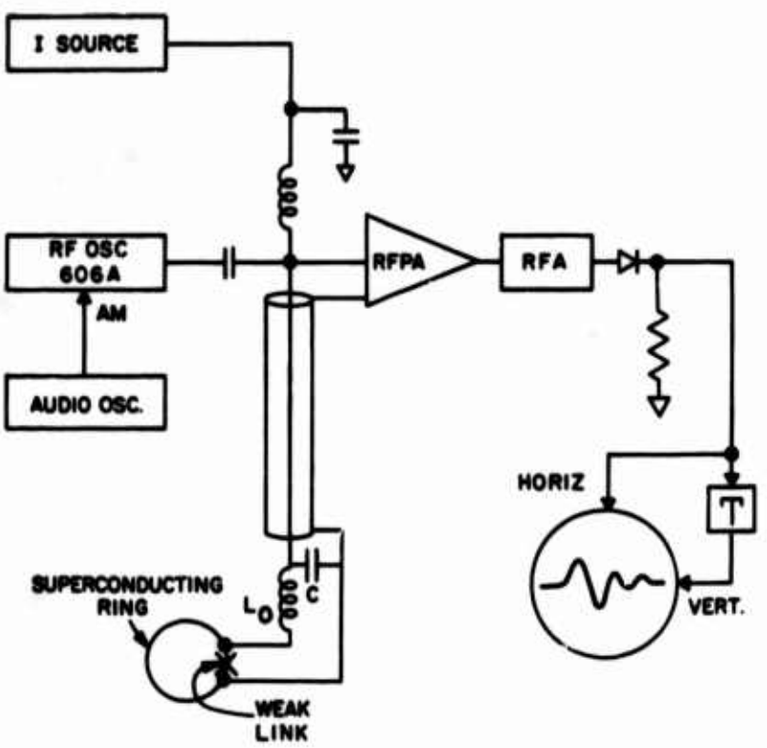
I SOURCE
RF OSC 606A
AM
AUDIO OSC.
RFPA
RFA
HORIZ
T
VERT.
SUPERCONDUCTING RING
L_O
C
WEAK LINK

Fig. F-6

am going to discuss will substantiate this claim.

Next I want to discuss measuring the critical current. Figure 6 is a little bit of review again in that it shows the way in which one can measure the critical current and behavior of the superconducting ring with a weak link. And the way we have don. these experiments is to excite this ring with an rf oscillator which is very weakly coupled to this system, so essentially you have a constant rf current flowing down the cable. Then we observe the reflected voltage with the rf receiver. We vary the level of that oscillator which varies the rf current amplitude and of course we expect to get a linear signal. We want to eliminate this linear behavior and look for nonlinearities in the voltage. So we use a rejection T-network and observe the response of the system on the oscilloscope. Figure 7 shows the actual oscilloscope traces for a superconducting ring excited in this manner. The first break in these curves occurs when the input rf current equals the critical current. Each succeeding oscillation occurs when the rf current amplitude is increased by Φ_o/L. This form of V-I curve therefore demonstrates the quantum behavior of the superconducting ring and also measures the critical current. The two curves shown are for variations of the ambient field by half a flux quantum. You get a large change in the voltage pattern and of course that is the basis of a magnetometer.

Let us now go back and do the same experiment except that we put a small resistance in the ring as shown in Figure 8. The question is what will we see with this non-superconducting ring. We certainly expect to see something when we reach the critical current. Figure 9 shows the experimental results. The upper curve is the Josephson radiation observed by adjusting the dc current, I. The lower one is reminiscent of Figure 7 and the first break in fact measures the critical current of the point contact. Each succeeding signal is at a position where the input current is increased by Φ_o/L. So even in this non-superconducting ring we have a clear exhibition of flux quantization if we observe it fast enough. These experiments were performed at 30 Mcps and the time constant of these rings, L/R, gives a frequency of about 10 kilocycles. Presumably if the observing frequency is large enough compared to R/L there will be a clear exhibition of the flux quantization. If you vary the critical

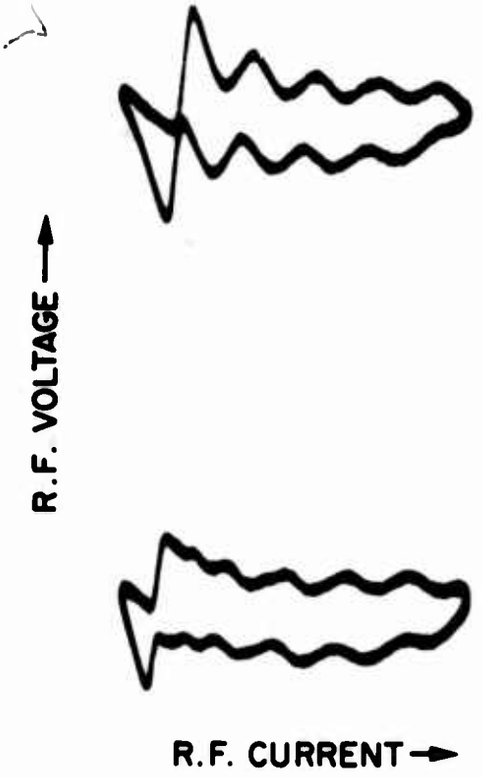
R.F. VOLTAGE
R.F. CURRENT

Fig. F-7

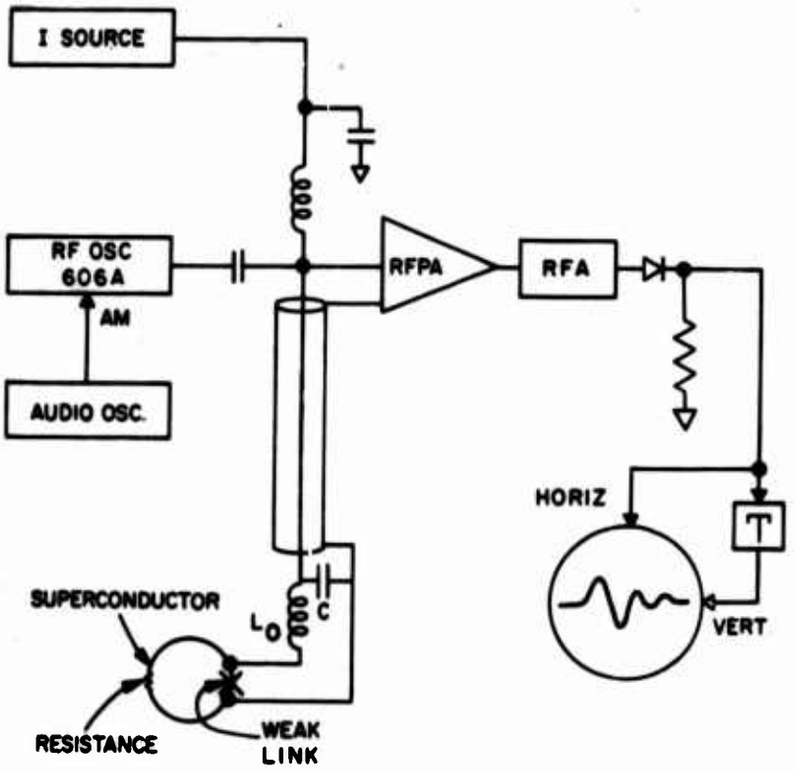
I SOURCE
RF OSC
606A
AM
AUDIO OSC.
RFPA
RFA
HORIZ
VERT
SUPERCONDUCTOR
L_O
C
RESISTANCE
WEAK
LINK

Fig. F-8

current of the contact you only change the position of the initial signal and the rest of the behavior remains the same.

Figure 10 is really more of the same thing. The important first thing to notice is that the upper curve is the actual voltage versus current before we reject the linear term. One sees a linear signal with very small kinks which we can enhance by rejecting the linear term as shown at the bottom.

The second point to notice is that the breaks are very sharp. In the previous figure they wiggled around and appeared to be unstable. This turns out to be a very useful property which I shall come back to a little later.

The question now is how do we make a detector with this oscillator? Figure 11 diagrams the experimental setup. It is again basically the same experiment, with the voltage biased superconducting point contact oscillator at the lower left of the diagram. We voltage bias the oscillator to the frequency

$$\omega_J = \frac{2\pi iR}{\Phi_o}$$

with the current source at the upper left. A damped oscillator ω_o is coupled to the inductance L of the Josephson oscillator and we wish to detect this absorber by observing the electrical characteristics of the point contact at a fixed frequency, ω_D. Again this is nominally 30 Mcps and in order to make the observation we excite the system very weakly with the current i_D at the frequency ω_D. Thus the detected voltage $V(\omega_D)$ is plotted as a function of ω_J by varying i. One might expect to see a signal near $\omega_J = \omega_o$ since the I-V characteristic of a point contact in the flux-flow state depends on the rf losses that are involved.

Figure 12 shows the results of this experiment. Let us look first at the upper graph. I have plotted $V(\omega_D)$ as a function of the dc current and the corresponding Josephson frequency. The resonant absorber was a coaxial line terminated with a coil coupled to the ring inductance and its lowest frequency mode is about 60 Mcps and indicated by ω_o at the upper left. This corresponds to the resonance of the cable capacity and the terminating coil. Ignoring the signal at ω_D and $2\omega_D$, we observed signals at ω_o and $\omega_o \pm \omega_D$. Similar results are shown in the same graph for the next highest mode near 190 Mcps.

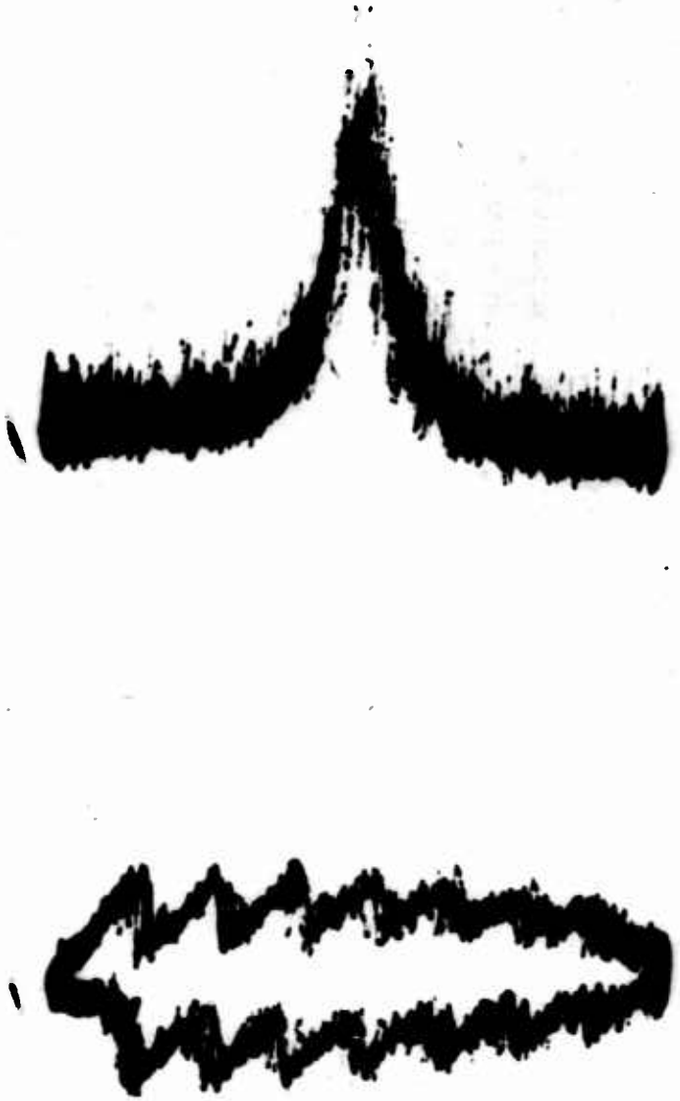

Fig. F-9

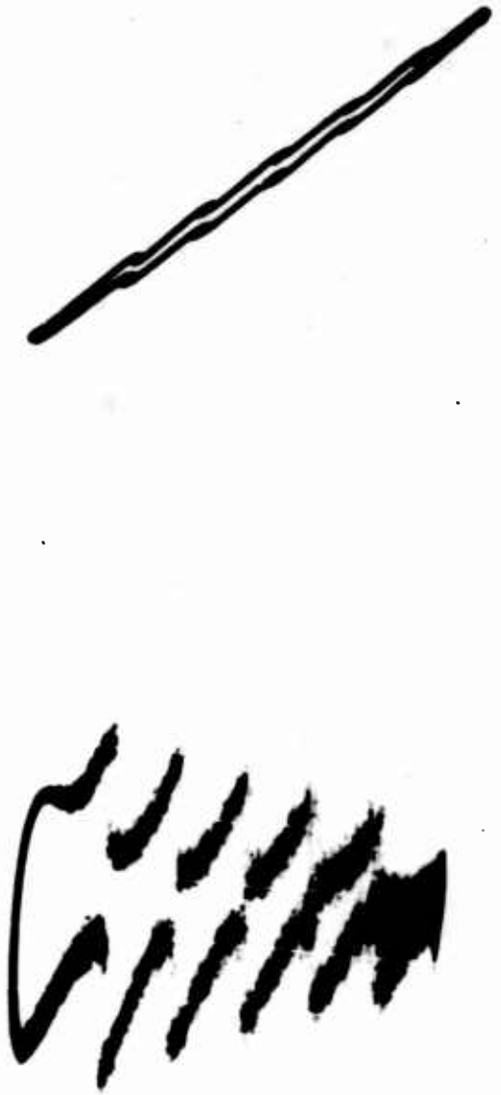

Fig. F-10

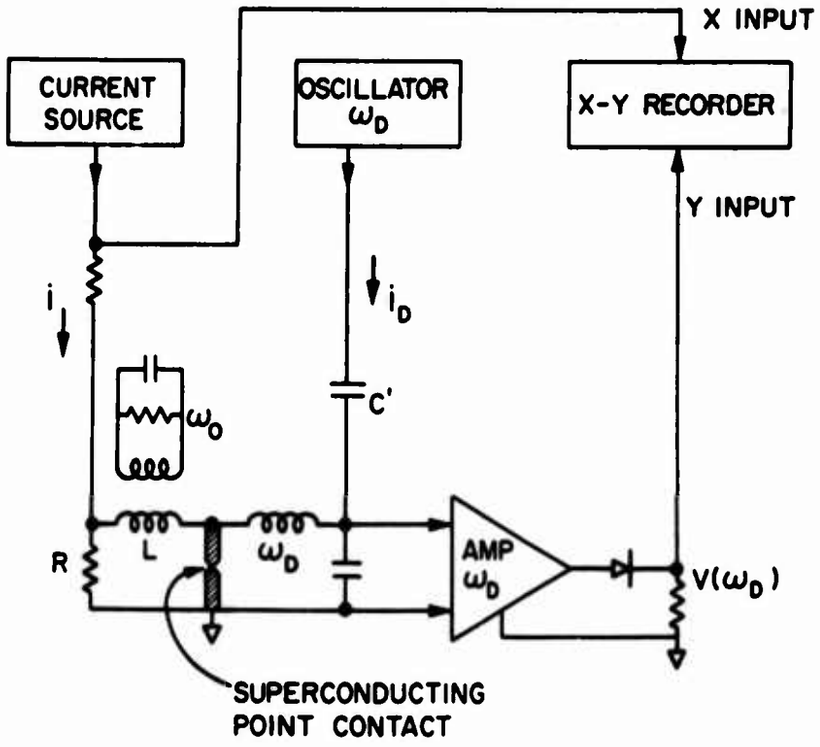

Fig. F-11

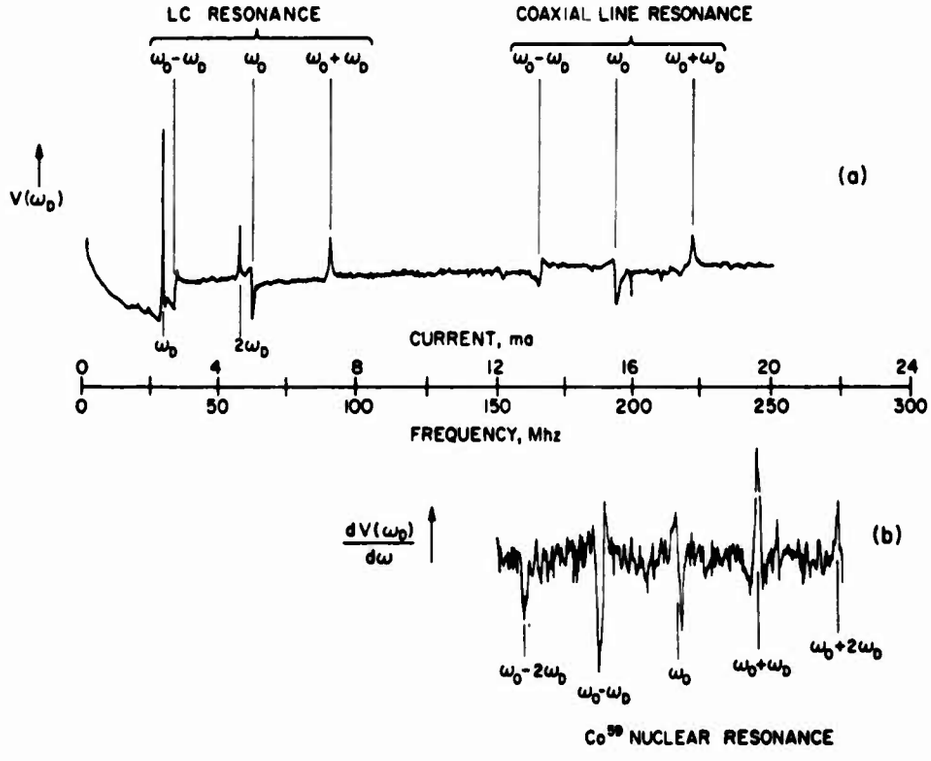

Fig. F-12

A further experiment was to fill the little inductor in the voltage biased oscillator itself with some cobalt powder, and to look for the Co^{59} nuclear resonance frequency. This result is plotted at the lower part of Figure 12. Here $\omega_o \approx 218$ Mcps and there are sidebands $\omega_o \pm \omega_D$ and then a second set of sidebands, $\omega_o \pm 2\omega_D$. The relative intensity of the various sidebands depends upon the power level, i.e., upon i_D/i_c.

Figure 13 gives us an idea of why these sidebands show up by characterizing this as a multi-level system in which the absorber is a two-level system which can only absorb power when we match its frequency ω_o with a photon of frequency ω_o. We expected something to happen when the Josephson frequency matched the resonance frequency. We interpret our result as essentially the derivative of the I-V curve, which should have a peak in it at the voltage corresponding to ω_o due to this resonant absorption.

The sidebands are regarded as nonlinear or multi-photon processes. For example, on the low frequency sideband $\omega_J < \omega_o$. However the contact is a highly nonlinear element. It mixes the Josephson frequency ω_J which it is generating with the rf excitation ω_D and the resultant quantum $\omega_J - \omega_D$ can be absorbed when it matches ω_o. The low frequency sidebands have a general absorption behavior. On the high frequency side we again get mixing and an absorption of ω_o but in fact, at the detector frequency we see emission. There is a stimulated emission of a photon at ω_D associated with the absorption of an ω_o photon in order to match up the frequency condition. And similarly for the other sidebands.

In the remaining time I want to mention the apparent instability in the radio frequency V-I curves to which I alluded earlier. This has only been investigated in the last few weeks and was not originally to be part of this talk. However, I think it is very interesting and pertinent so I shall discuss it briefly. These are not instabilities but coherent oscillations due to small dc voltages which appear across the biasing resistor and hence across the point contact. In the figure which I showed earlier the voltage was due to a small temperature gradient across the metal resistance element and the associated thermoelectric voltage. If we adjust the rf current to the critical current, i.e., to the first break in the rf V-I curve, we can observe this oscillation

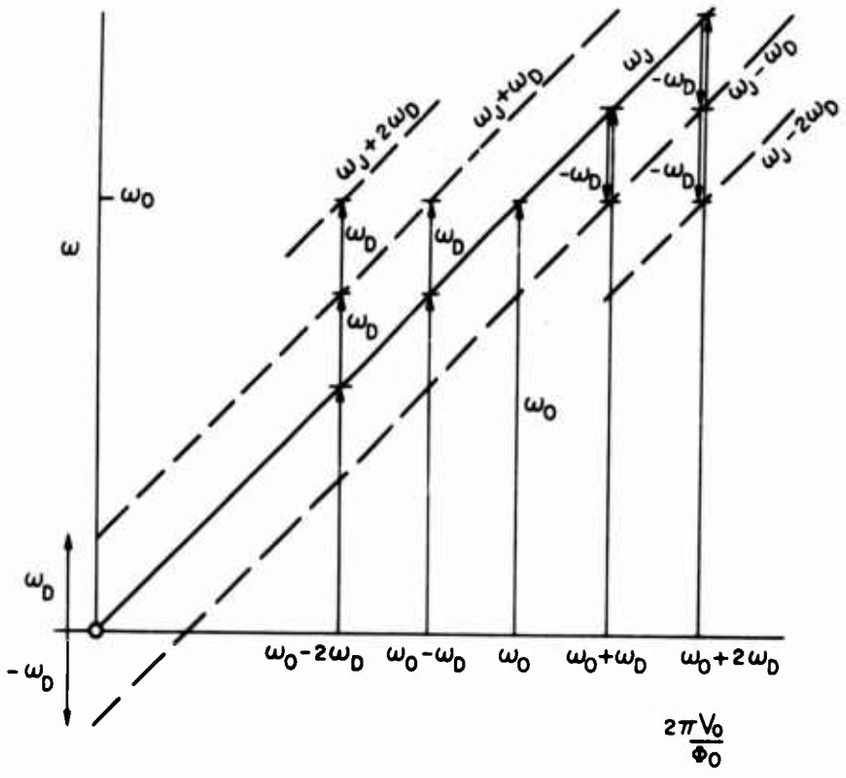

Fig. F-13

Fig. F-14

Figure 14 shows the region near the critical current expanded and although it is difficult to perceive in this type of picture, there is a uniform modulation of this curve. The frequency in this case is about 10 kcps, which corresponds to a voltage of 2×10^{-12} volts. This is essentially a Josephson oscillation at 10 kcps, induced by a 2×10^{-12} volt bias voltage, which then mixes with the 30 Mcps rf current which is externally injected. The rf detection system then demodulates the combined signal at (30 Mcps $\pm \omega_J$) and we can actually observe the Josephson frequency directly. This can then be useful in detecting very small voltages via very low frequency oscillations.

In conclusion, the experiments we have reported are all radio frequency studies of superconducting point contacts in which the quantum behavior is dominant. In the oscillating detector we observed the loss of power from the oscillator to an external circuit at extremely low power levels. I believe that in the small signal limit this should be reversible in the sense that one should now be able to detect very small amounts of rf power incident on the Josephson oscillator, and that furthermore this can be done in a narrow band, frequency selective manner. Frequency selection is determined only by an applied dc voltage which is adjustable over a very wide range. We have scanned this particular oscillating detector from essentially dc to 40 kMcps in a single scan. Clearly the potential is here for a cryogenic detector of very low power and very great sensitivity.

CURRENT FLUCTUATIONS IN SUPERCONDUCTING TUNNEL JUNCTIONS*

D. J. Scalapino**
Department of Physics and Laboratory for Research on the Structure of Matter
University of Pennsylvania, Philadelphia, Pennsylvania

As we heard this morning, and will hear more of later in this conference, superconducting devices have tremendous sensitivity and stability. The sensitivity is such that one can measure voltages of something like 10^{-14} to 10^{-15} volts, magnetic fields of 10^{-10} gauss, and detect millimeter radiation at a level of 10^{-13} to 10^{-14} watts with a one-cycle bandwidth. The stability has been illustrated in many ways. One of the first was experimental work by Goldman and Kreisman at Stanford, in which metastable current carrying states in loops of superconducting material containing Josephson junctions were observed. Another measure of this stability is the recent observations of the spectral purity of the Josephson radiation carried out at Pennsylvania by Dahm and Parker. They find, for a Sn-Sn oxide-Sn junction biased to emit x-band (10^{10}Hz) radiation, that the line width is a function of temperature. At a reduced temperature T/Tc = .3 this width is 2KHz, giving a spectral purity of parts in 10^{7}. With these sensitivity and stability properties in mind, what I will do is address myself to the general question of fluctuations in Josephson junctions. Some of my remarks apply to other types of weak link systems, but they are all calculated with models appropriate to a junction.

First, let's get an idea of the type of quantity that we want to calculate by remembering how the noise properties of a resistor are treated.

---

*Work supported by the Advanced Research Projects Agency.

**A. P. Sloan Foundation Fellow.

In device noise analysis, a resistor can be replaced by an ideal resistor and a noise current generator.

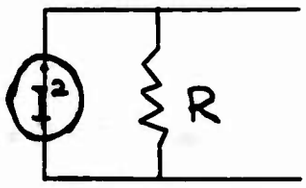

The important quantity to know is the power spectrum $P(\omega)$ which describes the frequency distribution of the current fluctuations. It represents the power dissipated in a 1 ohm resistor per unit frequency interval.

$$\langle I^2 \rangle = \int_0^\infty d\omega\, P(\omega) \tag{1}$$

If we have $P(\omega)$, then the noise calculation for the device containing R is straight forward.

For the resistor, the power spectrum is just the Nyquist relation.

$$P(\omega) = \frac{2\omega}{2\pi R}\left(1/2 + \frac{1}{e^{\beta\omega}-1}\right) = \frac{\omega}{\pi R}\coth\left(\frac{\beta\omega}{2}\right) \tag{2}$$

Here R is the resistance (at frequency ω) and ω is measured in radians which accounts for the factor of $(2\pi)^{-1}$. The factor of 1/2 in Eq. (2) represents the contribution of the zero point fluctuations and the Bose factor is just the thermal fluctuations. In the limit $kT \gg \hbar\omega$ this reduces to the well known expression for Johnson noise.

$$P(\omega) = \frac{4kT}{2\pi R}$$

Now relations of the type given by Eq. (2) are special cases of the Callen-Welton fluctuation dissipation theorem. This theorem states that the thermal equilibrium fluctuations of an observable are related to the dissipative part of a transport coefficient. In this case, the current-current fluctuations are proportional to $R^{-1}(\omega)$. We would like to be able to characterize a

tunnel junction by a power spectrum, and it is some attempts to do this that I want to describe this afternoon.

To begin with, consider a tunnel junction with an oxide layer sufficiently thick ($\sim 30\ A^{o}$) to exclude Josephson tunneling. In Figure 1 some data of Taylor's for an aluminum tunnel junction which exhibited no Josephson tunneling is shown. Above the transition temperature the characteristic is quite linear, while below T_c the gap opens up and the standard Giaever non-linear tunneling characteristic is observed. At low temperature, the tunneling current is suppressed until a voltage of $2 \cdot \Delta_o / e$ is reached. Now, what is the power spectrum for this junction when it is operated at a bias voltage V? This is a steady-state situation, but not a thermal equilibrium one so that the standard fluctuation dissipation theorem can not be invoked. However, a straight forward calculation is possible.

Figure 2 shows a sketch of a tunnel junction with an applied bias voltage V. The dynamics are determined by the Hamiltonian consisting of the full many-body Hamiltonians for sides 1 and 2, a phenomenological tunneling Hamiltonian of the type introduced by Cohen, Falicov and Phillips, and a term representing the applied voltage. The electrons on sides 1 and 2 are labeled by momentum indices k and q respectively. The tunneling Hamiltonian transfers electrons from one side of the junction to the other side. For the important states near the Fermi surface, the tunneling matrix element is such that

$$| T_{kq} |^2 \sim e^{-\ell/2}$$

where ℓ is the oxide thickness in Angstroms. This means that there is a really good expansion parameter available. In the absence of Josephson pair phase coupling we can simply expand in powers of the tunneling interaction H_T.

The current operator is shown at the bottom of Figure 2, and to second order in H_T it is straight forward to calculate the power spectrum of the tunneling current defined by

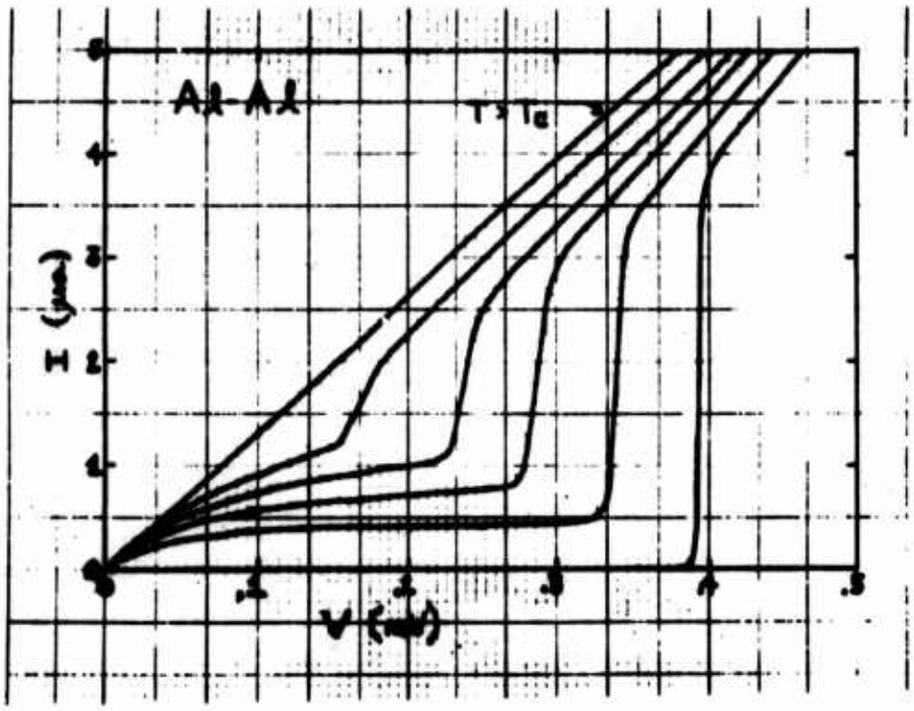

Fig. G-1

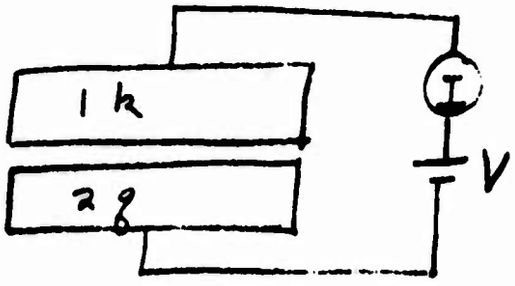

$$H = H_1 + H_2 + H_T - eVN_1$$

$$H_T = \sum_{kg} T_{kg} C_k^+ C_g + h.c.$$

$$j = e\dot{N}_1 = ie \sum_{kg} T_{kg} C_k^+ C_g + h.c.$$

Fig. G-2

$$\mathrm{Re} < j\ (t)\ j\ (o)> = \int_o^\infty P\ (\omega) \cos \omega t\ d\omega$$

Here j(t) is the Heisenberg current operator and the expectation value represents an ensemble average. We have assumed that the voltage was turned on adiabatically. I won't bore you with the details of the calculation. The final form is in fact surprisingly simple. The multiple Green's functions which enter can be directly related to the observed device current and the resulting expression for the power spectrum at a voltage V is shown in Figure 3. As you can see it depends only upon the observed dc current at voltages $V \pm \omega/e$. There are two limiting properties of this form which are worth noting. If eV is much less than $\hbar\omega$ then this expression reduces to the Nyquist form with

$$R^{-1}(\omega) = \frac{e}{2\omega} (I(\omega) - I(-\omega))$$

This is exactly the tunnel resistance at frequency ω so we have in this limit just the fluctuation dissipation result. If eV is large compared to $\hbar\omega$, the power spectrum reduces to

$$P(\omega) = \frac{2eI(V)}{2\pi} \coth \left(\frac{\beta eV}{2}\right)$$

over a bandwidth determined by the tunneling matrix element which may be of order electron volts. This is just the shot noise result and $I(V)\coth(\beta eV/2)$ is the effective noise current. The $\coth(\beta eV/2)$ factor converts the current I(V) to the sum of the absolute values of the forward and backward junction currents. Since these two currents are incoherent to order $|T|^2$ this is just what one should expect. It is interesting that it comes directly out of the formal calculations. These two limiting results give us some confidence in the validity of the general expression shown in Figure 3.

Next I would like to discuss the situation when there is phase coherence across the insulating region and Josephson tunneling occurs. Figure 4 shows the I-V characteristics for a Sn-Sn Oxide-Sn junction. The sharp vertical rise at zero bias in the Josephson dc current and the slanted steps

$$P(\omega) = \frac{e}{2\pi}\left[I\left(V+\frac{\omega}{e}\right)\coth\beta\frac{(eV+\omega)}{2} + I\left(V-\frac{\omega}{e}\right)\coth\beta\left(\frac{eV-\omega}{2}\right)\right]$$

$$\simeq \frac{\omega}{\pi R(\omega)}\coth\beta\frac{\omega}{2} \qquad eV \ll \omega \quad \text{Nyquist}$$

$$\simeq \frac{2eI(V)}{2\pi}\coth\beta\frac{eV}{2} \qquad eV \gg \omega \quad \text{Shot}$$

Fig. G-3

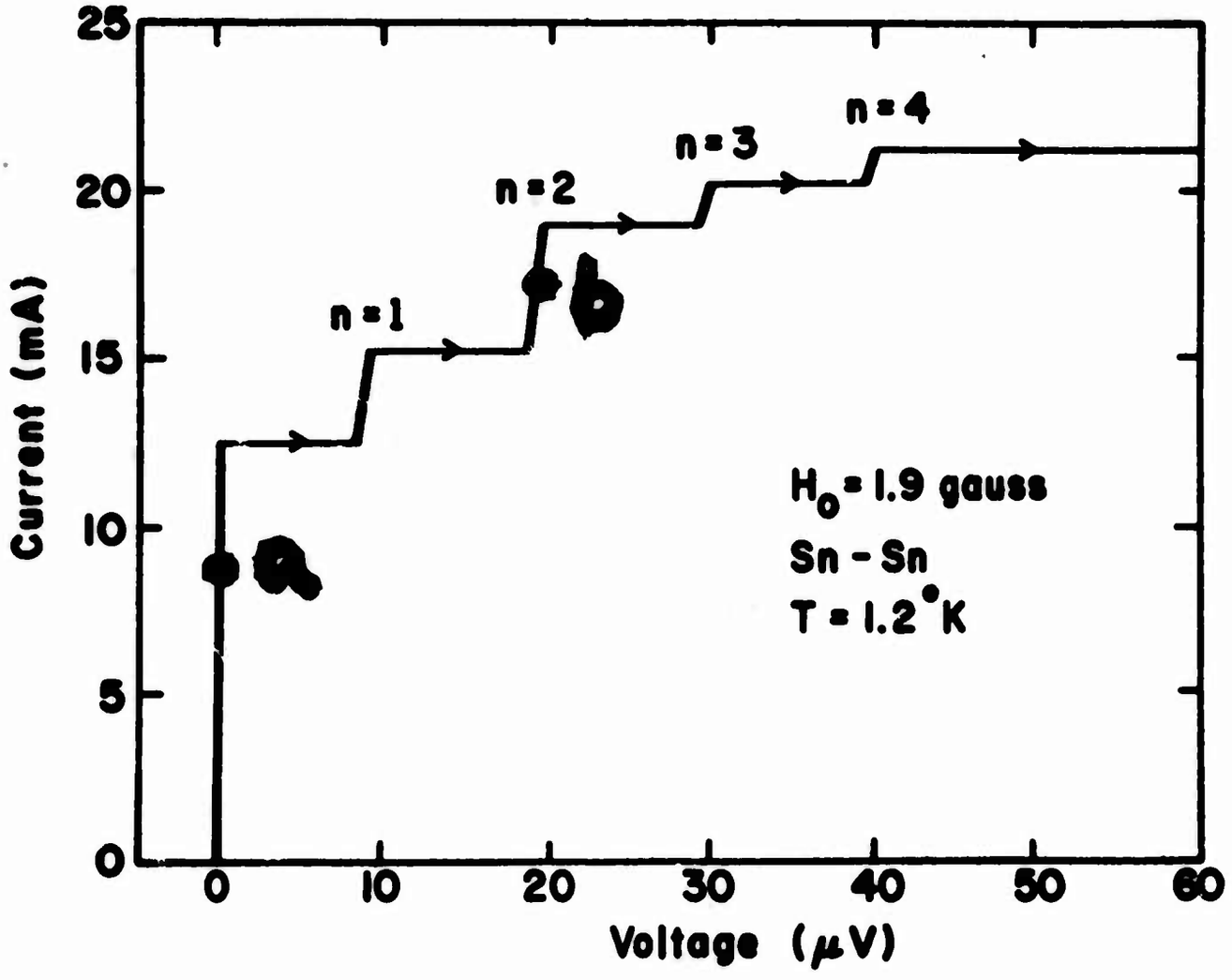

Fig. G-4

represent the various cavity modes of the metal-oxide-metal structure which can be excited. The characteristics of the current-current power spectrum for this type of junction depend upon the operating point. Two cases of particular interest are marked as a and b on Figure 4. At a the junction is operating on the Josephson dc step while at b the junction has a finite bias voltage and radiation is emitted. The line shape of this radiation provides a direct measurement of the low frequency part of the power spectrum at the operating point b.

Before discussing some approximate results for these cases, it is useful to review the theory of the steps which occur in the I-V characteristic. They were first reported by Fiske at the Colgate meeting on superconductivity in 1963. They are simply understood on the basis of some work by Eck, Taylor and myself which showed that the Josephson current can couple to TEM waves which propagate along the junction barrier region. The electric field associated with these waves is large in the insulating region while the magnetic field extends a penetration depth on either side of the insulator. This means that the phase velocity is considerably reduced below the velocity of light. This reduction is determined by $(\ell/\epsilon d)^{1/2}$ where ℓ is the oxide layer thickness, ϵ is the effective dielectric constant of the oxide, and d is equal to twice the penetration depth plus the insulator thickness ℓ. In practice this reduction factor is of order 1/20. These waves are strongly reflected at the edges of the junction so that a set of allowed modes are determined by the junction geometry. Figure 5 shows a plot of a theoretical calculation of the I-V characteristic from some work by Eck, Taylor and myself. Folded into this result is the coupling of the Josephson current to a given cavity mode for different external magnetic fields. The external magnetic field controls the wave length of the Josephson current distribution and hence the overlap of the current distribution with a given cavity mode. An extensive discussion of this is given in the L T 9 Proceedings and I won't discuss it further here. Now, the usual external circuit is basically a current source so, with the inclusion of the Josephson dc current spike, the observed I-V characteristic looks like the dashed line drawn in part b of Figure 5.

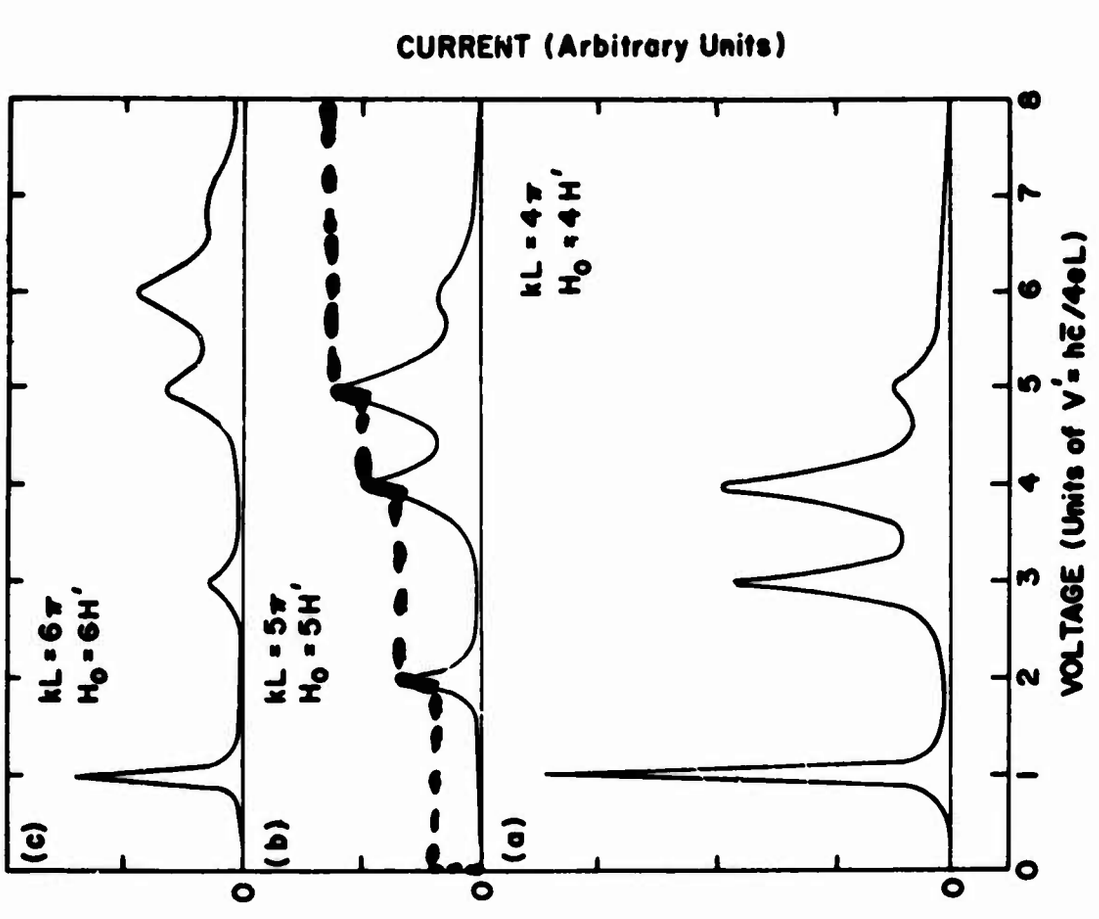

Fig. G-5

$$P(\omega) = A\,\delta(\omega) + B \coth \beta\frac{\omega}{2} \; \frac{\Gamma/\pi}{(\omega-\tilde{\omega}_0)^2+\Gamma^2}$$

$$A = (j_1 \sin\theta_0)^2 \left(1 - \frac{\tilde{\omega}_0}{4\tilde{E}_1} \coth \beta\frac{\tilde{\omega}_0}{2}\right)$$

$$B = (j_1 \cos\theta_0)^2 \, \frac{\tilde{\omega}_0}{2\tilde{E}_1}$$

Fig. G-6

In order to determine the power spectrum when there is phase coupling across the barrier, the two particle collective states are important. In the bulk material the s-wave part of the two particle collective state has a part which corresponds to an oscillation of the gap (or order parameter) and has an excitation energy of order $2\Delta_o$. There is also a component which corresponds to the oscillation of the phase of the gap (order parameter). This latter excitation involves an oscillation of charge density and is essentially the plasmon. In the case of a barrier, this latter type of mode, associated with a variation in the relative phase across the barrier, has a much lower plasma frequency due to the insulating layer and couples strongly to the electromagnetic field.

Rather than approach this problem by an analysis of the two-particle Green's function for these collective states, it is simpler and equivalent (for the limited frequencies and wave lengths of importance) to study the dynamics of an effective Hamiltonian.

$$H = -\int E_1 \cos \varphi(s)\, ds + \frac{1}{8\pi}\int (\epsilon E^2 + H^2)\, dV$$

Here $\varphi(s)$ is the relative pair phase across the barrier at position s and

$$E_1 = \frac{\hbar j_1}{e}$$

with j_1, the current density. The first term is just the energy associated with the phase coherence across the barrier. The bulk of the electric field energy is confined to the insulating region and can be expressed in terms of the local relative pair transfer field density n(s) and the junction capacity per unit area C.

$$\frac{1}{8\pi}\int \epsilon E^2 dV = \int ds \quad \frac{2e^2}{C} \quad n^2(s)$$

Using the Josephson relation

$$\bar{\nabla}\varphi = \frac{2ed}{\hbar c}\ \bar{H} \times \bar{n}$$

relating the gradient of the phase to the magnetic field cross the normal to the junction interface, the magnetic energy term becomes

$$\int dV \frac{H^2}{8\pi} = \int ds \frac{E_1}{2} \lambda_J^2 |\overline{\nabla} \varphi|^2$$

The full Hamiltonian is therefore

$$H = \int ds \left\{ -E_1 \cos \varphi + \frac{2e^2}{C} n^2 + \frac{E_1}{2} \lambda_J^2 |\overline{\nabla} \varphi|^2 \right\} \qquad (3)$$

with the commutation relation

$$[\varphi(s), n(s')] = i\delta(s-s')$$

The equations of motion for the field φ leads to the non-linear wave equation

$$\left(\nabla^2 - \frac{1}{\bar{c}^2} \frac{\partial^2}{\partial t^2}\right) \varphi = \left(\frac{\omega_o}{\bar{c}}\right)^2 \sin \varphi$$

where $\bar{c}$ is the electromagnetic TEM wave velocity discussed earlier

$$\bar{c} = (\ell/\epsilon d)^{1/2} c$$

and ω_o is the plasma frequency associated with phase oscillations across the barrier.

$$\omega_o^2 = (2e)^2 E_1/C$$

The noise problem is intimately tied up with the fluctuations of the φ-field. The power spectrum of the current-current fluctuations depends upon

$$\text{Re} \langle j(t)j(o) \rangle = \text{Re} \langle j_1 \sin\varphi(t) \; j_1 \sin \varphi(o) \rangle = \int_o^\infty P(\omega) \cos \omega t \, d\omega$$

Under small signal conditions, the non-linear wave equation can be expanded and solved in the harmonic approximation. In this way, results appropriate to

operating at zero Josephson current are obtained. To find the power spectrum at point a we must include the condition that a d.c. super-current is flowing and determine its effect on the spectrum of excitations.

Reading back over this, it appears that the tendency to want to give general results has removed what simplicity (and insight) there might have been in the original talk. Since most of this will in fact be submitted for publication elsewhere, I'll stop trying to give the general results and return more closely to the transcript of the talk. There, in dealing with the noise at point a, I considered a short junction in which the dynamics was well described by the simple "lumped circuit" equivalent of the Hamiltonian given by equation (3) which was first introduced by Anderson.

$$H = -E_1 \cos \varphi + \frac{(2en)^2}{2C} \tag{4}$$

The commutation relations are now just $[\varphi,n] = i$. To treat the case in which the junction carries a Josephson dc current we must add a term which describes the coupling energy to the external circuit. Anderson suggested $-\lambda\varphi$, which corresponds to a picture in which the external circuit acts to fix the average phase $\langle\varphi\rangle$. Another possibility is to add $-\lambda \sin \varphi$ which corresponds to treating the external circuit as a current generator which fixes the average current $\langle j_1 \cdot \sin \varphi\rangle$ through the junction. One of the points I would like to make is that the resulting current-current power spectrum depends critically on which of these is the correct choice. I believe that the average phase model is a better representation for most circuits, but an experiment is needed to see. Later on I'll return to this point and describe some experimental work going on at the University of Pennsylvania to test this question.

Taking the Hamiltonian

$$H = -E_1 \cos \varphi + \frac{(2en)^2}{2C} - \lambda\varphi$$

and linearizing about the operating point φ_o by setting

$$\varphi = \varphi_o + \delta\varphi$$

one gets

$$H \simeq \frac{E_1 \cos \varphi_o}{2} (\delta \varphi)^2 + \frac{(2en)^2}{2C}$$

where φ_o is determined by the condition

$$E_1 \sin \varphi_o - \hbar J_1/e = o$$

This Hamiltonian is simply that of a harmonic oscillator with frequency

$$\tilde{\omega}_o = \sqrt{\cos \varphi_o}\ \omega_o \qquad \text{(fixed average } \varphi\text{)}$$

where ω_o is the previously defined plasma frequency. Since $\cos \varphi_o$ goes to zero as the Josephson d.c. current is increased, the plasma frequency ω_o in the presence of the current is decreased. If, on the other hand, the coupling to the external circuit was of the form $-\lambda \sin \varphi$ a similar analysis would show that

$$\tilde{\omega}_o = \omega_o / \sqrt{\cos \varphi_o} \qquad \text{(fixed average current)}$$

which increases as the Josephson d.c. current increases.

Linearizing the current

$$j = j_1 \sin \varphi_o \left(1 - 1/2 (\delta \varphi)^2\right) + j_1 \cos \varphi_o\ \delta \varphi$$

the calculation of $P(\omega)$ is simple and the results are shown in Figure 6. Here $\tilde{E}_1 = E_1 \cos \varphi_o$ and Γ is a width introduced to take into account the cavity losses at frequency ω_o. The δ-function spike represents the memory of the dc current response and the current which flows is proportional to $A^{1/2}$.

This form for $P(\omega)$ was arrived at by linearizing about a given operating point. One of the consequences of this procedure is the delta function at

zero frequency. In order to understand the nature of the power spectrum in this region it is necessary to solve the problem in more detail. We will see that it is in fact closely related to the metastability of persistent current carrying states in a loop of superconductor containing a Josephson junction. In rough terms, the width of the "delta function" is just one over the life time of the metastable state. Now let me see if I can formulate this idea a little better. Suppose that $\lambda = 0$, that is, zero d.c. current is flowing. Then setting $n = \frac{1}{i}\frac{\partial}{\partial\varphi}$ the Hamiltonian, Eq. (4), becomes

$$H = -E_1 \cos\varphi - \frac{(2e)^2}{2c}\frac{\partial^2}{\partial\varphi^2}$$

This describes a one dimensional band problem. The linearization procedure corresponded to generating a harmonic well with discreet levels. It is clear that the full problem has a sequence of bands. The lower bandwidth is just the width of the low frequency spike in the power spectrum.

Before estimating this, consider the problem of metastability of persistent currents. For a loop with one junction, Goldman, Kreisman and I found that the metastable states could be determined by considering the energy (free energy) form

$$-E_1 \cos\varphi + 1/2\ L\ I^2$$

Here L is the inductance and the second term is just the magnetic energy associated with a current I. Now the relative phase φ is related to the current by integrating A around the loop.

$$\varphi = \int_1^2 \frac{2e\bar{A}}{\hbar c}\cdot d\ell = \frac{2e}{\hbar c}\int H\cdot ds = \frac{LI}{(h/2e)}$$

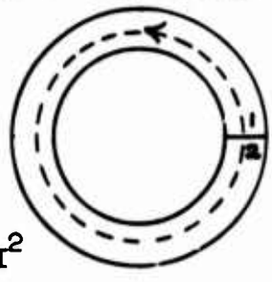

This means that the energy is given by $E = -E_1 \cos(AI) + 1/2\ LI^2$

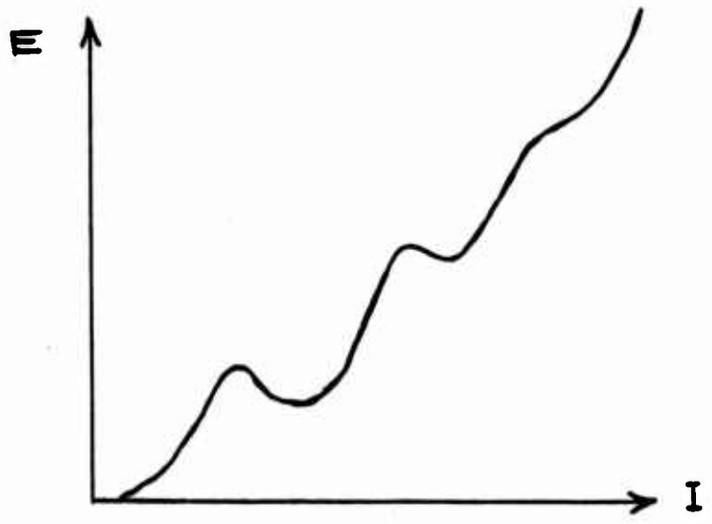

which shows a certain number of metastable states. Now replacing $(1/2)\ L \cdot I^2$ by $\alpha\ \varphi^2$ and adding the electrostatic energy $(2 \cdot en)^2/2C$. We have a Hamiltonian for a one-dimensional particle moving in the potential shown in Figure 7. At zero temperature, it can tunnel from one metastable state to another. The time associated with this for the low lying states is of course inversely proportional to the bandwidth of the previous problem. The higher lying metastable states become exponentially easier to tunnel out of. At finite temperature, thermal activation occurs as indicated in the slide. The life times for the low lying states are shown in the figure. Here ω_o is the plasma frequency, of order 10^9 to 10^{10}, E_1 is the barrier energy of order 10^{-10} to 10^{-12} ergs and C is the junction capacitance of order 10^{-8} farads. Putting in these numbers, one finds for the spontaneous tunneling lifetime (the inverse of this is an estimate of the width of the "δ - function" spike in the power spectrum)

$$\frac{1}{\tau} \sim 10^{10}\ e^{-10^5}$$

which is incredibly long. The thermal life time is about the same. however, since E_1 varies as the current density and hence as $|\ T\ |^2$, it depends

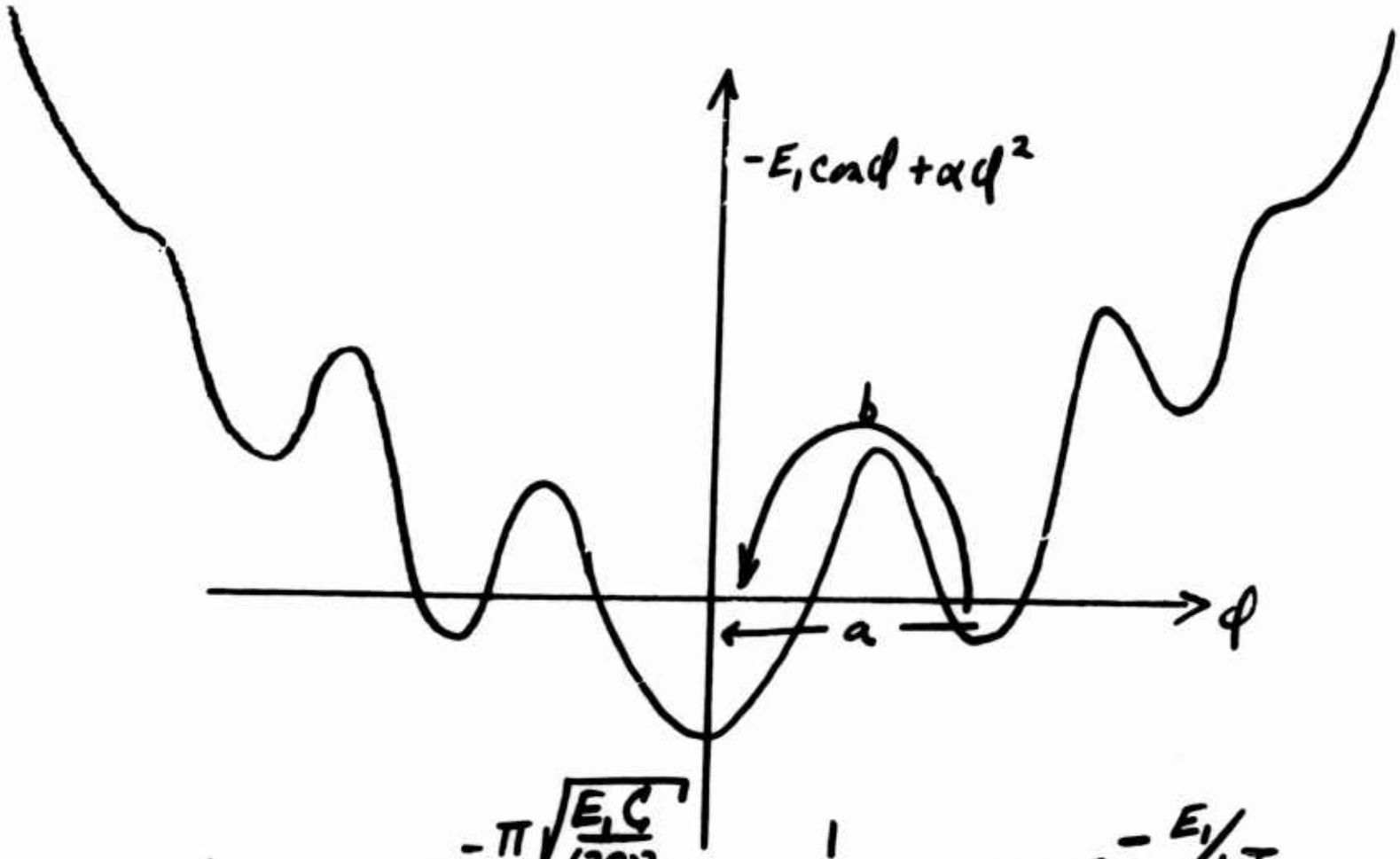
$-E_1 \cos\phi + \alpha\phi^2$
b
a
ϕ
$\frac{1}{\tau_a} = \omega_0 e^{-\pi\sqrt{\frac{E_1 C}{(2e)^2}}}$
$\frac{1}{\tau_b} = \omega_0 e^{-E_1/kT}$

Fig. G-7

exponentially on the separation of the superconductors. This means that as the superconductors are separated, this separation enters the exponential in τ^{-1} in an exponential manner. A matter of 10 or 20 A^{o} is sufficient to make $\tau \sim 10^{-10}$ sec. and at least this discussion shows one possible model which goes continuously between the normal and superconducting state.

Finally, let's turn to the case in which the system is operating at b in Fig. 4. The current is given by

$$j = j_1 \sin \varphi$$

and

$$\dot{\varphi} = \frac{2e}{\hbar} V$$

The system is now operating in a resistive state and the noise problem can be separated into two parts: (1) Given the power spectrum of the voltage fluctuations what is the power spectrum of the current fluctuations? and (2) What is the power spectrum of the voltage fluctuations? The answer to the first part of this problem is well known from F. M. noise theory. The results car be summarized as follows: If $j = j_1 \sin \varphi$ and the power spectrum of φ is $P_{\varphi}(\omega)$ then the power spectrum of j is

$$P(\omega) = \frac{j_1^2}{2\pi} \int_0^{\infty} dt \cos(\omega t) \cdot \exp\left(\int_0^{\infty} P_{\varphi}(\omega') (\cos \omega' t - 1)\, d\omega'\right) \qquad (5)$$

In the present case

$$\dot{\varphi} = \frac{2eV}{\hbar}$$

so that the power spectrum of φ is linearly related to that of V.

$$P_{\varphi}(\omega) = \left(\frac{2e}{\hbar}\right)^2 \frac{1}{\omega^2} P_v(\omega) \qquad (6)$$

If the fluctuations in V occur over a small bandwidth compared with the breadth of the current power spectrum $P(\omega)$ determined from them, the power

spectrum is well approximated by a Gaussian of width $2eV_{rms}/\hbar$. If, on the other hand, $2eV_{rms}/\hbar$ is small compared to the bandwidth of the voltage fluctuations, then the power spectrum $P(\omega)$ is Lorentzian in shape with a width $\Delta\omega$ reduced from the Gaussian result by roughly a factor of the square root of the ratio of $\Delta\omega$ to the bandwidth of the voltage power spectrum. This is nothing but the well known "motional" narrowing in magnetic resonance.

Perhaps an example for the case of shot noise will clarify what I've just tried to say. In this case the voltage power spectrum is

$$P_V = R^2 \cdot \frac{2eI(V)}{2\pi} \coth\left(\frac{\beta eV}{2}\right) = \frac{e\, I_n R^2}{\pi}$$

and the average voltage squared is

$$V^2 = \frac{e\, I_n\, R^2}{\pi} \Delta\omega_V$$

where $\Delta\omega_V$ is the bandwidth of the voltage fluctuations. In the Gaussian limit, the width of the current power spectrum would be of order

$$\frac{2e}{\hbar}\sqrt{\frac{eI_nR^2}{\pi}\Delta\omega_V}$$

Putting in numbers for a typical junction this is orders of magnitude smaller than $\Delta\omega_V$ (and orders of magnitude larger than the observed line width of the Josephson radiation would indicate it should be). The point is, the integration in Eq. (5) gives a Lorentzian in this case. Its width is narrowed from the Gaussian result just calculated by the factor $(\Delta\omega/\Delta\omega_V)^{1/2}$ telling us how much of the voltage fluctuation spectrum is effective in broadening the line. The result is a line width

$$\Delta\omega = \frac{2e}{\hbar}\sqrt{\frac{eI_nR^2}{\pi}\Delta\omega_V}\cdot\left(\frac{\Delta\omega}{\Delta\omega_V}\right)^{1/2}$$

or

$$\Delta\omega = \left(\frac{2e}{\hbar}\right)^2 \frac{eI_nR^2}{\pi}$$

The remaining part of the problem is to determine the low frequency power spectrum of the voltage fluctuations. Clearly there will be shot noise from the quasi-particle current as previously discussed. There should be no shot noise associated with the phase coherent super current flow. One would expect that there will be Johnson noise from the dynamic resistance associated with the underlying excitations of the cavity modes. By taking the Johnson and quasi-particle shot noise into account, Parker, Dahm, Langenberg and I have obtained an order of magnitude fit to the observed line width of the Josephson radiation.

If I have just one more minute, I would like to mention an experiment in progress which I think is extremely relevant to the whole question of phase fluctuations. It is an experiment Parker and Dahm are doing at the University of Pennsylvania. They send 6 GHz onto a junc ion operating on the dc step and detect any output radiation at 12 GHz. The amount of power coming out at 12 GHz is plotted as a function of the dc Josephson current passed through the junction. When the plasma frequency passes through 6 or 12 GHz we expect to see a sharp increase in the frequency doubling. This should provide a direct observation of the plasma excitation and with care allow them to determine whether this excitation increases or decreases with the amount of d.c. current carried by the junction.

Discussion

DR. BARDEEN: Does anyone have a question?

DR. FERRELL: In the situation with the persistant current, you came up with a lifeline that is very long, but of course that depends upon which one of these trapped flux situations you are dealing with.

Isn't it entirely possible that the rest of the persistant current circuit could be made variable, so that you could adjust to give you a shorter lifetime?

What is the situation?

DR. SCALAPINO: What happens is the following: You could move up towards a state that is more metastable in the sense that there is a smaller potential minimum you have to go over. One always finds that you have to go down to around a millidegree in order to get the system to go by tunneling. Otherwise,

it seems that the thermal activation process dominates, and you are in a position to say all right, this is a very simple model to check Anderson's theory of flux creep, in which you don't have to worry about pinning centers, and other things, you can do to the details of the dynamics, but when you are all through there's a question as to what you have, plus the fact that the thing goes and you have to recycle and set it up. It is a hard experiment, because unlike the flux creep experiment, where you had many flux lines and you could watch them creep out, here you have only two or three flux lines included in this sort of a situation. And it technically is difficult to recycle the experiment.

QUANTIZATION AND FLUCTUATIONS IN SUPERCONDUCTORS

Ronald E. Burgess
University of British Columbia
Vancouver, B.C., Canada

INTRODUCTION

On several occasions one may come across certain misconceptions about fluctuations in supercurrents and their decay. For instance, it has been said that supercurrents cannot possibly decay, but must have an infinite lifetime because scattering does not affect the momentum of a Cooper pair. One has also heard that supercurrents cannot fluctuate because the quantization of the fluxoid implies clamping of the flux and hence of the supercurrent. Also one reads that supercurrents cannot fluctuate because the resulting magnetic dipole radiation from a superconducting loop would dissipate energy from the supercurrent, inconsistent with the persistence of the supercurrent.

All of these statements are erroneous and based on irrelevancies or misconceptions. The main omission in these arguments is the contribution of the normal (current) component. Let's take the 2-fluid model as a very convenient and useful starting point. The normal current in a system contributes to the instantaneous flux and the energy of the system, yet one does not usually find this included in the customary expressions for a superconducting ring.

I will discuss a number of cases using simple treatments and since this conference contains the word "device" in its title, I will suggest equivalent circuit techniques for doing some of these calculations.

We will consider thermal equilibrium which is straightforward since it is a matter of applying the fluctuation-dissipation theorem suitably. As a check when one integrates the spectral density one should get in the classical limit the equipartition theorem in a form depending on the number of degrees of freedom of the system.

If a persistent current is flowing, the system is not in equilibrium. No matter how long the life of a metastable persistent current, the system

nevertheless is not strictly in thermal equilibrium. If one waits long enough it will eventually relax to the equilibrium state of zero supercurrent.

Three systems: a superconducting ring, a superconducting ring with a Josephson junction, and a d.c.-biased Josephson junction will be considered.

THIN ROUND HOLLOW CYLINDER

For a cylinder of inner radius r, length ℓ, and wall thickness d the magnetic inductance for circulating currents is

$$L = \mu_o \pi r^2 / \ell$$

(MKS units will be used throughout)

We assume that the radius is large compared with the London λ while the wall thickness is small compared with λ. In the two-fluid model the kinetic energies of the normal and superfluid components are then simply expressible in terms of "kinetic" inductances.

$$L_n = \frac{2\pi r}{\ell d} \frac{m}{n_n e^2} \qquad L_s = \frac{2\pi r}{\ell d} \frac{m}{n_s e^2}$$

The total energy associated with electron motion is magnetic and kinetic and given by

$$E = 1/2\ LI^2 + 1/2\ L_n I_n^2 + 1/2\ L_s I_s^2$$

Now the fluxoid enclosed by any contour lying within the superconductor and circling the axis once is

$$\Phi_c = LI + 2\pi r \Lambda J_s = LI + L_s I_s$$

where $\Lambda = m/n_s e^2 = \mu_o \lambda^2$

The fluxoid is independent of the contour and is quantized:

$$\Phi_c = n(h/2e) \qquad (n = \text{integer})$$

If the normal component of current I_n is ignored the flux Φ through the cylinder is given by

$$\Phi = LI = LI_s = \frac{nh/2e}{1+L_s/L} = \frac{nh/2e}{1+2\lambda^2/rd}$$

It therefore seems that Φ is strictly quantized too and cannot exhibit fluctuations but this false inference arises from the neglect of I_n. When this is included we have for the flux

$$\Phi = LI = L(I_s+I_n) = \frac{nh/2e + L_s I_n}{1 + L_s/L}$$

which can fluctuate because of the term I_n.

On the basis of the equations of motion of the two fluid components it is

possible to devise a simple equivalent circuit which depicts the macroscopic and fluctuation aspects of the electrodynamics (Fig. 1).

The resistance R_n represents the dissipation in the normal fluid arising from its interaction with the lattice and is given by

$$R_n = \frac{2\pi r}{\sigma \ell d} = \frac{2\pi r}{\ell d} \frac{m}{n_n e^2 \tau_n}$$

where σ is the normal conductivity and $\tau_n = L_n/R_n$ is the momentum relaxation time of the normal fluid.

The equivalent circuit is applicable up to frequencies typically of the order of 10^{10} - 10^{11} HZ. The fluctuation e.m.f., e_n, is associated with the dissipation R_n in the normal fluid and will be taken as

$$\langle e_n e_n^* \rangle_\omega = kTR_n/\pi$$

This is the classical form of Nyquist's theorem since it will be throughout assumed that the dominant frequencies in the fluctuation spectrum lie below kT/h.

The circuit has a loop LL_s which contains no resistance and is therefore consistent with fluxoid conservation in the absence of a varying external field:

$$LI + L_s I_s = \text{const.}$$

The quantization of the fluxoid is not implied by the circuit but imposed as an additional condition.

In equilibrium the energy is a minimum with respect to I_s and I_n for a given value of the fluxoid. The system needs a single continuous variable (e.g. the flux) to specify its dynamic state if the fluxoid number n is given, since

$$I_s = \frac{\Phi_c - \Phi}{L_s} \qquad I_n = \Phi\left(\frac{1}{L} + \frac{1}{L_s}\right) - \frac{\Phi_c}{L_s}$$

The energy is a minimum with respect to Φ when

$$\Phi = \bar{\Phi} = \frac{\Phi_c}{1+L_s/L} = \frac{nh/2e}{1+2\lambda^2/rd}$$

for which $I_n = \bar{I}_n = 0$ $\qquad$ $I_s = \bar{I}_s = \frac{\Phi_c}{L+L_s}$

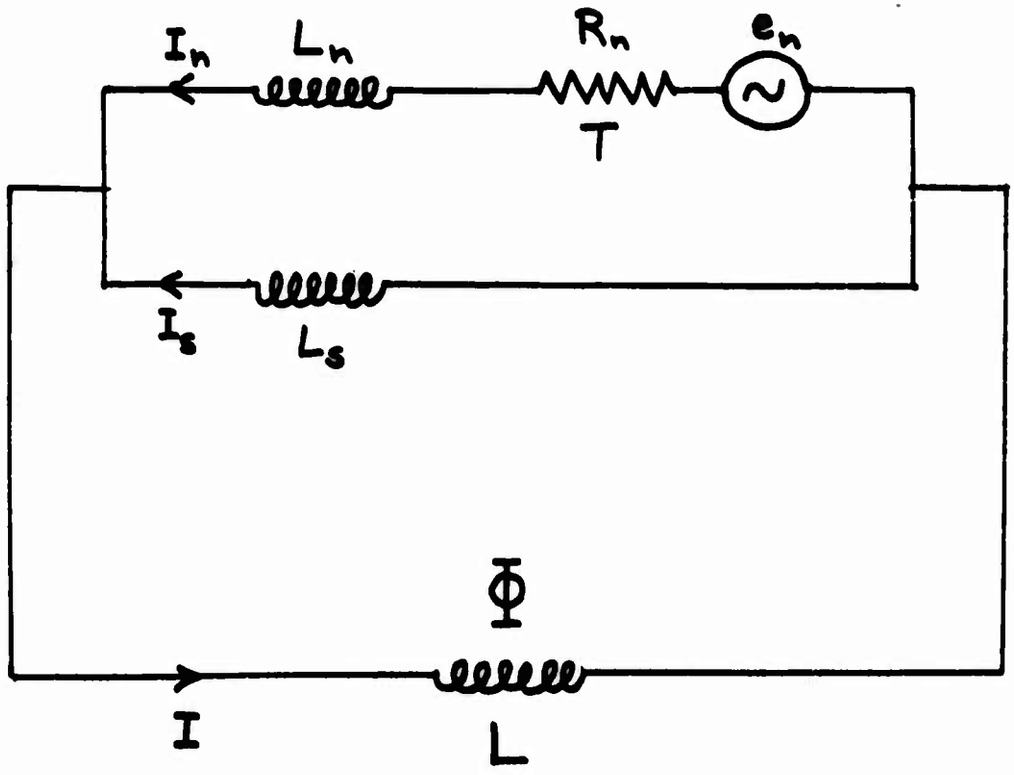

Fig. H-1 Representation of Superconducting Ring.

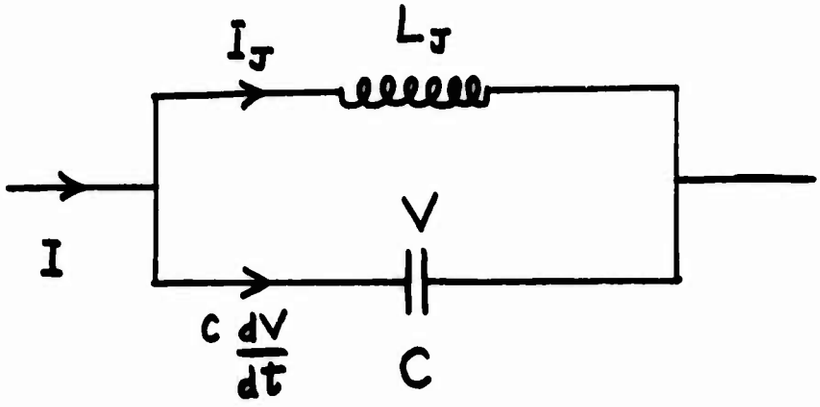

Fig. H-2 Representation of Junction.

Thermal fluctuations of the currents I_n and I_s around these equilibrium values are present. It should be remarked that the fluctuations of I_s do not occur directly by scattering (since the pair momentum is unaffected) but by an indirect mechanism. The normal component is scattered by phonons and this results in a fluctuating I_n which causes a fluctuating flux whose rate of change provides a driving force which acts on both the normal and superfluid components. In terms of the stochastic equations of motion, the normal component is subject to a Langevin force associated with the dissipative interaction with the lattice as well as the $\dot{\Phi}$ force while the superfluid component experiences only the latter force. There is no dissipation directly associated with the superfluid and hence no Langevin force.

Differentiating the energy a second time with respect to the flux enables us to find the fluctuations of the flux:

$$\text{var } \Phi = kT/\frac{d^2E}{d\Phi^2} = \frac{kTL^2L_s^2}{(L+L_s)(LL_s+L_sL_n+L_nL)}$$

Here we note that this result is equally applicable to a cylinder of normal metal by putting $L_s = \infty$. Then the flux fluctuations are

$$\text{var } \Phi = \langle \Phi^2 \rangle = \frac{kTL^2}{L+L_n} \simeq kTL$$

which is the value to be expected from considerations of equipartition of energy. Since in the normal metal $I = I_n$ the statement $\langle E \rangle = \frac{1}{2}\langle I^2 \rangle (L + L_n) = \frac{1}{2}\,kT$ immediately gives the above result.

Reverting to the superconductor where typically L_s and L_n are very small compared with L

$$\text{var } \Phi = \frac{kTL_s^2}{L_s+L_n} \ll kTL$$

Thus the fluctuations of flux are very much smaller than the value kTL which might be expected from equipartition considerations. Closer examination shows indeed that the sum of the contributions to the mean energy from the fluctuations of I, I_s, and I_n correctly add up to give $\frac{1}{2}$ kT. In the superconducting state

the magnetic contribution (from var I or var Φ) is usually much smaller than the kinetic contribution and there is thus a reduction of fluctuations of flux as the temperature is reduced below T_c due not only to T decreasing but also to the accompanying decrease of L_s and increase of L_n.

The variance of the flux is the integrated fluctuation spectrum over all frequencies , but for some purposes we may be more interested in the spectral distribution of the fluctuations; for example, in certain experimental situations only the low frequency portion of the spectrum may be observed or in some devices it may determine the signal/noise ratio.

To find the flux spectrum we use the spectrum of the Nyquist e.m.f. associated with the resistance R_n of the normal fluid and find

$$\langle \Phi\Phi^* \rangle_\omega = \frac{kT}{\pi R_n} \left(\frac{LL_s}{L+L_s}\right)^2 \frac{1}{1+\omega^2\tau^2}$$

where $\tau = \frac{1}{R_n}\left(L_n + \frac{LL_s}{L+L_s}\right)$

This spectrum decreases monotonically with increasing frequency and falls to one half its low frequency value at $\omega = 1/\tau$. The relaxation time τ has a lower bound of $L_n/R_n = \tau_n$ which is the momentum relaxation time of the normal fluid. It is also seen that the flux spectrum tends uniformly towards the value for the normal cylinder as the temperature tends to T_c. Furthermore τ there has the value $(L + L_n)/R_n$ which is the time constant of a ring of normal metal and includes the term in L_n (usually ignored) taking account of the kinetic energy of the electrons. Thus no discontinuity in fluctuations occurs on reaching the normal state.

A check on the flux spectrum is obtained by integrating it over all frequencies and it is correctly found to give the variance of the flux derived earlier from energy considerations.

Up to now we have assumed that the fluxoid number is fixed. However, this number can make a transition to an adjacent integer either spontaneously (a rare event) or under the influence of a varying external magnetic field. If the flux due to the external field is Φ_e then the energy of the system is a minimum when

$I_n = 0$ as before and when the flux has the value

$$\Phi = \bar{\Phi} = \frac{L_s \Phi_e + L\Phi}{L_s + L}$$

in which case the energy has its minimum value

$$E_{min} = (\Phi_e - \Phi_c)^2 / 2(L+L_s)$$

The fluxoid number which minimizes this energy is the integer which gives $|\Phi_e - nh/2e|$ its smallest value. As Φ_e changes n will change stepwise and it is of interest to evaluate the time constant for the resulting changes of flux. Referring to the equations of motion of the two-fluid model or to the equivalent circuit it is found that the equation for the flux variation is

$$\Phi(t) = \frac{(R_n + pL_n)[L_s \Phi_e(t) + L\Phi_c(t)]}{R_n(L+L_s)(1+p\tau)}$$

where $p = d/dt$ and the relaxation time τ has exactly the value found in the fluctuation spectrum of the flux.

If either Φ_e or Φ_c changes abruptly at $t = 0$ the flux exhibits a prompt stepwise response

$$\Phi(0) = \frac{\tau_n}{\tau} \frac{L_s \Delta\Phi_e + L \Delta\Phi_c}{L_s + L}$$

followed by an exponential rise with time constant τ to the asymptotic value

$$\Phi(\infty) = \frac{L_s \Delta\Phi_e + L\Delta\Phi_c}{L_s + L}$$

When a fluxoid transition of magnitude $h/2e$ occurs the flux changes by $\frac{L}{L+L_s} \frac{\tau_n}{\tau} \frac{h}{2e}$ immediately. This determines the locus of the transition in the energy, flux diagram which consists of a sequence of intersecting parabolas, corresponding to the integer values of n. The position of the representative point oscillates about the minimum of one of the parabolas and may with very small probability jump to an adjacent parabola. This mechanism is responsible for the ultimate decay of a persistent current. The fluxoid number can be

regarded as a random variable in a discrete Markov process in which the transition probabilities greatly favor a decrease of the number rather than an increase.

The fluctuations of flux in a ring cause electromagnetic radiation from the ring and therefore an energy loss. The source of the energy is the lattice (not the supercurrent) acting through the intermediary of the normal fluid. For a system in thermal equilibrium the ring would receive energy from the environment at the same rate by transferring energy from the radiation field through the electrons back to the lattice. Arguments that a persistent current can decay by virtue of energy radiation by current fluctuations are misconceived.

An interesting possibility is that if initially we have a ring with no quantized flux in it, there is a possibility that at some later time we will observe it with one quantum of flux, and this can be in either axial direction with equal probability.

Spontaneous fluxoid transitions are low probability processes and if one puts in numbers for typical cylinders, one finds that the lifetime is enormously long except at temperatures extremely close to the critical temperature. Therefore, the chance of comparing these results with the experiment is very slender, because technological difficulties of stabilizing temperatures to perhaps one microdegree or even better, make it impossible to prevent observation of the more fundamental effects. So although in principle, spontaneous fluctuations are the fundamental limitation of the lifetime, in practice other effects intervene and result in a shorter lifetime for temperatures very close to transition temperature.

When a supercurrent flows around a ring the system is not in thermal equilibrium and it may be asked if there is any component of noise (which would be current-dependent) additional to the thermal fluctuations calculated above. As in the case of semiconductors we might expect an extra term proportional to the square of the current and generally termed modulation noise.

Indeed just such an effect can occur in a superconductor due to fluctuations of the order parameter which in the Ginzburg-Landau model can be represented in terms of $|\psi^2|$ or $|\Delta^2|$ or n_s.

For temperatures close to T_c the correlation distance of n_s becomes large, being given approximately by $\xi_o(1-T/T_c)^{-1/2}$ where ξ_o is the coherence length. Also λ becomes large and if these two distances are large compared with the perimeter $2\pi r$ of the ring one can to a first approximation in a small ring regard n_s as fluctuating in time uniformly around the ring. The consequence of fluctuations of n_s in the presence of a supercurrent is readily seen by noting that for constant fluxoid

$$0 = \delta\Phi_c = \delta\Phi + \bar{L}_s\, \delta I_s + \bar{I}_s\, \delta L_s$$

The bars denote time-averaged values. The first two terms on the right hand side correspond to those already used in the previous analysis but the last term is new and corresponds to an additional mechanism of flux variation due to modulation by variations of L_s. The fluctuation of L_s is given in terms of δn_s.

$$\delta L_s = -(\bar{L}_s/\bar{n}_s)\, \delta n_s$$

and the fluctuation δn_s is derived from the second derivatives of the free energy in the Ginzburg-Landau model with respect to Φ and n_s.

Detailed calculations of the effect of n_s fluctuations have been made and the resulting expressions are rather complicated. It will here suffice to remark that for typical cylindrical structures investigated the effect on the flux fluctuations is small except perhaps extremely close to T_c. This implies that a ring carrying a supercurrent even up to the order of the critical current can be fairly accurately regarded as being in thermal equilibrium from the viewpoint of fluctuations.

RING WITH JOSEPHSON JUNCTION

If a very narrow cut is made along a cross section of a superconducting ring so as to form a Josephson junction the electrodynamical relations are greatly modified even though the system can still support a circulating supercurrent. Additional terms appear in the energy which are associated with the junction:

$$E_J = \tfrac{1}{2} CV^2 - \frac{\hbar I_1}{2e} \cos\varphi$$

where C = junction capacitance, V = potential difference,

I_1 = critical Josephson current, φ = phase difference across junction.

The Josephson equation is here important:

$$\frac{d\varphi}{dt} = \frac{2eV}{\hbar}$$

as well as the expression for the total current

$$I = \frac{1}{V}\frac{dE_J}{dt} = C\frac{dV}{dt} + I_1 \sin\varphi$$

consisting of the displacement current and the current transported by pairs across the junction.

An equivalent circuit for the junction is shown in Figure 2 and consists of C in parallel with an inductance L_J given by

$$L_J = V_J/\frac{dI_J}{dt} = \hbar/2eI_1 \cos\varphi$$

The expressions given here assume that the phase fluctuations are small (var $\varphi < 1$) which is to be checked a posteriori.

It is readily seen that the phase φ and voltage V are conjugate and similarly that V and I are uncorrelated. The system is now trivariate i.e. three continuous variables such as φ, V and Φ specify the state of the system in addition to the fluxoid number.

The fluxoid relation for the system is found from demanding that the integral of the gradient of the phase around a closed contour be $2\pi n$ whence

$$\Phi_c = 2\pi n(\hbar/2e) = LI + L_s I_s + \frac{\hbar}{2e}\varphi$$

Once again the variances and covariances can be found:

$\overline{V} = 0$ $\qquad\qquad$ $\langle V^2\rangle = kT/C$

$$\text{var } \varphi = \left(\frac{2e}{\hbar}\right)^2 kTL_J$$

$$\text{var } \Phi = kT\left[L_J + \frac{L_s^2}{L_s + L_n}\right]$$

$$\text{cov } (\varphi,\Phi) = -kT\frac{2eL_J}{\hbar}$$

These simple results are found when L is much greater than L_s and L_J and when the critical current I_1 is greater than $2ekT/\hbar$. These are reasonable assumptions for temperatures not extremely close to T_c. It is also assumed that the transverse dimensions of the junction are small compared with the Josephson length

$$\lambda_J = (\mu_o \hbar/2eJ_1 d)^{\frac{1}{2}}$$

where J_1 is the critical current density.

The spectral density of the flux fluctuations exhibits features not present in the closed ring, a minimum at the frequency ω_o and a maximum at the higher frequency ω_J where

$$\omega_J^2 = 1/CL_J \qquad \omega_o^2 = \frac{1}{C}\left(\frac{1}{L_J} + \frac{1}{L}\right)$$

The fluctuation spectrum of the voltage V rises from zero to a maximum at a frequency somewhat below ω_J and then decreases. The phase fluctuation spectrum decreases monotonically with increasing frequency.

The mean values of the currents in the ring are found to obey:

$$\bar{I}_n = 0$$

$$\bar{I}_s = I_1 \overline{\sin \varphi} = I_1 \sin \bar{\varphi} \quad \exp\left(-\frac{1}{2} \operatorname{var} \varphi\right)$$

The latter result is based on the gaussian distribution of the phase about its mean value, and arises from the non linear dependence of the supercurrent on the phase.

The equipartition principle for this system is confirmed by the sum of the contributions of the fluctuations of voltage, phase, and flux to the energy being found equal to 3kT/2.

DC BIASED JOSEPHSON JUNCTION

In the case of a DC biased Josephson junction the external circuit essentially contains a normal segment so no longer are fluxoid or phase considerations appropriate in dealing with the complete circuit.

"An approximate treatment of the line width of the current oscillation in the junction is now given. The conductance G shunting the junction includes the internal and external contributions". From the Josephson equation, the time evolution of the phase is

$$\varphi(t)-\varphi(0) = \frac{2e}{\hbar}\int_0^t V(s)\,ds$$

$$= \omega_o t + \frac{2e}{\hbar}\int_0^t u(s)\,ds$$

where $\omega_o = 2e\bar{V}/\hbar$ and $u = V - \bar{V}$ is the fluctuating component of the potential difference.

Thus

$$I(t) = I_1 \sin\left[\omega_o t + \frac{2e}{\hbar}\int_0^t u(s)\,ds\right]$$

There is manifested line broadening around ω_o due to the frequency modulation produced by the voltage fluctuations.

Using the Wiener theorem one may determine the line shape of the oscillation. Without going into the details, the essential result is found to be that the line is Lorentzian near the center and gaussian in the wings, and thus all moments of the line width are finite as they must be.

Furthermore the Lorentzian region extends quite appreciably about the center of the line, certainly beyond the half-intensity points; the criterion for this to be so is that kTC/G^2 shall be small compared with $(\hbar/2e)^2$ and this condition is satisfied in typical experimental systems. The half-intensity full line width is then found to be

$$\Delta\omega = \left(\frac{2e}{\hbar}\right)^2 \frac{2kT}{G}$$

This result is based on taking $\langle V^2\rangle = kT/C$ and therefore assumes that shot noise is negligible. For this to be the case the average current through the junction should be small compared with kTG/e.

CONCLUSIONS

We have outlined methods for calculating the thermodynamic fluctuations in various superconducting systems and indicated the possibility of using simple equivalent circuits for first order evaluation.

These techniques would seemingly be equally applicable to superfluid helium for calculating fluctuations of flow and vorticity.

Among the outstanding points which have not been dealt with adequately and are being further investigated we may mention:

Order parameter fluctuations of finite correlation distance

Dynamics of fluxoid transitions

Shot noise of tunnel currents across Josephson junctions

DISCUSSION

DR. FERRELL: There are a couple of points. The first is the discussion of the fluctuations in phase, or the fluctuations in order parameter. Have you seen that you included in your discussion the fluctuations in magnitude in the order parameter? But you did not include the fluctuations in the phase of the order parameter which gives a much bigger effect. And I wonder why you did not discuss the fluctuations in phase.

The other question is: In the discussion of the free energy curve, with the cusps, it seems to me that it is very difficult to get conclusions from such considerations, because such a diagram is incomplete. The free energy curve should cross and represent a sort of a supercooling and superheating that could take place. We could consider fluctuations away from these local minima passing through these places where the curves cross. So the cusps really are not very relevant for questions of the metastability of the supercurrents, and there I think it is extremely important to make a distinction between the type of situation that I think you were discussing and the situation that Scalapino was discussing, where you have a weak link and the actual curve does go up and down and up and down and there is no cusp separating the two. And I think that this supercooling and superheating thing is well established in experiments such as Mercereau and Silver and others have carried out, which shows that you could

cross right through. You don't have to pay any attention to the fact that another free energy curve comes crossing there. So I don't see how you can reason about the lifetime of supercurrent in that situation.

DR. BURGESS: My intent here was to obtain an upper bound on the transition probability, assuming that the fluctuation in a free energy picture gave the possibility of making a transition on the first possible passage. In other words, this gives an upper bound while with supercooling phenomenon we have to wait much longer.

Answering the first part, I think I will have to give this further consideration, but the influence of the phase fluctuations around the completely enclosed system on an observable such as flux fluctuations should be negligible under the assumptions made.

DR. SCALAPINO: I would like to make one comment and ask two questions. You are right about the factor that sits in the exponential. What I did was a linear expansion, so that I calculated only to the next lowest order, which amounts to taking your exponential and expanding.

The other two questions: One is that I notice in the power spectrum distribution that the power spectrum of phase showed no structure and plasma frequency. I wonder whether you might want to comment on that.

The second thing is that I tried to calculate the shot noise due to the supercurrent and find there is no shot noise component. And I feel this is associated with the phase coherence of it as opposed to the shot noise which comes from the quasiparticles. I wonder whether you might express why you feel there should be a shot noise associated with superflow.

DR. BURGESS: Yes. This is attained by applying effectively Campbell's theorem to a charge transition across the boundaries extending approximately lambda in each side from the junction area, and bearing in mind that the external circuit is normal.

And I guess I can't make any further comment on this, except that one assumes that there was a real charge transfer across the system which occurs randomly in time, i.e. there is no periodicity in the transitions for the pairs.

DR. SCALAPINO: How about the resonance of omega-zero?

DR. BURGESS: This was assumed to lie outside the region I was depicting.

DR. SCALAPINO: How do you get any weight down below? I wonder where the weight comes at low frequency.

DR. BURGESS: On the phase? or the flux?

DR. SCALAPINO: The phase.

DR. BURGESS: This is thermal noise.

DR. SCALAPINO: I wonder what the frequency scale is. Where does omega zero sit on this spot roughly? And secondly, where are you getting the weight in your curve that I see at low frequency below what is called omega-J? Plus: where are the plasma?

DR. BURGESS: That is ω_J while ω_o is the higher frequency, which includes the loop in parallel with L_J. This phase spectrum is an amendment essentially a correction of the Shin-Schwartz result.

If one integrates the total area under either the phase fluctuation curve or the flux fluctuation curve, one finds it disagrees in the very low temperature limit with the Shin-Schwartz results where they have only the zero point. But these results are intended to be extrapolations true at any temperature.

DR. BARDEEN: I would like to ask whether you think that the general explanation, qualitative explanation, that Fritz London gave long ago for persistent currents is essentially correct. You have a persistent flow defined by macroscopic wave functions, and in the many-dimensional phase space of all the electrons there are very few which take you downhill in free energy; and that this is the qualitative explanation for persistent currents. There are few paths in phase space which will take you downhill, and you are not likely to find the sort of fluctuation required to bring you downhill.

DR. BURGESS: I think we agree on this.

DR. BARDEEN: Any other questions?

DR. LITTLE: One point, I'd like to question, about the size of the region which you considered to fluctuate. You used in the analysis the correlation length which is the Ginsberg-Landau correlation length. And if you do a similar analysis, where you consider the thermodynamic fluctuations, which would give rise to a fluctuation of the order parameter as well, you find that this is limited to the mean free path of the electrons.

DR. BURGESS: That is included in the normal component fluctuations.

JOSEPHSON EFFECT FAR INFRARED DETECTOR

Sidney Shapiro*
Bell Telephone Laboratories, Incorporated
Murray Hill, New Jersey

My talk today is about the use of Josephson junctions at high frequencies. By high frequencies, I mean frequencies up to and beyond the superconducting energy gap. This means we will be dealing with millimeter and submillimeter wavelengths or, in general, with far-infrared frequencies. In particular, I am going to describe experiments which Mike Grimes, Paul Richards and I have carried out[1] which demonstrate that Josephson junctions are sensitive high speed, far infrared detectors.

I shall use the term Josephson junction[2] to refer to any superconductor-barrier-superconductor system which is capable of passing a zero-voltage current. As shown in Figure 1, a number of different forms of Josephson junction have been used. The thin-film tunnel junction (A) was the first to be studied and the existence of the Josephson effects[2] was first verified using such junctions. The films of course would be made of superconducting metal and the barrier would be a thin dielectric layer, shown shaded in the figure. Closely related in form is the crossed wire junction (B)[3]. The dielectric barrier would be the natural oxide on the wires and for niobium wires, for example, this works quite well. The crossed wire form is really just a mechanical contact and a slight extension of this idea leads to the point-contact form of junction (C)[4]. In experiments with this form of junction it is not at all clear whether a dielectric barrier plays an essential role or whether a very tiny contact area between two superconductors is sufficient. In any event, such junctions exhibit the Josephson effects and it is such point contact junctions that were used in the high frequency experiments I shall discuss today. The figure also shows a superconducting ring broken by

*Present address: Department of Electrical Engineering, The University of Rochester, Rochester, New York 14627.

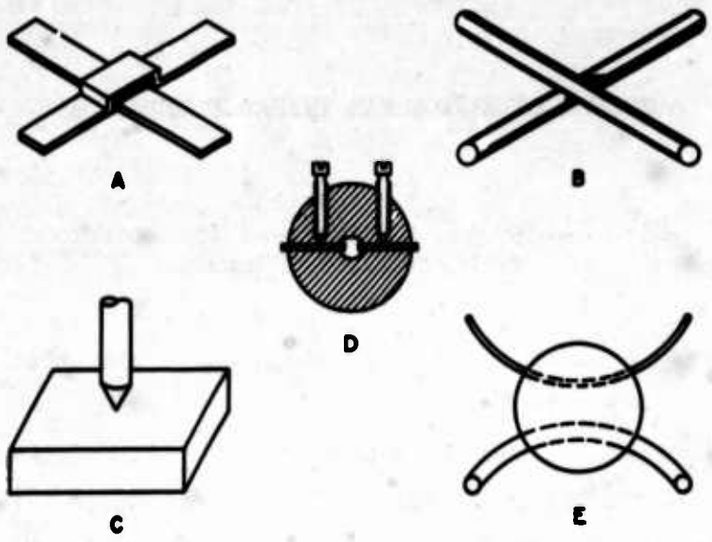

Fig. I-1 Several forms of junction which exhibit the Josephson effects. See text.

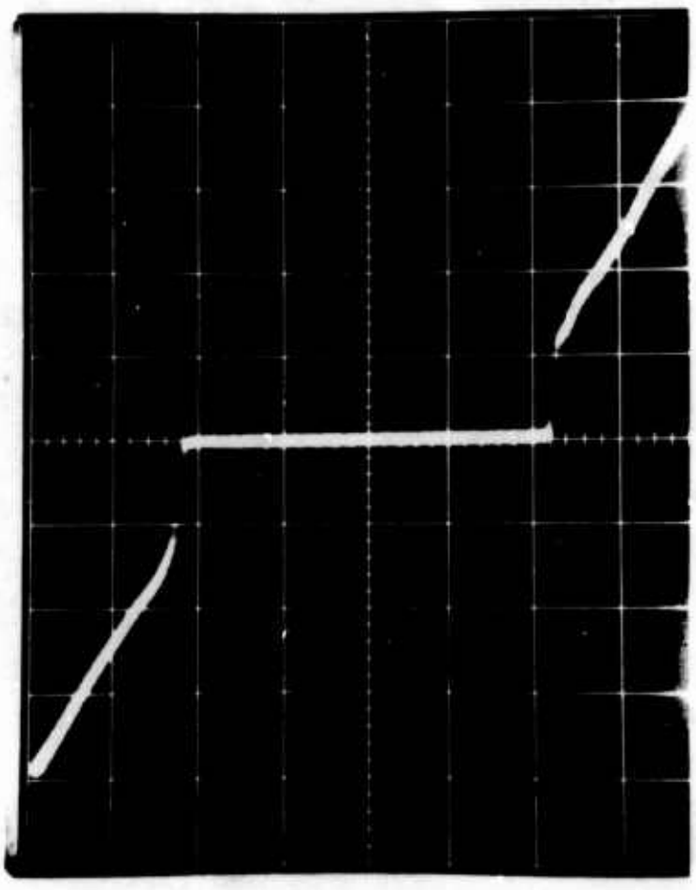

Fig. I-2 Voltage vs. current for a Nb-Nb point contact Junction at 4.2°K. Scales: (V) 0.050 mV/large division; (H) 2.50 mA/large division.

two point contacts or weak links (D) - a structure whose properties have already been discussed at this conference[4,5]. And finally, the solder blob junction (E)[6,7], some of the properties of which Clarke discussed this morning. Let me reiterate that the junctions used in the experiments I shall be describing were point-contact junctions.

The junctions were made by pressing together two pieces of wire - 30 mil was a convenient size. One of the wires was flattened and the other sharpened by filing, by cutting with a razor blade, or by a chemical etch. For junctions involving niobium (Nb) or tantalum (Ta) we used Nb or Ta wires directly; for junctions with indium (In) or lead (Pb) we used copper wire tinned - so to speak - with In or Pb. By adjusting the contact pressure through a suitable mechanism[8], the voltage-current curve of the junction could be adjusted while the junction was immersed in liquid helium.

Figure 2 shows a typical voltage-current characteristic, here for a Nb-Nb point contact junction at 4.2°K. Note that here as for all such V-I characteristics that I shall show the voltage is plotted vertically and the current horizontally. The presence of zero-voltage current is clearly indicated. When a magnetic field is applied the maximum amplitude of the zero-voltage current is affected and goes through a series of maxima and minima. This indicates the existence of the DC Josephson effect in such junctions. It is to be contrasted to the behavior of thin-film tunnel junctions in which the zero-voltage current is actually reduced to zero at certain field values.

Note also that when you leave the region of zero-voltage current, voltage appears smoothly and continuously. This too is in contrast to the case of thin-film tunnel junctions. I do not have time now to go into these differences and can only say that they are characteristics of point-contacts and have also been observed by other investigations[4,5,7,9].

That these point-contact junctions exhibit the AC Josephson effect[7,10] is shown in Figure 3. Here again you see the V-I curve for a Nb-Nb point contact junction only here some rf power has been applied at a frequency of 9.51 GHz. The beating between the applied rf - or harmonics of the applied rf - and the Josephson AC currents gives rise to constant voltage steps whenever the voltage -

Fig. I-3 V-I characteristic for a Nb-Nb junction at 4.2°K in the presence of radiation at 9.51 GHz Scales: (V) 0.020 mV/large division; (H) 0.200 mA/large division.

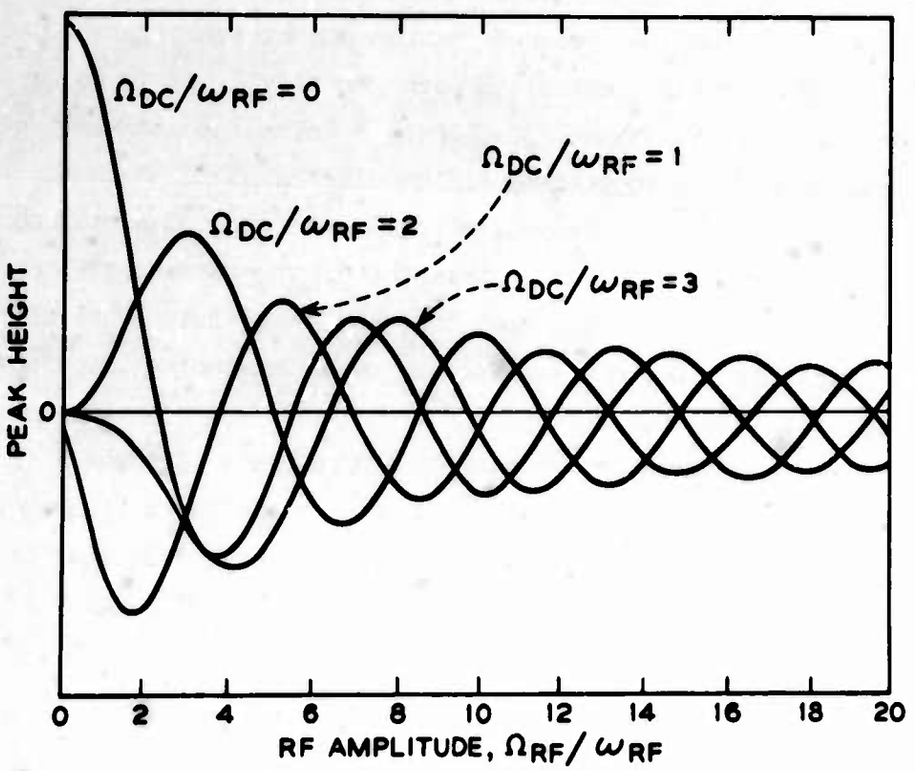

Fig. I-4 Amplitude of the current in several constant voltage steps as a function of rf amplitude as obtained on an analog computer.

and therefore the Josephson frequency - equals the applied frequency or one of its harmonics. The voltage scale here is 20 μV per large division and the voltage separation between the steps corresponds to the applied frequency of 9.51 GHz. Let me call your attention to the fact that since the applied rf has produced an observable change in the V-I curve that change represents a detection of the presence of the rf. The amplitude of the current in any one of these steps - including the step at zero-voltage - varies as the rf power is applied. Figure 4 indicates how that goes. The current amplitude is plotted versus the rf power level for a number of different steps - at zero voltage, on the first step, on the second step etc. These data are the result of an analog computation[11] showing the solution of the relevant equations. The form of the variation is simply a Bessel function of order equal to the order of the step - 0, 1, 2 etc. - and whose argument involves the applied power. The experimental data agree reasonably well with this prediction.

So far, what I have shown is for the case of frequencies well below the superconducting energy gap. At frequencies near the gap new things happen which should come as no surprise considering the central importance of the gap singularity in other properties of superconductors - including tunnel junction characteristics.

Riedel[12] was the first to point out that the AC Josephson current amplitude should have a singularity at the gap frequency. Werthamer[13] carried out a detailed calculation for a tunnel junction and extended Riedel's result.

Figure 5 is one of Werthamer's figures for the case of identical superconductors at absolute zero. In his notation j_1 represents single-particle tunneling processes. Note $\mathrm{Im} j_1$. It is what is measured in conventional tunnel experiments and you see the familiar behavior - no current flows until you get to the gap frequency (or voltage) and then there is a sharp rise in current. Now note $\mathrm{Re} j_2$. This is what is measured by the amplitude of the Josephson current. It has a finite amplitude at zero frequency - the DC Josephson effect - and at higher frequencies it increases in amplitude to singularity at the gap. Above the gap it falls off but only gradually and there is still appreciable amplitude at twice the gap.

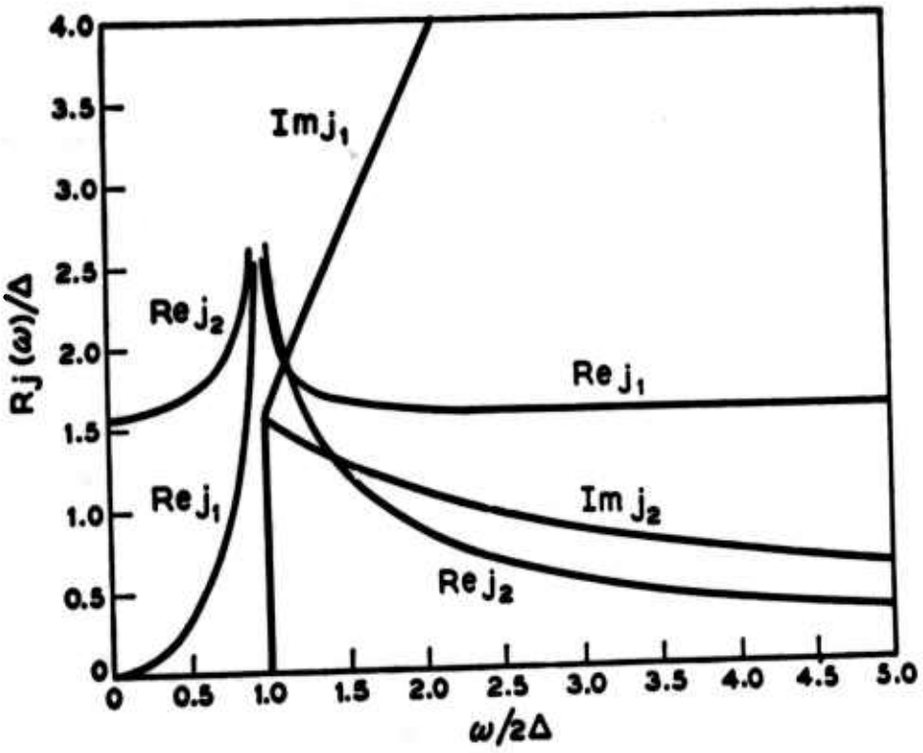

Fig. I-5 Real and imaginary parts of the tunneling current amplitudes at zero temperature and for identical superconductors. (After Werthamer, reference 13).

Fig. I-6 V-I characteristic for an In-In point contact junction at 1.3°K in the presence of about 10^{-9} W of radiation at 150 GHz. Scales: (V) 0.200 mV/large division; (H) 0.050 mA/large division.

Such singularities occur in the theory of other properties of superconductors and what is found experimentally is a peak in the quantity being observed. So we would expect such a peak to show up in the Josephson effect. One other consequence of this peak also pointed out by Werthamer[13,14] is that if radiation at the gap frequency falls on a Josephson junction then the amplitude of the current in the constant voltage steps such as in Figure 3 will not have a simple Bessel function variation with rf power. There will be a very complicated behavior with power level. In fact, a similar complicated variation of step current with rf power should also occur if the applied frequency is 1/2 the gap, or 1/3 the gap, or 7/8 the gap or 3/2 the gap, or in fact, any prominent fraction of the gap frequency.

These theoretical predictions were the stimulus for us to extend our experiments on Josephson junctions to high frequencies.

Figure 6 shows some data for an In-In point contact which has been exposed to a small amount of power at 150 GHz - i.e., 2 mm radiation. This is a frequency that is higher than 1/2 the indium superconducting energy gap and even at these high frequencies the constant voltage steps characteristic of the Ac Josephson effect are present. The voltage scale is 200 μV/large division and the interval between steps is the expected amount for the applied frequency.

Now this photo was taken with only about 10^{-9} W of rf incident on the junction and yet it produces several steps in the V-I characteristic. Thus this junction as a 2 mm video detector already shows high sensitivity with no effort at optimizing the coupling of the radiation field to the junction nor using any fancy detection scheme.

Encouraged by this result we wanted to measure directly the response of Josephson current as a function of frequency. To do this we used the point-contact Josephson junctions as detectors in a far-infrared Fourier transform spectrometer[15]. In this spectrometer broad-band radiation of very low power falls on the junction so no constant voltage steps can be seen but rather the initial decrease of zero-voltage current in the presence of radiation is what we observe.

The schematic of the spectrometer is shown in Figure 7. Broad band,

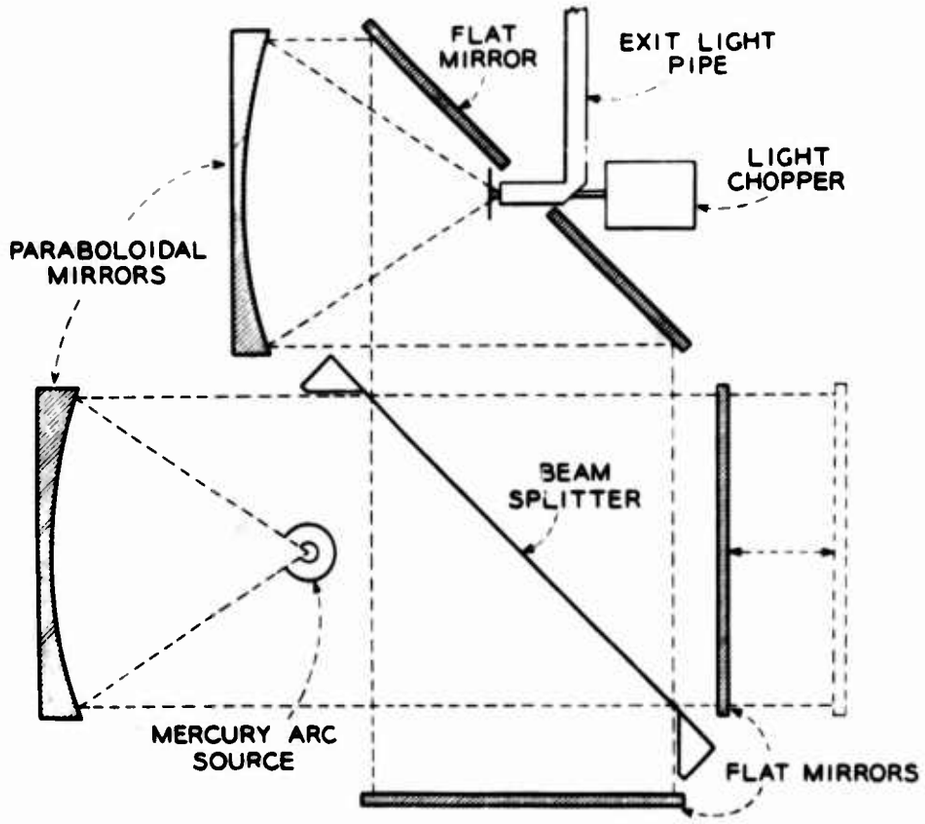

Fig. I-7 Schematic of far-infrared spectrometer.

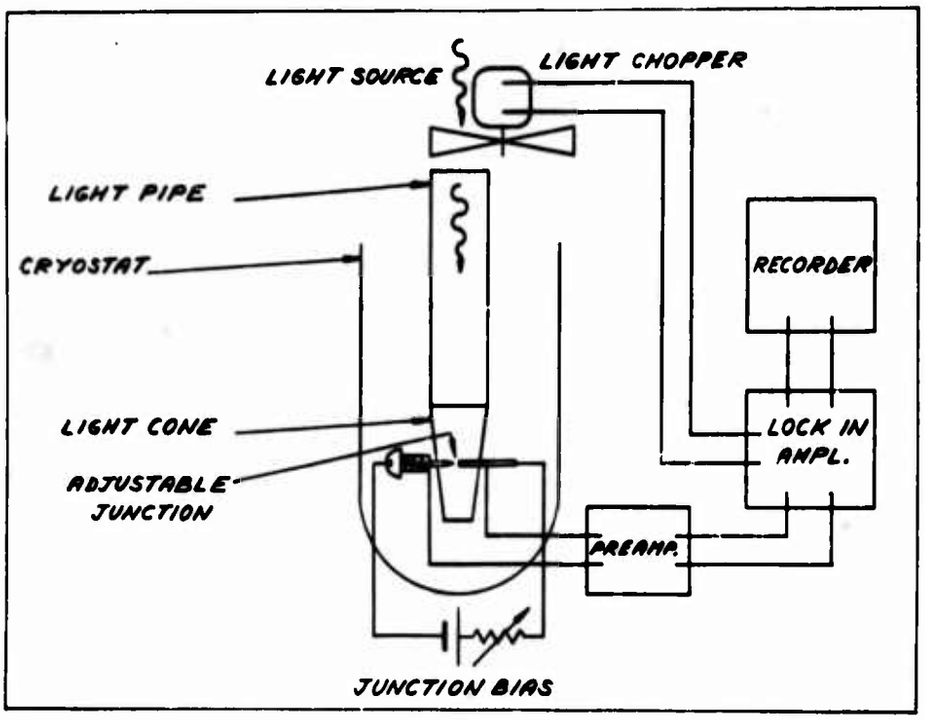

Fig. I-8 Schematic of detection experiment.

incoherent radiation from a mercury arc lamp illuminated a Michelson interferometer, one arm of which was adjustable. After the light was recombined it was chopped before entering the exit light pipe. As shown in Figure 8, the light passed down the light pipe into the liquid helium dewar and after some focussing by means of a light cone it fell on the adjustable point contact which was immersed directly in the liquid helium.

Leads were brought in to provide bias for the junction and to permit measurement of the V-I curve. The radiation diminished the maximum amount of zero voltage current that could flow through the junction. A voltage at the chopper frequency related to the change in zero-voltage current was developed across the junction and served as detector output.

Figure 9 shows schematically how this was done. The solid curve shows the junction characteristic in the absence of radiation. The current through the junction was set to a point of high resistance. In the presence of radiation, the characteristic shifted to that indicated by the dashed line. The bias current however was held constant and so a voltage appeared across the junction at the chopper frequency. This voltage, suitably amplified and phase detected, was plotted on a chart recorder as a function of the path difference in the interferometer.

Figure 10 shows a typical recorder chart or interferogram as it is called. This was taken at 0.3 sec time constant and is indicative of the signal to noise available. The length of the interferogram determines the resolution. This is a rather short interferogram and so the spectrum has rather low resolution. The spectrum is obtained by taking the Fourier transform of the interferogram.

The spectrum for a typical In-In junction is shown in Figure 11. It should be born in mind that signal-to-noise information is largely lost in presenting the spectral response curve. This is because the raw data - the interferogram - is first smoothed before the computer takes the Fourier transform; and then the transformed data points are smoothed to get the spectral response curve shown here. The points to note about these data - which are representative for all In-In junctions - are first that there is a peak in the response and second that the response is broad extending up to about twice the energy gap. The peak is

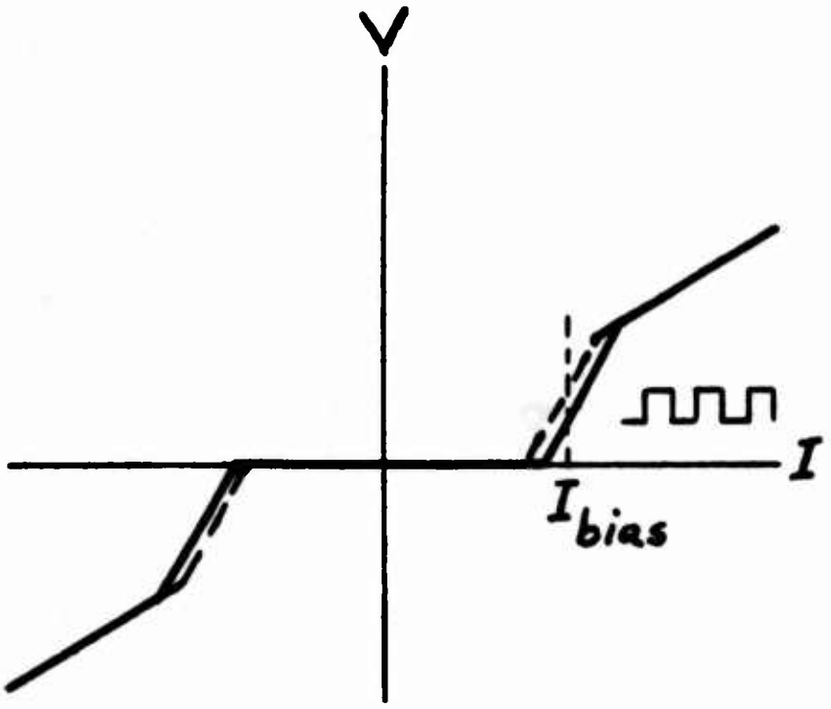

Fig. I-9 Schematic V-I curve indicating how constant current bias permits detection signal voltage to be developed across junction. See text.

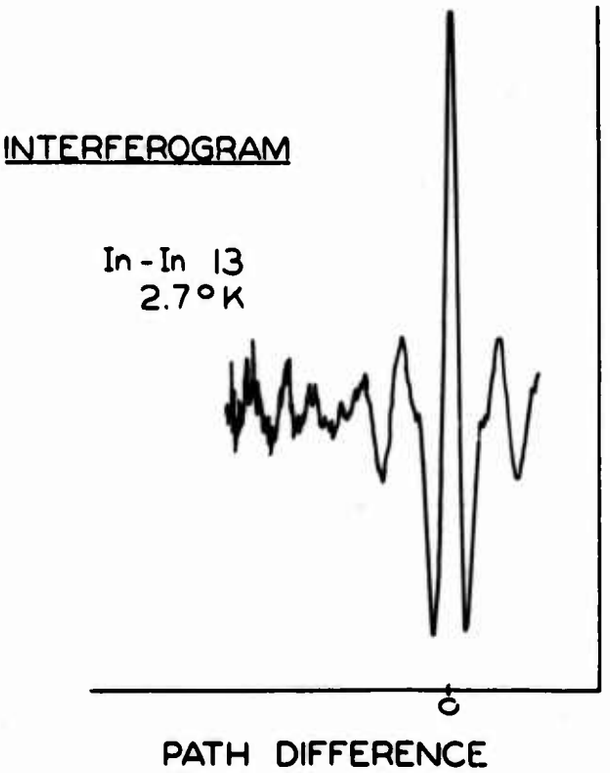

Fig. I-10 Typical interferogram representative of form of raw experimental data. Time constant was 0.3 sec.

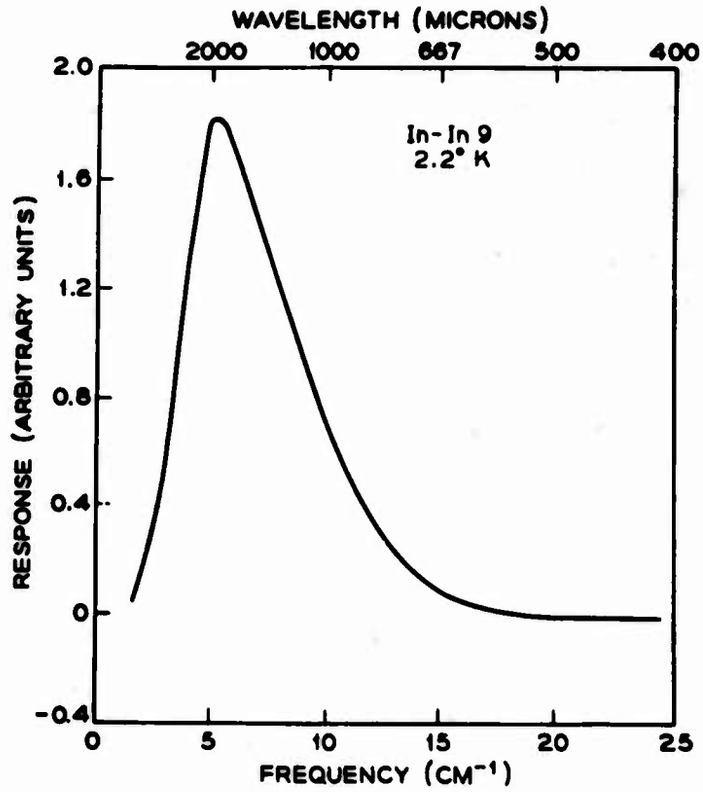

Fig. I-11 Spectral response of an In-In superconducting point contact.

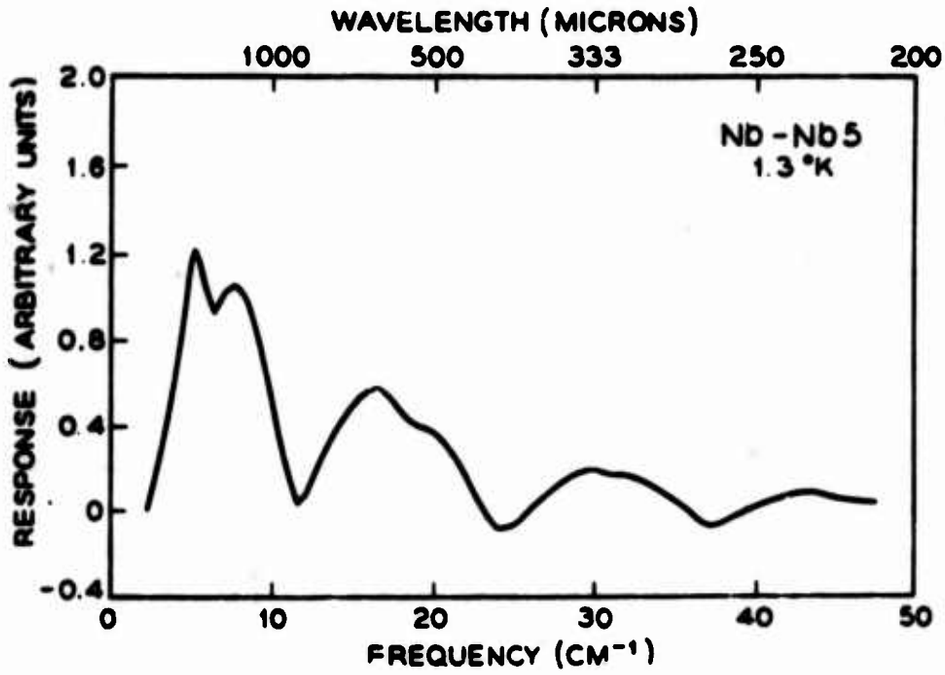

Fig. I-12 Spectral response of a Nb-Nb superconducting point contact.

not quite at the energy gap however which for this temperature occurs at about 7.2 cm^{-1}. At lower temperatures the response sharpens somewhat but not appreciably.

In Figure 12, are shown data typical for all Nb-Nb junctions. Nb has a much higher transition temperature than In and consequently a much larger energy gap and so we would expect the response to extend to higher frequencies and it does being still appreciable at wavelengths smaller than 300 microns. The form of the response curve, however, instead of agreeing more or less with the Riedel-Werthamer calculations as in the case of In, is quite different. In fact, instead of a peak in the response at the gap there is nearly a minimum there (at about 24 cm^{-1}) and at 1/2 the gap, 1/4 the gap and 3/2 the gap too. However, regardless of the shape of the response curve it is at least true that Nb-Nb junctions also respond out to about twice the gap as did the indium junctions.

To supplement these infrared spectral response results and with the help of Marty Pollack we were able to carry out some preliminary experiments[16] using a cyanid laser as a monochromatic source at 311 microns. We found constant voltage steps appearing in the V-I characteristic of a Nb-Nb junction when irradiated with the laser just as shown in Figure 3 for microwave experiments. And the steps appear at the right voltage for the laser frequency used. In effect, this checks one point on the response curve. Note that in these laser experiments the monochromatic frequency applied was already well above the gap, yet constant voltage steps arising from the AC Josephson effect were still seen.

We have taken spectral response curves for junctions formed from a number of other superconductors and I want quickly to run through these data. In each case the curves are different - both from the data shown up to now and from the Riedel-Werthamer theory.

Figure 13 shows the spectral response curve for a Nb-Ta junction. The response is at frequencies well below the energy gaps involved which would be at frequencies well off the figure. Note however the prominent structure in the solid curve as about 2 cm^{-1} and the presence of similar structure at just twice the frequency. The dashed curve was taken for the same junction by applying a small magnetic field to counteract the effect of some trapped flux and to

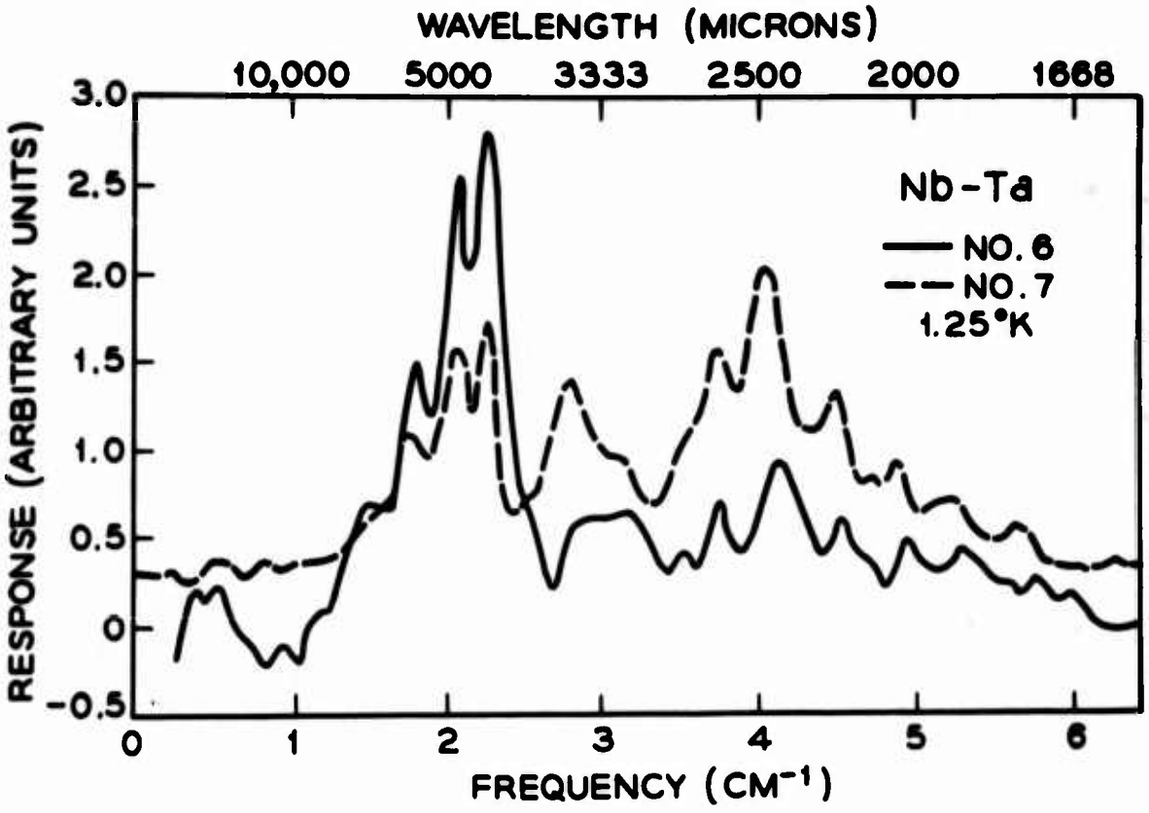

Fig. I-13 Spectral response of a Nb-Ta superconducting point contact at two different values of applied magnetic field.

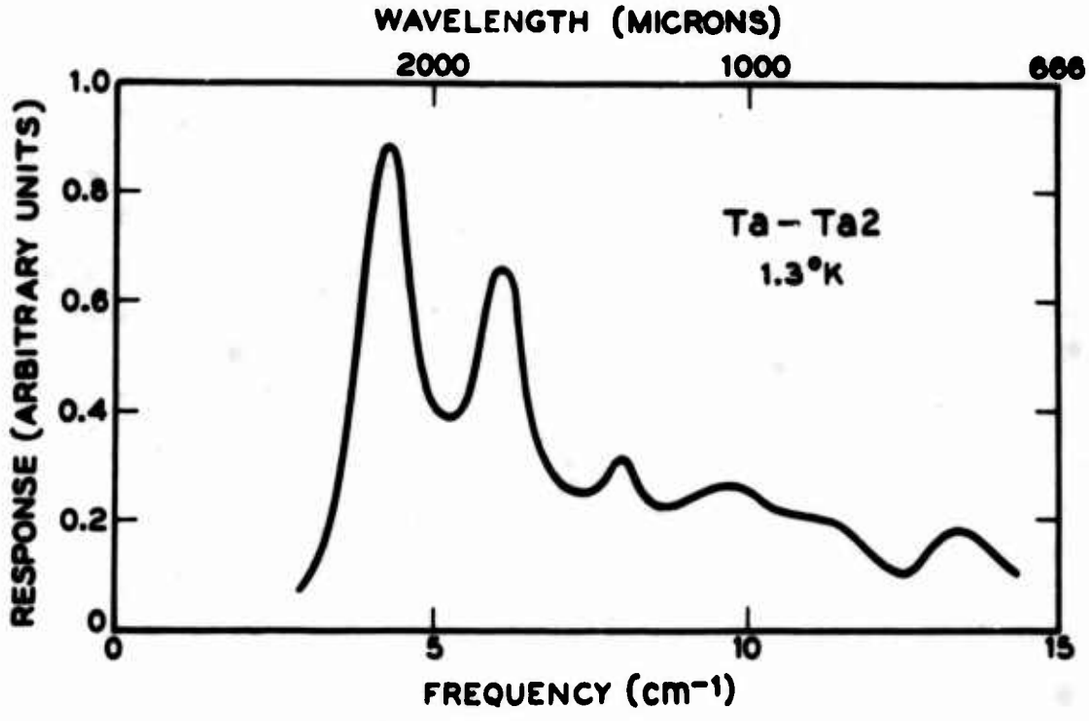

Fig. I-14 Spectral response of a Ta-Ta superconducting point contact.

increase the Josephson current. Again, the harmonically related structure is present. In fact, the second harmonic has been emphasized relative to the fundamental.

Figure 14 shows data for a Ta-Ta junction. Again the response is largely at frequencies below the energy gap and there is some indication of periodicity in the response.

We have also looked at Pb-Pb junctions and invariably they give rise to very strong, very sharp response curves at a frequency far below the Pb gap. Figure 15 shows a portion only of an interferogram for a Pb-Pb junction. You can clearly see that there is a dominant frequency in the spectrum and that the Q is rather high as measured by the slow decrease in amplitude of succeeding interference peaks. The resulting spectrum is shown in Figure 16.

There is a strong response at essentially one frequency which is well below the gap. Upon repeating the measurement with other Pb-Pb junctions there seems to be a strong tendency always to get a dominant response at some low frequency. We have seen such peaks as low as 1.5 cm^{-1} and as high as 14 cm^{-1} though usually not as narrow as in Figure 16.

We believe that the narrow response peaks seen for Pb and the harmonically related peaks in Nb-Ta junctions and the suggestion of periodicity in the response of Ta-Ta and Nb-Nb junctions reflect the fact that we are dealing with an active device.

It is well known that a Josephson junction wants to generate high frequency radiation especially if there is any kind of resonant circuit coupled to it - even if the Q of the resonance is very weak[10,17,18]. We know that such resonances can exist in our experimental light-pipe rig because it is really nothing but a metal box in which radiation can bounce around for a while before decaying. And so the junctions may be generating some radiation of their own as well as detecting the incident radiation and thereby giving rise to complicated response curves.

But regardless of the ultimate explanation for the exact form of the response curves, these infrared experiments are noteworthy for several reasons. They show that Josephson currents exist at frequencies well beyond the

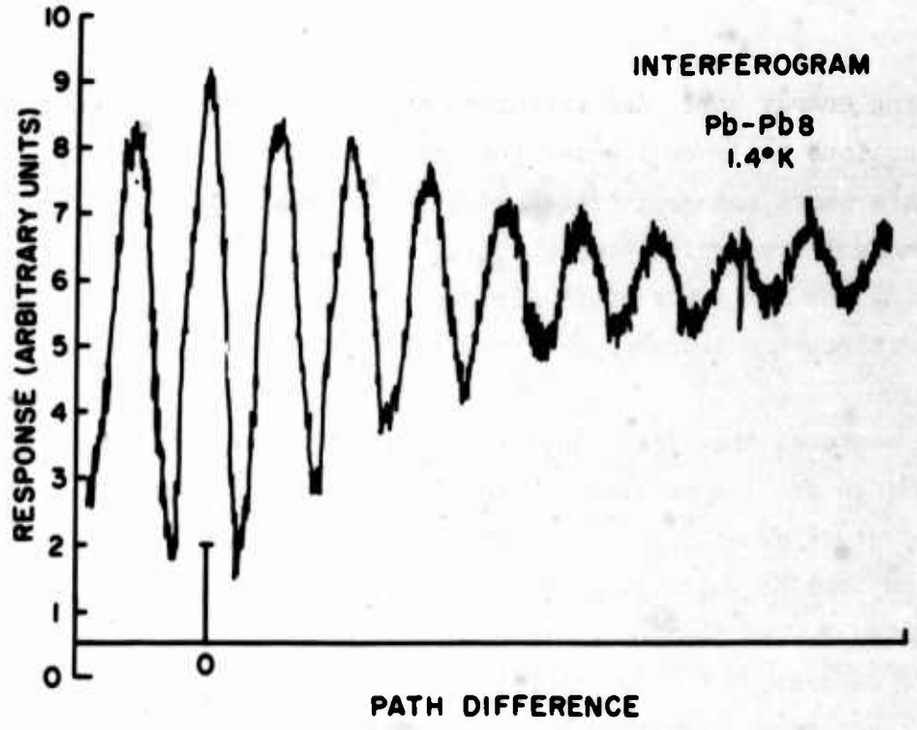

Fig. I-15 Portion of an interferogram for a Pb-Pb superconducting point contact.

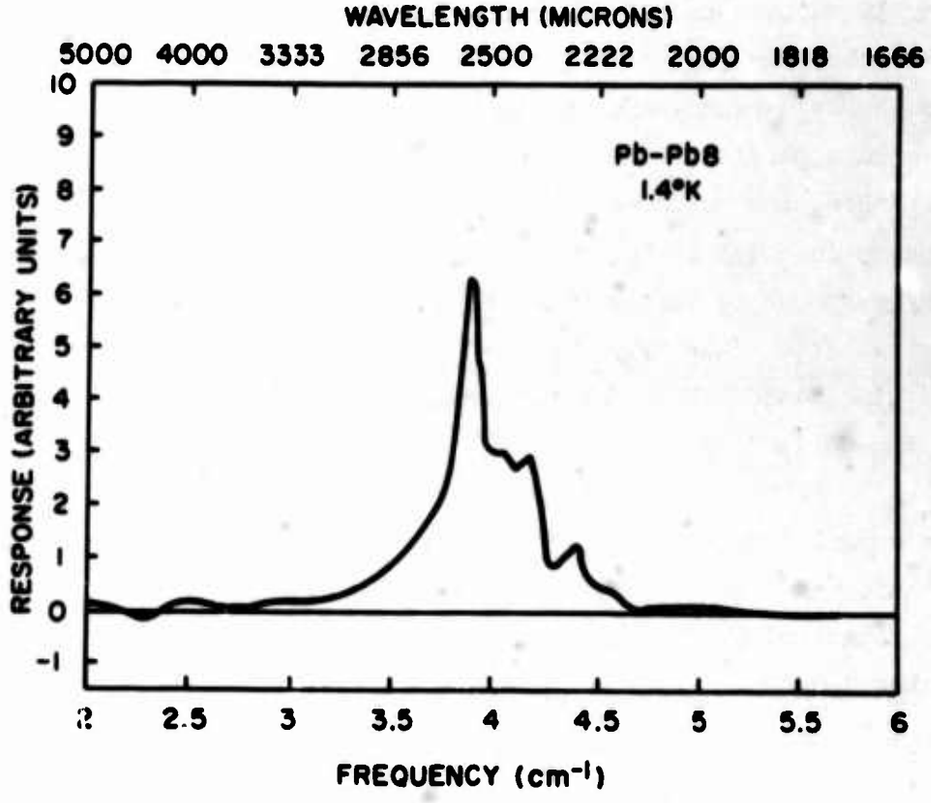

Fig. I-16 Spectral response of a Pb-Pb superconducting point contact.

superconducting energy gap. And therefore anything that can be done with Josephson junctions at lower frequencies can be done at infrared frequencies - provided we are smart enough to figure out the necessary circuits.

Furthermore the very fact the spectral response experiments could be done at all considering the low power available from standard arc lamps indicates that Josephson junctions are indeed sensitive detectors of millimeter and submillimeter radiation.

We have measured the video sensitivity of a Nb-Nb junction using available microwave sources at 4 mm and find, with a one second time constant, a noise equivalent power of about 5×10^{-13} W. Note that the frequency of this measurement was well below that at which we get maximum response. Yet the measured value compares favorably with that of other helium temperature infrared detectors.

Finally, we believe the detector to be capable of extremely high speed and to check this out we have carried out a relatively crude experiment in which a pulse of 4 mm radiation with a rise time of 10 nanoseconds, as observed with a conventional room temperature crystal detector, was applied repetitively to a Nb-Nb junction. The junction output voltage was observed on a sampling scope and reproduced the 10 nanosecond rise-time of the pulse.

Let me add that the Josephson junction is <u>not</u> a thermal detector and though it has response over a broad-band it can be used as a narrow-band detector with suitably designed apparatus.

To sum up then, the performance figures already achieved for the point-contact Josephson junction detector are:

Frequency response to wavelengths shorter than 300 microns.

Sensitivity better than 5×10^{-13} W noise-equivalent-power.

Response time better than 10 nanoseconds.

Acknowledgments

The work reported here was carried out in collaboration with C. C. Grimes and P. L. Richards and, in part, in collaboration with C. C. Grimes and M. A. Pollack. The technical assistance of G. Adams, A. Contaldo, and F. DeRosa is gratefully acknowledged.

References

1. C. C. Grimes, P. L. Richards and S. Shapiro, Phys. Rev. Letters 17, 431 (1966); and to be published.
2. See, for example, B. D. Josephson, Advan. Phys. 14, 419 (1965). Also, P. W. Anderson in Progr. in Low Temp. Phys., Vol. 5, ed. by C. J. Gorter, to be published.
3. J. E Zimmerman and A. H. Silver, Phys. Letters 10, 47 (1964).
4. J. E. Zimmerman and A. H. Silver, Phys. Rev. 141, 367 (1966).
5. A. H. Silver and J. E. Zimmerman, Phys. Rev. (to be published).
6. J. Clarke, Phil. Mag. 13, 115 (1966).
7. S. Shapiro, J. Appl. Phys. March 15, 1967.
8. A. Contaldo, (to be published).
9. J. I. Pankov , Phys. Letters 21, 406 (1966) and Phys. Letters 22, 557 (1966).
10. See, for example, D. N. Langenberg, D. J. Scalapino and B. N. Taylor, Proc. IEEE 54, 560 (1966).
11. N. R. Werthamer and S. Shapiro (to be published).
12. E. Riedel, Z. Naturforsch, 19a, 1634 (1964).
13. N. R. Werthamer, Phys. Rev. 147, 255 (1966).
14. N. R. Werthamer, private communication.
15. For details of the method and the instrument see P. L. Richards, J. Opt. Soc. Amer. 54, 1474 (1964).
16. C. C. Grimes, M. A. Pollack and S. Shapiro (unpublished).
17. A. H. Dayem and C. C Grimes, Appl. Phys. Letters 9, 47 (1966).
18. J. E. Zimmerman, J. A. Cowen and A. H. Silver, Appl. Phys. Letters 9, 353 (1966). See also, A. H. Silver and J. E. Zimmerman, Appl. Phys. Letters 10, 142 (1967).

QUANTUM GENERATION AND DETECTION OF PHONONS IN SUPERCONDUCTORS

A. H. Dayem
Bell Telephone Laboratories
Murray Hill, New Jersey

In a superconductor an excited quasi-particle of energy E (measured from the Fermi level) relaxes first to the top of the energy gap (of width 2Δ) emitting a phonon of energy $(E-\Delta)$ and then recombines with a mate to form a Cooper pair with the emission of a phonon of energy 2Δ.

In the experiment we use two identical Sn-Sn^{o}_{2}-Sn tunnel diodes evaporated on opposite ends of a sapphire single crystal. In the first diode, the generator, quasi-particles are excited by tunneling; they then relax, recombine and generate phonons, which are detected by the second diode, the receiver. Using pulse techniques one establishes that the received signal is produced by phonons propagating in the sapphire crystal from the generator to the receiver. The dependence of the received signal on the frequency of the generated phonons shows that the receiver responds only to phonons of energy $\geq 2\Delta$. Thus a tunnel diode can be used as a quantum counter.

It is obvious that this new technique for phonon generation and detection has great potential both for experimental research as well as device application

This work was published in Phys. Rev. Letters 18 125 (1967).

ON THE USE OF THE AC JOSEPHSON EFFECT TO MAINTAIN STANDARDS OF ELECTROMOTIVE FORCE

B. N. Taylor
RCA Laboratories
W. H. Parker and D. N. Langenberg
University of Pennsylvania

It was shown how a particular phenomenon arising from the ac Josephson effect in tunnel junctions and point contacts, namely, microwave induced constant-voltage current steps, can be used to provide a comparatively simple and inexpensive means for (1) checking on the constancy of reference standards of emf at the one ppm level for long periods of time, and (2) inferring at this same level of accuracy the relationship between the national reference standard of emf of one country and that of another country, thereby contributing to a better international assignment of the volt. The results of recent high accuracy, five ppm measurements of the above phenomenon[1] and the relative ease with which the techniques used in these measurements can be extended to the one ppm level were presented as evidence that these two goals can be reached in the immediate future. Practical considerations such as cost were also discussed as well as the future possibility of using the effect to calibrate emf reference standards in absolute units.

A detailed discussion of this work will appear in the October, 1967 issue of the quarterly journal, Metrologia, the International Journal of Scientific Metrology, published by Springer-Verlag.

---

1. W. H. Parker, B. N. Taylor, and D. N. Langenberg, Phys. Rev. Letters, 18, 287 (1967).

HIGH CIRCUIT Q's WITH NIOBIUM STANNIDE AT RADIO FREQUENCIES

K. Siegel, R. Domchick, F. R. Arams
Airborne Instrument Laboratory
Melville, New York

This work was supported by the U.S. Army Electronics Command. The program has as its goal the development of a simple refrigerated radio frequency preselector to reduce interference in radio communications.

Earlier models we have developed[1] have been of lead and have operated in liquid helium but obviously cooling by a small closed cycle refrigerator is preferred. Therefore, the investigation of niobium stannide with its high transition temperature.

The first portion of the talk will be about open cycle data.

A self-resonant coil was wound of commercial vapor deposited niobium tin ribbon 0.090 inch wide with no silver plating. It was wound on a teflon form and had a resonant frequency of 27 MHz. Inductive coupling loops were adjustable, so unloaded Q could be measured directly.

Figure 1 gives the results in a lead shield at 4.2 degrees K and below. There is good evidence that even these Q's are not limited by the niobium tin material but are due to dielectric loss. The low Q at room temperature is related to the fact that the 3 mil, nonmagnetic stainless steelsubstrate has nearly the same high resistivity as the niobium-sn.

In Figure 2 are the results at higher temperatures in an 8.0 inch diameter copper shield, as the system is allowed to warm slowly after liquid helium is transferred. The Q of 500,000 is limited by the copper shield with the small drop near 7 degrees believed due to the lead tin coupling loops going normal.

At 15 degrees, we see that the Q of the niobium tin itself is still better than 500,000.

A coil of 1/8 inch wide diffused niobium tin ribbon was tested in the same environment with essentially the same geometry, see Figure 3. The surface has been etched to remove any excess tin. This ribbon also yielded a Q of 4 million at 4.2 degrees and below in a Pb shield, even though it has this very marked

TEMPERATURE (°K)	UNLOADED Q
290	35
4.2	3.7 MILLION
2.1	4.2 MILLION
1.8	4.2 MILLION

Fig. L-1

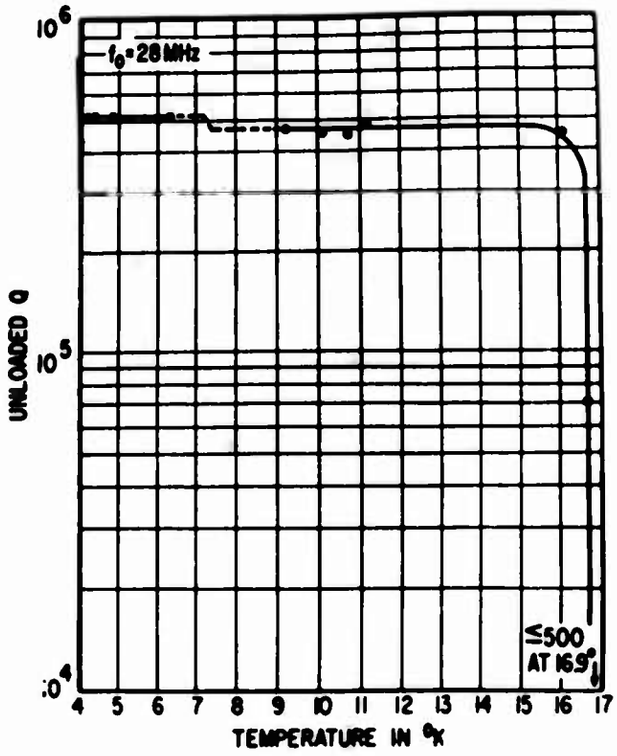

Fig. L-2

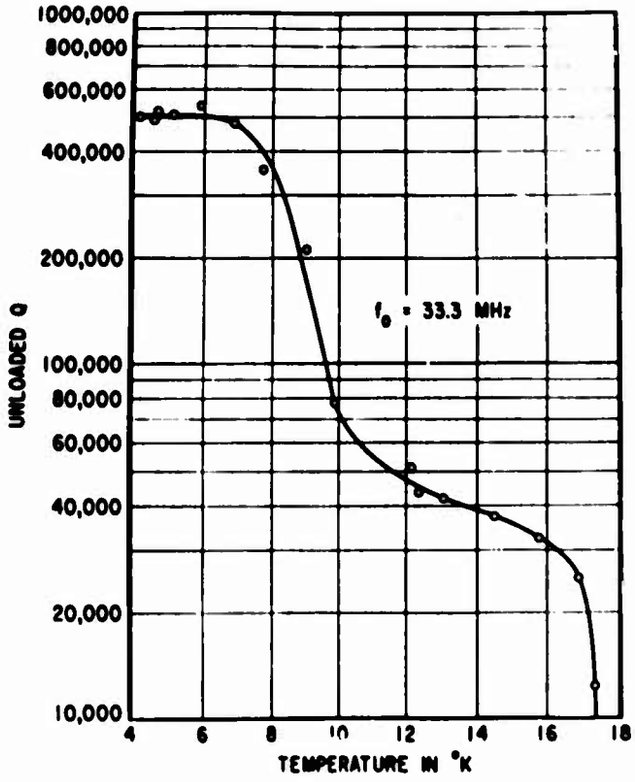

Fig. L-3

	PRESENT DATA	ROSENBLUM ET AL	EXTRAPOLATE $f^{3/2}$
T(°K)	R_S/R_N (26 MHz)	R_S/R_N (23 GHz)	TO 23 MHz
4.2	$< 3\,(10)^{-5}$	$< 10^{-3}$	$< 3(10)^{-8}$
16	$\doteq 3\,(10)^{-4}$	$5\,(10)^{-2}$	$1.5(10)^{-6}$

$Q_N \approx 100$ FOR SOLID Nb_3Sn RIBBON WITH THICKNESS $> \delta$

Fig. L-4

deterioration at the higher temperatures, indicating that the superconductor is not setting the limit on Q at 4.2^{o}. Also measurements of the loss tangent of the teflon used for this coil form were 9×10^{-6}, namely 3 per cent of the capacitance in the teflon form would limit the Q to 4 million.

Figure 4 is a listing of R superconducting to R normal where Q normal now is estimated from the room temperature numbers and the published values of resistivity for niobium-tin, but to be meaningful, it is assumed that the thickness of the superconductor is greater than the penetration depth when normal.

In the third column is the data of Rosenblum and associates[2], taken at 23 gc for H external equals zero. In the last column I put the classical three halves power extrapolation to 23 MHz, which assumes no gap effects or flux trapping.

You can see that these numbers come out to be much lower than the numbers we acually have. But as I say, we are limited by other things than the niobium-tin itself. You would have to have a variation of at least $f^{5/6}$ to agree with our 16 degree data. If it was slower than $f^{5/6}$ then the loss would be too high and we would have been able to measure it.

Figure 5 shows the results of the vapor deposited coil in a shield made from the diffused niobium tin foil. The helically wrapped shield and the open tops and bottoms are enclosed in a copper can. You see the fall-off with temperature, mainly due to the shield of the diffused niobium tin material. The three million data at 4.2 degrees doesn't quite go as high as 4 million and that is believed due to the copper tops and bottoms.

The second part of the talk is about data taken on a small closed cycle 10 degree refrigerator. Figure 6 is a photo showing the coil mounted on the cold plate of the refrigerator. The cold plate has been extended to fit the large copper shield. The coil is wound on lucalox, a poly crystal line aluminum oxide, which we measured to have a loss tangent of 1.4 times 10^{-6}, which is about the best material we have found. The thermal conductivity of the lucalox is extremely good.

Figure 7 is a plot of Q versus temperature taken on that coil on the refrigerator, for vapor deposited niobium-tin and a copper shield. The limit is imposed by the copper at 300,000.

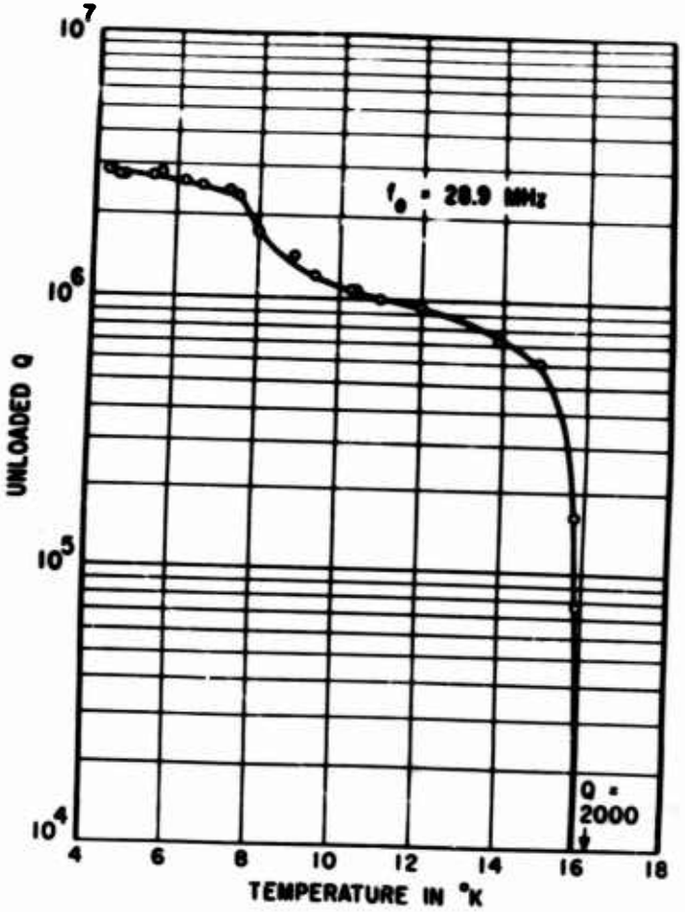
10^7
10^6
10^5
10^4
UNLOADED Q
f_o = 28.9 MHz
Q = 2000
4
6
8
10
12
14
16
18
TEMPERATURE IN °K

Fig. L-5

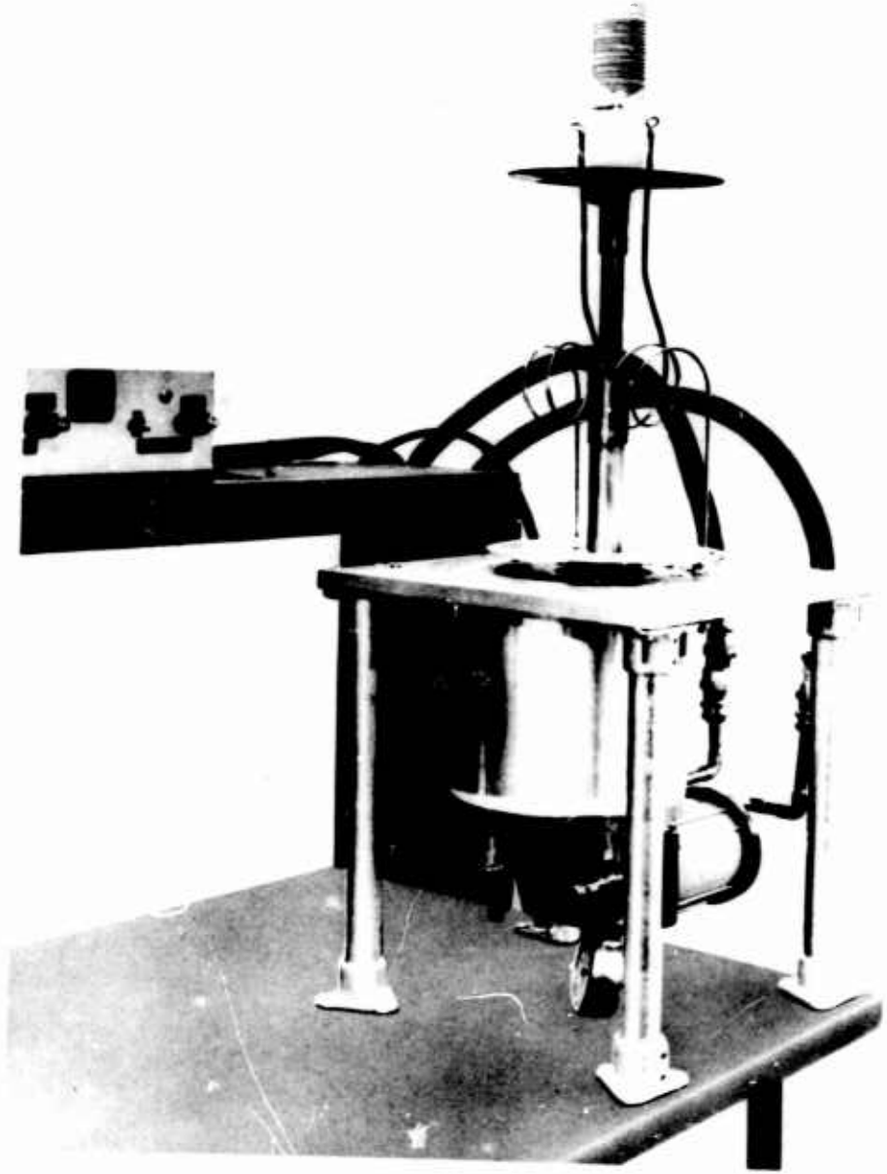

Fig. L-6

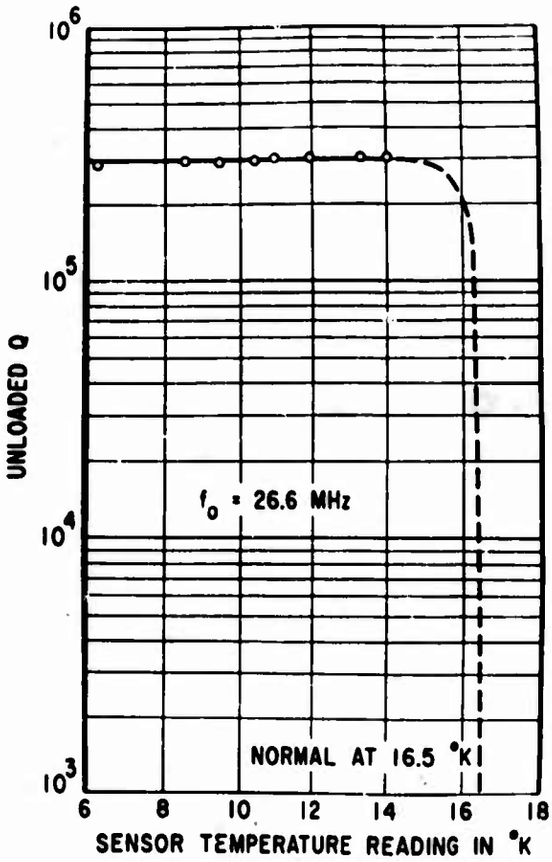
10^6
10^5
10^4
10^3
UNLOADED Q
f_o = 26.6 MHz
NORMAL AT 16.5 °K
6
8
10
12
14
16
18
SENSOR TEMPERATURE READING IN °K

Fig. L-7

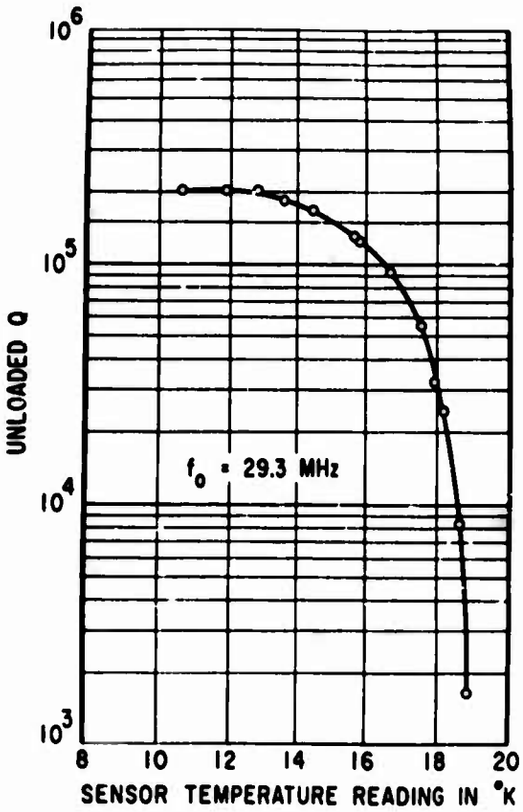
10^6
10^5
10^4
10^3
UNLOADED Q
f_o = 29.3 MHz
8
10
12
14
16
18
20
SENSOR TEMPERATURE READING IN °K

Fig. L-8

Figure 8 is essentially the same but for diffused niobium tin. Again the fall-off with temperature is noted for the diffused material.

A very interesting phenomenon was noticed during the last few months. There is an extreme nonlinearity which occurs, which is not reactive nonlinearity, of the type that you make parametric amplifiers out of because there is no detuning that takes place, just short of the threshold. The circuit is still tuned perfectly. Figure 9 is a plot of output versus input for vapor deposited niobium tin in a copper shield. Notice the initial run which is not restored by warming above the transition temperature. It seems to say something about flux trapping. At first we looked to see whether voltage breakdown could be the mechanism. That was ruled out. The maximum possible electric field of 400 volts per cm is much too low for the 10^{-6} ton pressure, and the threshold is not gas pressure dependent. We varied the gas pressure and checked that the threshold did not change.

The threshold is also not temperature dependent, which rules out local heating. And it is Q dependent. So it seems to be a critical current type of phenomenon, but the values of I and H are very small compared with Hcl of about a hundred gauss for niobium tin at this temperature[3]. Namely the peak current was 60 milliamperes and the peak magnetic field 0.16 gauss calculated at the ribbon surface. The low critical current may be due to a phenomenon described by Buchold[4] a few years ago to explain low frequency losses in superconductors, namely, surface voids with circulating currents in very small regions with high current density.

See Figure 10. This is the same coil material, but now, the vapor deposited ribbon is in a tight fitting shield of niobium tin. The shield was fabricated at an outside laboratory by diffusing tin into a niobium can and cover. Now this is the first time the diffused material did not degrade with temperature. Possibly, it may be related to the fact that the other materials were made for magnet applications and defects were introduced to improve the critical current density, whereas this was just done to provide a niobium tin surface.

The source of the 300,000 Q limitation is not really known at the present time. It may be due either to the fitting of the cover on the can, the can itself, or possibly due to the copper loops, by which energy was coupled in and out.

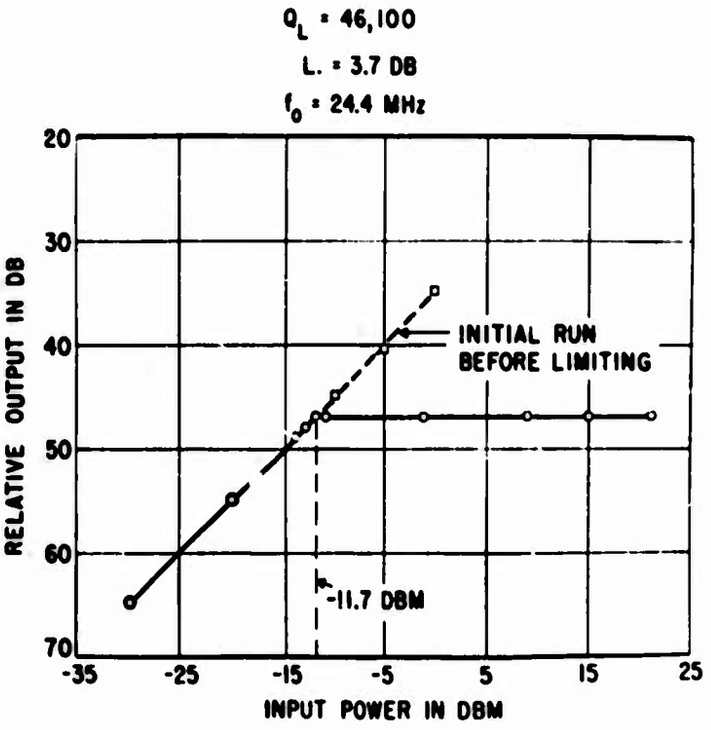

Fig. L-9

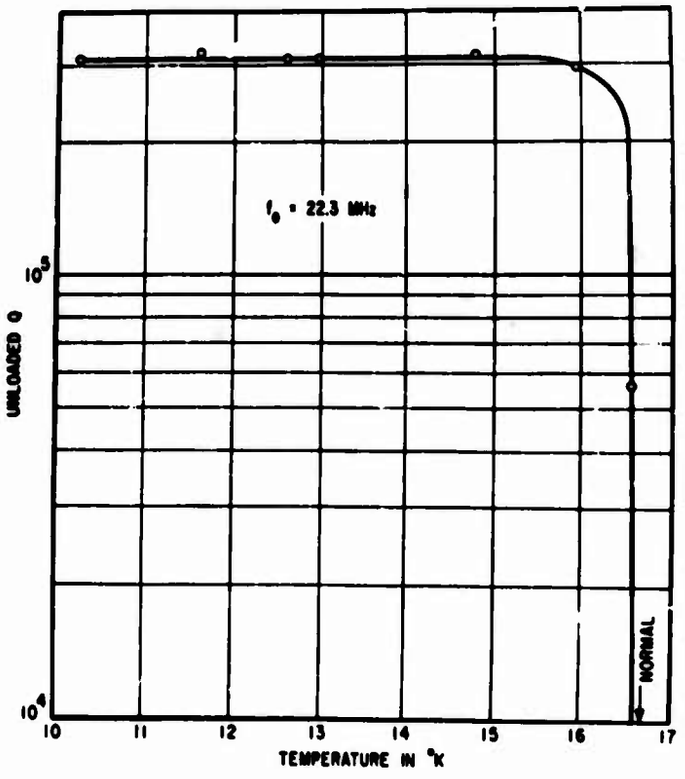

Fig. L-10

One very interesting fact related to the limiting, is that in this configuration, with the same coil as used before, no limiting was observed when this superconducting shield was present, up to more than one watt incident power, the maximum power available. The same coil was taken out of the circuit, put back into the copper can, and gave the marked limiting effect.

It was first thought by us that possibly a good portion of the earth's field was excluded from the inside by the superconducting shield. So I put a small magnet inside to supply a field comparable to the earth's field and coated it with copper so there wouldn't be too much loss. It had absolutely no effect so I think we have to throw out that possibility.

One other thing I can say about this, in the copper shield where it did limit, the threshold was found to be a function of the ambient field but not of the field when it went through the transition point, namely, not the trapped field.

Maybe somebody here may be able to figure out what is going on at these extremely small values of rf field. As I say, the order of a 10th of a gauss.

In summary, small signal radio frequency superconducting devices using niobium stannide appear quite feasible.

QUESTION: Did I understand you correctly that you found that you could not remove it by warming up and cooling once more?

SIEGEL: In the next experiment the process repeated. The virgin line was followed again. I was able to go up on that virgin curve and then drop down. I could not repeat that virgin curve without going to the next experiment. Just warming above the transition temperature would not restore me to the virgin curve. It just took me again to that same level. I didn't have a chance to check all the points in between; or whether heating to nitrogen temperature would have restored it.

References

1. F. Arams, J. Fradkin, E. Sard, and K. Siegel, "Superconducting Ultrahigh Q tunable R. F. Preselector", presented at the 1966 Communications Conference, Philadelphia, Pa.
2. B. Rosenblum, M. Cardona, and G. Fischer, "Microwave Studies of Niobium Stannide", RCA Review Vol. 25, No. 3, Sept. 1964, pp. 491-509.
3. R. Hecht, "Lower Critical Field of Niobium Stannide", RCA Review Vol. 25, No. 3, Sept. 1964, pp. 453-465.
4. T. A. Buchold, "About the nature of the Surface Losses of Superconductors at Low Frequencies," Cryogenics Vol. 3, No. 3, Sept. 1963, pp. 141-149.

MILLIDEGREE NOISE THERMOMETRY*

R. A. Kamper
Cryogenics Division, Institute for Materials Research
National Bureau of Standards, Boulder, Colorado

I would like to make it clear right at the beginning that what I want to discuss is a suggestion only. I have as yet no experimental demonstration that it works. [1]

The suggestion is that since the linewidth of Josephson radiation is temperature dependent, we might use it for thermometry. In order to discuss the expected performance and limitations of such a thermometer, I shall take as a model Zimmerman, Cowen and Silver's circuit for observation of Josephson radiation [2] at 30 MHz, which is represented in essence in Figure 1.

The Josephson junction is connected in parallel with a small resistance R which provides the bias voltage. Although one cannot neglect the inductance of the connections when considering the radio-frequency aspects of the system, it will turn out that the important components of the noise which we will consider are at low frequencies, so we may take the circuit as it is drawn.

Both the junction and the bias resistor generate noise. In his talk, Scalapino discussed the various mechanisms of junction noise, which depend on the properties of the individual junction and may impose a low temperature limit on thermometry if there is a significant temperature-independent component. However, if the bias resistor has a low impedance, compared with the junction, then its thermal noise will be the largest contribution and I want to concentrate on that.

The effect of noise is to introduce a random frequency modulation of the emitted radiation, which is thereby spread over a band of finite width. We

* This work was supported in part by NASA

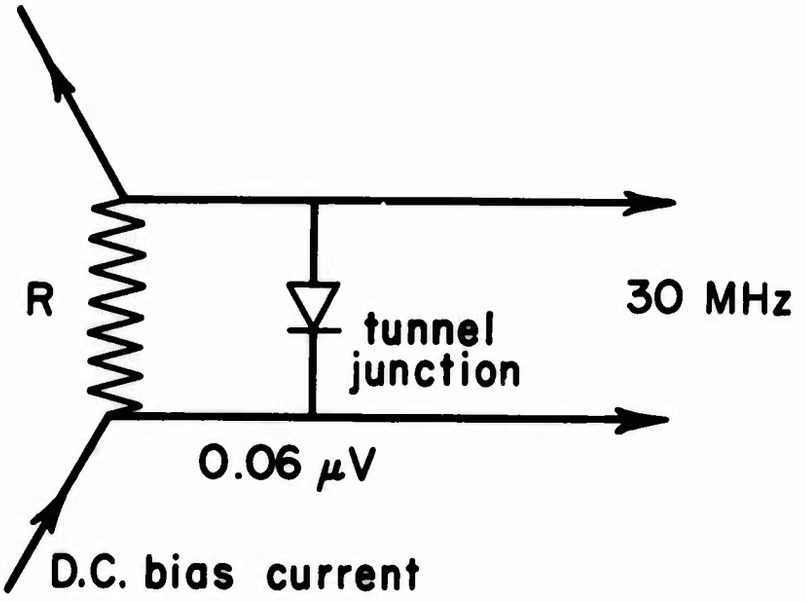

Fig. M-1 Circuit for generating radio-frequency Josephson radiation.

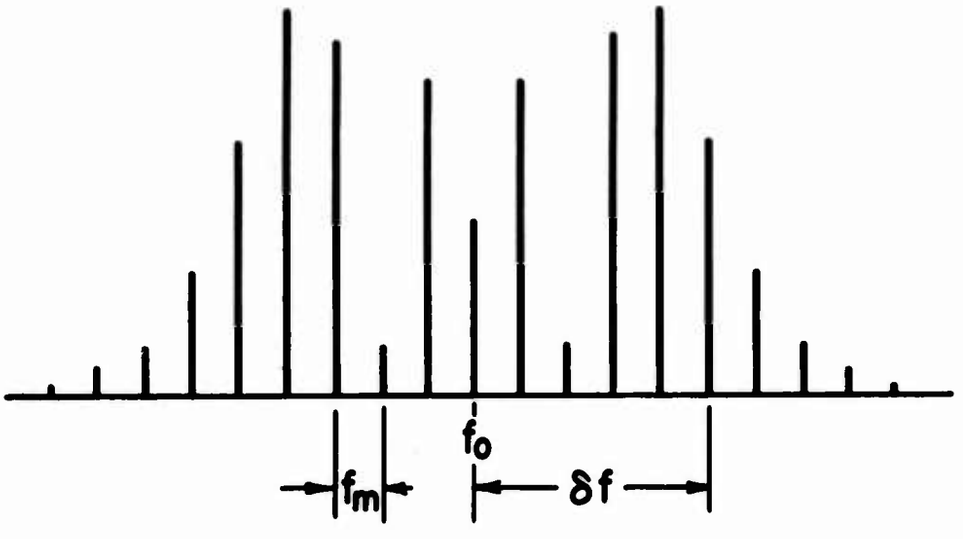

$$\cos\left[2\pi f_o t + \frac{\delta f}{f_m}.\cos(2\pi f_m t) \right]$$

Fig. M-2 Spectrum of a frequency-modulated sine wave.

can estimate this linewidth by a very simple physical argument, which leads to a result similar to one which Burgess obtained in his talk by much more respectable mathematics.

Figure 2 is a reminder of what the spectrum of a frequency modulated wave looks like. It represents a sine wave whose frequency is modulated over a range δf, on either side of a center frequency f_o, at a modulation frequency f_m. As you can see, the result is an array of evenly spaced side-bands at interval f_m. All the side-bands of significant amplitude lie in a range δf on either side of f_o. If the modulation is at a high frequency, it may happen that f_m exceeds δf. Then there would be no large side-bands. Most of the signal would be in the central peak at f_o and a receiver would not detect the modulation. Physically this corresponds to the situation where the variation of phase due to the modulation is less than one cycle.

Thus high frequency components of frequency modulation are not effective in broadening the line unless the depth of modulation δf exceeds the modulation frequency f_m.

Bearing this in mind, we take Nyquist's formula for the thermal noise voltage V on a resistance R

$$\langle V^2 \rangle = 4kTRf_c \tag{1}$$

where T is the absolute temperature and f_c is the width of the band of noise to which the system is sensitive. This extends from zero frequency up to the cutoff we have just discussed, where the frequency of the modulation is too high for effective line broadening.

The depth of modulation δf resulting from this noise is given by Josephson's formula

$$\delta f \approx 2e \sqrt{\langle V^2 \rangle} /h \tag{2}$$

Equating δf to f_c and combining equations (1) and (2) we find that the linewidth $2\delta f$ is given, at least in order of magnitude, by

$$2\delta f \approx 32kTRe^2/h^2 \tag{3}$$

Thus the linewidth of the radiation depends upon the value of R, and for thermometry this should be as large as possible.

Zimmerman, Cowen and Silver [2] discussed the limitations on R and showed that there are two which one must worry about. One is that the current passing through R to provide the bias voltage must exceed the DC critical current of the junction, and the other is that the larger R becomes the smaller is the signal power available for detection. With a bias resistor of 3.6μΩ they got a big enough signal to detect directly with a sensitive receiver. By using lock-in detection one could use a signal at least an order of magnitude smaller, so 100μΩ would be an easily attainable value for R which would not impose too stringent requirements on the junction. In that case the linewidth $2\delta f$ of the radiation would be

$$2\delta f \approx (3 \times 10^3)T \text{ Hz/deg.K},$$

so if one can measure it to one cycle per second one would get a resolution of the order of one millidegree.

The receiver for such a measurement would be no problem. The lower limit of the attainable bandwidth of a receiver is imposed by the stability of the local oscillator. A very simple crystal-controlled oscillator would suffice for this purpose. It is quite common practice to achieve bandwidths less than one cycle per second at radio frequencies.

As for the bias current supply, one has to worry about stability and flicker noise. Most electronically stabilized power supplies would not be good enough. However, it has been shown [3] that at least the flicker noise from an ordinary flashlight battery is small enough to be tolerable for our purpose. Hopefully, a mercury cell would have just as little noise combined with the advantage of long-term stability.

Thus with simple equipment one could measure temperatures down to one millidegree, provided that there is no significant source of noise, independent of temperature, which could mask the effect of the bias resistor at low

temperature. As a thermometer this would have the great virtue that one is measuring the temperature of the conduction electrons in a block of metal, which can be soldered directly to the other metal parts of a cryostat, ensuring good thermal contact.

REFERENCES

1. For a preliminary experimental test see: A. H. Silver, J. E. Zimmerman and R. A. Kamper, Applied Physics Letters (to be published).
2. J. E. Zimmerman, J. A. Cowen and A. H. Silver, Applied Physics Letters 9, 353 (1966).
3. K. F. Knott, Electronics Letters 1, 132 (1965).

DISCUSSION

Zimmerman: I might say that we have recently measured the line-width of the Josephson radiation at $4^{\circ}K$, and we get about 5kHz, which would be exactly what you have there.

Kamper: Thank you.

Zimmerman: You said that the limit on the bias resistance might be something like $100\mu\Omega$. I didn't get the argument there.

Kamper: That was a conservative guess. I hope that one might do better.

Zimmerman: I think the resistance could be much larger without limiting the detectability of the signal.

THE JOSEPHSON JUNCTION AS A SWITCHING DEVICE

J. Matisoo
IBM Watson Research Center
Yorktown Heights, New York

I would like to describe yet another device application of Josephson junctions: that of a switch or logic element. This application uses the Josephson junction as a two state device. One state is the zero voltage pair tunneling state, the other, the quasi-particle tunneling state. Transition between states is controlled by a combination of fields and currents in the junction.

The first figure shows the structure I'll be talking about. The junction is made in the usual way by evaporating tin, oxidizing it, and evaporating the second layer. The structure is somewhat unusual in that the junction is formed by the overlap of the ends of the two tin strips. Under the junction is a ground plane.

Above the junction is a lead line, the so-called control, by means of which perpendicular magnetic fields are applied to the plane of the junction. That is, the field is perpendicular to the direction of current flow in the tin strips.

I'd now like to go over the junction characteristics pertinent to the device and only then go into details of device operation.

Figure 2 shows a junction i-v curve, to orient you to the scale of currents and voltages. There is a zero voltage region with a maximum zero voltage current of approximately 30 ma. There is a quasi particle tunneling region showing the tin gap of approximately 1 mv. and a limiting resistance of a hundreth of an ohm. Transitions are indicated by the dotted lines.

The region of interest is shown in greater detail in Figure 3. This curve as well as the previous curve was traced with a current source. As the current is increased from zero, the voltage is zero, up to in this case a maximum of 32 ma.

As the current is further increased the junction undergoes a transition to the quasi particle tunneling state. An important device parameter is the time duration of this transition which will be discussed later. As current is decreased the quasi particle curve is followed until $V = \Delta$, then there is an abrupt

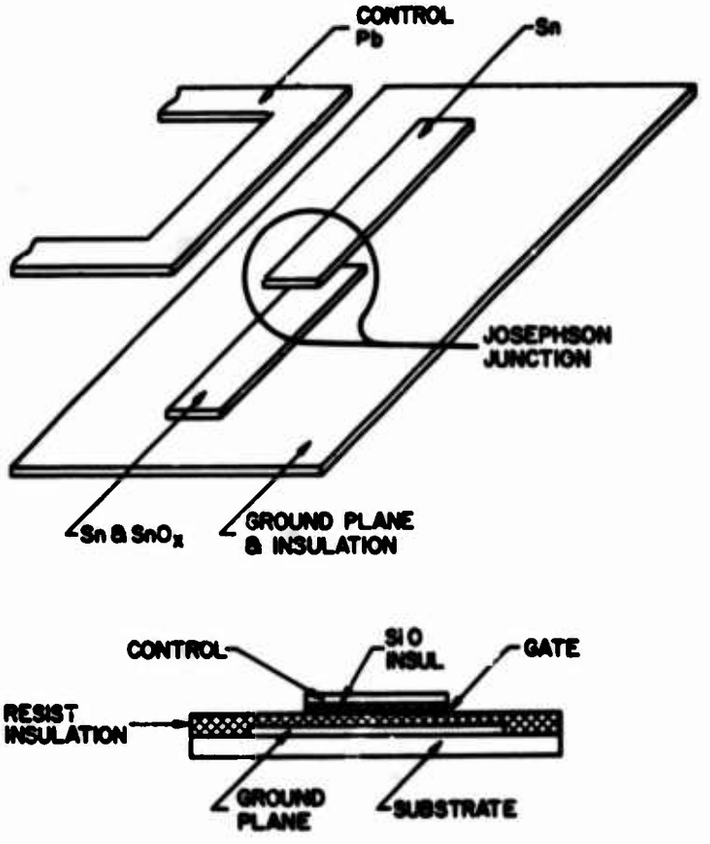
CONTROL
Pb
Sn
JOSEPHSON
JUNCTION
Sn & SnO_x
GROUND PLANE
& INSULATION
CONTROL
SiO
INSUL.
GATE
RESIST
INSULATION
GROUND
PLANE
SUBSTRATE

Fig. N-1

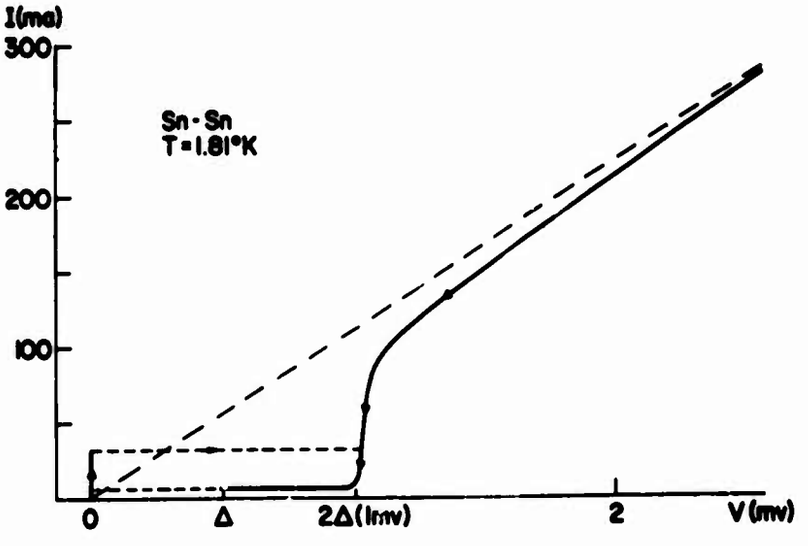
I(ma)
300
200
100
Sn - Sn
T = 1.81°K
0
Δ
2Δ(1mv)
2
V(mv)

Fig. N-2

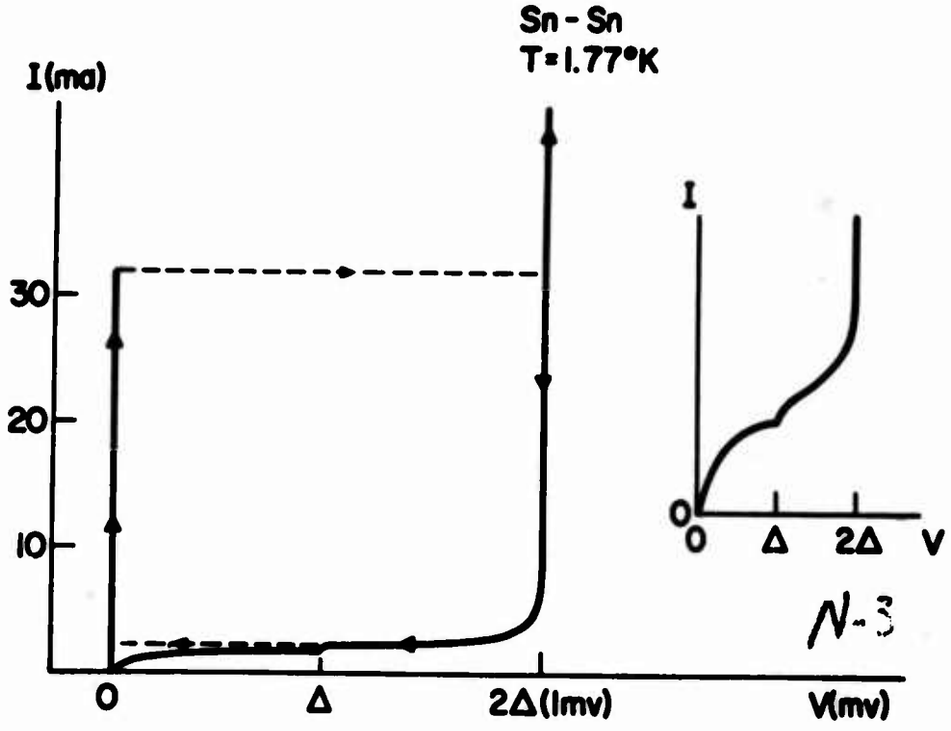
Sn - Sn
T = 1.77°K
I(ma)
30
20
10
0
Δ
2Δ(1mv)
V(mv)
I
0
Δ
2Δ
V
N-3

Fig. N-3

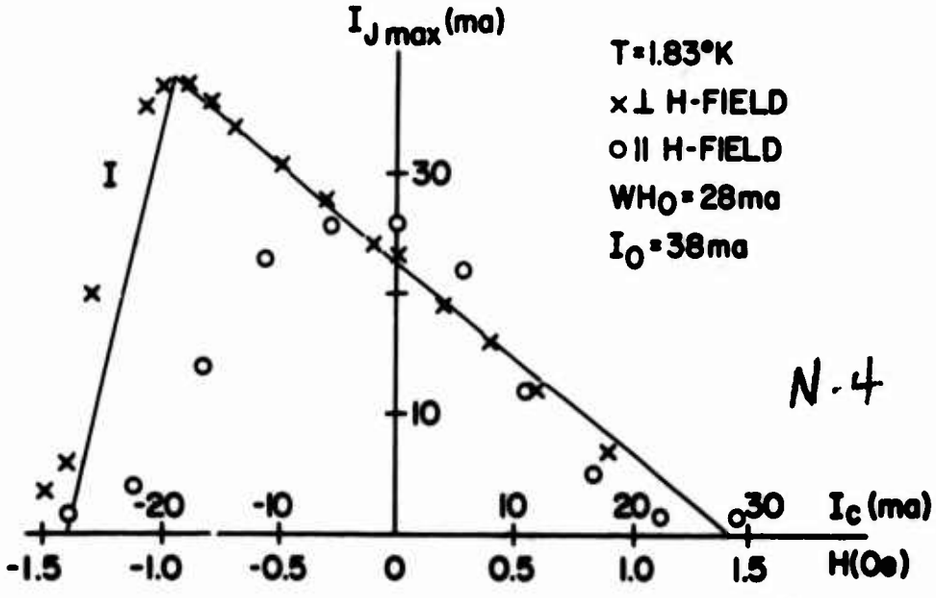
$I_{J\,max}$(ma)
T = 1.83°K
× ⊥ H-FIELD
○ ∥ H-FIELD
WH_0 = 28ma
I_0 = 38ma
I
30
10
-20
-10
10
20
30
I_c(ma)
-1.5
-1.0
-0.5
0
0.5
1.0
1.5
H(Oe)
N-4

Fig. N-4

transition to the zero voltage state. Thus this region between $V = \Delta$ and $V = 0$ is generally not visible. It can, however, be made visible by completely suppressing the zero-voltage current by applying a sufficiently large field, in this case, approximately 20 gauss. The insert shows the current on an expanded scale. The discontinuous onset of the two particle process at $V = \Delta$ is clearly visible. Thus, the current value at which the junction reverts to the zero voltage state consists of the thermally excited quasi particles and the small contribution from two-electron tunneling.

The reason for this junction behavior is that as the zero voltage critical current is exceeded we externally constrain the current to remain constant. The only stable operating point is on the quasi particle curve having the same current. This has been chosen so that $V = 2\Delta$. Clearly, for V greater than or equal to Δ, $\frac{\partial \psi}{\partial t}$ of the phase difference is such that the oscillating supercurrents are in excess of gap frequency. Thus, not only are the phases of the two superconducting regions not locked in time, nor increasing steadily in time, but there is no particular relationship between them. For a current such that $V \leq \Delta$, the zero voltage region is re-established (recall that the <u>voltage</u> is unconstrained).

With the application of a magnetic field the critical zero voltage current changes. How, is shown in Figure 4. This is a plot of maximum zero voltage current as a function of external field. Consider the "x"'s. The field in this case is applied via current through the control. In fact, on the horizontal axis, the field is given both in units of current and field. The open circles are for the case in which the external field is along the axis of the junction. We'll consider these curves in greater detail in a moment. The thing I would like to point out now is that one can lower the critical zero-voltage current by 40 ma by a change of only 10 ma in the control current.

These curves can be understood by a simple scheme. In fact, the solid line through the x's represents theoretical fit.

Assume that the <u>total</u> critical zero-voltage current is determined by the <u>total</u> field, the self field as well as the external field and that the fall-off of this critical current is linear in field. For the perpendicular case or current through the control, the external field either adds or subtracts from the self

field. Thus, H is just given by the second equation in Figure 5. The factor of two in I_g comes from the fact that on the average only 1/2 of the tunneling current contributes to the field in the junction. The final equations are obtained by substituting (2) into (1). The resulting curves are plotted in Figure 6. As you can see one obtains a curve of the appropriate character.

In the case in which the external field is along the tin strips there is no asymmetry in this curve since the external field is at right angles to the self field.

After this somewhat lengthy introduction, it is obvious how a switch might be built, and how it will operate (see Figure 7).

Suppose that the tunneling junctions have been biased so that the critical current is at its maximum value. Recall from the previous slide that in this case the application of a control field of appropriate polarity drastically reduces the critical current.

Switching then is achieved in the following way. Consider (1). A current I_g, chosen to be less than $I_{J_{max}}$ with $I_c = 0$ is forced through the junction. If a pulse of appropriate polarity is passed through the control, $I_{J_{max}}$ is suddenly lowered as indicated, with the result that the junction undergoes a transition to (2).

If there is a superconducting path in parallel with the junction, current will transfer to this parallel path. During the major portion of this current transfer process, the equivalent circuit of the junction is that of a battery shown in the insert. R is $\frac{dV}{dI}$ of this quasi particle current region, typically $10^{-3}\ \Omega$. This implies that the time required for the current to transfer is determined solely by the inductance of the superconducting path, with the result that this time can be very short, indeed a few hundred picoseconds.

The time of the transition itself from the pair tunneling to the quasi particle tunneling state has been measured by only establishing an upper bound, the measurement rise time having been restricted by the inductance of an unshielded portion of the measurement apparatus. Nevertheless, Figure 8 shows the transition from the pair to the quasi particle state and back.

The bottom trace is taken with the current through the junction below the

$$I_g(H) = I_0\left(1 - \frac{|H|}{H_0}\right)$$

$$|H| = \frac{\left|\frac{I_g}{2} + I_c\right|}{w}$$

$$\therefore\ I_g = \frac{I_0}{1 + \frac{I_0}{2wH_0}}\left[1 - \frac{I_c}{wH_0}\right]\quad I_g \geq 0;\ I_c \geq -\frac{I_0}{2}$$

$$I_g = \frac{I_0}{1 - \frac{I_0}{2wH_0}}\left[1 - \frac{|I_c|}{wH_0}\right]\quad I_g \geq 0;\ I_c \leq -\frac{I_0}{2}$$

Fig. N-5

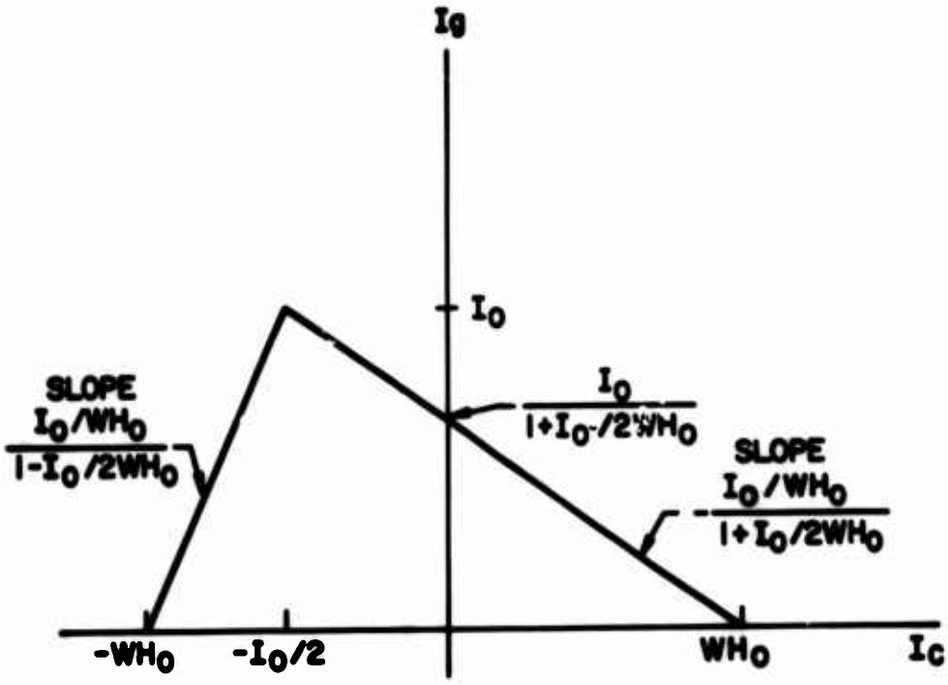

Fig. N-6

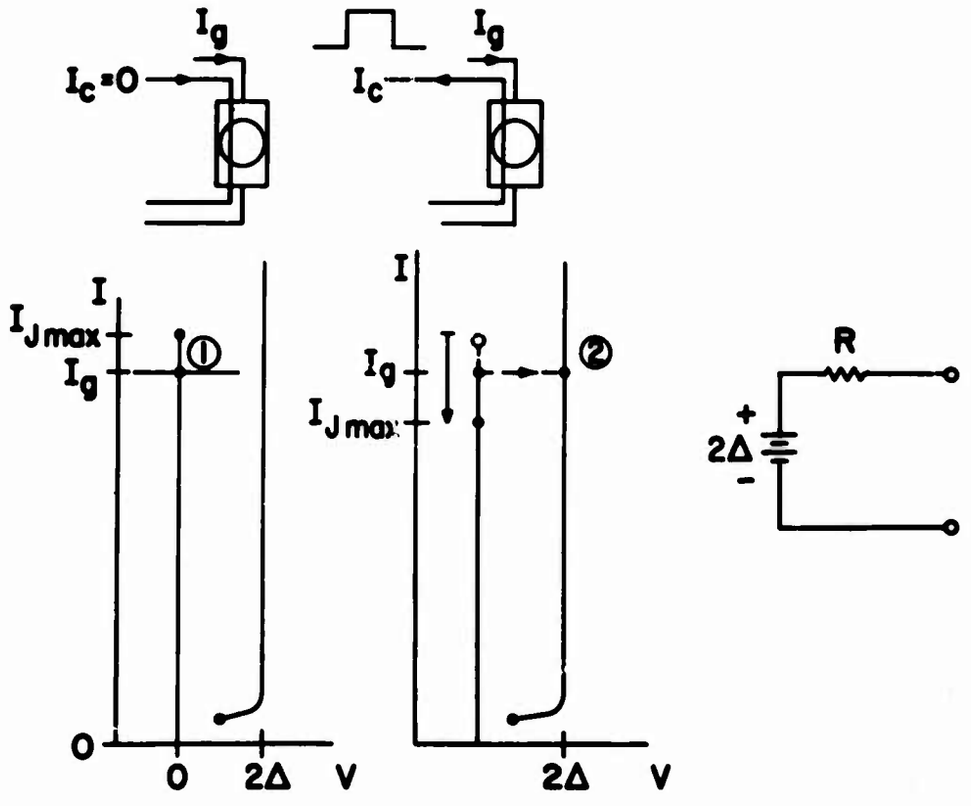

Fig. N-7

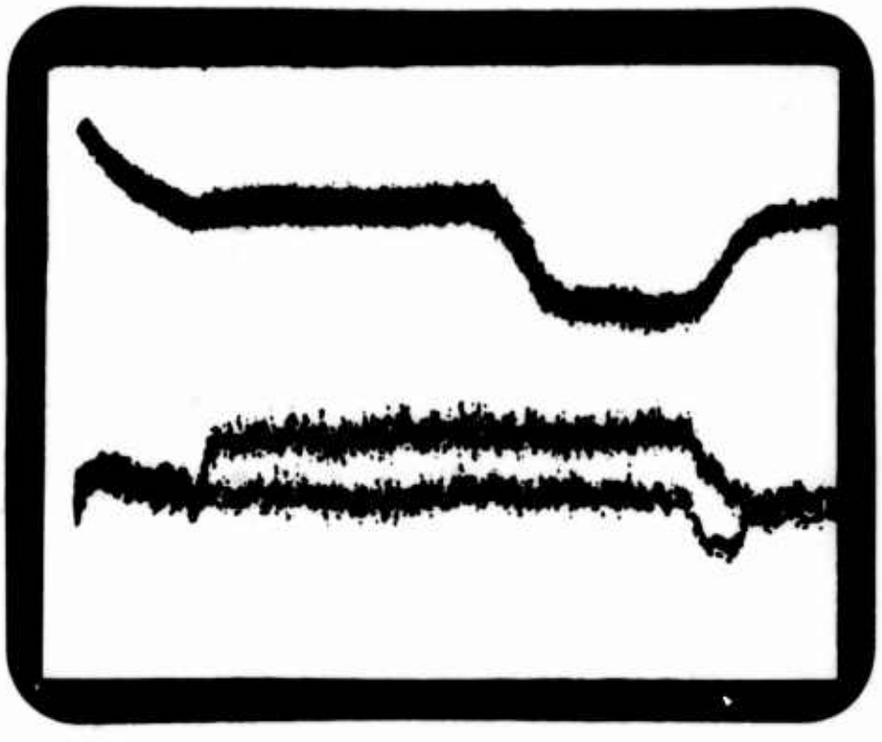

Fig. N-8

threshold the upper trace with current immediately above. The vertical calibration is 1 mv/cm; the horizontal calibration is 10 ns/cm. The uppermost trace is a double exposure of the drive pulse (and reflection). The rise time of the driving pulse is $\sim$ 15 ns. It is obvious that the rise of the voltage across the junction is substantially shorter.

In fact, Figure 9 shows the transition on an expanded scale. Again we have traces below and above the threshold. Here, however, the time scale is 0.5 ns/cm. Thus the transition time is bounded by $\sim$ 1 ns.

Finally, Figure 10 shows the transition from the quasi particle to the pair state at the end of the pulse. The time scale is 2 ns/cm. Since the transition begins at $V = \Delta$ and ends at $V = 0$, the transition time is again bounded by $\sim$ 1 ns.

Typical junction characteristics are summarized in Figure 11.

In summary, the Josephson junction as a switching device exhibits the following device characteristics: Transition times of $\leq$ 1 ns; current transfer times of 1 ns or less depending upon circuit characteristics. Finally current gain is achieved since the amount of current required to control the threshold is substantially less than the current flowing through the junction.

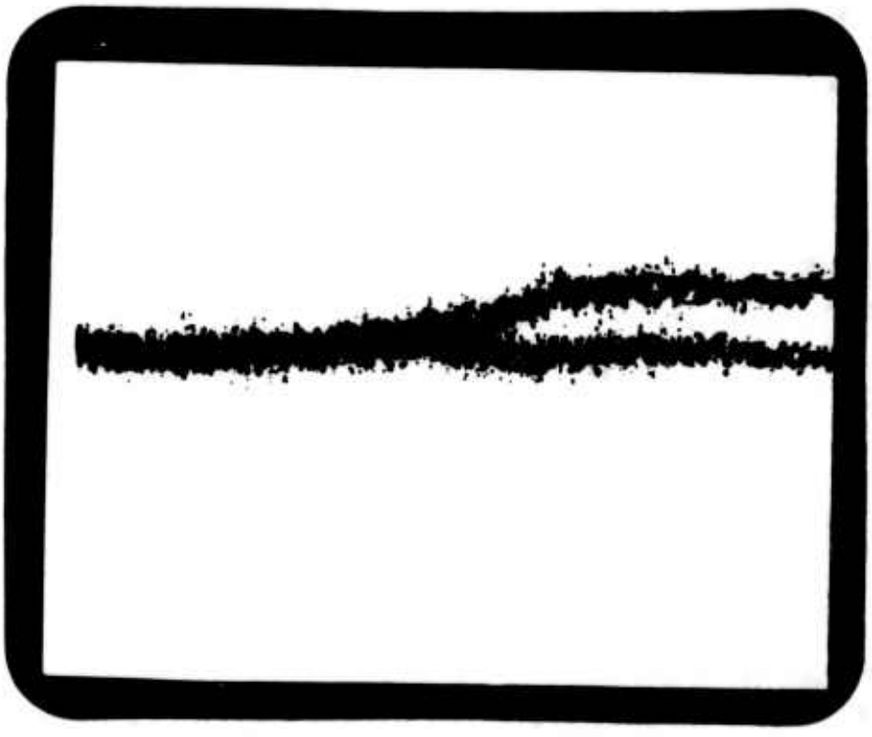

Fig. N-9

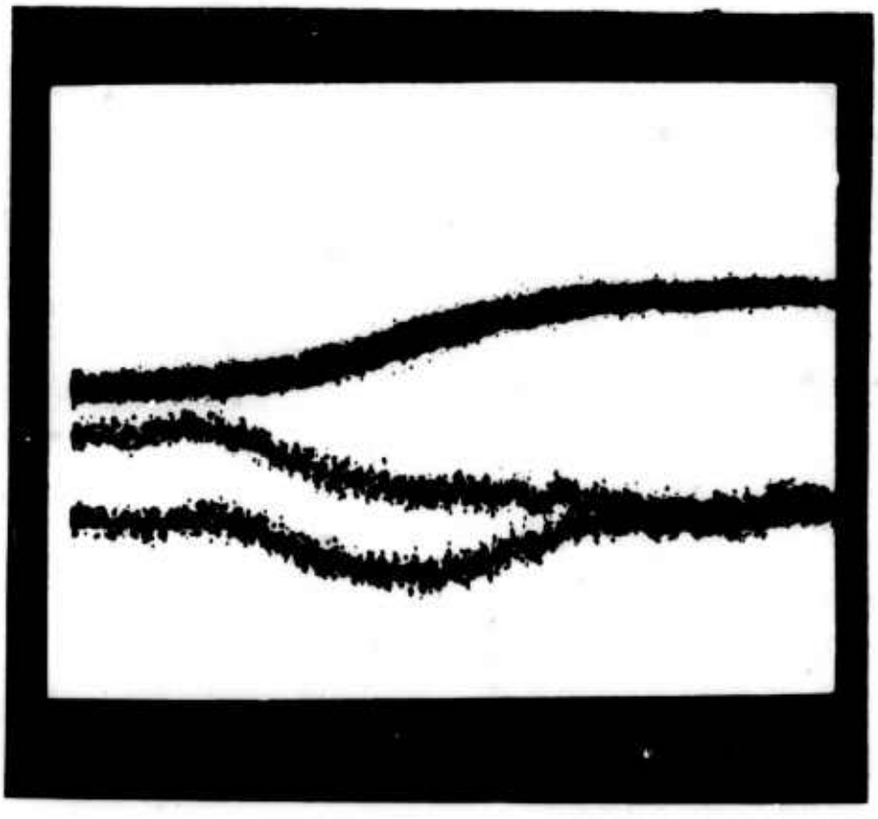

Fig. N-10

TYPICAL JUNCTION PROPERTIES

1. Sn-Sn junctions; thermally grown oxide
2. Junction size: roughly circular 10 mil diameter
3. Maximum Josephson current: 25 ma (zero external field)
4. $\lambda_J \cong 0.05$ mm.
5. Effective junction inductance: $\sim 1.5 \times 10^{-14}$ h
6. Junction capacitance: $\sim 5 \times 10^{-10}$ f
7. Josephson cut off frequency:

$$\omega_0 = \left(\frac{2e I_{J_{max}}}{\hbar C} \right)^{1/2} \cong 3 \times 10^{11}$$

N-11

8. On quasi particle curve:

$$\frac{dV}{dI} \cong \text{const} \cong 10^{-3}\,\Omega \quad \begin{cases} 3 \text{ ma} \leq I \leq 70 \text{ ma} \\ V > 2\Delta \end{cases}$$

Fig. N-11

THE ATTAINMENT OF ZERO MAGNETIC FIELD IN A SUPERCONDUCTING LEAD SHELL*

A. F. Hildebrandt
Physics Department, University of Houston
D. D. Elleman
Jet Propulsion Laboratory

Static magnetic fields of less than 2×10^{-6} gauss have been realized by utilizing the Meissner effect in a superconducting lead shell, shown in Fig. 1, in a room-size μ-metal shield. The length of the lead shell was 37 cm. with a radius of 7.5 cm. and a wall thickness of .025 cm. The fabrication technique consisted of fusing freshly cut lead sheets of 99.9999% purity. Fusing was accomplished with a clean copper soldering tip which was controlled with a variac. A heat sink was used to prevent flowing of the lead and solder flux was omitted.

Figure 2 shows a sectional view of a double walled prefabricated μ-metal shield. The inside dimensions are those of a six foot cube and the outside dimension is eight feet. A partial vacuum of .2 psi between the inner and outer door provided a stable magnetic contact as suggested by B. J. Patton.[1] To provide adequate breathing air for the operator during a helium transfer it was necessary to use a rubber air line (standard SCUBA gear is unsatisfactory because of its magnetic nature).

The ambient field inside the μ-metal shield was less than 100 microgauss provided the surrounding lab temperature was constant within a few degrees. Actually when the room was first assembled it had a field of about 5,000 microgauss but this was reduced to 100 microgauss with a tape degausser. The field could be cancelled further with triaxial Helmholtz coils of 1 meter diameter. The field variation over a 7.5 cm sphere could be reduced to less than 10 microgauss. Field

*Research supported by the National Aeronautics and Space Administration under Contract No. NAS 7-100.

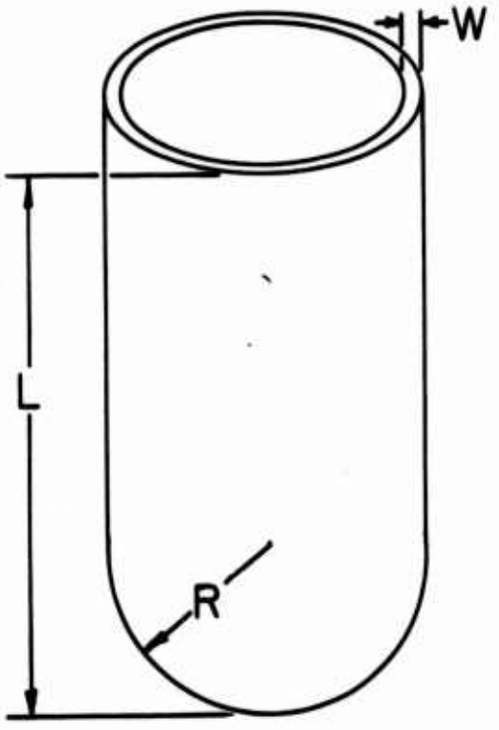

LEAD SHIELD

Fig. O-1

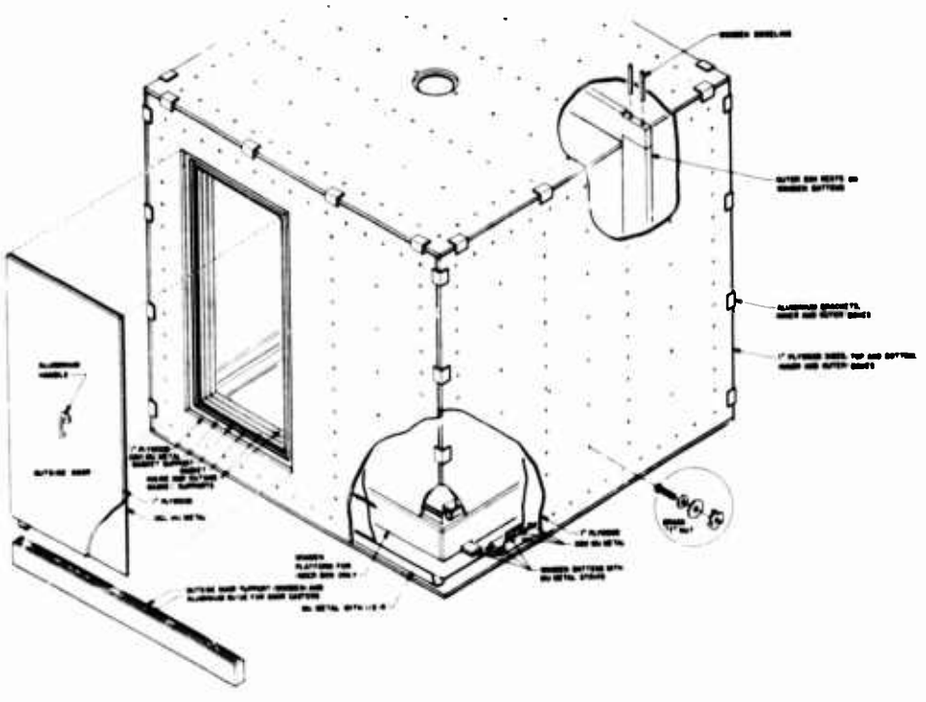

Fig. O-2

measurements were made with a Hewlett Packard Fluxgate probe. In order to attain .2 microgauss sensitivity with the device it was necessary to assure voltage stability and to flip the probe through 180°.

The results of six separate experiments of the lead shell in a reduced field are shown in Figure 3. To obtain a low B_t (axial field trapped in the lead shell) one must exercise care during the transfer. First, a non-magnetic extension such as glass must be added to most transfer tubes and second, the transfer of liquid should be slow (fifteen minutes or longer). With this procedure it was found that no fluxoid was trapped within experimental error over an axial length of 15 cm for each initial field except for one run at 500 microgauss. The field perpendicular to the axis was also found to be negligible. Thus, it is concluded that a pure lead hemispherical shell in small fields exhibits a good Meissner effect.

It should be noted that the cylindrical geometry used here is ideally suited for A. C. magnetic shielding. Any time-varying fields having a frequency less than cut-off are attenuated logarithmically with axial distance by a perfectly conducting hollow tube. Since the superconductor is a perfect conductor down to zero frequency it will attenuate all frequencies less than cutoff.

When hollow tubes without a closed end were made to go superconducting in zero applied field quite different results were obtained. For pure lead tubes of 2.5 cm diameter and 7.5 cm length fields of 10-15 microgauss were found to be trapped. Similar results were reported earlier for lead electroplated on brass where a larger effect was first suspected to be due to ferromagnetism.[2] These effects have been studied further in pure lead tubes by adding a warm helium gas switch shown in Fig. 4. The glass tube has been bonded to the lead tubes in a variety of ways including thick coatings of polystyrene cement, Dow Corning #11 vacuum grease and epoxy cement. No major difference between the bonding agents used has been observed. This method of switching was used to eliminate the possibility of any extraneous magnetic fields.

The activation of the switch, with a flow of warm helium gas in zero applied field leads to trapped axial fields as large as 5 milligauss. This effect is not

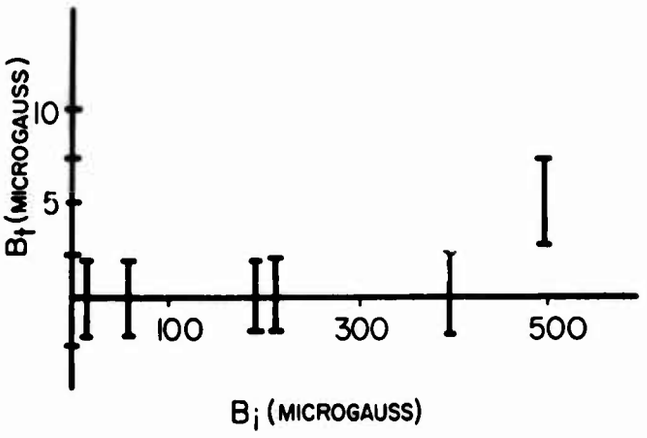

Fig. 0-3

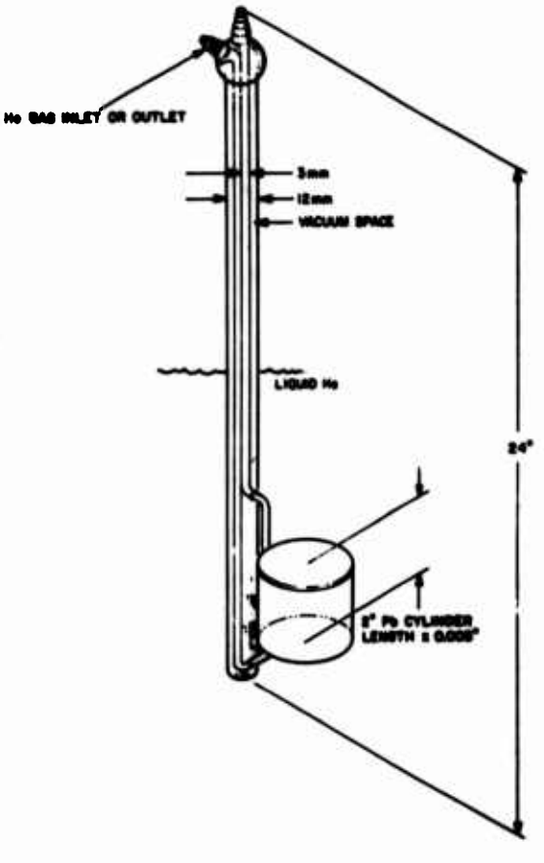

HELIUM GAS SUPERCONDUCTOR SWITCH (PYREX GLASS)

Fig. 0-4

due to noise fluctuation discussed earlier but a dc effect which does not disappear. When the switch is activated the field in the hollow of the tube does not decay but can be varied by applying an external field. This indicates that the warmed region is normal but that a large current is flowing. This result is surprising since no thermoelectric effect is expected for a pure superconductor.

This effect is not quantitatively understood but is believed due to strain and temperature gradients. Evidence to support this hypothesis is that the effect can first be modified by reversing the direction of gas flow, second, it becomes smaller upon continued switching and third that the fluxoid that was obtained when the transition occured while rotating[3] (where a more uniform temperature profile is expected) was in agreement with the London theory. It should be noted that the effect was virtually absent in Niobium.

References

1. B. J. Patton, Private Communication
2. A. F. Hildebrandt, Physical Review Letters, 12, 190 (1964).
3. A. F. Hildebrandt and M. M. Saffren, Proceedings of the IXth International Conference on Low Temperature Physics, Plenum Press (1965).

Discussion

DR. CAMPBELL: Did you have any idea how big the temperature gradients were across the mu metal shield or the hemisphere? Do you have any idea what sort of gradients you might have had across it? You said you had to cool it slowly. But did you make any effort to measure what sort of temperature gradients there were on it?

DR. HILDEBRANDT: No, I have no good number on it. It took 15 minutes to transfer a height of 37 centimenters.

DR. FERRELL: Could you explain again how you get these currents started that you record?

DR. HILDEBRANDT: The currents are spontaneous. I have a lead shield in zero-magnetic field, and when the switch is actuated the field appears and is trapped when the gas flow is stopped. It is due to the heating of the gas switch.

MICROWAVE MIXING WITH WEAKLY COUPLED SUPERCONDUCTORS

G. K. Gaule', R. L. Ross, and K. Schwidtal
U. S. Army Electronics Command
Fort Monmouth, N. J.

Diodes with Josephson or similar characteristics are promising as microwave mixers. When the diode current is below the critical current I_o the diode acts like a nonlinear inductance which may be obtained by inverting the Josephson formula,[1] as shown in the top lines of Table 1. More complicated nonlinearities enter when I_o is exceeded. Nevertheless, unambiguous expressions of the voltage V as a function of the current I can be found for cases of practical interest in which most of the higher Fourier components of the voltage are "shorted" by the diode capacity which, together with the external circuit, is assumed tuned to the local oscillator frequency. The higher Fourier components of the current, however, will be substantial. Self-consistent sets of all essential Fourier components have been determined with a digital computer by stepwise inserting improved estimates of the higher Fourier components of the current. Tables 1 and 2 indicate the method by which this carried out. Estimates for optimum local oscillator amplitudes and dc bias are thus obtained. Figures 1 and 2 are logarithmic presentations of the Fourier components of the voltage for various bias conditions. To facilitate computation, the local oscillator frequency was assumed to be 10 ω, the signal frequency 9ω, and the intermediate frequency, the desired mixer output, 1ω. It is seen that a substantial bias is necessary to obtain this output. The capacitive "shorting out" of the higher frequency voltage components is not taken into consideration in computing the curves of Figures 1 and 2. Therefore the third and fifth harmonics are predominant for all bias conditions.

Experimentally, a local oscillator and a signal generator, both operating near 10 GHz, were applied Figure 3 is a block diagram of the mixing experiment.

$$I = I_o \sin\varphi = I_o \sin[-(2\pi/\Phi_o)\int V dt],\quad \Phi_o = 2.1 \cdot 10^{-15}\ \text{V·sec}$$

$$V = -\dot{\varphi}\,\Phi_o/2\pi = (d/dt)\ \arcsin(I/I_o) = \dot{I}\,L_o\,[1-(I/I_o)]^{-1/2},\quad L_o = \Phi_o/I_o$$

$$\left.\begin{aligned} &u = V/\omega I_o L_o,\quad f = I/I_o,\quad r = R_{dyn}/\omega L_o \\ &u = r(f+1) \quad \text{for } f \le -1 \\ &u = -f\,(1-f^2)^{-1/2} \quad \text{for } -1 < f < 1,\ \text{always } (1-f^2)^{-1/2} > 0 \\ &u = r(f-1) \quad \text{for } f \ge 1 \end{aligned}\right\} \quad (1)$$

$$\left.\begin{aligned} &f = g_o + \sum_{q=1}^{\infty} g_q \cos 2\pi qy + h_q \sin 2\pi qy,\qquad 2\pi y = \omega t \\ &\dot{f} = \sum_{q=1}^{\infty} q(h_q \cos 2\pi qy - g_q \sin 2\pi qy) \end{aligned}\right\} \quad (2)$$

$$\left.\begin{aligned} &g_o = I_{bias}/I_o,\quad g_1 = h_1 = 0 \\ &h_9 = I_{signal}/I_o \end{aligned}\right\} \quad (3)$$

$$h_{10} = I_{LO}/I_o\ ,\quad \text{all other } g_q,\ h_q = 0$$

Insert f, $\dot{f}$ from (2), (3) into (1) and compute a_p, b_p according to

$$u = a_o + \sum_{p=1}^{\infty} a_p \cos 2\pi py + b_p \sin 2\pi py \quad (4)$$

Table P-1 Basic relationships between Josephson current I and Josephson voltage V. R_{dyn} represents the average dynamic resistance for $I > I_o$.

Compute an improved f by using values from (3), but now, instead of last line

$g_q = ka_q/q,\qquad h_q = -k\,b_q/q$

for $q = 18, 19, 20, 27, 28, 29, 30, 50$

$g_q = h_q = 0$ for all other $q > 10$

$k = (1 - g_o^2)^{-1/2} > 0$

Use improved f to recompute u, and a_p, b_p, and so forth.

Table P-2 The high frequency components of the relative current, f, are successively re-adjusted such as to make the high frequency components of the relative voltage, u, vanish. This takes account of the "shorting" of the latter by diode capacity and external circuit.

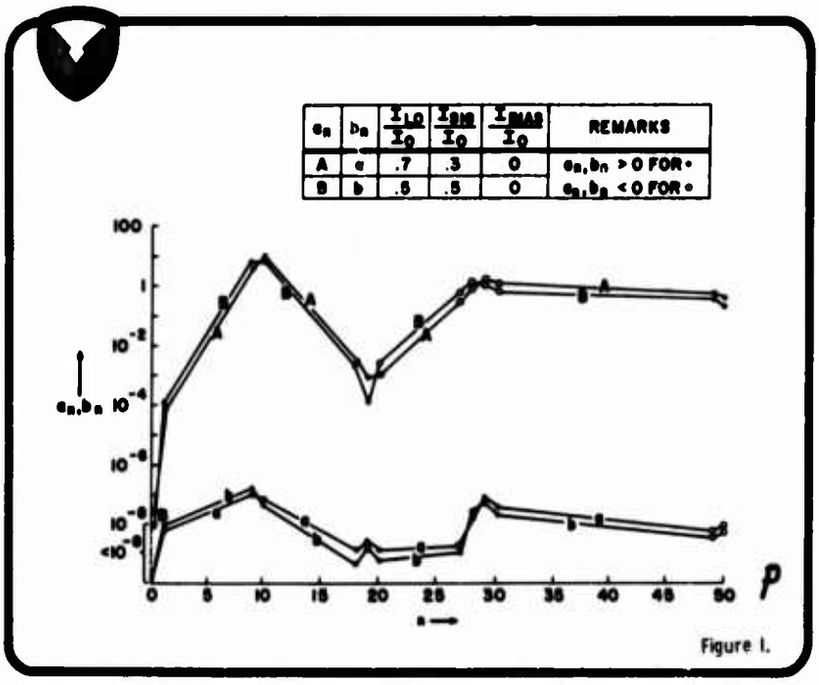

Fig. P-1 Logarithmic presentation of the Fourier components of the voltage for the case of no dc bias. The correction given in Table P-2 is not yet applied and third harmonics or equivalent (n = 27, 28, 29, 30) are much in evidence.

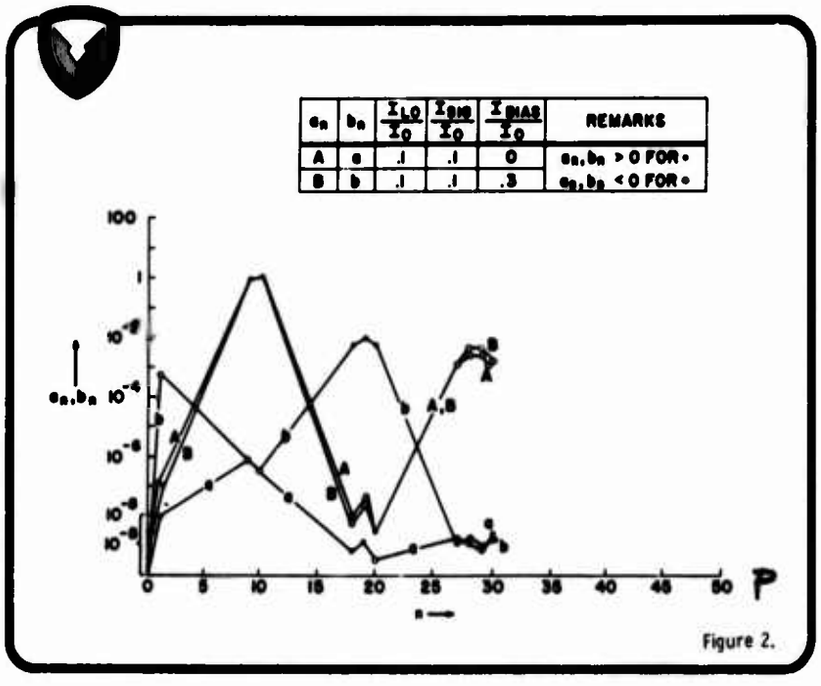

Fig. P-2 Similar to Figure P-1, but in the B case, substantial bias is applied, leading to a large desired mixer output (n = 1).

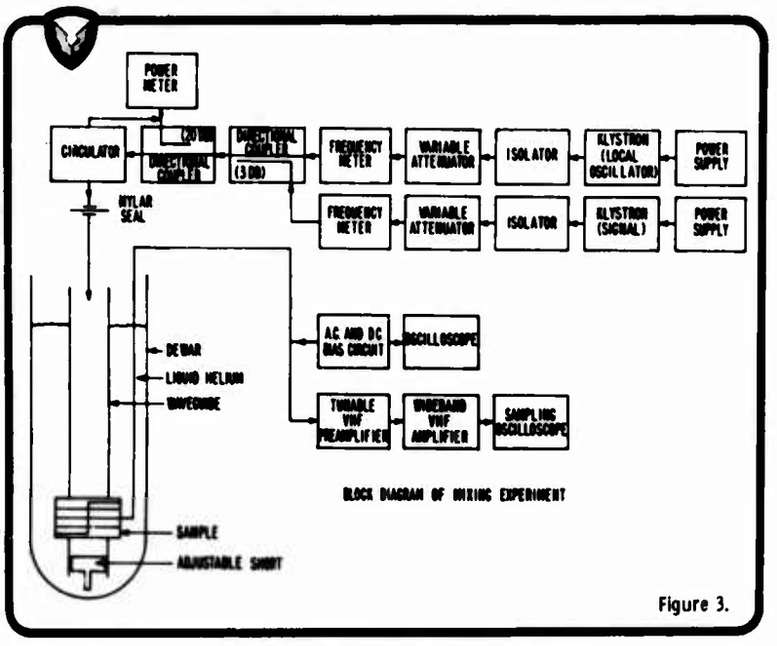

Fig. P-3 Block diagram of experiment. Three junctions could be measured in one run. Signal could be modulated and was monitored by separate detector.

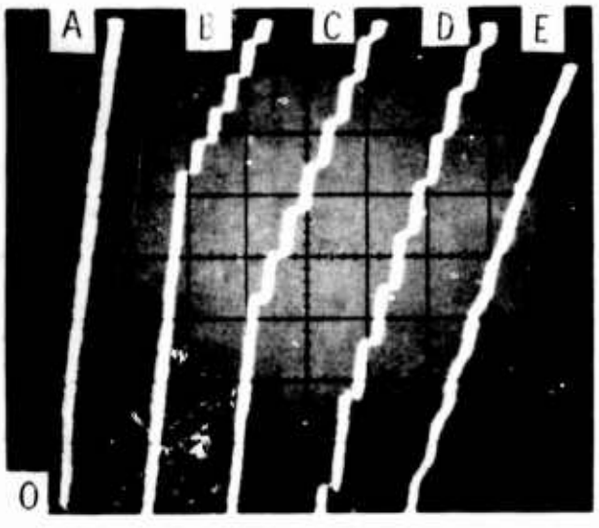

I (.1ma/cm) vs V (100uv/cm)

$T=4.2^{0}K$, H=0 Gauss

$f_{LO}=9.54GHz$, $f_{SIG}=9.74GHz$

A. $P_{LO}=0uw$ $P_{SIG}=0uw$

B. $P_{LO}=100uw$ $P_{SIG}=0uw$

C. $P_{LO}=200uw$ $P_{SIG}=0uw$

D. $P_{LO}=300uw$ $P_{SIG}=0uw$

E. $P_{LO}=300uw$ $P_{SIG}=3uw$

Fig. P-4 I vs. V characteristic of typical Nb-Nb-oxide-Nb diode as function of the local oscillator and signal power level (measured at entrance of waveguide). Signal unmodulated.

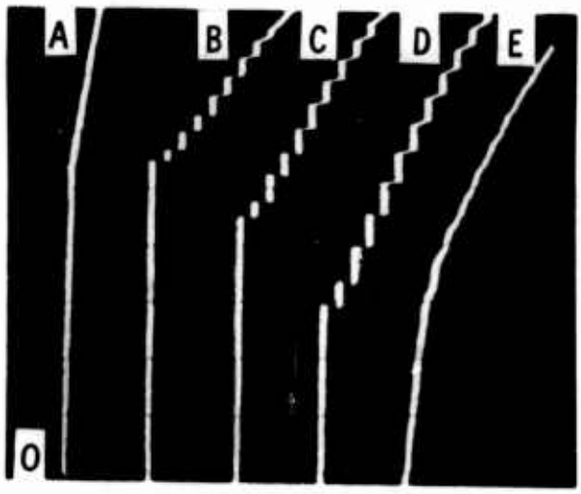

I (.1ma/cm) vs V (100uv/cm)
T=4.2°K, H=0 Gauss
f_{LO}=11.84GHz, f_{SIG}=12.04GHz
A. P_{LO}=0uw P_{SIG}=0uw
B. P_{LO}=10uw P_{SIG}=0uw
C. P_{LO}=20uw P_{SIG}=0uw
D. P_{LO}=30uw P_{SIG}=0uw
E. P_{LO}=30uw P_{SIG}=.3uw

Fig. P-5 Like Figure P-4, but power levels greatly reduced.

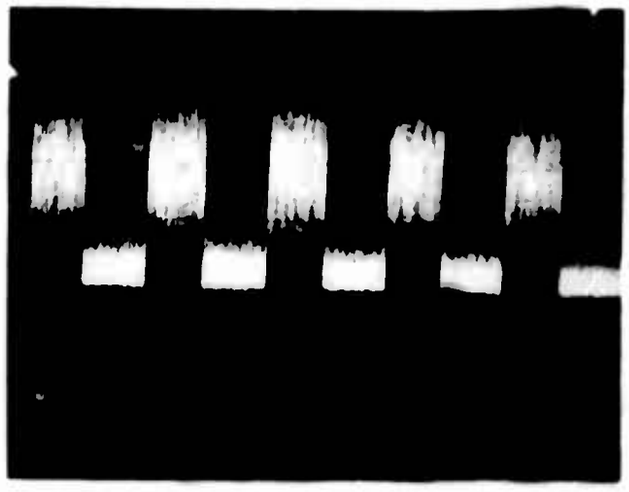

200 MHz Mixed Frequency Signal,
Square-Wave Modulated at 1 KHz

Fig. P-6 Mixer output obtained under condition of Figure 5E, but signal now square wave modulated. To make scope display possible, signal is transposed from the first intermediate frequency 200 MHz to 30 MHz in the wideband VHF amplifier (Figure 3). I_{bias} I_o.

The local oscillator power needed to produce the step structure described by Shapiro[2] was less at 12 GHz than it was at 9 GHz. The most conspicuous effect of even a very weak signal was to make the step structure disappear. Figures 4 and 5 illustrate the I vs. V characteristics of typical diodes under various local oscillator and signal power level conditions. Figure 6 shows the mixer output, taken under the condition given by Figure 5E, when the signal was square wave modulated. To display the mixer output on the scope screen, the 200 MHz signal was transposed to 30 MHz in a second (conventional) mixer. Bias current was $>I_o$.

Pressure contacts of oxidized Nb were far more radiation sensitive than crossed vacuum deposited Pb strips (preparation of the latter is described elsewhere[3]). Within each group, diodes with smaller critical currents responded more strongly to radiation. In Shapiro's terminology,[2] our Nb junctions are "tunnel-like", while our Pb film junctions are probably "bridge-like".

The authors wish to thank Mr. J. B. Herder for assistance in the Fourier analysis.

REFERENCES

1. A. H. Silver, R. C. Jaklevic, J. Lambe, Phys. Rev. 141, 362 (1966).

2. S. Shapiro, submitted to Journal Applied Physics.

3. G. K. Gaule', K. Schwidtal, J. T. Breslin, R. L. Ross, and J. J. Winter, 10th International Conference on Low Temperature Physics, Moscow, 1966.

MEASUREMENT OF THE ANISOTROPIC ENERGY GAP IN NIOBIUM SINGLE CRYSTALS BY TUNNELING

M. L. A. MacVicar and R. M. Rose
Massachusetts Institute of Technology

I am reporting on some preliminary results of tunneling characteristics taken on single crystal niobium at 1.9°K. The resistivity ratio of the samples was almost 800, and the crystal sections were of approximate orientation [110]. Current experiments involve crystals of simple directions: ⟨111⟩, ⟨112⟩, and ⟨100⟩ in addition, and are being carried out at 0.9°K.

The results are in qualitative agreement with the ultrasonic data of Dobbs and Perz, presented at the 1964 Colgate Conference. This means that I am observing low values of gaps in the ⟨100⟩; gap values along the ⟨110⟩ and ⟨111⟩ are very nearly equal to one another. The average value of the energy gap I observe is 3.0 millivolts. Gaps range from 3.1 to 2.9 millivolts, an anisotropy which is on the order of 6%, compared to the 5.7% of Dobbs and Perz.

The method I used to look at this anisotropy promises to be powerful. It is a direct approach and should see application in other studies. I have taken 1/8th inch diameter niobium rods and grown single crystals by electron beam zone melting in ultrahigh vacua. By this, I mean 10^{-9} or 10^{-10} torr. The growth was done at speeds of 4 inches, or 1 inch, per hour. Resistivity ratios varied from 350 to 800.

Figure 1 shows the steps of fabrication of the junctions. The vacuum system was backfilled with nitrogen, and the crystal removed for sectioning into $1\frac{1}{2}$ inch sections. These sections were oxidized for 20 to 40 minutes at temperatures of about 110°C, and then masked as shown, with a 3% formvar solution. The samples were then placed in an evaporation system and stripes of indium were evaporated at intervals around the circumference. These stripes were tried at width 0.030 inches and at 0.008 inches; as small a width as 0.003 inches is planned. The stripes were parallel to the crystal cylindrical axis, and provided 7.3° sampling in the case of the 0.008 inch stripes.

The samples were originally completed with lead stripes, but the lead was

1.

XTAL

3

DEPOSIT INDIUM STRIPES

2.

FORMVAR MASK

Fig. Q-1

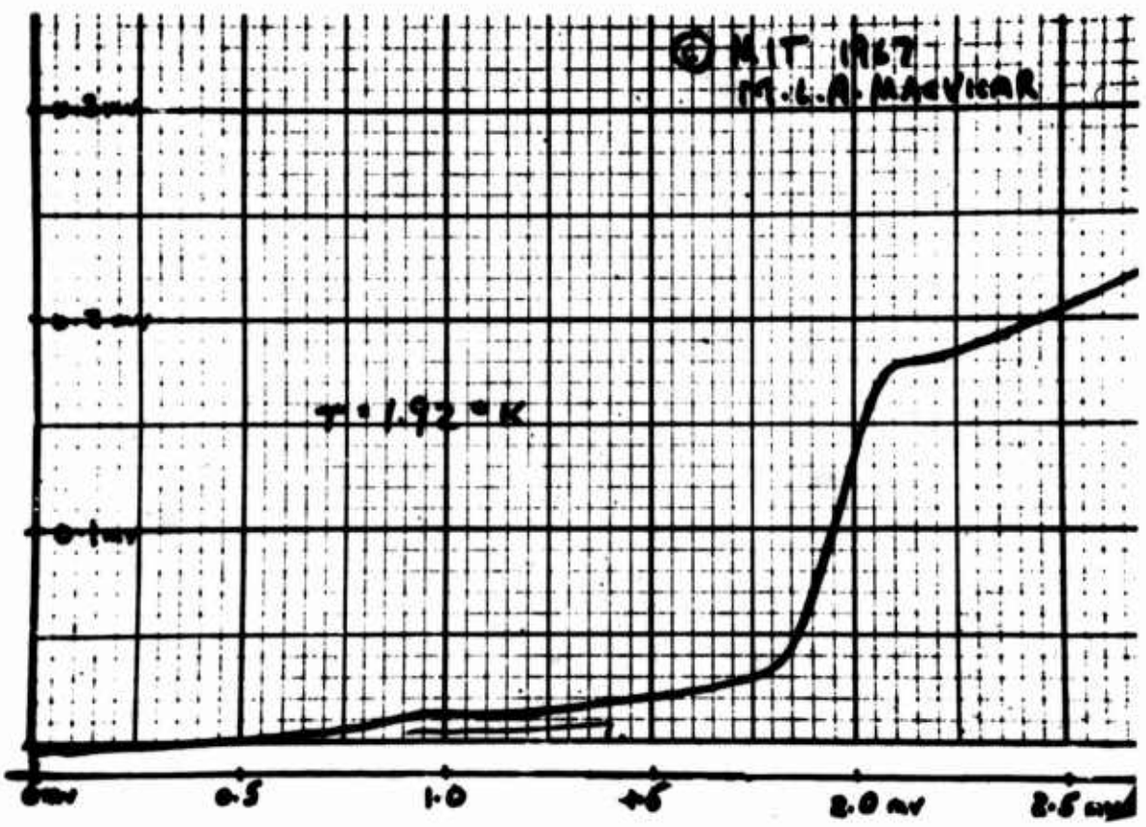

Fig. Q-2

found to show aging and oxidation effects when the temperature was cycled between liquid helium and room temperatures.

Electrical connections consisted of spotwelded leads to the crystal: these were nickel leads - two of them, one for common current and one for common voltage - ; and 5 mil gold wire leads, two, to each stripe. The gold leads were attached by a flexible silver paint.

Of the 15 junctions in which tunneling occurs, 4 junctions exhibit I-V characteristics showing the strange knee structure of Figure 2. This structure was reproducible for each sample in runs spaced over days. The four orientations fell within 5° of 65° off of $\langle 110 \rangle$. However, the insufficiency of the statistics prevent any conclusion of crystallographic sensitivity. Many junctions are presently under test; more information should be forthcoming from them.

The anisotropy is the most definite result I wanted to present today. The next matter draws on the fact that this is an informal meeting. I have just completed derivative tracing circuitry design and construction. The day before yesterday I took the first two junctions' derivatives with a 5000 cps, 30 microvolt signal (peak to peak). See the curve in Figure 3. The low bias regular structure present in the derivative of this curve shown in Figure 4 is similar to that described recently by Zawadowski. Zawadowski observed structure of a $2\Delta p/n$ type, and felt that metallic bridge shorts were responsible, and oxide effects probable. Note that I have swept from negative bias through to positive bias in an attept to locate a true zero bias.

A second type of low voltage structure is observed in the derivative taken for this junction. Figure 5 also exhibits low voltage structure, for a second junction.

Shen et al have taken specific heat measurements on niobium of resistivity 110, and found evidence of a second energy gap of magnitude about 1/10th the usual value. Much theoretical activity is taking place on the possibility of a second gap and its implications. When I looked at the low voltage structure, a possible explanation came to mind: i.e. a second gap a la Shen et al. Analysis in this direction is difficult, however, and I am running more samples to complete the necessary statistics. The only promising approach to analysis at present,

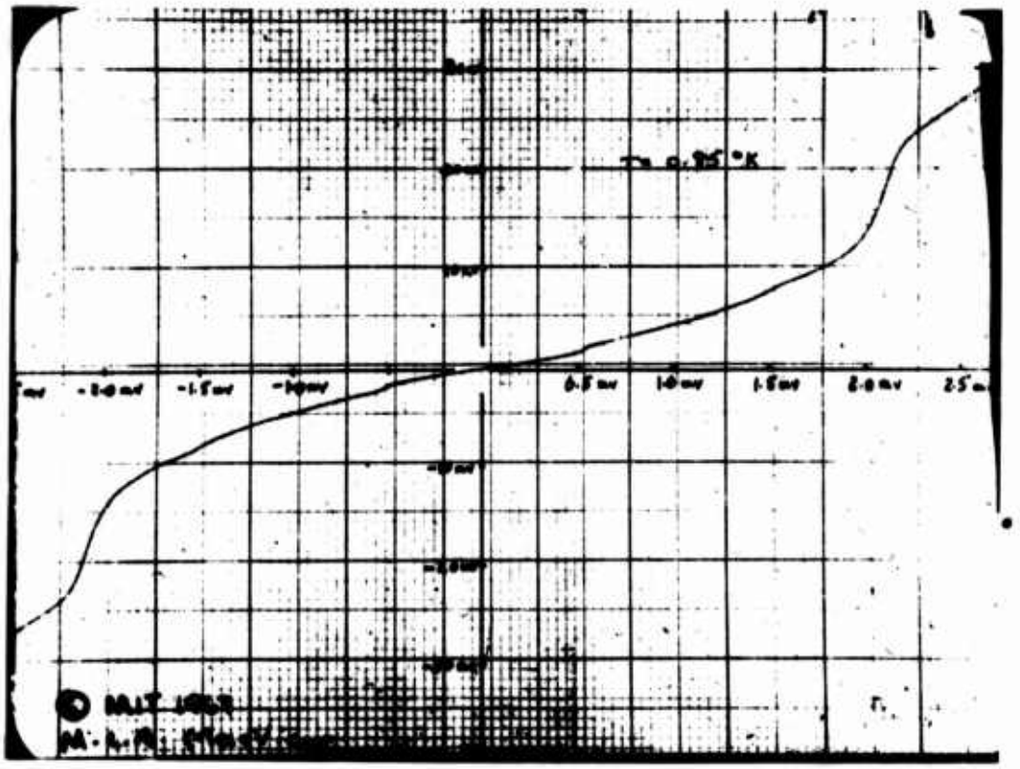

Fig. Q-3

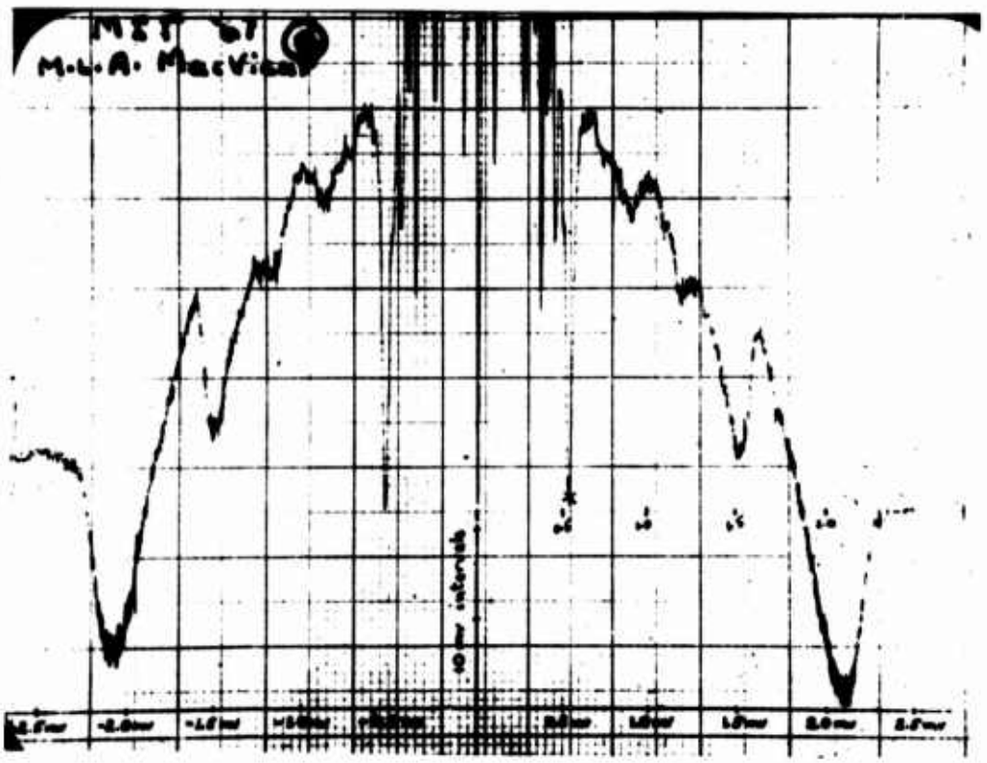

Fig. Q-4

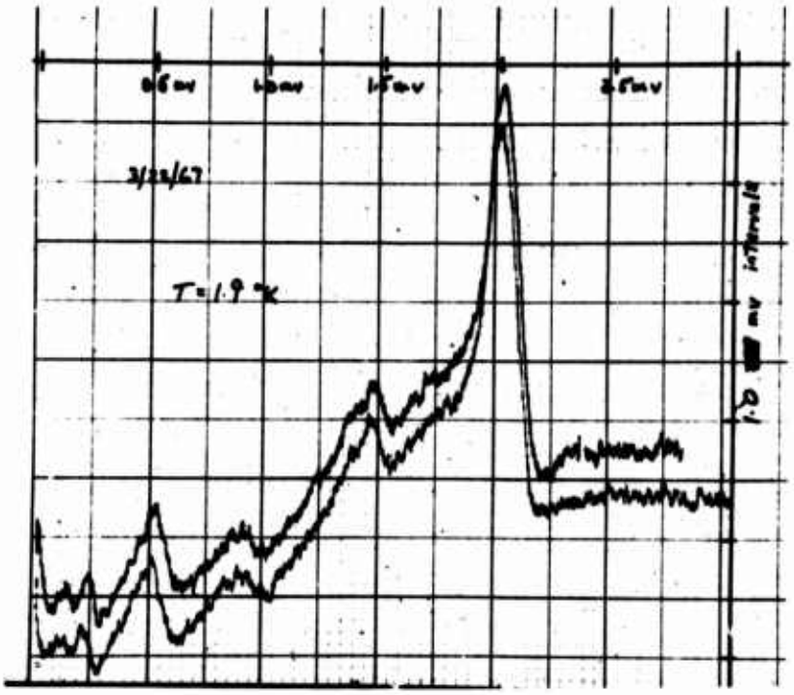

Fig. Q-5

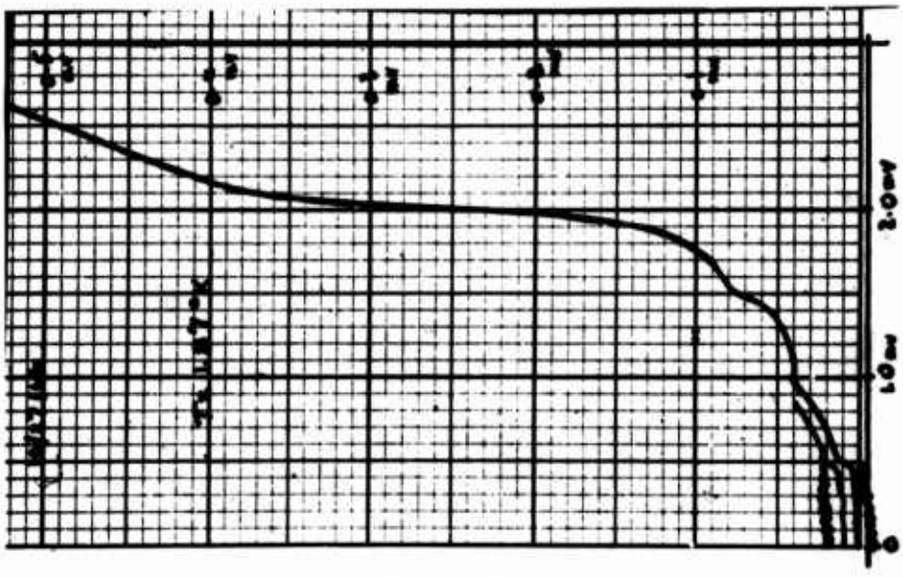

Fig. Q-6

seems to be the assumption of existence of two small gaps: one about 1/10th, and one about 1/5th, that of the usual value.

Discussion

DR. SHEN: I want to make two statements. One is the I-V characteristics of pure niobium junctions has a terrible background current flowing below the step, which is about a third of the current above the step.

And this just indicates that there is lots of tunneling current flowing this way. Of course, niobium is a very hard material to work with. I get the background currents.

The second is the conductance measurement. It doesn't look like the B.C.S. type of parabolic gap to me.

DR. MACVICAR: This is a good observation. My only comment is that the background current always appears higher in higher dynamic resistance junctions. One excellent I-V characteristic I haven't shown you is in Figure 6, if I can have it now. The double particle peaks of indium and niobium are particularly definitive here. Note the low voltage region ripple.

A SUPERCONDUCTING PARAMETRIC AMPLIFIER FOR THE MEASUREMENT OF SMALL DC VOLTAGES*

Roger P. Ries and C. B. Satterthwaite
University of Illinois

A device for detecting and quantitatively measuring very small dc signals in low impedance circuits has been developed employing a time varying mutual inductance between a set of input and output coils to produce parametric amplification of the input signal. The use of superconducting wire in the coils reduces loss caused by resistance and allows substantial power gain to be produced. A useful configuration uses one input and two output coils. The output coils resemble a Helmholtz pair but the two coils are connected in phase opposition. The input coil is mounted co-axially with and centered between the two output coils. It is vibrated with approximately simple harmonic motion along the axis of the three coils.

For small vibrations the mutual inductance between the input and output coils will very linearly with displacement along the axis (the x direction) so that the mutual inductance may be written as

$$M(t) = m_x \alpha \sin \omega t$$

Where m_x is $\partial M/\partial x$, α the amplitude of vibration and ω the vibrating frequency. The schematic of a typical amplifier is shown in Figure 1, which also includes a signal source and an associated source resistance. R_L is the resistance of the load connected to the amplifier. C is a capacitor which resonates the output circuit to the frequency of vibration and serves to maximize the power gain. The network equations are

$$L_i \frac{di_i}{dt} + R_s i_i = v_s - \frac{1}{R_L} \frac{d}{dt} (Mv_o) - C \frac{d}{dt} (M \frac{dv_o}{dt}) \qquad (1)$$

---

*This work was supported in part by the Joint Services Electronics Program (U. S. Army, U. S. Navy, and U. S. Air Force) under Contract DA 28 043 AMC 00073 (E).

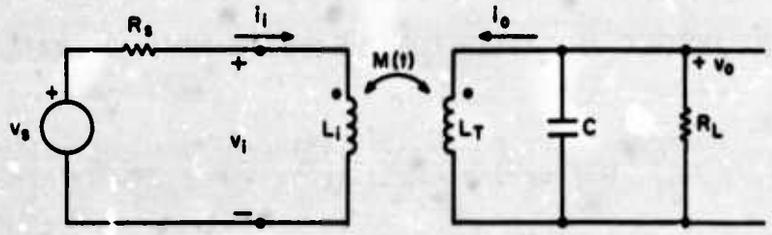

Fig. R-1 Schematic of the parametric amplifier.

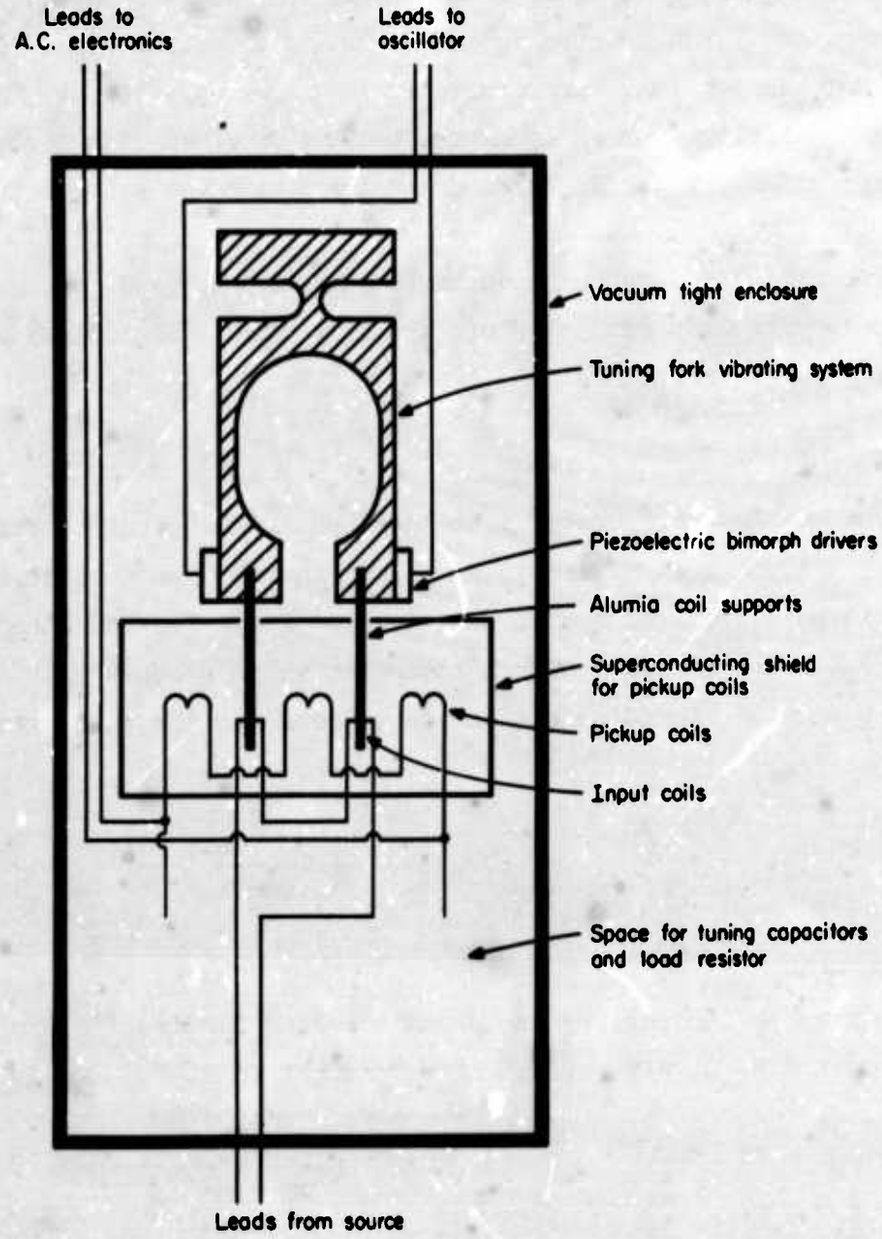

Fig. R-2 Layout of Picovoltmeter III.

$$L_T C \frac{d^2 v_o}{dt^2} + \frac{L_T}{R_L} \frac{dv_o}{dt} + v_o = \frac{d}{dt}(Mi_1) \quad . \tag{2}$$

The last two terms in Eq. (1) may be discarded with negligible error. If this is done, it is a simple matter to solve the equations for amplifier properties of interest.

The response to a step function input is a simple exponential with time constant τ equal to the input inductance divided by the source resistance. The voltage amplification is

$$A \equiv \frac{v_o}{v_s} = \frac{\alpha m_x R_L}{L_T R_S} \quad , \tag{3}$$

and is typically 3×10^6 or more.

The transducer power gain, in the limit of zero signal frequency is

$$G_{TO} = k_x^2 \alpha^2 \omega^2 \frac{\tau}{\gamma} \quad . \tag{4}$$

k_x is a geometric factor which describes the degree of coupling between the input and output circuits. γ is the loss decay rate of the output tuned circuit. Transducer power gains of 200 or more have been attained in experimental amplifiers, although such high gains are usually not required for maximum sensitivity.

Noise analysis indicates that the amplifier is capable of extremely high sensitivity. Since the actual voltage sensitivity is theoretically dependent upon the source resistance and the time constant used, we introduce a "sensitivity factor," S, as a basis for comparing the sensitivity of cryogenic dc detectors. S is defined as the ratio of the noise present at the output of the detector to the noise expected from the Johnson noise in the source resistance, and is thus a measure of how closely the amplifier approaches the ideal noisless amplifier. The ultimate sensitivity (as limited by Johnson noise) of a dc voltage detector is given by

$$V_{th} = \sqrt{\frac{k T_s R_s}{\tau}} \tag{5}$$

The actual limiting sensitivity of a practical amplifier is thus

$$V_m = S\, V_{th} \quad . \tag{6}$$

The sensitivity factor of a detection system using a parameter amplifier input stage can be shown to be[1]

$$S = \left\{ 1 + \frac{4(T_L + T_{eff})}{T_s G_{TO}} \left(1 + \frac{\tau}{\tau_L}\right) \right\}^{1/2} \quad . \tag{7}$$

T_L and T_{eff} are the temperature of R_L and the effective noise temperature of the ac amplifier connected to the output of the parametric amplifier. T_s is the source temperature. The system is assumed to include a lock-in amplifier as a detector, which has a time constant τ_L. T_{eff} can be about $20^{\circ}K$ for a good (commercially available) low noise ac amplifier or lock-in. If $\tau_L \approx \tau$ so that maximum sensitivity is obtained, but response time is not appreciably reduced, then

$$S \approx \left(1 + \frac{48}{G_{TO}}\right)^{1/2} \text{ at } 4^{\circ}K \quad .$$

Thus a transducer gain of about 16 should be adequate to achieve sensitivities within a factor of 2 of the limit set by Johnson noise at $4^{\circ}K$. For a source resistor of 10^{-7} and time constant of 10 seconds, voltage sensitivity would be

$$V_m \approx 10^{-15} \text{ volts} \quad .$$

The most recent version of the amplifier was built around a small tuning fork with a resonant frequency of about 1200 Hz, shown schematically in Figure 2. Two input coils were vibrated by the tuning fork in close proximity to three output coils as shown in the schematic. The driving frequency was locked to the resonant frequency of the fork. Tuning capacitors were chosen so that the output circuit was resonant at the frequency of vibration. The total inductance of the two input coils was about 5×10^{-7} hy. With a 4×10^{-7} ohm source resistance the noise level was about 4×10^{-14} volts rms. τ was 1.3 seconds so the Johnson noise level would have been 4.5×10^{-15} volts rms. The sensitivity factor was thus about 10.

The ac electronics consisted of a Keithley 103 low noise amplifier followed by a PAR JB-5 lock-in amplifier and a strip chart recorder. The transducer power gain of the parametric amplifier was about 4 while the noise figure of the Keithley amplifier was about 0.3 db. The lock-in amplifier time constant was 1 sec so the theoretical sensitivity factor was about 3.6. The discrepancy between sensitivity predicted and that observed was believed to be due to spurious vibration of the output coils in the presence of remnant magnetic field.

Figure 3 shows the chart recording of the response of the amplifier to a 2.4 picovolt square wave signal with a period of 5 minutes.

The amplifier is extremely linear (over a range of 6 to 7 orders of magnitude variation in the input signal) and offers a high degree of isolation between input and output circuits, the two being coupled through a stray capacitance of a few picofarads. The amplifier has true differential input with common mode rejection of over 200 db for maximum resistance to ground loop problems and other problems caused by extraneous signals. The amplifier will recover from sustained overloads as large as 10^{10} times the signals being measured, and will do so without loss of accuracy or sensitivity.

The input impedance of the amplifier is a small inductance (a fraction of a microhenry) so that the amplifier operates well with very low source impedances. If source loading is a problem, or if the source resistance is not accurately known, the amplifier may be included in a potentiometric type of feedback system which will minimize the current drawn from the source to a few nanoamperes. Such a system could be very similar to the feedback systems used in present day chopper stabilized dc amplifiers. The parametric amplifier would essentially replace the chopper in such a system.

The amplifier can be built with quite small size and mass. The smallest experimental amplifier measured 1 inch by 1 3/4 inches by 3 1/2 inches and weighed about 200 grams, though no attempt was made to miniaturize the amplifier. Power requirements are modest (less than a milliwatt) so that the amplifier's dissipation does not introduce an intolerable heat leak into the cryogenic apparatus.

Experimental amplifiers have demonstrated dc sensitivities which closely approach the maximum attainable by any device. The main obstacle to even higher

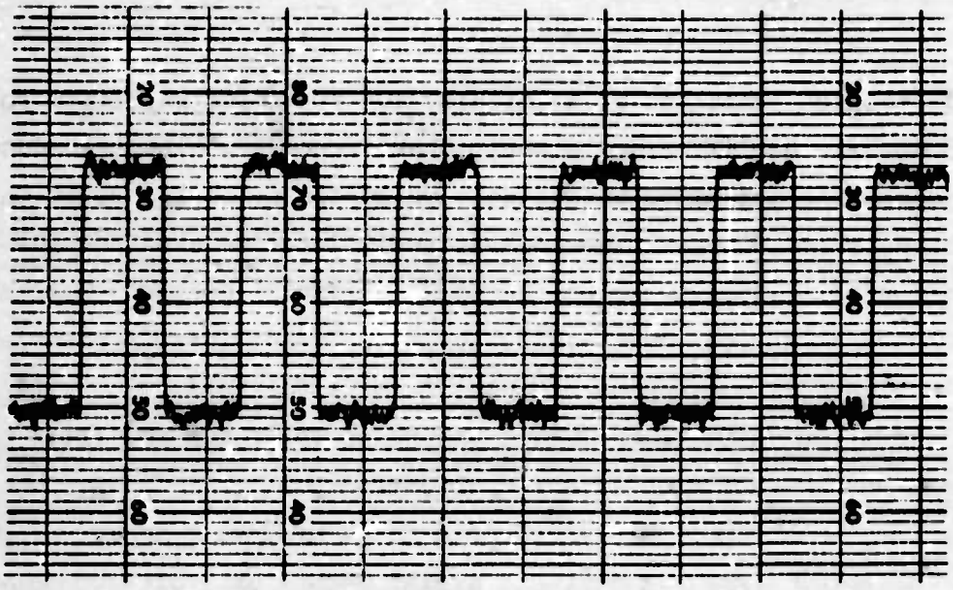

Fig. R-3 Response of the amplifier to a 2.4 picovolt square wave.

sensitivity appears to be a spurious effect which one should be able to eliminate through a better mechanical design. The ultimate sensitivity appears to be limited only by the noise present in the source itself.

References

1. Roger P. Ries and C. B. Satterthwaite, Rev. Sci. Instruments (to be published).

DEVICE APPLICATION OF SUPER-INDUCTORS

W. A. Little
Stanford University

DR. LITTLE: Much of the early work on superconductivity which was oriented towards devices was concentrated on the use of the perfect conductivity. The cryotrons, for example, and superconducting magnets are based on this use of superconductivity. But as most of you know, London pointed out that superconductivity is more than just perfect conductivity. In recent years these predictions of London have shown up very strongly, in particular, at this conference the importance of the long-range order, which he stressed has now been taken out of the academic part of the laboratory and is being used in many different devices. Since the initial discovery of flux quantization and the predictions of Josephson, several extremely sophisticated and yet sometimes simple devices have been developed.

London also had some remarks to make about the collective modes of electron systems, and what I want to talk about is more closely connected with this aspect of superconductivity than with either of the other two aspects of superconductivity. Some years ago we picked up some of the ideas that London had suggested and considered whether one could have superconductivity in a long, thin molecular system. It was brought home rather forcibly to us that the collective density modes in this particular system play an extremely important role.

Professor Ferrell was the first to show that if you consider the zero-point motion of the density modes these are capable of destroying the long-range order which is believed to be important for superconductivity. Another problem was raised by Professor Onsager. He made a rather cryptic remark which I will try and interpret for you. This was that in one dimension, he said, there were baby plasmons and these baby plasmons would lie under the gap and could destroy superconductivity. I don't know exactly what he meant but it at least got us thinking that the role of the plasmons was an extremely important one in superconductivity and should be looked at rather carefully.

You may recall that in an infinite 3-dimensional system of Fermi particles, the single particle Excitation spectrum is given as in Figure 1, and because of the peculiar form of the coulomb interaction, the density modes or plasmons are well separated from the quasi-particle continuum. The plasmon energy ω_p in typical metals is somewhere around 15 electron volts. Because of the enormous difference between the energy characteristic of the plasmon and the energies which are characteristic of the superconducting state there is very little interaction between the two, and so one can make a separation between the quasi-particle modes and the plasmon modes.

But that is just the theoretical position. In the laboratory we do not have an infinite 3-dimensional system. What one has, is a sample, usually a fairly small sample which has ends on it, and one should concern oneself with what role the ends play and what role the size of the sample plays.

Obviously here you do have baby plasmons, if you think about them a little bit, and as we shall show these baby plasmons could lie below the energy gap. The question is whether these plasmons would destroy superconductivity or not. Apparently they do not destroy superconductivity in this case.

You may recall that there must be a different series of plasmons for any finite sample. This is familiar to you in a somewhat different context. These are the antenna modes. See Figure 2. A T. V. transmission excites plasmons in the antenna system. The charge oscillations from end to end of the dipoles are real density modes. As you change the geometry of the dipoles going from a small dipole at one end of the array to a large dipole at the other end, the characteristic plasmon associated with these geometries changes from a high frequency mode to a low frequency mode and it is obvious if you make the sample long enough and thin enough or of the right shape, you can allow these modes to become arbitrarily low in energy. Thus, they could lie under the energy gap in the superconductor and might interfere in some way with it.

In Figure 3 I have tried to picture what the real situation would be like for the plasmons for a sample of finite size. You find that close to the origin there should be additional modes, the antenna modes, which in the case of dipoles, will have a slope given by the velocity of light. Also there will be the quasi-particle excitations.

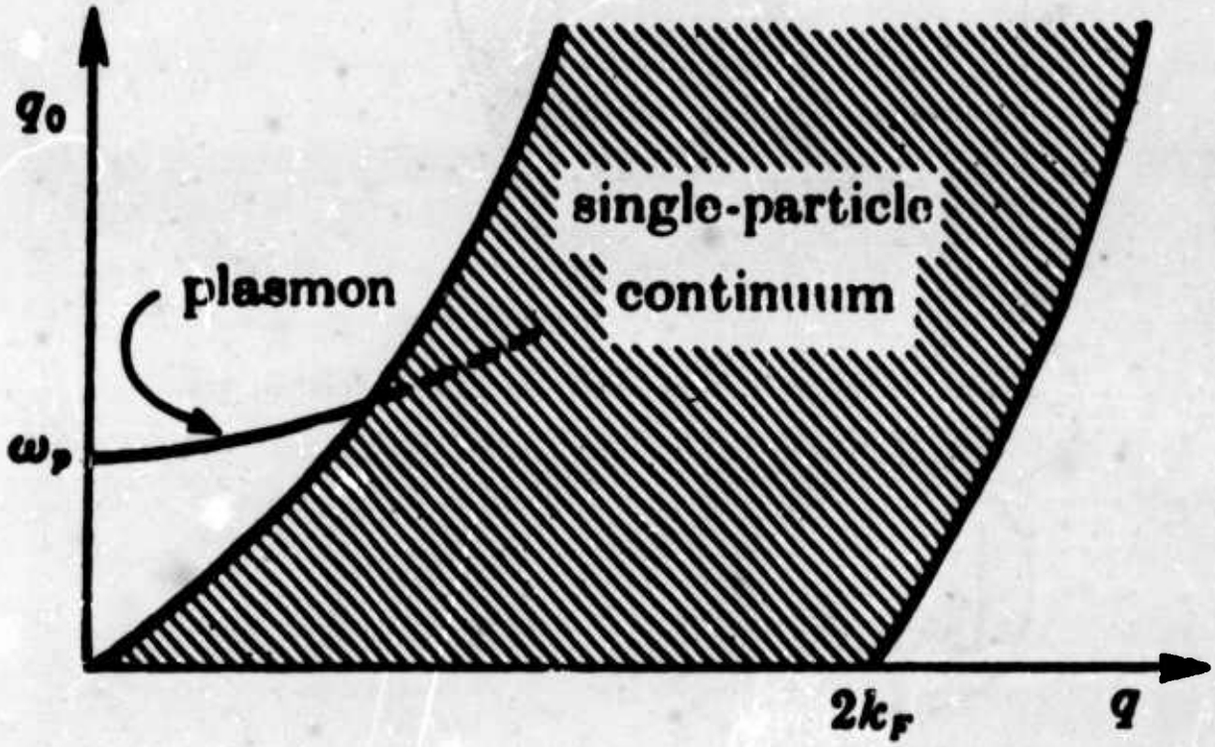

Fig. S-1 A plot of the excitation spectrum of the electron gas.

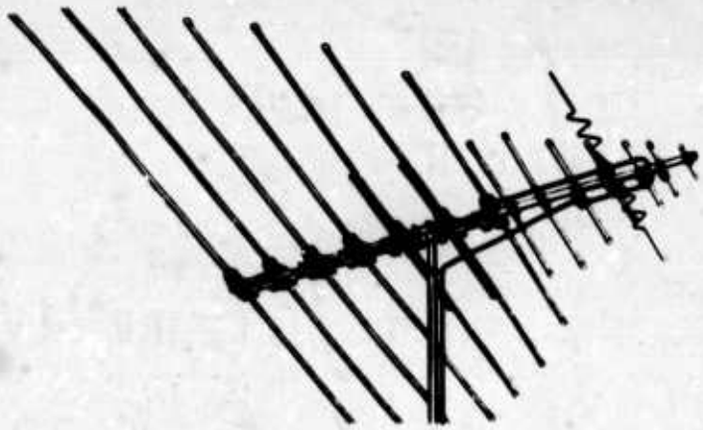

Fig. S-2

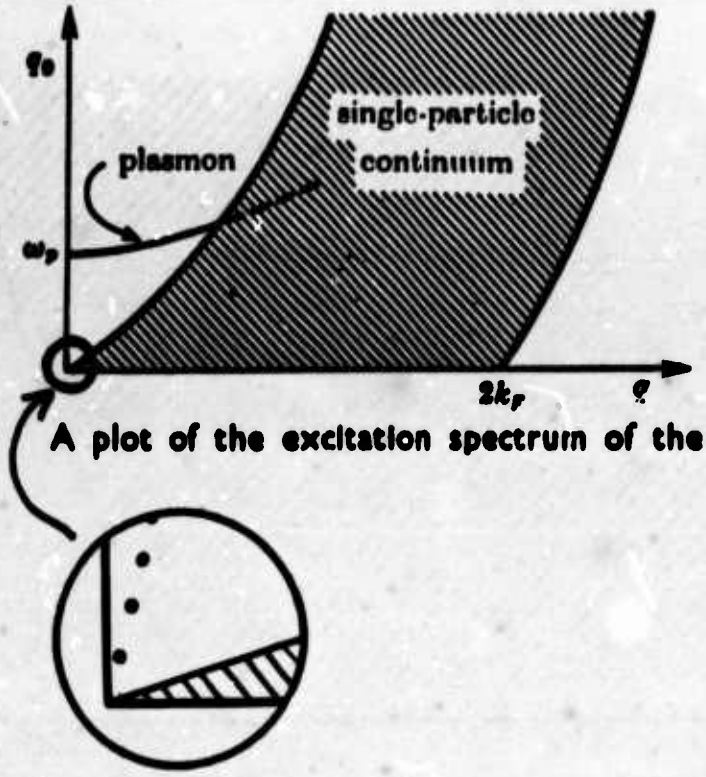

A plot of the excitation spectrum of the electron gas.

Fig. S-3 A plot of the excitation spectrum of the electron gas.

$$U = \frac{1}{2} L i^2$$

$$= \int_{\Omega} \frac{B^2}{8\pi} d\Omega$$

$$+ \int_{V} n \left(\frac{1}{2} m v^2\right) dV$$

$$L = L_n + L_e$$

Fig. S-4

In a superconductor the continuum is lifted up somewhat and you can have the quasi-particles excitations degenerate with some of these plasmons. I will come back to that problem somewhat later.

At first sight you may think this is totally irrelevant because nothing which is characteristic of the superconductor or of the metal shows up when you consider these modes. The frequency of the modes is determined entirely by the inductance and capacitance of the dipole, i.e. the actual shape of the piece of metal. The frequencies are only determined to second order by the intrinsic properties of the electrons. The resistivity only comes as a second order effect in determining the frequency of the dipole.

So that you might think, as the electromagnetic field is really determining the property of this dipole, it could not tell us anything about superconductivity. But that is only an accident. It just turns out that in most of the things with which we are familiar, the geometry is such that the frequency is determined in this particular way. You can have a situation however, where the inductance and capacity are determined by the properties of the electrons, themselves, i.e. the intrinsic properties of the superconductor or of the metal.

I want to turn to this particular situation, and rather than keep attacking the plasmons I would like to consider just one aspect of this, the inductance per unit length, which is one of the terms which determines the frequency and I shall pay special attention to this.

When a current flows through such a conductor a certain amount of energy will be stored in its neighborhood. This total stored energy U is equal to $\frac{1}{2}Li^2$ where L is its effective inductance. See Figure 4. It is often convenient to equate this stored energy to the energy which is stored in the magnetic field and we obtain the result that the integral of $\frac{B^2}{8\pi}$, integrated over the total volume where the field B exists is equal to the stored energy. However, this is not quite correct for there is an additional term which represents the energy stored in the kinetic energy of the moving charge carriers. This is the kinetic energy of each of the carriers, $(\frac{1}{2}Mv^2)$ integrated over the total volume of the conductor. The total inductance can thus be considered to be the sum of a magnetic term due to the energy of the magnetic field and an electronic term L_e which

represents the contribution of the kinetic energy of the moving charge carriers. One can readily write this kinetic energy term in the form shown in Figure 5 i.e. $L_e = \left(\frac{M}{ne^2}\right)\left(\frac{\ell}{A}\right)$. From the form of this inductive term one sees that it increases as the area of cross section of the sample decreases. On the other hand the magnetic term can be shown to increase only logarithmically as the radius of the conductor is decreased. Consequently by making a sample which is thin enough one can make the kinetic energy term in the inductance dominate the total inductance. In this case the frequency of the antenna modes will depend upon the intrinsic properties of the material rather than upon the properties of the electromagnetic field.

At this point where we were concerned about these plasmons, Professor Angell of our Department of Electrical Engineering was showing us over the work they were doing on microminiature integrated circuits. And he made a rather interesting remark about the problems of making these circuits. He said that the problems there are the exact opposite of the problems that we have in large scale electronic circuits. The active elements like the transitors and diodes and so on, these are easy to make. But the passive elements, things like the resistors, capacitors and inductors are extremely difficult to make. And the worst of the lot are inductors, which are extremely difficult to make for such miniature circuits. We noticed that here as you micro-miniaturize, as you go to the smaller and smaller cross-sectional areas A, you find that the inductance grows and grows. We have the unusual situation here where one can make an inductance of arbitrarily large magnitude by making the conductor arbitrarily small in diameter. In practice this is of very little use for if we consider the resistive term of any such conductor then as we decrease the area, so we increase the total resistance of the sample with the net result that we have a large inductance but an extremely lossy one. However, by considering a superconductor it is possible to obtain a useful device based upon this property.

In a superconductor one can consider that two interpenetrating electron fluids exist and we must consider the inertial properties of each of these as well as the term contributed by the magnetic field. In Figure 6 we show the effective circuit description of a thin superconducting wire similar to that used

$$L_e = \left(\frac{m}{ne^2}\right)\left(\frac{\ell}{A}\right)$$

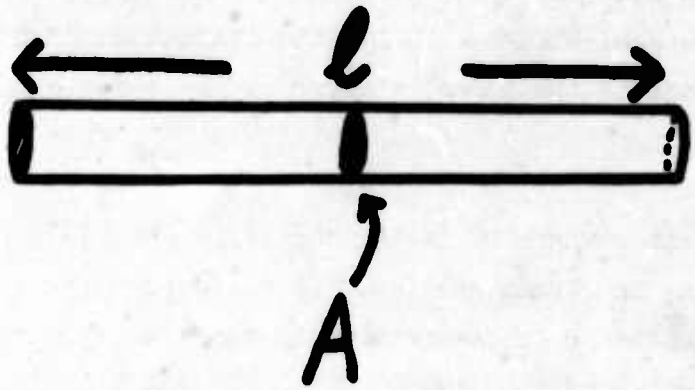

Fig. S-5

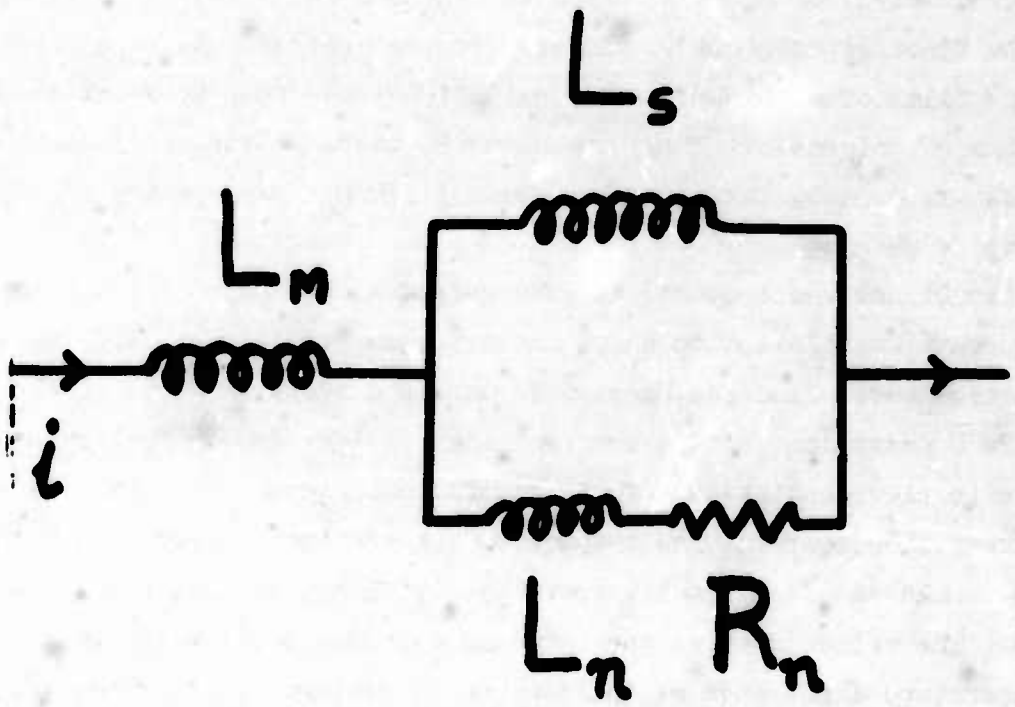

Fig. S-6

by several of the other speakers. The current flowing through such a wire will have a distribution which is essentially the same in the normal as in the superconducting stage. For this reason the inductance produced by the magnetic field L_m will be essentially the same in the two cases. However, the current may be carried partially by the normal fluid or by the superfluid and the circuit branches to indicate the two possible choices here. The division between them depends upon the impedance of each of the arms of the circuit. We have L_s, the inductance of the superelectrons with L_n, the inductance of the normal electrons and R_n, the resistance of the normal electrons; the super electrons exhibiting no resistance.

The kinetic inductance of the superelectrons can be put into a simple form, $L = \mu_o(\frac{\lambda^2}{A})$ Henries/meter where μ_o is the constant $4\pi \times 10^{-7}$ and λ is the penetration depth and A the cross section. (See Figure 7) And now of course the area of cross section can be made arbitrarily small and you can make your inductance as large as you please.

We were just a little bit suspicious about some of the magnitudes predicted. If you put in the numbers you find you can get magnitudes of the order of microhenries for a sample of about a centimeter and for reasonably thin films. So some of the first experiments we did were to prepare some of these materials by evaporating films of aluminum. After oxidation they ended up being about 40 or 50 angstroms of thickness. They were about 20 microns wide and 3 centimeters long. This was done by taking a thin glass fiber and evaporating on it so as to get a strip of metal.

The inductance was measured at 10 megacycles in a Raleigh frequency bridge and the current was limited to about one micro amp in the sample. The work was done by George Possin and Ken Shepard of our laboratory.

Figure 8 shows some of the behavior that you get here. The induction is given here in microhenries as a function of the temperature -- this is aluminum and the transition temperature is somewhat higher than the accepted value. The thinner you make the film the higher it gets. This goes to about 1.8 degrees in this case. The solid curve is the inductance that you get by putting in the known temperature dependance of the penetration depth. This agrees very well

$$L_s = \mu_o \left(\frac{\lambda^2}{A}\right)/\text{meter}$$

$$\lambda = \lambda(T, H, j)$$

Fig. S-7

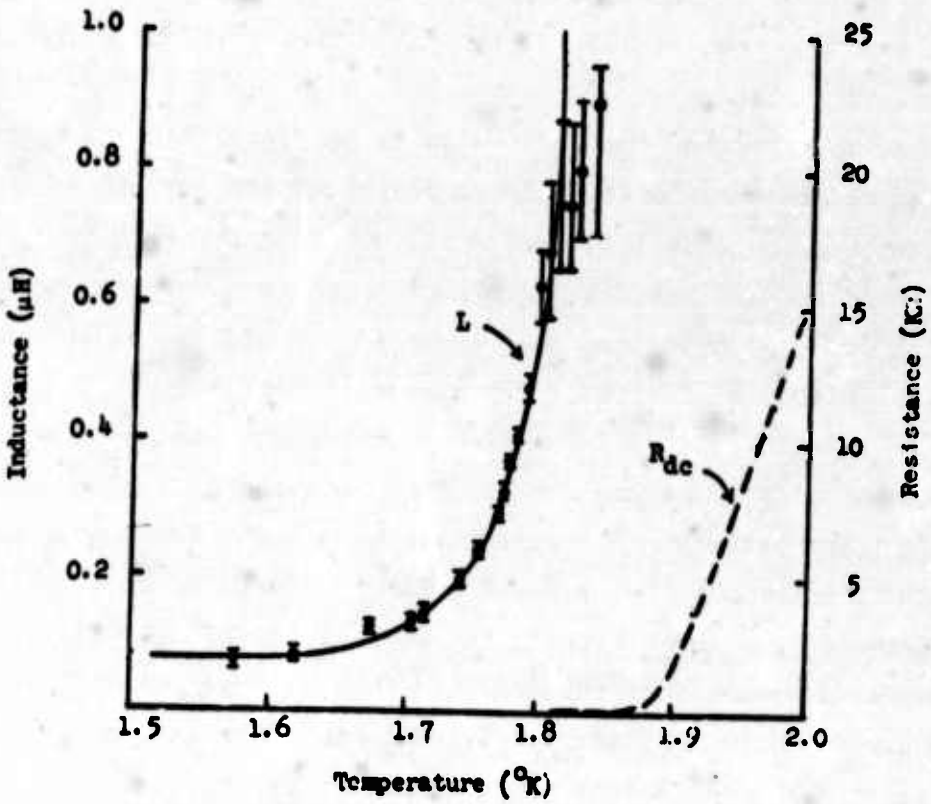

Fig. S-8

with what one would expect. This curve is normalized at one point, somewhere near the bunch of error bars near the top and the rest seems to follow from this.

Notice that it has been well known, of course, that if you have a superconducting circuit you will have a change of inductance as you approach the transition temperature because of the penetration depth change, however, these results are in the opposite sense to what one normally gets. Because here you are not changing the configuration of the magnetic field but changing the part which involves the current. So here the inductance increases as you approach the transition temperature, rather than decreases.

On this curve the calculated magnetic inductance is approximately the size of one of the dots so that it would be negligible compared to the kinetic inductance. Then in this particular case the kinetic inductance is very much greater than the magnetic inductance. In this case it goes up to about fifty times the value of the magnetic inductance. This is part of the excuse for calling these things "Super-Inductors." The inductance, while not as spectacularly large compared with the change that we have in the conductivity, is appreciably greater than the magnetic inductance.

Notice the dc resistance has become quite negligible in the region where the inductance has become very large. The ac resistance is not quite as low as this as it comes in at a somewhat lower temperature.

One of the more exciting features about these inductances is not so much the large inductance, because you can make large inductances if you are not interested in the microminiaturization by making several turns and then you can rapidly get an extremely large inductance of course. But the interesting part is that the inductance is of course a modulable inductance. As I pointed out, the inductance is proportional to the square of the penetration depth, and the penetration depth is determined by the temperature; it depends upon the magnetic field, and depends upon the current which is flowing through this. So each one of these things can cause the inductance to change.

I have already shown the temperature dependence in this curve of the inductance. It is very appreciable in the region near T_c and if one puts such an inductance as the frequency determining element in an oscillator, in the tank

circuit of an oscillator, then this could be used directly to measure temperatures, where even at a temperature well below one degree the inductance changes are enormous so that the total frequency change would be very large. In fact, if one could go down to millidegrees one could still get sufficiently large changes in the penetration depth so as to detect differences of temperature. There are problems in the power involved here, but these can be run at very low power.

At first sight we thought that the magnetic field would not be a particularly useful way of modulating these devices because the films are so thin compared to the penetration depth that we thought there would be a rather weak interaction. But of course the magnetic field is perpendicular to the film, and it is possible for vortices to enter the film, and this could of course influence the over-all inductance of the sample, so that some measurements were made on a strip, in this case a somewhat broader strip, .28 millimeters wide and about 40 angstroms thick. Figure 9 shows what happens here.

One finds that the inductance in this case is, in the absence of a field, considerably lower than in the presence of a field, and it changes now approximately linially with the field. Again the magnetic inductance is about a 50th of the maximum value that you get for the total inductance. As a function of temperature you find that the rate of change of the inductance increases as you approach the transition temperature.

Why this is so is not absolutely clear. I mean that there are good reasons for believing that there should be some such effect, but the magnitude of the effect is considerably bigger than we expected.

I think part of the reason is shown perhaps in Figure 10. If you imagine such a strip with a magnetic field on, then the vortices will enter. At the core of the vortex you will have a reduced number of super electrons; when you pass a current through this the total number of super electrons in the current will be reduced and in this case they must run faster for the same total current through the sample. So the kinetic inductance must go up. But that is not encugh to explain the effect. It is still out by an order of magnitude at least. And it seems there is the additional effect that the electrons now must run in a grand slalom. They have got to go around the various vortices to go from end to end.

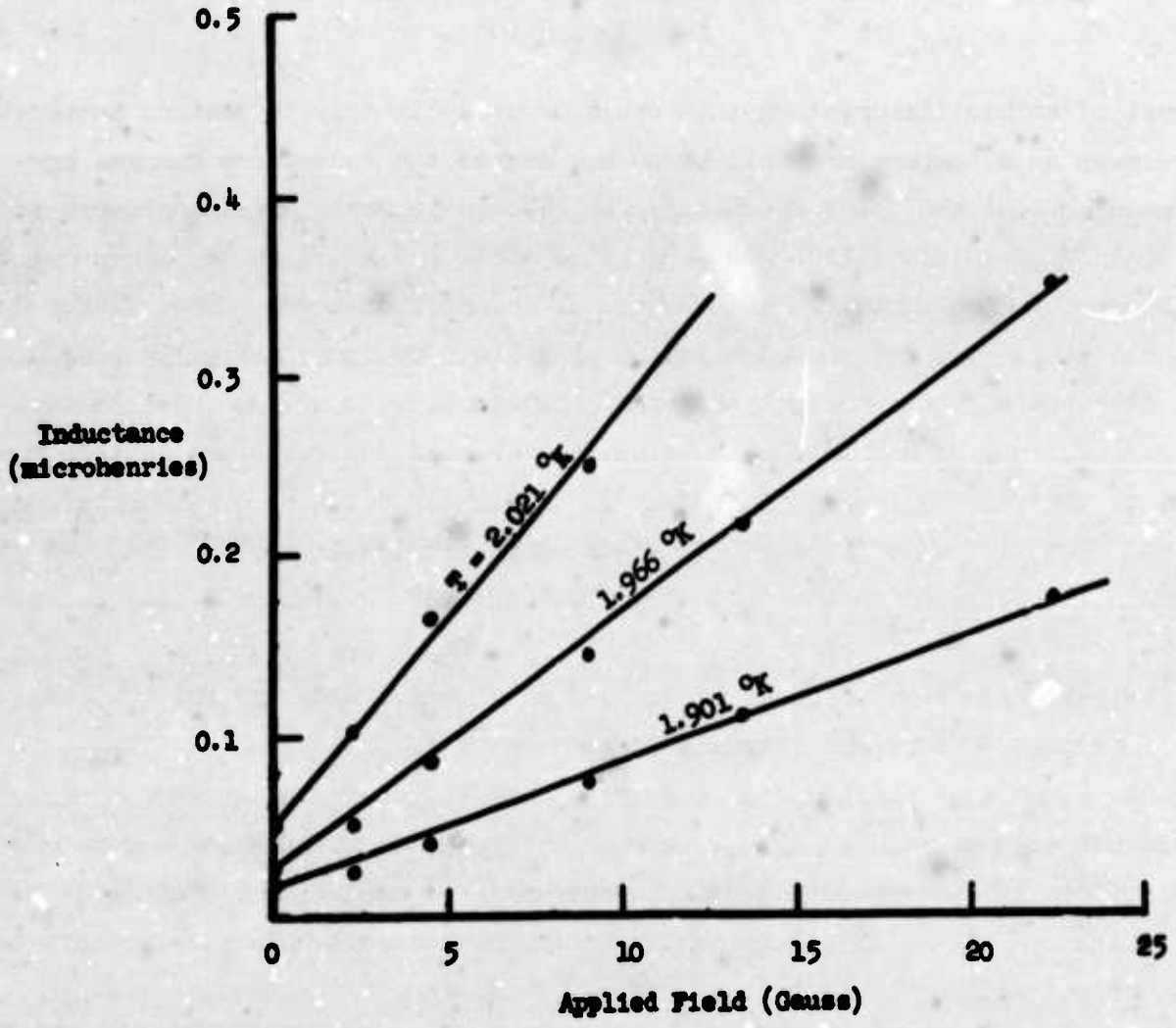

Fig. S-9

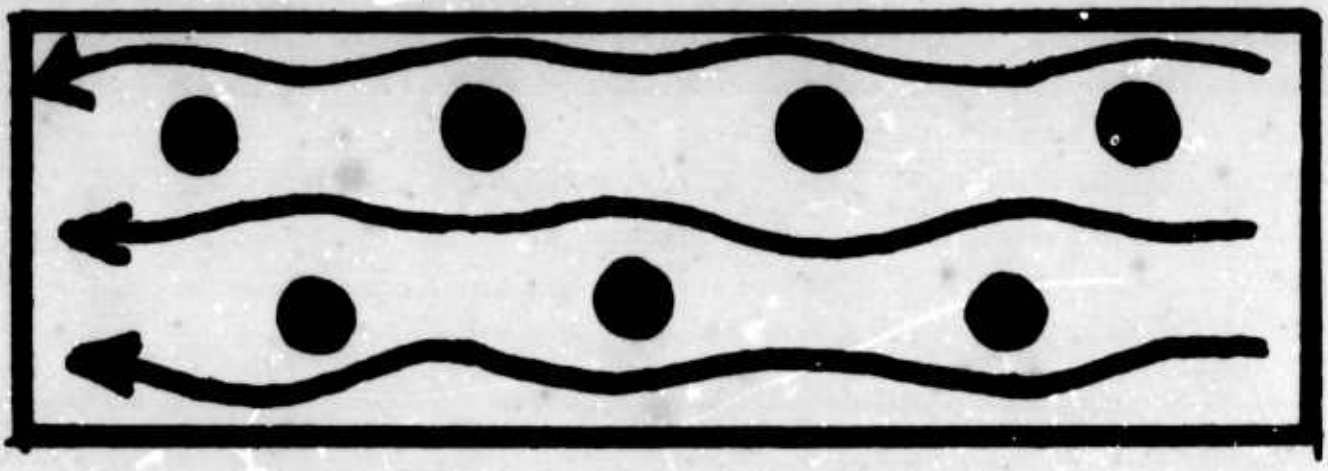

Fig. S-10

So to cover the same distance to produce the same current they must run faster. So there seems to be an additional effect here too.

The other reason seems to be that in regard to the core. In the core of the vortex we know that the order parameter drops down and then comes up again, but when you are near the transition temperature it seems as if you have two effects, one is that the correlation length is going to change so that the slope will be somewhat broader so that the size of the core will get larger. But in addition to that, as you get very close to the transition it seems that the inner core would have to get fatter. Because the electrons are running in it, and if they run as fast as they have to, they will have too great a free energy so that they will be driven normal. So, presumably there is an effect not only of the change of the coherence length but of the change of the size of the core.

In this case, again, we got a kinetic inductance which was about 50 times as large as the magnetic inductance and was completely controllable.

One thing which we hoped to have some results on -- but we haven't got it yet -- and this was what happens if you have a strip which is so thin that the applied magnetic field is too small to allow the first vortex to enter. As you increase the field you should have rather a low inductance, until the first vortex goes in, and when it goes in then the current must go around it and one would get a rather large effect, similar to the effect which Parks' studied, looking at the resistance transition. But this type of experiment on the inductance has the advantage that one should see it without digging deep into the noise of the resistance as it would be a very large, first order effect.

With the number of applications which one might make of such devices, one of them of course would be to use it as a low noise parametric amplifier, seeing that you can modulate this inductance over to a factor of about 30. And this might be used in the flux detectors of the type that Professor Fairbank discussed earlier. One might use this also in logic devices because current flowing through a superconducting network will take the route of lowest impedence, and this can be controlled by the magnetic fields or by thermal means in various ways. So that one might be able to devise some logic device which would determine the direction that a current pulse would pass through a particular maze.

Another application is the possibility of using this in delay lines. If you recall the velocity of propagation Vp of a distributed line is given by 1 over the square root of the inductance and the capacitance of unit length. The impedence R is given by the square root of L over C. So that in these where you have a kinetic inductance which is about 50 times larger than the magnetic inductance you get from an ordinary line, for the same impedence you can tolerate a much greater capacity per unit length. Thus you can increase both the inductance by using the kinetic inductance, and the capacity to get a total velocity of propagation which would be down from the velocity of light by a factor of the order of 50. So Vp $\sim$ order of 1/50th C.

Now this might be used as a storage element where you could put a series of pulses into a loop, and if the losses are small enough they could continue to circulate and you could read this out very much like a disc on a computer, where you have a real rotation of the disc and you read out at different points. The propagation velocity is significantly lower than you can get with any other type of delay line of miniature size.

The attraction of such devices, especially for microminiature circuits, of course, is that they can be made extremely small. You can get a large inductance in a small space. They seem simple to construct.

The other interesting point is that in parametric amplification you can get extremely high gain in a small volume. Because the inductance is stored in the interior of the conductor and not in the field round about it. You can stack these individual inductors within a distance of the order of the diameter of the conductor from one another. The mutual inductance would be smaller than the magnetic inductance alone, so it would be about a fiftieth of the total inductance so the cross talk between these elements would be extremely small.

The problems which remain are that we don't know what the frequency limitations are, we don't know what the Qs are, we don't know whether they modulate at very high frequencies. These should be studied.

In conclusion, to return to the problem of plasmons, what would be particularly interesting to see is whether one can indeed separate the plasmon and the quasi-particle excitations at these very long wave lengths where the energy of

the quasi-particle and the energy of the plasmons are in fact degenerate with one another. Normally the difference depends upon the separation of energy of these. It would be interesting to know what the situation is where they lie closer to one another. The situation then is much closer to that of zero sound.

Discussion

DR. SCALAPINO: I want to perhaps comment on some of the things you were saying with respect to Josephson junctions.

In the Josephson junctions there exists of course a mode of propagation down between the two superconductors that Sweihart first analyzed but without the Josephson coupling. In fact, you pick up exactly the type of effects you are talking about in which the Kinetic inductance is large, and typically in these you get a speed that is a 20th of the speed of light.

Furthermore, that speed of light differs where the normal modes sit. And so if you look at the step structure and you measure the position of these steps as a function of temperature, you pull out exactly the type of temperature dependent changes you are talking about here, and you can in fact track the change of your kinetic induction with temperature by watching how the normal modes move in their voltage positions. And that has been done by this. Plus you see these things exist right up to 2 delta. After you hit 2 delta they suddenly disappear. So depending upon the length of your junction, as the junction gets shorter they will get very closely spaced. So you see these small lines. You sometimes couple more strongly into one. What happens is that when you hit 2 delta they go away. So I think in part this is an experiment associated with what happens when the collective modes, which these are, lie below the gap, and what happens as they move towards the 2 delta.

LITTLE: Do they lie in the gap?

SCALAPINO: In the gap, and you can see them all the way up to 2 delta. So your quasi-particle continuum would be lifted up so you see them sit right up to the continuum. Once they get to the continuum they completely disappear on the scope, for example. How low they lie I don't know.

HAYDEN: Does the reactance remain dominant?

LITTLE: When you apply the dc magnetic fields, this increases the inductance that you are measuring at 10 megacycles. And it is always dominant over the magnetic inductance.

HAYDEN: I mean over the resistance.

LITTLE: Yes, sir. We don't know what the Q is. We don't observe it, but it could be a factor of 10 or a factor of 100 of the impedence of the inductors.

FERRELL: I had some questions, if I may. I wondered if you could comment on the disappearance of the dc resistances. Do you understand that, how it goes down to zero gradually? Is that unusual?

LITTLE: If the film is dirty enough. It always has that effect.

FERRELL: Do you have also some comments about the enhancement of T_c. That is seen in aluminum usually. I wondered if you had any ideas about that.

LITTLE: I don't. I wish I did know what was causing this. These were aluminum films.

MASON: I can speak to the question. I have done this experiment with transmission lines, which you suggested to Lalock. You can make Q's or several at temperatures well below the critical temperatures. This is with indium. As you approach the critical temperature the Q drops very rapidly, so when you get large inductances and large arrays, you find you get Q's down in the order of 10. In fact, that is a limitation that is close to how well you can make it, it gives that technique.

LITTLE: How large a kinetic inductance were you able to get over the magnetic inductance?

MASON: I guess I would have to phrase it in terms of velocity but the velocity would be as low as 1/20th the speed of light.

ROSENBLOOM: I suspect the Q's will depend critically on the frequency that you choose. If you choose a frequency that is higher, what we have referred to as a natural relaxation frequency of the vortex lines in the pinning potential, if the frequency is higher than this, you will get a very low Q; if the frequency is low I suspect that you will be very high. And typically for films -- well, I don't know about 30 angstrom of aluminum films, but for 500 or 1000 angstrom

indium films, these are in the 100 megacycle range in critical frequencies.

MASON: These measurements are made right in the range.

ROSENBLOOM: That depends on the particular film.

FLUXFLOW AND DIRECT CURRENT TRANSFORMERS

I. Giaever
General Electric Research and Development Center
Schenectady, New York

If a type II superconductor is placed in a sufficiently high magnetic field, the magnetic field will penetrate the superconductor in certain small areas which will become normal, leaving the rest of the material superconducting. According to Abrikosov's[1] theory, each normal area contains one unit of flux, and it is customary to refer to them as quantized vortices or fluxons. Now if in addition, a sufficiently large current is passed along the type II superconductor, the current will interact with the fluxons causing them to move, as was first suggested by Anderson.[2] The relative motion between the fluxons and the lattice causes a voltage to appear along the superconductor. Thus, it is possible for a type II superconductor to be in a resistive, yet superconductive state.

By properly taking advantage of the fluxflow which occurs in type II superconductors, a new class of electronic devices can be constructed,[3] such as dc transformers, controllable rectifiers, and fluxpumps. Some of the advantages and inherent limitations of these devices were discussed.

---

1. Abrikosov, A. A., Soviet Phys. J.E.T.P. 5, 1174 (1957).
2. Anderson, P. W., Phys. Rev. Letters 9, 309-311 (Oct. 1, 1962).
3. Giaever, I., IEEE Spectrum, 3, 117-122 (September 1966).

MODULATED FLUX FLOW IN SUPERCONDUCTING FILMS

J. E. Mercereau
Ford Scientific Laboratory
Newport Beach, California

What we have done is to build an ac version of Giaever's transformer, and he cautions me that I should give the proper credit to Faraday.

Let me draw a circuit, Fig. 1. We have a transformer which I will schematically draw this way. This is a superconducting circuit of some sort.

If you apply a voltage, V(0), to the primary at some frequency, under the proper circumstances what you get out is a voltage, which is at the same frequency you put in, plus something else, which may be at another frequency and whose amplitude depends on the voltage that you apply, the frequency that you apply, and the amounts of magnetic flux, Φ, the steady magnetic flux that links this circuit.

Now, as Giaever pointed out, we don't have any adequate theory for explaining what goes on so what I would like to do is only to describe what goes on in a very simple kind of model which is essentially a quantized Faraday induction law. But it turns out that it is not even necessary to put quantization into the thing, you must put something discrete into it, and then you can do the experiments to find out in fact the discreteness is really quantization. What we will do is to consider a transformer with a completely superconducting secondary. And we will attempt to analyze the situation when the flux enclosed by the superconducting secondary is forced to change.

Suppose you had a superconducting thin film ring like so (Fig. 2,a), and you apply a magnetic field parallel to the axis, then of course a circumferential current is induced. Let me plot the density of the currents induced in the ring (Fig. 2,b). Of course what happens is the current is induced mostly at the edges of the ring because the ring doesn't want to let the flux penetrate through the walls.

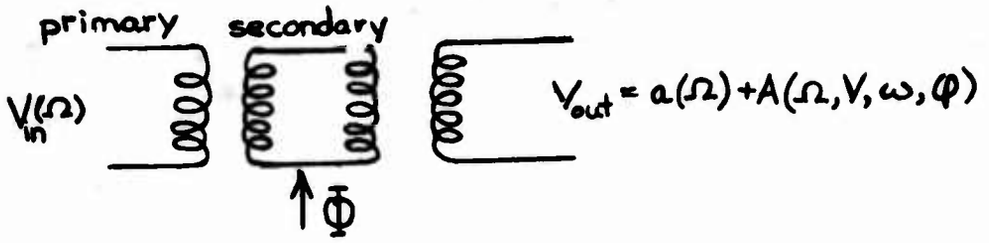

Figure 1

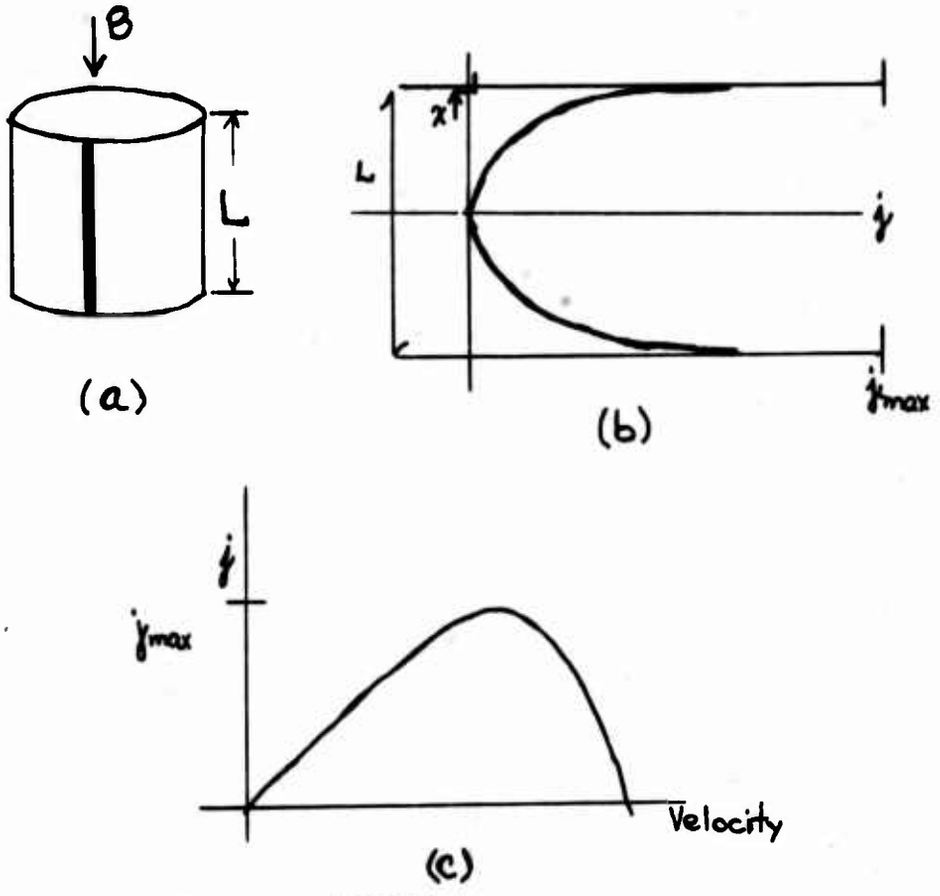

Figure 2

If you try to measure the emf induced around this circuit at the top, this loop at the top, it is of course zero because just exactly as much current flows as is required to keep the flux through the circuits constant.

Sooner or later what is going to happen is that there is some limit on the current that you can flow in this thing, some critical current. And, if you insist on changing the magnetic field until you get a critical current at the edge, then something happens. If you try to exceed that point then the superconductor has no choice but to let the magnetic flux penetrate through the walls.

What has happened is that the flux at the edge has begun to penetrate, because you are increasing the flux outside, it has no choice, it has to come through the wall. So at some point the enclosed flux begins to change. In these experiments the ring is deliberately weakened at some point to localize the flux flow. Nominal ring geometry is one-two mm diameter, one centimeter long. The "weakening" is usually done by shortening the ring at one spot to a constriction of about .1 mm x .1 mm.

This induction technique is essentially a voltage source for the ring. In the superconducting state the electrons are accelerated by the applied voltage to a current required to keep the flux in the ring constant. At low velocities current and velocity are related in a linear way but at higher velocities nonlinear effects appear, Fig. 2,c. When the current limits at j_{max} a voltage will continue to accelerate the electrons, but create a lower current. This "inverse" Lenz law drives the current to zero as the flux penetrates the wall. For a thin film structure as we have here the process begins at the film edge, Fig. 3. If the flux moves in a stable way the process can repeat. The current at the edge will again rise to j_{max} before allowing a second flux bundle (ϕ_o) to enter and pass through the film. The flux flow across the film will be at a rate to conserve flux, of course, so that the average rate of generation (Ω) of the bundles (ϕ_o) will be:

$$\Omega = 2\pi \frac{\dot{\phi}_{applied}}{\phi_o}$$

But now if you ask what is the emf around this circuit, around the top, the emf now is different than it was before because now the flux is passing

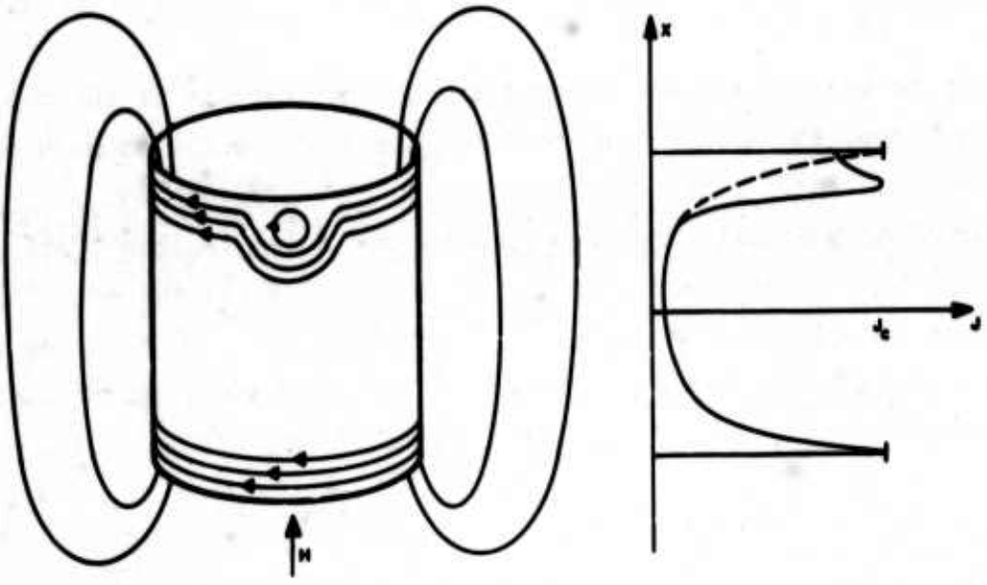

Fig. U-3

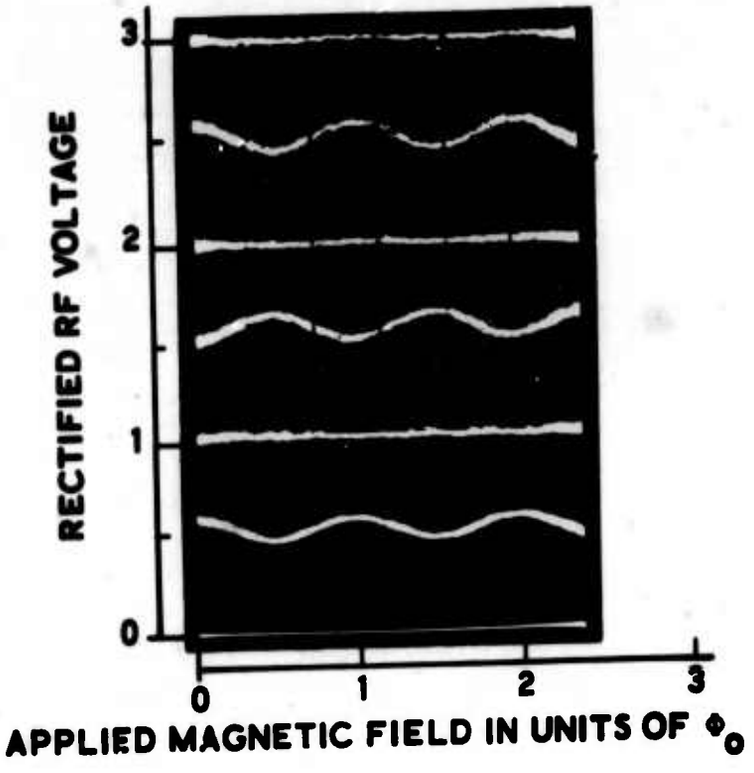
RECTIFIED RF VOLTAGE
0
1
2
3
0
1
2
3
APPLIED MAGNETIC FIELD IN UNITS OF Φ_0

Fig. U-4

into the ring in a non-continuous fashion, it is passing through as these little bundles at frequency (Ω). The emf produced is also going to be periodic in frequency (Ω). The first term in any mathematical expansion is going to be proportional to $\sin\int_{\Omega} dt$, plus terms in higher harmonics however complex the function must be to describe what actually happens. At least to lowest order there must be a term that looks something like this:

$$\text{emf} = V_{\text{classical}} + A \sin \int \Omega \, dt + \ldots$$

Let me go through the arithmetic. The physics, however, is quite simple. The superconductor is acting like a flux valve. It is allowing flux to pass through a certain circuit at a certain rate. All we have to do then is calculate the emf produced by the flux valve. This is a particular model that says the flux is allowed to pass only in a single size unit (ϕ_o). That then determines the frequency at which the process occurs. From here on it is arithmetic based on whatever rate of change you wish to assume for ϕ_{applied}.

But let me go through a particular arithmetic because we have done some experiments which tend to confirm the idea. I only want to get out a functional form that demonstrates the periodicity, because it is the periodicity we have confirmed, not of course the detailed functional form.

The non classical part of the emf we are taking to be:

$$\mathcal{E} \text{ (emf)} = A \sin \int \Omega \, dt,$$

where $\Omega = 2\pi \frac{\dot{\phi}_{\text{applied}}}{\phi_o}$. Since we are, at present, only interested in the functional form of this voltage we will take A to be a constant. It can, in principle, be determined from the details of the flux flow process. Substituting for Ω:

$$\mathcal{E}(\text{emf}) = A \sin \frac{2\pi}{\phi_o} \int \dot{\phi}_{\text{applied}} \, dt$$

$$\delta\,(\text{emf}) = A \sin \frac{2\pi}{\phi_o} [\phi(t)_{\text{applied}}]$$

$$= A \sin \frac{2\pi}{\phi_o} [\int v\,dt + \Phi]$$

We are assuming that the flux is Φ until the voltage (v) is applied.

If the voltage that you apply is some function of time itself, $v = v_o \sin \omega t$, then the emf at (ω) is found to be $\propto J_1 (\frac{2\pi v_o}{\omega \phi_o}) \sin \frac{2\pi\Phi}{\phi_o}$. So what this says is if the superconductor acts as a flux valve to let flux through at a certain rate, what you are going to have is an emf produced which is dependent upon the amplitude of the voltage by which you drive it (v_o), the frequency of the drive voltage (ω), and the amplitude of the time independent part of the flux, Φ. The functional dependence of this emf is identical with that expected from a Josephson junction. But, this is a non-tunneling process in fact the superconductor is not even "weakly connected". It's just that you are allowing the superconducting ring to act as a flux valve. The flux comes through at a certain rate, Ω. The only physics to this, now, is to do the experiment to measure ϕ_o and see whether the voltage that you see out here does depend somehow periodically on the amplitude and the frequency of the applied voltage, and for a constant amplitude and frequency whether the voltage depends on the amount of the flux through that circuit.

Rather than using the transformer as indicated in Figure 1, the experiments done by Dr. Nisenoff of our laboratories consist of a single coil and the superconducting shorted turn secondary formed by the ring. You put a signal in and take it out of the same coil. Effects of this type have been found in several different superconducting materials, particularly evident in thin films (< 1000Å) of Sn, Al, and In-Sn alloys. These experiments were done at 30 mc sec^{-1} where it was found that the voltage of form $J_1 (\frac{2\pi v_o}{\omega \phi_o}) \sin 2\pi \frac{\Phi}{\Phi_o}$ can be as large as the usual "classical" Faraday law voltage. However, in the data I will show you these quantum effects are only about 10% perturbation.

Figure 4 shows the rectified 30 mc sec^{-1} voltage on the coil as a function of steady magnetic flux through the superconducting ring.

A series of curves of rectified rf output at various levels of applied rf voltage is shown. For each curve the applied voltage is held constant.

However the curve at an rf level of (1/2) shows a periodicity in magnetic field of ϕ_o. This additional field dependent voltage arises from a modulated flux flow across the film at an average rate of one bundle (ϕ_o) per cycle. This voltage adds to or subtracts from the "classical" voltage depending on its phase. The phase, in turn, depends on the steady enclosed flux. Similar effects are seen at rf levels of (3/2), (5/2) where two and three "quanta" pass each cycle, etc. At levels 1, 2, 3 etc. no net flux flow occurs during a cycle which produces a voltage at this frequency. Many harmonics are also observed, as expected. Harmonics up to ten times the pump frequency have been observed, dropping off only slowly with frequency. No evidence of sub harmonics has been found.

From the observed periodicity in magnetic field and rf voltage and known values of the circuit parameters you get independent checks on the magnitude of the flux ϕ_o that is allowed to flow through. And it turns out that the smallest ϕ_o in all the experiments we have ever done with this thing, the smallest it can be is (h/2e). It may also be a multiple of this value but most often just (h/2e).

This then is one description which I think is adequate to describe how the magnetometer that John Goodkind was using works. Simply that the superconducting ring is acting as a flux valve, and since you have quantization the minimum size of flux that the value can allow to pass is (h/2e). Under those circumstances of operation you must therefore quantize Faraday's law as we have done.

What we have done is to actually build a magnetometer, several, as a matter of fact, based on this kind of principle and also the more conventional principle that you have heard yesterday using the Josephson junction or the point contacts.

What I would like to do next is present some actual data that comes out of using one of these magnetometers as a research instrument.

Vant-Hull, Simpkins, Harding
Physics Letters 24A, 736 (1967)

OPERATION OF SUPERCONDUCTING INTERFERENCE DEVICES IN APPRECIABLE MAGNETIC FIELDS*

M. R. Beasley and W. W. Webb

Department of Engineering Physics
Cornell University
Ithaca, New York

Recently the phenomenon of superconductivity has been used to develop extremely sensitive magnetometers. The two most prominent approaches are the modulated superconducting inductance[1,2], and the superconducting quantum interference device (or SQUID)[3,4]. The inherent sensitivity of these devices is remarkable. Price[2] claims a projected sensitivity of 10^{-10} gauss for a modulated inductance device and Silver and Zimmerman[4] have detected 10^{-9} gauss using a SQUID. Zimmerman and Silver[5] have also shown that one configuration of the SQUID shows the characteristic critical current modulation in rather strong magnetic fields. However, problems arise in developing a practical measuring device for measurement in strong fields. It is our objective in this report to discuss some of these problems and describe a device which we have been using to study flux creep in superconductors and that is capable of resolving field changes of less than 10^{-7} gauss, with a 1 sec time constant, in an applied field of 2500 gauss thus obtaining a field resolution of better than 1 part in 10^{10}. Higher field resolution was not necessary for our flux creep experiments so the resolution of the instrument has not been extended to the ultimate limit of the system.

Basically, the problems of reliable operation of a SQUID in appreciable magnetic fields fall into three categories: effect of the field on the SQUID, stability of the electrical characteristics of the SQUID, and environmental control (e.g. stabilizing magnetic fields and shielding of stray fields) which we will not discuss here except where it directly effects the operation of the device.

One fundamental limitation of any device which, like the SQUID, uses the dc Josephson Effect is the possibility of self-limiting of the weak contacts in a

*This research was supported by the United States Atomic Energy Commission and benefited from facilities provided the Materials Science Center by the Advanced Research Projects Agency.

magnetic field. This occurs when the field is large enough to put one flux quanta into the area of the contact. Thus to operate such devices it is necessary to have small contacts. We have found that a niobium point contact SQUID will successfully operate in any field up to at least 2000 gauss which implies that the individual areas which comprise a point contact are less than 10^{-10} cm^2. Presumably each point contact consists of many very small superconducting contacts enclosing non-superconducting regions.

While the SQUID will presumably function in a field at least up to H_{c2} for the material used, two other considerations usually make it impractical to exploit this property. The first is secondary modulation (i.e. the additional periodicities in the modulation of the critical current of the device as the applied field changes due to the areas enclosed by the individual superconducting contacts within each point mentioned above). While these areas are much smaller than the central area enclosed by the two point contacts and hence have much larger field periodicities they frequently have much larger amplitudes and in practice make it difficult to keep the magnetometer dc biased at the critical current, where the primary modulation due to flux through the central area of the interferometer can be detected, as large field changes are made. Furthermore, the secondary modulation makes it impossible to calibrate the SQUID output over one cycle at one level of applied field and have it reproducible at another field when making measurements of flux changes less than one full flux quantum through the device.

The second problem in use of the SQUID directly in a high field is flux creep[6] in the material which comprises the bulk of the SQUID. When the applied field exceeds $H_{c1}/(1-n)$, the field of initial flux penetration, where n is the appropriate demagnetization factor, flux will enter the bulk material of the device. When flux passes through the inner wall of the material of the device the critical current is modulated just as if the field through the central area had changed thus producing a "drift" in the magnetometer.

Although the SQUID can be used in strong fields if necessary, the problems of self-limiting and secondary modulation can be completely eliminated and the effects of flux creep can be made more manageable by the use of a superconducting

dc transformer to connect the SQUID, which is then placed in a constant low field region, to the variable high field region as shown schematically in Figure 1. In this arrangement, possible self-limiting by the applied field is eliminated. By winding the secondary of the superconducting transformer inside the central area of the SQUID and making it long compared to the axial dimension of the SQUID, it is possible to eliminate all varying fields on the points themselves and hence eliminate secondary modulation entirely. In addition, the SQUID output wave form is much cleaner which facilitates further signal processing. The actual arrangement and the SQUID construction are shown in Figure 2.

Since flux will eventually begin to creep in the material of the transformer windings, flux creep remains a major problem in this design (or in any system incorporating a superconducting transformer). For fields in excess of $H_{c1}/(1-n)$, which under the best circumstances will only be a few hundred gauss, some means of reducing the creep may be necessary.

In our investigations of flux creep we have found that the rate of change of flux in a hard superconductor always decreases inversely with time, is roughly proportional to the critical current density of the material and was undetectible for fields which do not penetrate the bulk of the material. Flux creep can be vastly reduced by a small change of applied field (1-10 gauss) in a sense opposite to the preceeding large field change or by a small temperature decrease (10-100 m deg) after setting the final magnetic field. The details of creep behavior will be highly dependent on the particular material used but the properties described appear quite general and should provide means for reducing creep effects in superconducting instruments.

The degree of isolation between the high field and the low field regions necessary in this system are quite lenient. It is only necessary to keep the field at the SQUID due to the high field magnet below the level which would produce any significant secondary modulation (typically never less than a fraction of a gauss). In our system this is achieved by locating the SQUID 5 inches above the end of the one inch diameter solenoid and enclosing it in a superconducting Pb shield. Figure 3 illustrates the arrangement of the complete magnetometer.

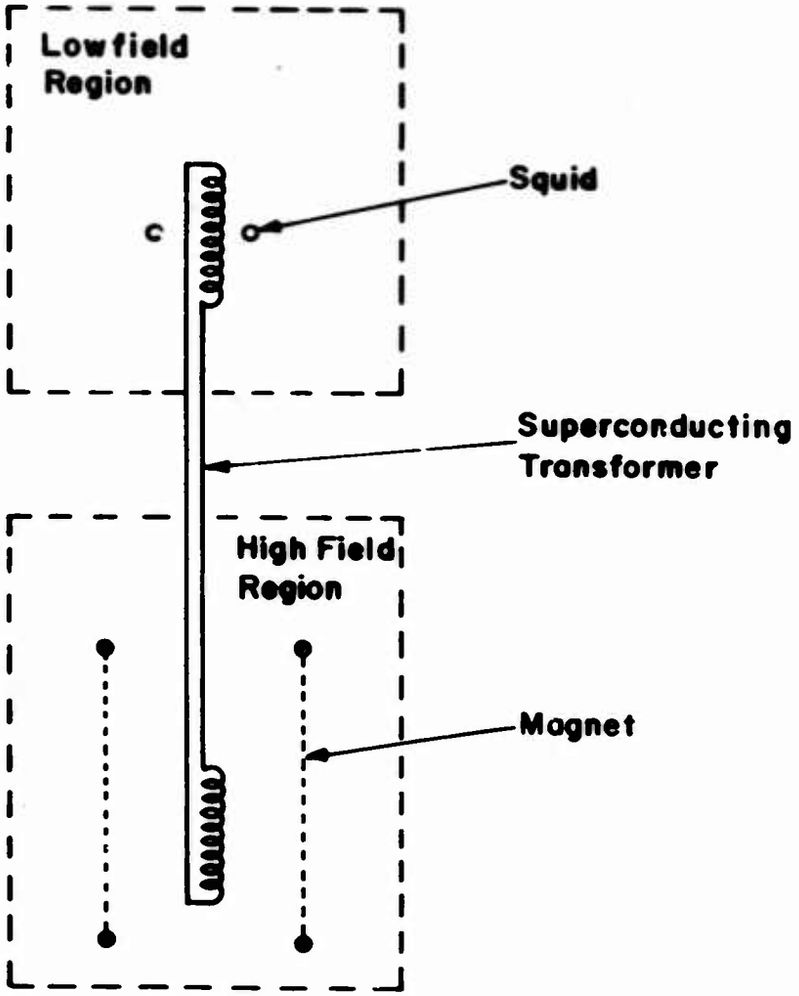

Fig. V-1 Superconducting dc transformer.
(See V-5 for Figure Captions)

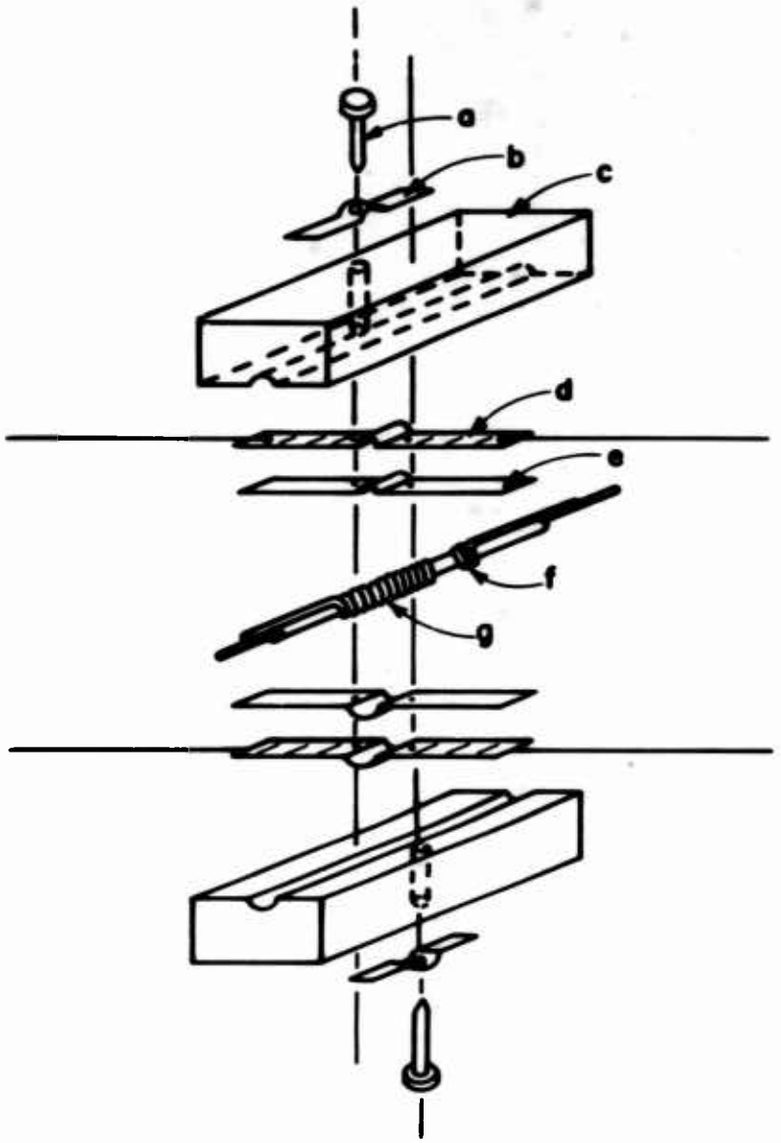

Fig. V-2 SQUID construction.
(See V-5 for Figure Captions)

Figure Captions

Figure 1. Superconducting dc transformer.

The persistent current of the superconducting coils transfers flux changes in the high field region to the low field region where they are detected by the SQUID.

Figure 2. SQUID construction.

The SQUID consists of two strips of .001" Nb foil (d) separated by two sheets of .001" myl r (e). The point contacts are made by pushing pointed .030" Nb wires (a) with a lever (not shown) controlled from outside the dewar through one Nb foil and the mylar sheets to make contact with the other Nb foil. Springs (b) provide a restoring force to back off the Nb wires. The secondary of the superconducting dc transformer is wound from .005" Nb wire on a brass rod and is placed between the two mylar sheets. The length of the coil is about twice the width of the Nb foils. The entire assembly is held together by a micarta jig (c) which has guide holes for the Nb wires. The small field modulating coil (f) is used in the detection circuit.

Figure 3. Complete magnetometer system.

a) SQUID surrounding superconducting transformer secondary.
b) Superconducting dc transformer.
c) Additional inductance in superconducting transformer circuit to change transfer ratio between primary and secondary.
d) Superconducting Pb shield.
e) Thermal switch to open transformer circuit during large field changes.
f) Shoulder to seat magnetometer assembly firmly to top plate of magnet in order to reduce motion of transformer primary in the high field.
g) 2500 gauss persistent current superconducting Nb solenoid.
h) Copper solenoid to make small field changes when superconducting magnet is in persistent current mode.
i) Magnetic specimen in superconducting transformer primary.
j) Tapped hole and stud to secure magnetometer assembly firmly to bottom plate while seating shoulder (f).
k) and l) "Mu-metal" magnetic shielding.
m) Liquid nitrogen dewar
n) Helium dewar.

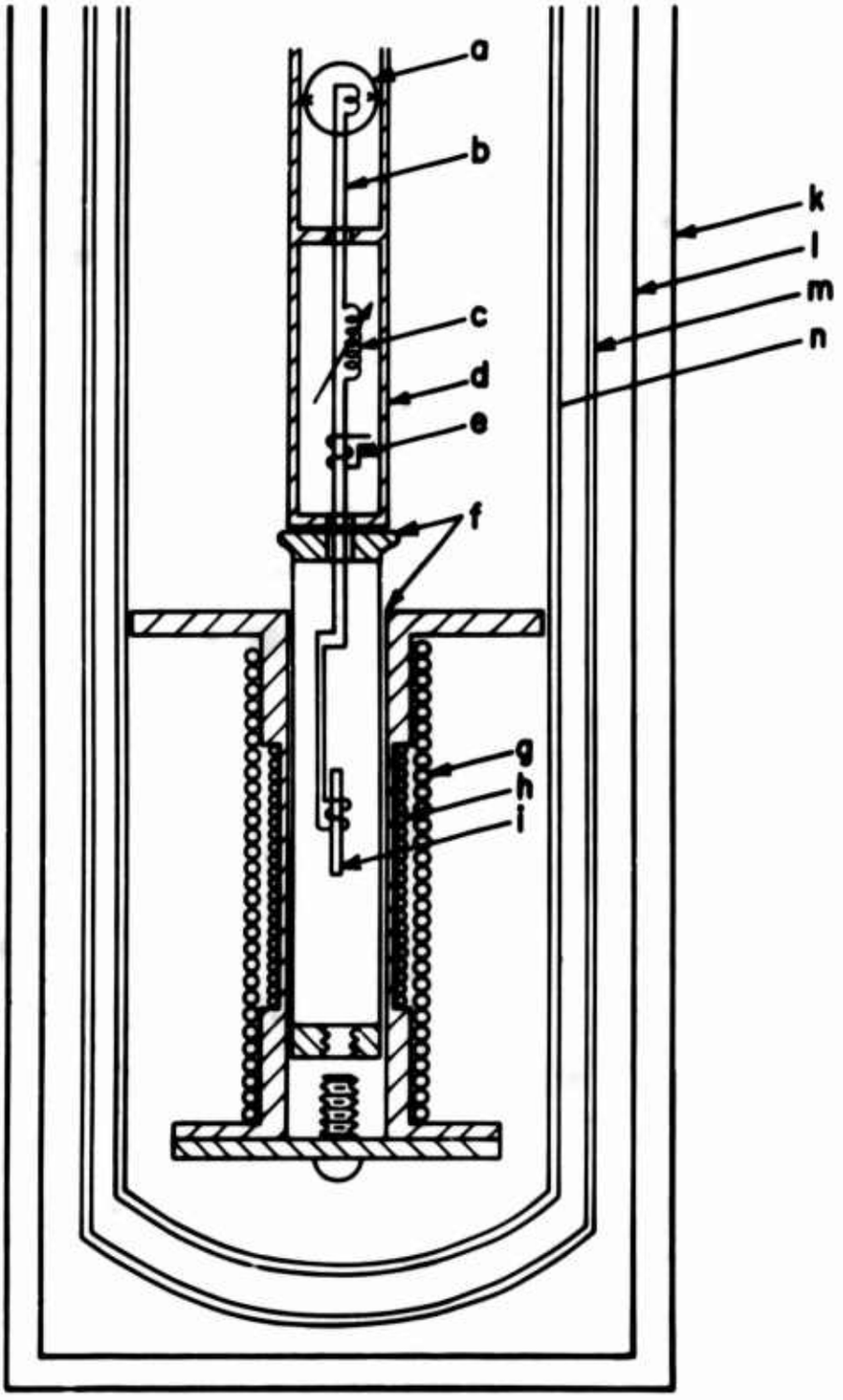

Fig. V-3 Complete magnetometer system.
(See V-5 for Figure Captions)

For applications at any magnetic field level the stability of a SQUID and hence its long term reproducibility is primarily a matter of maintaining the same weak coupling contacts in the presence of mechanical and electrical disturbances. The mechanical stability of point contact SQUIDS does not seem to be a major problem except perhaps at the very greatest sensitivities[4]. Our particular point adjustment mechanism has considerable deliberate backlash which provides a means of mechanically decoupling the points from the external vibrations transmitted by the mechanism. In addition, the entire dewar is vibration isolated. Electromagnetic noise seems to be the most important source of instability of a SQUID. Electromagnetic fields alter the basic electrical characteristics of the point and thus stray electromagnetic fields make the critical current modulation irregular resulting in a poor quality signal and producing "magnetic noise" in the SQUID output. To eliminate these instabilities some kind of electromagnetic shielding is necessary. In our system the dewar is surrounded by two "mu-metal" cans and the entire dewar and signal detection electronics are enclosed in a shielded enclosure. This arrangement has proven quite satisfactory.

With these precautions and using the transformer arrangement described above we have found it possible to operate the SQUID over the course of a day without any readjustment of the points and achieve critical current modulation which does not change in time and is independent of the applied magnetic field to within the experimental accuracy of 1% to which it was measured. Despite the disadvantages of slow drift due to flux creep, the transformer coupled SQUID currently provides reliable field resolution of better than 1 part in 10^{10} in a magnetic field of 2500 gauss.

We would like to acknowledge very useful conversations with A. H. Silver and J. E. Zimmerman, the support of the United States Atomic Energy Commission, and the facilities of the Advanced Research Projects Agency.

REFERENCES

1) B. S. Deaver, Jr., and W. S. Goree, Rev. Sci. Instr. 38, 311 (1967).
2) J. M. Pierce, Symposium on the Physics of Superconducting Devices, University of Virginia, Charlottesville, Va., (1967).
3) R. C. Jacklevic, J. Lamb, J. E. Mercereau, and A. H. Silver, Phys. Rev. 140, A1628 (1965).
4) J. E. Zimmerman, and A. H. Silver, Phys. Rev. 141, 367 (1966).
5) J. E Zimmerman, and A. H. Silver, Physics Letters 10, 47 (1964).
6) P. W. Anderson, and Y. B. Kim, Rev. Mod. Phys. 36, 39 (1964).

SUMMARY OF PROCEEDINGS

M. Tinkham
Harvard University

I think that the first thing I should do in my talk, since it is the last talk of the meeting, is to express the thanks that I am sure all of us feel are due to the organizers, particularly Bascom Deaver, who I am sure has been working on this conference at the expense of his physics for the last N months.

The second thing I should do is excuse myself for giving an incomplete summary talk. For one thing, this Conference, despite its excellent organization, was so compact that there was no time for me to think about what I have heard. This problem was aggravated by Dick Ferrell, Chairman of this session, whose birthday party last night took the time I had planned to prepare my talk ! Moreover, because of the short time available for a summary compared to the number of talks, I shall have to omit any mention of some talks to avoid trying to summarize each talk in one minute.

Instead of making an effort at a detailed summary, what I will start off with are a few rather general remarks about the subject of our meeting, aimed not at the speakers who know all about this, but at the people who are here who are not experts, but have been trying to find out about this area.

The idea which underlies all these devices is the existence of long-range order or coherence in superconductors. This is described by saying that there is some sort of macroscopic wave function like the Ginsburg-Landau wave function, ψ, which is a complex quantity with phase as well as amplitude, and of course both of these may be functions of position. Thus we write

$$\psi(r) = |\psi(r)| e^{i\varphi(r)} \qquad (1)$$

In terms of such a macroscopic wave function, one can write expressions for the current and magnetic field, which we operationally observe. Without going through any detail, the basic relation we need is just the usual relation between the canonical momentum $\vec{p}$ and the velocity in the presence of a magnetic field, described by a vector potential $\vec{A}$, namely

$$\vec{p} = m^* \vec{v} + \frac{e^*}{c} \vec{A} \tag{2}$$

where m^* and e^* are the effective double mass and charge of the paired superconducting electrons. The current should then be proportional to the density of superconducting electrons (i.e. to $|\psi|^2$) times a superconducting drift velocity $\vec{v}_s$. Thus we write

$$\vec{j} \sim |\psi|^2 \vec{v}_s \sim |\psi|^2 \left[\vec{\nabla}\varphi - \frac{2\pi}{\varphi_o} \vec{A}\right] \tag{3}$$

where the flux quantum $\varphi_o = hc/2e$. In deriving the second form, we have used the fact that the momentum is related to the gradient operator by a factor of $\hbar/i$. Hence we expect an expression of this sort to determine the current density in a material which has such a coherent macroscopic wave function.

Now from this formulation we can easily get such things as the London theory, which describes so many of the properties of superconductors. In the London gauge choice, the phase of the macroscopic wave function is taken to be constant everywhere, so the term in $\nabla\varphi$ drops out, and one finds simply that $\vec{j}$ is proportional to $-\vec{A}$, a familiar result. By taking derivatives with respect to time and space it leads to the two London equations. These relations commonly underlie the devices which involve what I might call strong superconductivity. By contrast, we might refer to weak superconductivity, to describe things having to do with junctions, weak links, tunneling, etc., in which a spatially localized weak part is intentionally put in the superconducting circuit.

To approach these weak cases, let's first think of an actual Josephson tunneling junction, where we have a very thin insulating layer between two superconductors. If we try to discuss the current that flows through the junction in terms of (3), we can do this in a very crude way by saying that in this junction the material is a very weak superconductor because the only conduction electrons out here are those that tunnel out into this forbidden region, so that $|\psi|^2$ approaches

zero. This would suggest that the current flowing through such a junction should go to zero. But this leaves out the possibility that the gradient of the phase may in fact approach infinity in such a way that the phase difference $\Delta\varphi$ across this very thin junction remains finite. If we have such a situation, we can see that the vector potential term, being a constant $\vec{A}$ times the vanishing quantity $|\psi|^2$, drops out, leaving the current proportional, according to this argument, to the difference in phase $\Delta\varphi$ across the junction. But this is obviously an oversimplified result, because phase is only defined modulo 2π. Intuitively we generalize from $j \sim \Delta\varphi$ to

$$j \sim \sin \Delta\varphi \tag{4}$$

which reduces correctly to $\Delta\varphi$ when the phase difference is small, but yet which has the desired periodicity property. To be fair, though, we must note that this isn't the only periodic function which reduces properly for small $\Delta\varphi$. As we have heard from Silver, in narrow metallic weak links (rather than thin oxide-insulated junctions) one often finds something other than a sine wave response. In fact one may find a sawtooth wave, but the general idea remains that the current should be some periodic function of this finite phase difference.

Equation (4) gives us one of our necessary equations, the relation between the current and the finite phase difference across the junction or weak link. The other equation we need in order to treat ac effects is

$$2e(\Delta V) = \hbar\, \partial(\Delta\varphi)/\partial t = h\nu \tag{5}$$

where ΔV is the voltage difference across the junction, and ν is the frequency of the ac tunneling current, which is also the frequency with which flux quanta cross between the two contacts of the junction. This relation can be derived in an elementary way, by considering a case in which ΔV is sustained by magnetic induction, or by more general quantum theoretic arguments.

These are the equations we need to understand most of what we have heard, and fortunately they are quite simple. I don't mean we can understand everything with these equations, but at least they give a framework. In terms of

this analysis, we may try to distinguish strong superconducting effects requiring no weak links or Josephson junctions, from the weak superconductor effects, depending critically on the existence of such phenomena.

Now to proceed to the summary itself, I have tried to skim through all the papers which were presented and picked out a representative few of the things in each of these categories which have been done.

As a first example of the strong superconducting effects consider Fairbank's plan to make a superconducting linear accelerator, in which the high conductivity characterized by the London equations gives microwave cavity wall power losses 500,000 times less than would copper. That is a major improvement, just by having better conductivity. (Superconductors are perfect conductors only at dc or T = 0.) Also of course the superior cooling ability of superfluid liquid helium plays a key role in making this practical.

A related requirement for the superconducting accelerator to be practical is that the microwave losses be about as low as theoretically expected. There is quite a long history of this subject, with extraneous losses dominating the low-temperature behavior. For example, shortly after World War II people started trying to make very high Q superconducting cavities, taking advantage of the advent of microwave technique and the increased availability of liquid helium, thanks to the development of the Collins liquifier. The present results reported by McAshan, seem to be about 1000 times better, i.e., with 1000 times lower residual losses or 1000 times higher Q, than the results obtained at that time. The reason for this great improvement is not entirely clear; a rational explanation is that great care is taken to prevent any magnetic flux trapping in the cavity walls, since the normal spot associated with such trapped flux gives a loss which does not vanish at low temperatures. Beyond the rational, however, the speaker referred to judicious use of new forms of "black magic" in fabricating particularly clean and perfect metallic joints and surfaces in the cavity. Both types of improvements seemed essential for the excellent results reported. The temperature-dependent part of the absorption, above this reduced residual value, was observed to be in reassuring agreement with the expectations of the Mattis-Bardeen calculation.

Another striking observation was that the Q of these cavities remained constant at these high values up to power levels at which the peak value of the RF magnetic field was equal to the static critical field. This shows that the situation is quite ideal, and that these cavities can be used up to very high power levels without a preliminary onset of heating.

Another type of thing that Fairbank described was his general relativity experiment. In this, the persistent current, a strong superconducting property, makes his gyro possible, but to sense the position of the gyro he plans to use a Josephson, or weak superconducting, device to detect the magnetic field produced by the so-called London magnetic moment of the rotating superconductor. Thus, in this application, both strong and weak superconductivity play a role.

The perfect diagmagnetism of London superconductors has suggested to various speakers the possibility of reaching absolutely zero magnetic fields inside a superconducting shield. The superconductor provides a quantized scale of magnetic flux, so that the total flux threading an enclosure must be an integral multiple of ϕ_o. Thus, if one can get out the last quantum of flux, one should have really zero gauss. At this conference, Hildebrandt has reported reaching fields of less than 2×10^{-6} gauss over a spherical volume of 7.5 cm radius. About the only ultimate limit discussed was that of thermal noise, described by Mercereau. The fluctuations of $B^2V/8\pi$ should be $1/2\ kT_c$ at T_c, and below T_c the superconducting flux quantization will preserve whatever value of flux was present at T_c.

Among the demonstrations of things superconductors can do better was that of the "superinductor" by Little. This is based on the simple ideas of the London theory of superconductivity in which an electric field accelerates the supercurrent, giving it a kinetic energy proportional to v_s^2, and hence to the square of the current. Equating this kinetic energy to $1/2\ Li^2$, we define an effective inductance of the element. This superinductance has the advantages that: (1) it can be 50 times as great as that of a non-superconducting microelement of the same size (because the energy is stored internally rather

than in an external magnetic field), and (2) the inductance is a function of temperature, magnetic field, and current (since all these affect $|\psi|^2$, or the number of superconducting electrons), allowing convenient modulation for the inductance in a parametric amplifier application.

Continuing with our list of possible types of applications, we come to the report of Matisoo, who reported on the possible use of a tunnel junction as a computer switching device. The switch between the Josephson (zero-voltage) and the normal single-particle (non-zero-voltage) tunneling characteristic could be induced by a 10 ma control current and occured in less than 10^{-9} seconds.

Giaever's paper on flux-flow and DC transformers made it clear that despite the alluring concept of a DC transformer, the actual practice was not very attractive from an application point of view because the efficiency was limited to something like 20%. The problem is that there is dissipation in the primary even if there is no load on the secondary. A further practical limitation arises because in the thin films which must be used to make these transformers, fluxon pinning is generally severe (because of the thickness variations due to the granular structure of thin films). Thus extra dissipation will always ensue from the overcoming of the pinning resistance. Perhaps the most practical of the applications he discussed was the "flux-pump", a type of DC transformer in which flux is pumped into a higher concentration by passing flux bundles across a superconducting circuit. Such devices are used in building up strong fields in superconducting solenoids with heavy windings without the need for heavy conductors to carry heavy currents down into the cryogenic region.

At this point, we turn to a long list of detectors, all of which use a weak superconducting element as the critical element. As I shall develop in a little more detail, these devices can measure voltages down to 10^{-15}, magnetic fields down to 10^{-10} gauss, gravitational g's to 10^{-8}, flux to 10^{-3} of flux quantum, etc. With further development, such detector elements may well be among the most useful of the superconducting devices.

The detector which I most keenly appreciated hearing about was the far-infrared detector reported on by Shapiro. This device uses a point contact between two superconducting wires as the Josephson weak link. With a suitable DC current bias just beyond the limiting zero-voltage Josephson current, the output voltage is a very rapid function of incident radiant energy. In fact, he reported being able to detect 5×10^{-13} watts, which compares favorably with the best cryogenic bolometer detectors. A striking property of these detectors is their frequency-dependent sensitivity. This seems to depend on the material, but also to vary somewhat depending on junction geometry. There can be very sharp peaks in response, suggesting the highly sensitive, but tricky, response of a regenerative circuit in early radio circuitry. This analogy is probably more than superficial, because the Josephson contact plays both an active and a passive role in its interaction with the radiation field. Shapiro showed that these detectors work (with reduced sensitivity) even above the gap frequency, where the materials are strongly lossy, and successfully detected a 300 micron laser beam. The response time is less than 10 nanoseconds. Countering these attractive features, the devices are very sensitive to stray electrical impulses, requiring work in a shielded room to extract the potential sensitivity. Also, they are generally less stable, reliable, and broadband than a bolometer. Of course, if the selective response can be brought under control, it could offer a considerable advantage.

Closely related to this detector, with its possible regenerative behavior, is the oscillator-detector described by Silver. In this device a controlled voltage is developed across a point-contact weak superconducting link by passing a current through a brass shunt. This voltage determines the frequency of the AC Josephson current. When this circuit is coupled to an external resonant structure, whether macroscopic transmission line or microscopic nuclear spins, structure is observed in the characteristic of the junction (probed at 30 Mhz) when the Josephson frequency 2eV/h is equal to the external resonant frequency ($\pm$ 30 Mhz). This simple voltage tuneable spectrometer has already been used by Silver and coworkers to detect NMR in metallic

cobalt, and it seems a most attractive prospect for future development to allow sweeping up to the energy gap frequency and even above. If successful, it would certainly be extraordinarily much simpler than the cumbersome far-infrared techniques now used for our work in the submillimeter wavelength range.

In connection with the Josephson frequency relation, basic to the above application, discussion was directed to the question of the line width of this Josephson radiation. Kamper suggested that it would be determined ideally by thermal fluctuations in the voltage across the junction, i.e., by Nyquist noise, which would lead to frequency modulation. He proposed turning this limitation into an advantage by using the bandwidth as an absolute temperature thermometer. With reasonable assumed values, he argued that temperatures could be determined to 1 millidegree. Some experimental support for this conjecture was offered in discussion by Zimmerman, who reported finding a finite line width in general agreement with this prediction.

The question of noise in superconductors and junctions was taken up in more detail by Scalapino and Burgess. Scalapino reported that, despite the extreme non-linearity of tunnel junctions and the complex underlying theory of the tunneling process, it is possible to relate the theoretical noise spectrum to the observed static I-V characteristic of the junction without explicit dependence on the microscopic theory in the results. This provided a welcome bit of simplification for future discussions. The report of Burgess emphasized the utility of simple equivalent circuits in discussion of noise and fluctuations in superconductors, with particular attention to the extremely rare fluctuations which lead to the slow decay of a persistent current.

Returning, now, to the list of detectors, we come to the superconducting gravimeter reported by Goodkind. As in Fairbank's gyro, superconducting persistent currents are used here for levitation purposes, leading to great long-term stability. Position sensing by either superconducting flux sensing or by ordinary capacitive sensing allow the position of the levitated sphere to be sensed to within 1Å! At present, the performance of the gravimeter matches or betters the best in conventional techniques, and there is hope of

increasing the sensitivity and stability to allow detection of a possible secular variation of the gravitational constant at the rate of 10^{-11} per year. Such sensitivity would not only allow precise measurements of "earth tides" but also allow explorations of cosmological interest.

Finally, we come to the devices which really are the most basic application of the flux quantization Josephson junction ideas; the devices which basically measure and count individual flux quanta. Perhaps the first of these to be used was the SLUG, or Superconducting Low-inductance Undulating Galvanometer, introduced by Clarke. This simple device, consists basically of a solder blob around a niobium wire, with the solder making weak Josephson contacts to the wire. When a current passes through the wire, the magnetic flux enclosed by the solder causes the critical current that can be passed through the junction to oscillate with the period of the flux quantum. Since these oscillations remain clean for thousands of periods, this allows a "digital" measurement of the current in units of the flux quanta produced. This does not make a particularly sensitive ammeter, but because the resistance is so low, it does make an extraordinarily high sensitivity voltmeter. For example, with a circuit with intrinsic time constant of one second, a voltage change of 2×10^{-15} volts makes a complete cycle of one flux quantum. With suitable feedback circuitry it is possible to subdivide this by at least a factor of 100, leading to a sensitivity of the order of 10^{-17} volts. By combining two SLUGs and by using DC transformers ("real" ones with multi-turn superconducting windings, not Giaever-type film sandwiches) to give a step-up, sensitive DC amplifiers and more convenient impedance levels may be obtained.

More or less equivalent to the SLUG is the SQUID, or Superconducting Quantum Interference Device, usually having a configuration in which the two junctions between which the interference occurs are separated by more exactly controlled geometry. Beasley's short report on work at Cornell is typical of the potential applications of SQUIDs. In this work, he counted the individual flux quanta leaving or entering a type II superconducting

rod, demonstrating with great conviction the remarkably characteristic logarithmic time dependence predicted by the Kim-Anderson flux creep theory.

This brings us to the final paper of the Symposium, that of Mercereau on modulated flux flow. In this paper he reported on a very sensitive type of weak-link magnetometer, with a specific application to measurement of thermal magnetic noise. Integrated over all frequencies, $1/2\ Li^2 = 1/2\ \Phi^2/L$ should have the equipartition value 1/2 kT. Although these rms flux variations are about 100 times smaller than a flux quantum, he was able to confirm the expected value and temperature dependence in normal samples. However, when a tin rod was put in the pickup coil and cooler, the noise dropped below the level of detectability below T_c. This result does not really contradict the expected result; rather, it is a manifestation of the fact that the persistent currents of a superconductor trap flux over such a long time period that fluctuations must occur much, much too slow to be observable in an experiment of this sort.

To conclude, I would say that this conference has been a very interesting one to me, in which I have seen tremendous activity in developing practical applications of the simple relations which I summarized at the beginning of this talk. In the sense that a device is defined as something which can be sold at a profit, the conference may have been premature. But if we include devices which are already practical for laboratory use and promising for more general application, the conference was indeed timely. If I am not mistaken, many of us will now go home and put together a few SQUIDs, SLUGs, or other weakly connected superconductors so that we will have new results to contribute to the next conference on this subject.